UNIVERSITÉ LAVAL

The effects of polyphenol-rich extracts on obesity-linked metabolic diseases

Thèse

Fernando Forato Anhe

Doctorat en physiologie-endocrinologie
Philosophiæ doctor (Ph. D.)

Québec, Canada

The effects of polyphenol-rich extracts on obesity-linked metabolic diseases

Thèse

Fernando Forato Anhê

Sous la direction de :

André Marette, directeur de recherche

Résumé

L'obésité et son large spectre de maladies associées ont atteint des proportions pandémiques inquiétantes, soulignant la nécessité d'identifier des stratégies alternatives afin de lutter contre ce problème. À ce titre, les régimes riches en fruits et légumes représentent des déterminants bien établis d'une incidence plus faible de ces désordres métabolique. Grandement soutenus par des évidences épidémiologiques reliant les régimes riches en polyphénols et un meilleur état de santé, des efforts considérables ont été déployés afin d'étudier les bienfaits de ces métabolites secondaires des plantes. Malgré tout, les mécanismes par lesquels ces phytoéléments améliorent la santé métabolique demeurent encore mal compris, ce qui en justifie une étude plus approfondie. D'autre part, de plus en plus d'évidences indiquent que les bactéries intestinales exercent un important contrôle sur des aspects clés du métabolisme, et on comprend aujourd'hui que plusieurs phytoéléments de baies ont une biodisponibilité limitée, atteignant ainsi le colon qui abrite la plus vaste part du microbiote intestinal. Le travail présenté dans cette thèse vise donc à étudier l'impact de phytoéléments de baies sur le syndrome métabolique de souris soumises à une diète obèsogène et d'en comprendre le rôle du microbiote intestinal dans ces effets. En traitant quotidiennement ces animaux avec des extraits riches en polyphénols d'une gamme de baies aux compositions polyphénoliques variées, nous avons montré que les extraits les plus bioactifs (c.-à-d., canneberge, cloudberry, alpine bearberry, lingonberry et camu camu) partagent la capacité de diminuer l'inflammation intestinale, l'entotoxémie métabolique, la stéatose hépatique et la résistance à l'insuline. L'analyse des populations microbiennes fécales par séquençage du gène 16S ARNr a révélé que l'état métabolique amélioré lié à l'administration de ces extraits était associé à un remodelage draconien du microbiote intestinal, marqué par une expansion d'*Akkermansia muciniphila*. Cette bactérie intestinale est fortement associée à un faible niveau d'adiposité chez l'humain et son administration à des souris obèses a été montrée suffisante pour renverser le syndrome métabolique. Par ailleurs, les résultats présentés dans cette thèse suggèrent que les polymères de polyphénols, à savoir les proanthocyanidines et les ellagitannins, pourraient bien être des

molécules clés dans les effets bénéfiques observés, ouvrant la voie à plus de recherche en ce sens. L'ingestion régulière de ces polyphénols par la consommation de canneberges, de cloudberry, d'alpine bearberry, de lingonberry et de camu camu représentent donc une stratégie efficace pour la prévention de désordres métaboliques associés à l'obésité. Cet ouvrage ouvre ainsi à de nouveaux concepts mécanistiques, ciblant l'axe intestin-foie et le microbiote intestinal pour expliquer les effets bénéfiques des polyphénols sur la santé métabolique.

Abstract

Obesity and its wide spectrum of associated diseases have reached worrisome pandemic proportions, underscoring the need for alternative strategies to fight this problem. Plant-rich diets are well-established determinants of a lower incidence of obesity-related diseases, and fruits are important components of these diets. Supported by strong epidemiological evidence linking polyphenol-rich diets and better health status, research has been focused on the potential health effects of these plant secondary metabolites, albeit the mechanisms by which these poorly bioavailable phytonutrients improve metabolic health remains are not yet fully understood. Since there is compelling evidence for a relationship between host metabolic control and the gut microbiota, the work presented in this thesis aimed to investigate the impact of polyphenol-rich berry extracts on features of the metabolic syndrome in diet-induced obese mice. The work presented in this thesis also focuses on the relationship between putative gut microbial alterations driven by dietary polyphenols and its relevance to host metabolism. By daily treating diet-induced obese mice with polyphenol-rich extracts of a wide range of berries (with varied polyphenolic concentration and composition) we demonstrated that the most bioactive extracts (*i.e.*, cranberry, cloudberry, alpine bearberry, lingonberry and camu camu) shared in common the ability to dampen intestinal inflammation and bacterial lipopolysaccharide leakage to systemic circulation, findings associated with reduced hepatic steatosis and improved insulin resistance. 16S rRNA gene-based analysis of fecal DNA revealed that the improved metabolic status linked to the administration of these polyphenolic extracts was associated with a drastic gut microbial remodeling, marked by a consistent bloom of *Akkermansia muciniphila.* This gut bacterium is strongly associated with leanness in humans and its administration to obese mice reversed features of the metabolic syndrome. The findings presented in this thesis suggest that polymers of polyphenols, namely proanthocyanidins and ellagitannins, may have a superior impact on the gut-liver homeostasis, supporting further research on these particular classes of phenolic phytonutrients. While bringing evidence that substantiate the regular consumption of sources of proanthocyanidins and ellagitannins as a strategy to prevent

prevalent chronic diseases associated with obesity, this work provides novel mechanistic insights pointing to the gut-liver axis and the gut microbiota as primary targets of dietary polyphenols in order to improve metabolic health.

Table of contents

List of figures

Introduction

CHAPTER I

CHAPTER II

CHAPTER III

CHAPTER IV

Conclusion

List of tables

List of abbreviations

^{18}F-FDG – ^{18}F Fluorodeoxyglucose

2-AG – 2-Arachidonoylglycerol

2-OG - 2-Oleoylglycerol

2-PG – 2-Palmitoylglycerol

AKT – Acute transforming retrovirus thymoma

ASBT/ IBAT – Apical sodium-dependent bile acid transporter/Ileal bile acid transporter

ATP – Adenosine triphosphate

BA – Bile acid

BAT – Brown adipose tissue

BMI – Body mass index

BMP – Bone morphogenetic protein

CA – Cholic acid

CBG – Cytosolic β glucosidase

CCK – Cholecystokinin

CD – Cluster of differentiation

CDCA – Chenodeoxycholic acid

Ceacam1 – Carcinoembryonic antigen-related cell adhesion molecule 1

ChREBP – Carbohydrate-responsive element-binding protein

CVD – Cardiovascular diseases

CYP7A1 – Cholesterol 7α hydroxylase

DCA – Deoxycholic acid

ER – Endoplasmic reticulum

FASN – Fatty acid synthase

FFA – Free fatty acids

FGF – Fibroblast growth factor

FGFR4 – Fibroblast growth factor receptor 4

FIAF/ANGPTL4 – Fasting induced adipose factor/Angiopoietin-like 4

FOXO1 – Forkhead BOX class-0 winged helix transcription factor-1

FXR – Farnesoid X receptor

GI tract – Gastro-intestinal tract

GLUT – Glucose transporter

GPR – G protein-coupled receptor

GSK3 – Glycogen synthase kinase

HCC – Hepatocellular carcinoma

HDAC – Histone deacetylase

HFD – High fat diet

HFHS – High fat high sucrose diet

HS – Hepatic steatosis

HSL – Hormone-sensitive lipase

IEC – Intestinal epithelial cells

IL – Interleukin

ILC – Innate lymphoid cells

INFγ – Interferon γ

iNOS – inducible nitric oxide synthase

Ins – Insulin gene

IR – Insulin receptor

Irgm 1 – Immunity-related GTPase family M

IRS – Insulin receptor substrate

JAK – Janus activated kinase

JNK - c-Jun N-terminal kinase

LCA – Lithocholic acid

LPH – Lactase phloridzin hydrolase

LPL – lipoprotein lipase

LPS – Lipopolysaccharide

MAPK – Mitogen-activated protein kinase

MCA – Murocholic acid

MCP1 – Monocyte chemoattractant protein 1

MRP – Multidrug resistance protein

mTOR - Mammalian target of rapamycin

MyD88 – Myeloid differentiation primary response 88

NAFLD – Nonalcoholic fatty liver disease

NASH – Nonalcoholic steatohepatitis

NFκB – nuclear factor κB

NK – natural killer

NLR – NOD-like receptor

NLRP - NLR family pyrin domain containing

NO – nitric oxide

NOD – Nucleotide-binding oligomerization domain containing

O_2^- - Superoxide

Ocln – Occludin

$ONOO^-$ - Peroxynitrite

PET – Positron emission tomography

PI3-K – Phosphoinositide 3-kinase

PRR – Pattern recognition receptor

RANTES - Regulated upon activation, normal T-cell expressed and secreted

ROS – Reactive oxygen species

S6K – Ribosomal protein S6 kinase

SCFA – Short chain fatty acids

SGLT – Sodium glucose transporter

SHP – Small heterodimer partner

SNS – Sympathetic nervous system

SREBP – Sterol regulatory element-binding protein

T1D – Type 1 Diabetes

T2D – Type 2 Diabetes

TGFβ – Transforming growth factor

TGR5/GPBAR1 – G protein-coupled bile acid receptor 1

TLR – Toll-like receptor

TNFα – Tumor necrosis factor α

TSLP – Thymic stromal lymphoprotein

UCP1 – Uncoupling protein 1

UDCA – Ursodeoxycholic acid

WHO - World Health Organization

ZO/TJP1 – Zonula Occludens/Tight junction protein 1

Aos meu pais, Silvio e Marilene.

Aos meus irmãos, André e Gabriel.

A minha esposa, Joana.

Acknowledgments

Throughout almost six years of intense work dedicated to my doctorate, I had the chance to meet several people, each one of them was essential for this journey in a particular way. In addition to long hours doing experiments, treating animals, reading papers and writing, the daily routine of a PhD student involves exchanging ideas and the constant observation of how his peers and mentors approach questions and put scientific thinking into practice. Soon it becomes clear that the scientific endeavour demands a great deal of collaboration, otherwise it is doomed to failure. The PhD is a long and winding road, but it leads to a beautiful place.

Below I acknowledge those without whom this work would not have been possible or who were important somehow to the accomplishment of this daring mission.

First and foremost, I would like to thank Dr André Marette, who welcomed me with open arms in his laboratory, gave me unrestricted intellectual freedom, provided an extraordinary research infrastructure and, above all, taught me how to be a scientist. There is nothing more altruistic than sharing knowledge. I will be forever thankful.

I am thankful to Dr Geneviève Pilon. With her kindness and passion for science, she attracted me (and many others) to the world of polyphenols and gut microbiota. In her passionate quest for links, insights, answers, she would devour articles, books and anything that brings any relevant information, then she would prepare sketches and hand written summaries hanging them on her office wall to keep these ideas at reach. Afterwards, little by little, she would always find order in chaos and come out with brilliant hypothesis. By observing that, I had one of the most inspiring and important lessons in my PhD and the most beautiful and pure demonstration of what being a scientist means. Thank you.

I am thankful to all former and current members of the Marette Lab with whom I had the pleasure to work aside. Thanks for the help, for sharing ideas and for the friendship. Thanks to Dr Patricia Mitchell, Dr Mauro Sola-Penna, Dr Patricia Zancan, Dr Annabelle Caron, Dr Kerstin Bellmann, Dr Michael Schwab, Dr Elaine

Foreword

The work presented in Chapter I of this thesis was published in *Gut* (2015 64(6):872-83; published ahead of print 30 July 2014) and it is presented as an author-created, uncopyedited version of the original article. As the first author, I was the main author involved in data integration and interpretation and wrote the manuscript. I was responsible for planning the studies along with Dr Geneviève Pilon and Dr André Marette. I carried out all the animal studies and I generated most of the data presented, except for the phytochemical characterization of the cranberry extract (Dr Stéphanie Dudonné), the bio-informatics analysis of fecal 16S rRNA gene sequences (Dr Thibault Varin and Dr Sébastien Matamoros) as well as some intestinal analysis (Dr Carole Garofalo, Dr Quentin Moine). All authors importantly contributed to the discussion and to the conclusions drawn in this manuscript.

Chapter II contains a manuscript accepted for publication in *Molecular Metabolism* (October 10th 2017, doi.org/10.1016/j.molmet.2017.10.003). This chapter provides a deeper understanding of the effects of a cranberry extract on diet-induced obesity and is presented as an author-created, uncopyedited version of the original article. I am the first author of this article and, as such, I planned the study along with Dr Émile Levy, Dr Geneviève Pilon and Dr. André Marette. I carried out all the studies, with the technical assistance of Dr Vanessa Vilela, and contributed to research directions. I am responsible for most of the data contained within, except for the bioinformatics analysis (Dr Thibault Varin).

Chapter III contains a manuscript accepted for publication in *Diabetologia* (article in press) and is presented as an author-created uncopyedited version of the original article. Dr André Marette, Dr Geneviève Pilon and I designed the study. I performed most of the experiments, with the valuable assistance of Dr Mélanie LeBarz. Dr Stéphanie Dudonné carried out the chemical characterization of the extracts of Arctic berries and published these data in a separate paper (*Journal of Food Composition and Analysis* 2015, 44:214-224), of which I am a co-author. Dr Thibault Varin analyzed fecal 16S rRNA sequences and generated plots of

bacterial taxonomic distribution. All authors were implicated in the discussion of the data and I wrote the manuscript.

The study presented in Chapter IV contains a manuscript in preparation. Dr André Marette, Dr Geneviève Pilon and I designed the study. As the first author, I conducted all the animal studies, with the technical assistance of Dr Mélanie LeBarz, was in charge of data compilation and analysis and was a major contributor to research directions. Dr Stéphanie Dudonné carried out the phytochemical analysis of the camu camu extract. Dr Thibault Varin conducted bio-informatics analysis of fecal 16S rRNA gene sequences and generated plots of gut microbial profile. Dr Jocelyn Trottier conducted bile acid quantification analysis in Dr Olivier Barbier's laboratory.

Introduction

1 Obesity: le mal du siècle

Obesity is an abnormal fat accumulation of sufficient magnitude to produce detrimental health consequences and it is caused by a continuously positive energy balance. Nutritonal transition to processed foods and high-calorie diets and sedentarism spread across the planet as societies became wealthier and modernized throughout the 20th Century. These environmental determinants coupled with genetic susceptibility (1) have been working together so that obesity and overweight have both reached worrisome pandemic proportions. Data from the World Health Organization (WHO) revealed that more than 1.9 billion adults were overweight and, of these, over 600 million were obese in 2014 (overweight BMI ≥ 25; obesity BMI ≥ 30; BMI = weight/height^2) (2). In other words, while 4 out of 10 adult individuals were overweight, 1 in 10 was obese in the world in 2014. Obesity and overweight are strongly prevalent in both developed and emerging economies, considerably impairing life quality, reducing lifespan and imposing important costs on public health systems (3, 4). While the worldwide prevalence of obesity more than doubled between 1980 and 2014, childhood obesity was found to be highly prevalent in children under the age of 5, with 41 million obese infants in 2014 (2). These data fuel alarming predictions that the global prevalence of obesity will easily surpass 1 billion people by 2030 (5).

2 The multifactorial etiology of obesity

The storage of triglycerides in the adipose tissues is influenced by the interplay of genetic, environmental, socioeconomic and behavioural determinants, which are all capable of altering the balance between energy intake and expenditure. Energy storage occurs when energy intake surpasses energy expenditure (*i.e.*, the amount of energy used to fuel physical activity, basal metabolism and adaptive thermogenesis). Economic development, growing availability of inexpensive and nutrient-poor food, industrialization and urbanization are achievements of both high-income countries and emerging economies that act as important obesogenic forces. However, the fact that individuals living in these

environments are not necessarily obese and display varied BMI highlights a role for genetic predisposition in the etiology of obesity. It is, however, surprising that while almost a hundred of genetic loci have been associated with obesity, they explain only a small fraction (~2.7%) of the total BMI variantion within populations (6, 7). Although it is not reasonable to disconsider the relevance of genetics in obesity, the relatively small differences in BMI between carriers and non-carriers of risk alleles in addition to the dramatic global rise in obesity over the last decades stress the importance of risk factors beyond genetics.

While dietary habits are obvious determinants of obesity, and caloric intake a well-known player, diet quality also plays a relevant part in the consortium of factors leading to obesity. According to the WHO, a healthy diet means at least 400g of fruits and vegetables a day, less than 10% of total energy intake from free sugars and less than 30% of total energy intake from fat (being unsaturated fat preferable over saturated and trans fat). Studies suggest that long-term weight management and other metabolic consequences of obesity that go beyond body size (eg, liver steatosis, low-grade chronic inflammation) are strongly influenced by diet quality (8, 9). Diet also strongly influences our "other genome" (*i.e.*, the gut microbiome) (10), modelling gut microbial community structure (11) and impacting host metabolism and energy partitioning (12, 13). Research conducted throughout the last decade has revealed a clear link between obesity and gut microbial dysbiosis, which is generally characterized by a reduction in bacterial richness and by major taxonomic and functional changes (14). (*This topic is better discussed below*). Interestingly, recent evidence also starts to shed light on transgenerational consequences of obesity and overweight. Parental obesity (15, 16) weight gain during gestation and gestational diabetes (17, 18) have been linked to increased obesity risk in the offspring. These studies suggest lasting effects of fetal programming that, possibly by means of epigenetic alterations, substantially impacts on life course health. These studies underscore the potential relevance of pre- and perinatal dietary/lifestyle habits on the obesity epidemic for generations to come.

2.1 BAT activity and WAT browning

Seminal studies with monozygotic twins (19) and with a particularly obese population of Native Americans (20) have underscored genetic-based differences in the metabolic rate and in the adaptive thermogenesis as contributors to human obesity. This was further supported by the demonstration that BAT depots are significantly present in adult humans and inversely correlated with BMI, adiposity and age (21-24). The BAT is specialized in producing heat in order to protect mammals from hypothermia by means of non-shivering thermogenesis. Its thermogenic capacity is conferred by the abundant presence of uncoupling protein-1 (UCP1) in brown adipocytes (25). In the mitochondria, the energy derived from the oxidation of fatty acid- or glucose-related molecules is either stored in the high-energy phosphate bonds of ATP or released as heat. ATP is synthesized when protons accumulated outside the inner matrix re-enter the mitochondrial matrix across ATP synthase (*i.e.*, coupled respiration). However, protons can leak back across the inner mitochondrial membrane and energy is therefore dissipated as heat (*i.e.,* uncoupled respiration). Although this latter process is inherent to the biology of several membranes, it is intensified by the action of uncoupling proteins (UCP), which are proton channels not linked to ATP synthesis (26). Indeed, when mice were bred in thermoneutrality (*i.e.,* 28-30 °C), UCP1 ablation induced obesity and abolished diet-induced thermogenesis (27).

BAT thermogenic activity is under control of the sympathetic nervous system (SNS). Postganglionic neurons of the efferent branches of the SNS release noradrenaline, which activates β-adrenergic receptors and triggers the breakdown of triglycerides into fatty acids. This process not only fuels thermogenesis as it stimulates BAT thermogenic activity (25, 28). Importantly, several endogenous signals coming from hormonal modulation or the action of dietary metabolites can alter BAT biology. Thyroid hormone (29), fibroblast growth factor-19 (FGF19, 15 in mice) (30), FGF21 (31), bone morphogenetic protein 8b (BMP8b) (32), bile acids (33, 34), short chain fatty acids (SCFA) (35-37), long chain free fatty acids (FFA)

(38), caffeine (39), green tea (40), apigenin (41) and naringenin (41) can all enhance BAT thermogenesis. In addition, another contribution to adaptive thermogenesis stems from white adipocytes that acquire a brown adipocyte-like phenotype (referred to as beige or brite adipocytes) (42). WAT browning is also under control of peptide/protein hormones and dietary metabolites, thereby responding to signals arising from catecholamines (secreted either from sympathetic terminals (43) or M2 macrophages (44)), prostaglandins (45), thyroid hormone (46), FGF21 (47), BMP4 (48), SCFA (49, 50) and from a wide range of polyphenolic phytochemicals (51-53). Interestingly, chronic hyperinsulinemia, which is as an early event of diet-induced obesity, was shown to hamper both BAT activity and WAT browning in mice, constituting another contributing factor to adaptive thermogenesis (54). Altogether, these findings stress the key role of UCP1 in controlling adaptive thermogenesis and justify a regain of interest in brown and beige adipocyte biology as a strategy to treat and prevent obesity and its related comorbidities. These studies also point out the myriad of molecules (several of which are gut microbial metabolites and phenolic phytochemicals) that potentially modulates adaptive thermogenesis by means of enhanced BAT activity and increased WAT browning.

3 Obesity-linked diseases

Obesity is associated with the onset and progression of a broad spectrum of diseases. Visceral obesity (also referred to as central obesity) is considered a hallmark of the metabolic syndrome, which consists of a cluster of key risk factors that increases the odds of developing metabolic maladies such as type 2 diabetes (T2D), cardiovascular disease (CVD), stroke and cancer (55). In addition to visceral obesity, hyperglycemia, hypertension and dyslipidemia are also major features of the metabolic syndrome (55). A deeper understanding of the physiological role of the hormone insulin, the pathophysiological bases of insulin resistance and the relationship between obesity, T2D and non-alcoholic fatty liver disease (NAFLD) are particularly relevant to the elaboration of this thesis and are better discussed below.

3.1 T2D

Diabetes mellitus is a chronic disease caused by inherited and/or acquired deficiency in the production of insulin by the pancreas, or by reduced responsiveness to insulin (56). While T1D is triggered by the autoimmune destruction of insulin-producing pancreatic β-cells, T2D initially results from the body's inability to respond properly to insulin (*i.e.*, insulin resistance), which ultimately evolves to β-cell failure and insufficient insulin secretion. T2D is more common than T1D and accounts for approximately 90% of all diabetes cases in the world (56). The prevalence of diabetes worldwide is worrisome: the number of people with diabetes has risen from 108 million in 1980 to 422 million in 2014, representing 8.5% of the global adult population (57). Diabetes is associated with several complications, being a major cause of blindness, kidney failure, CVD and lower limb amputation. The WHO projects that diabetes will be the 7th leading cause of death in 2030 (57), which emphasizes the need for more research on this field in order to fuel preventive policies, optimize existing curative approaches and to discover novel treatments.

Multiple risk factors contribute to the development of T2D, such as family history of T2D (58), glucose intolerance (59), sedentarism (60), poor dietary habits (61) and accumulation of visceral fat (62). In fact, the global rise in the prevalence and severity of obesity is the main underlying cause of the burden of T2D worldwide, which explains the fact that several risk factors for T2D overlap those associated with obesity.

3.2 NAFLD

Non-alcoholic fatty liver disease (NAFLD) is the hepatic manifestation of the metabolic syndrome and results from dysregulated lipid and glucose metabolism. NAFLD is the buildup of extra fat in the liver and comprises a group of common hepatic maladies whose severity progressively increases as hepatic fat accretion aggravates. NAFLD ranges from hepatic steatosis (HS) and non-alcoholic steatotic hepatitis (NASH) to hepatic fibrosis or cirrhosis and early stages of hepatocellular carcinoma (HCC). HS is characterized by an increase in triglyceride accumulation

that exceeds 55 mg/g of liver (63). HS may progress to NASH, where histological features such as hepatocyte ballooning, inflammation, cell death and fibrosis become apparent (64). Ten to 29% of the cases of NASH evolve to cirrhosis within 10 years (65). Cirrhosis may also progress to liver HCC with a rate of 4 to 27% (66). NAFLD and its subtype NASH are becoming the principal causes of chronic liver disease in the world, and this is driven by the global burden of obesity and diabetes (67).

3.3 The pathophysiology of insulin resistance

3.3.1 Insulin action and clearance

Insulin is a protein hormone synthesized and secreted by pancreatic β-cells in response to nutrients and, while glucose-stimulated insulin secretion is a key event, amino acids and FFA also act as insulin secretagogues (68). Insulin contributes to control lipid and glucose homeostasis by diverting energy substrates towards anabolism and maintaining normoglycemia (Figure 1). These effects are a product of a pleiotropic action of this hormone on multiple target tissues. The skeletal musculature is the main site of insulin-stimulated glucose clearance in the body. After binding to the insulin receptor (IR), insulin triggers a cascade of signaling events within the IRS/PI3K/AKT pathway that culminates in the translocation of GLUT4 to the sarcolemma and glucose entry into the cell (69). Insulin also stimulates glycogenesis and protein synthesis in the muscle, processes downstream AKT activation and linked to the inhibition of GSK3 (70) and FOXO1 respectively (71). In the adipose tissue, insulin stimulates glucose uptake through a PI3K/AKT/GLUT4-dependent process, favours lipid storage by activating lipoprotein lipase (72) (73) and decreases FFA release by inhibiting hormone-sensitive lipase (74) (75). This results in enhanced lipid storage and increased uptake of FFA from circulation.

The liver is functionally connected to the intestine through the enterohepatic circulation, being the first organ of passage of amino acids and sugars post absorption and therefore acting as a major orchestrator of energy homeostasis and nutrient metabolism. Insulin shuts down hepatic glucose output by downregulating

gluconeogenesis and glycogenolysis while stimulating glycogen storage. In sum, these anabolic outcomes are mediated by IRS/PI3K/AKT pathway-related inhibitory effects on FOXO1 (76), PGC1 (77) and activation of SREBP (78), being this latter factor also important in the regulation of hepatic lipogenesis (79). A brief summary of important insulin signalling events are illustrated in figure 2.
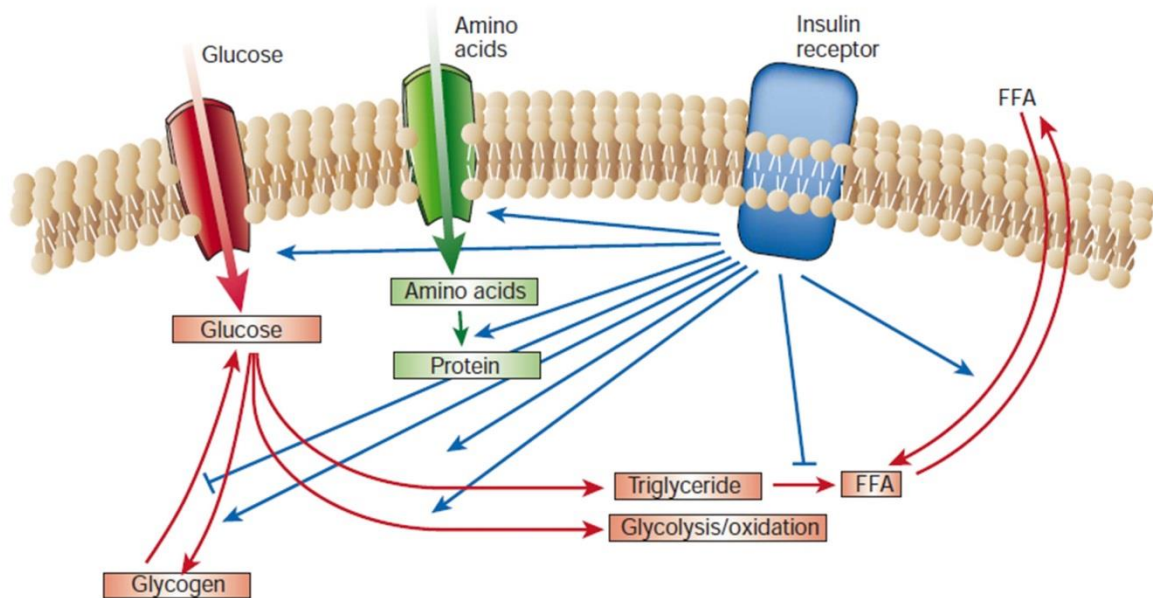
Figure 1: The anabolic effects of insulin.

Insulin promotes synthesis and storage of carbohydrates, lipids and protein while stimulating their storage and inhibiting their release into the bloodstream.

Adapted from Saltiel & Kahn (80). Insulin signalling and the regulation of glucose and lipid metabolism. Nature 2001;**414**:799-806.
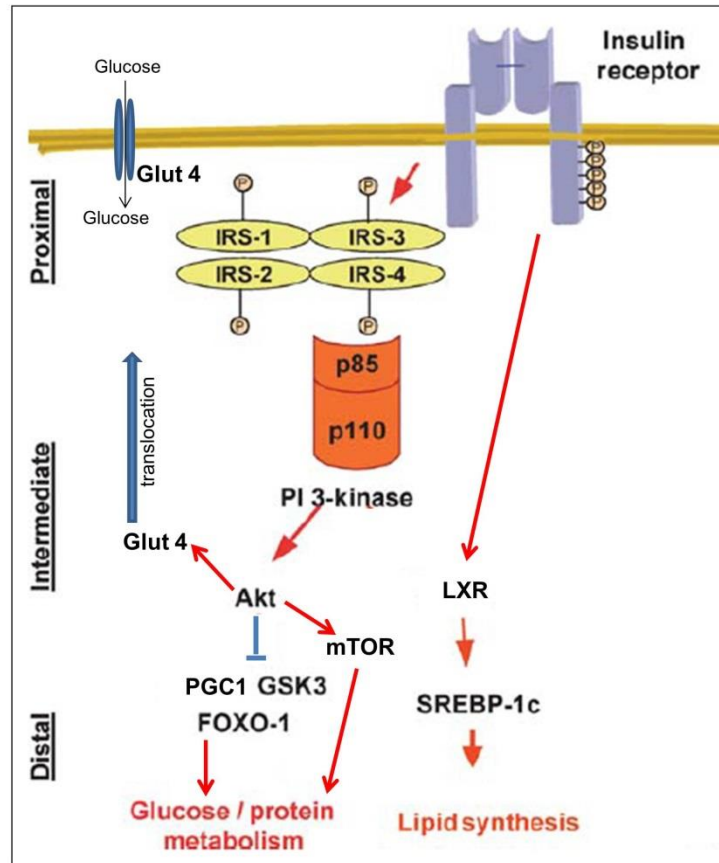
Figure 2: Schematic of key insulin signalling events.

Insulin action is mediated by its binding to the heterotetrameric transmembrane insulin receptor (IR). Activated IR elicits downstream phosphorylation of other substrates, including members of insulin receptor substrate (IRS) family, which in turn activate downstream signaling events via phosphatidylinositide 3-kinase (PI3K) and murine thymoma viral oncogene/protein kinase B (Akt/PKB). These signaling events lead to glucose uptake, glycogenesis and protein synthesis in the muscle; in the adipose tissue, insulin is a key driver of glucose uptake and lipid synthesis. Insulin-induced glucose uptake is dependent upon GLUT4 translocation to the cell membrane in muscle cells and adipocytes. In the liver, insulin leads to inhibition of gluconeogenesis and synthesis of glycogen and protein through PI3K/AKT-related inhibition of PGC1, FOXO1 and GSK3 and activation of mTOR. LXR and SREBP play a major role in the insulin-stimulated lipogenic program in the liver.

Adapted from Beddinger & Kahn (81). From mice to men: insights into the insulin resistance syndromes. Annu Rev Physiol 2006;**68**:123-58.

The efficient withdrawal of insulin from circulation is a key process to regulate the cellular response to this hormone by decreasing insulin availability (82). In fact, impaired insulin clearance is importantly related to insulin resistance

(83, 84) and it is a common trait associated with glucose intolerance (85), visceral obesity (86, 87), high circulating FFA (87) and NAFLD (88, 89). The latter is not surprising, since the liver is the primary site of insulin depuration, being 80% of endogenous insulin rapidly removed by this organ whereas the remainder is cleared out by the kidneys and muscle (90). Interestingly, impaired insulin clearance increases the risk of T2D in humans even when adjusting for lifestyle, obesity and insulin secretion, which underscores the major relevance of this process to glucose homeostasis (87).

Upon release of insulin in the portal circulation, insulin binds to the IR in the hepatocyte and stimulates its intracellular tyrosine activity, which in turn phosphorylates substrates such as the protein Carcinoembryonic Antigen Related Cell Adhesion Molecule-1 (Ceacam1). Once tyrosine phosphorylated, Ceacam1 has been shown to promote receptor-mediated insulin uptake into clathrin-coated vesicles, which then leads to insulin degradation (91-93). Ceacam1 also governs lipid metabolism in the liver by downregulating fatty acid synthase (FASN) enzymatic activity and therefore restricting hepatic *de novo* lipogenesis (94). Indeed, studies conducted in our laboratory by Dr Elaine Xu *et al.* demonstrated that Ceacam1 whole-body knockout mice are prone to hepatic steatosis in addition to impaired insulin clearance and hyperinsulinemia (95). Similar findings were reported by others in a context of liver-specific ablation of Ceacam1 (91, 96, 97). Taken together, these findings point to Ceacam1 as a major regulator of both insulin and lipid metabolism in the hepatocyte providing a potential mechanistic link between NAFLD, obesity and insulin resistance.

Another aspect of insulin clearance involves the insulin degrading enzyme (IDE). This enzyme is crucial to hepatic insulin clearance and, similarly to Ceacam-1, genetic deletion of IDE in mice causes hyperinsulinemia and insulin resistance (98). However, little is known about the interplay between these two major regulators of hepatic insulin clearance. While *in vitro* studies suggest that inflammatory cytokines may directly downregulate IDE, pointing to a link between metabolic inflammation and impaired insulin clearance (99), more studies are

warranted to determine the modifiers of IDE and Ceacam-1 and to clarify the role of insulin clearance in the metabolic syndrome.

3.3.2 The concept of insulin resistance

The pathological process whereby cells fail to respond properly to insulin is named insulin resistance. Insulin resistance is the cornerstone in the pathogenesis of obesity-linked metabolic diseases and, in T2D, it precedes β-cell dysfunction and the progression towards impaired glucose tolerance. Initially, pancreatic β-cells compensate for peripheral insulin resistance and prevent hyperglycemia at the expense of incremental insulin secretion. While hyperinsulinemia from the compensating β-cells ensures normal glucose tolerance for some time, chronic hyperinsulinemia is a deteriorating condition *per se* (100). Due to the adaptive nature of pancreatic β-cells, euglycemia coupled with chronic hyperinsulinemia can be sustained for years (101). As the metabolic injury persists, the pancreas finally fails to compensate for the waning metabolic response to insulin leading to overt T2D. Insulin resistance is therefore classically considered as a primary defect in the sequence of events associated with the development of T2D. However, this notion was challenged in an elegant study by Mehran *et al.* The authors genetically prevented diet-induced hyperinsulinemia in mice by partially deleting the pancreas-specific *Ins1* gene and knocking out the *Ins2* gene (*i.e.*, *Ins1*$^{-/+}$/*Ins2*$^{-/-}$). These animals were protected from diet-induced insulin resistance, which led the authors to the conclusion that the advent of chronic hyperinsulinemia precedes obesity and insulin resistance (54). In agreement with these findings, Templeman *et al* showed that suppression of hyperinsulinemia in growing female mice protects against obesity (102). While more studies are warranted to clarify the early events leading to diet-induced metabolic derangements, the role of the intestine and its colonizing bacteria in such events must be object of thorough analysis given the primordial relationship between diet, intestinal mucosa and gut microbiota. (*This topic is object of further discussion below)*

3.4 Insulin resistance and low-grade metabolic inflammation

In the early 1990's, Hotamisligil *et al.* reported increased mRNA expression of the pro-inflammatory cytokine tumor necrosis factor α (TNFα) in the adipose tissue of obese rats (103) and humans (104), unveiling a connection between inflamed adipose tissue and insulin resistance. These findings were the seeds of a whole new field, named immunometabolism, linking the recruitment of immune cells along with the secretion of cytokines and chemokines to the pathogenesis of obesity-linked diseases. Nowadays, the role of a chronic low-grade inflammatory state in the pathophysiology of obesity-linked insulin resistance is well demonstrated (105). For instance, genetic deletion of important inflammatory mediators, such as inducible nitric oxide synthase (106) (107) and c-Jun N-terminal kinase (JNK) (108), has been shown to prevent the development of insulin resistance in obese mice. Moreover, in addition to TNFα (103, 104), the presence of other cytokines and chemokines such as interleukin-6 (IL6) (109), IL1β (110), regulated upon activation normal T-cell expressed and secreted (RANTES) (111), monocyte chemoattractant protein-1 (MCP1) (112) and interferon γ (INFγ) (107) is also raised in the adipose tissue and in circulation during obesity, highlighting not only the complex mechanisms underlying immune cell aggregation within the inflamed adipose tissue but also the potential spillover of proinflammatory molecules and cells towards other metabolic organs. Indeed, immune cell infiltrates are also found in the muscle (113), particularly associated with ectopic fat depots (114), and in fatty liver (115, 116), where macrophages have been shown to encapsulate steatotic hepatocytes (117).

The infiltration of macrophages is a key event in adipose tissue inflammation, strongly correlating with BMI and being an important source of TNFα, IL6, NO and oxidative stress in the hypertrophic adipose tissue (114, 118). Bone marrow-derived macrophages are attracted to the visceral adipose tissue in response to adipocyte remodeling and death (119), and the chemokine MCP1 is critical to this process (120). These immune cells then form aggregates surrounding dying adipocytes histologically termed crown-like structures (121). Interestingly, obesity is associated with the recruitment of a particular subset of

F4/80^{+} CD11c^{+} proinflammatory M1 macrophages, as opposed to a polarization towards the anti-inflammatory IL10 producer M2 population found in the adipose tissue of lean mice (122). Apart from macrophages, proinflammatory subsets of T cells, such as CD8^{+} (123), NK (124) and Th1 (125) were found to be increased in the adipose tissue of obese mice, whereas T regs (125) and Th2 (125) populations are either reduced or unchanged. Such a T cell profile in the adipose tissue is thought to precede and to be necessary for macrophage recruitment. Moreover, expansion of neutrophil (126), eosinophil (127), mast cell (128) and B-cell (129) populations has been reported and also contributes to adipose tissue inflammation and insulin resistance.

Immune cell aggregation into the adipose tissue takes place in parallel to an expanding adipose tissue. While the subcutaneous adipose tissue is a more plastic depot, which copes with anabolic demands by means of hyperplasia, visceral adipocytes predominantly resort to hypertrophy in situations of excess energy intake (130), more promptly leading to cell death. Although the underlying mechanism of cell death is not yet determined, tissue hypoxia (131) and ER stress (132) are plausible and not mutually exclusive theories. Hypoxia would be a natural consequence of insufficient vascular supply due to cell overexpansion, whereas ER stress is thought to be linked to an exaggerated protein and lipid synthesis demand to comply with changes in tissue morphology and function.

Inflammation triggers the activation of protein kinases (*e.g.*, MAP kinases, mTOR/S6K1), lipid species (*e.g.*, ceramides, gangliosides) and transcriptional mediators (*e.g.*, NFκB) that altogether contribute to disrupt the insulin signaling pathway (133). The phosphorylation of IRS at serine 307 (312 in humans), which prevents its activation by the IR, as well as the blockage of Akt recruitment are points of convergence in the action of inflammatory mediators to impair insulin sensitivity (133). Moreover, NO generated by the activation of inducible NOS (106) can cause S-nitrosylation of IR, IRS1 and Akt (134, 135), whereas the product of the reaction between NO and O_2^- (*i.e.,* ONOO$^-$, peroxynitrite) is associated with the nitration of several tyrosine residues (136), also contributing to weaken the cellular

response to insulin. Important intracellular pathways leading to low-grade inflammation-induced insulin resistance are summarized in figure 3.

Obesity is also a state of mounting oxidative stress, characterized by an imbalance between tissue free radicals, reactive oxygen species (ROS) and antioxidants (137). Oxidized lipids and proteins may exert cytotoxic effects and damage cell membrane and membrane-bound receptors in addition to disrupting enzymatic function and signalling cascades (138, 139). Enhanced oxidative stress may also further inflammatory responses in the cell, damage nucleic acids and leads to cell death (138, 139).
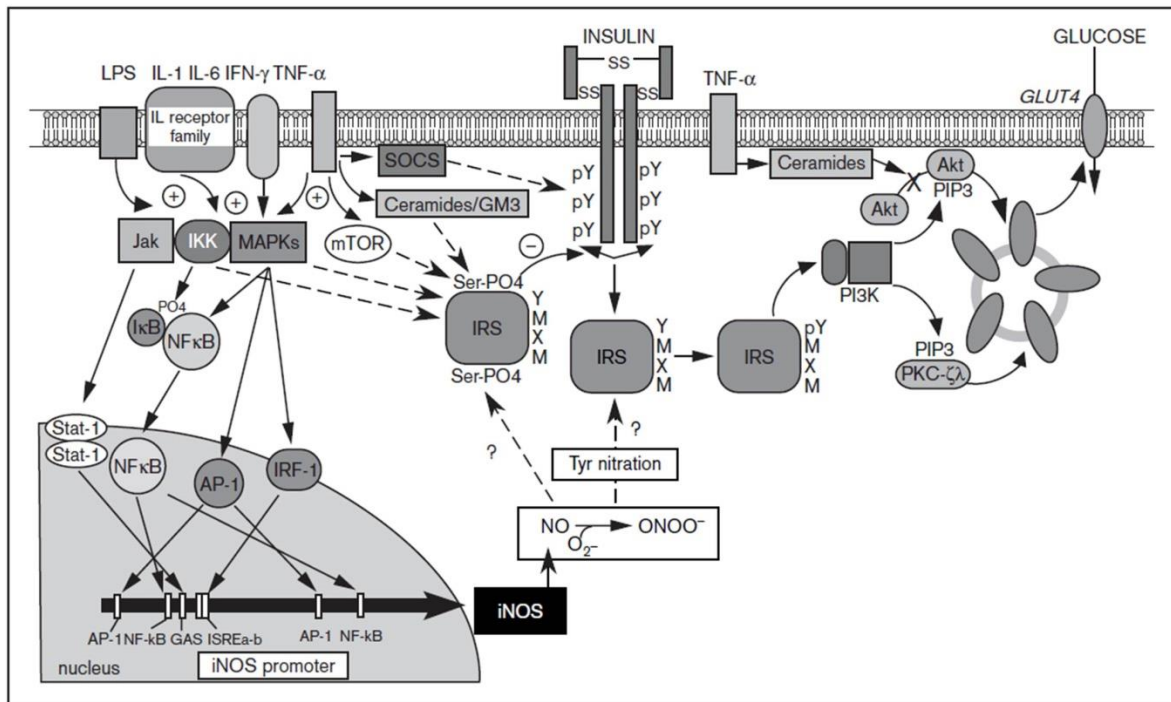
Figure 3: Low-grade inflammation-related intracellular pathways leading to insulin resistance.

Proinflammatory cytokines (*eg*, TNFα, IL1β, IFNγ) and bacterial lipopolysaccharide (LPS) activate multiple pathways in fat, muscle and liver cells. Activation of IκB kinase (IKK), mitogen-activated protein kinase (MAPK), and mammalian target of rapamycin (mTOR) pathways, as well as the generation of lipid species (*ie*, ceramides and the ganglioside GM3) increases insulin receptor substrate (IRS1) serine phosphorylation, leading to inhibition of downstream insulin signalling to phosphatidylinositol-3 (PI3)-kinase and glucose transport. Activation of Jak, IKK and MAPK

13

pathways by cytokines also triggers inducible nitric oxide synthase (106) expression and nitric oxide production. iNOS activation possibly impairs insulin signalling either by promoting IRS1 serine phosphorylation or by nitration of IRS1 tyrosine residues through formation of potent reactive nitrogen species such as peroxynitrite ($ONOO^-$). PIP3, phosphatidylinositol-3,4,5,-trisphosphate; PKC, protein kinase C; NFkB, nuclear factor-kB; Stat-1, signal transducer and activator of transcription-1; AP-1, activating protein-1; IRF-1, interferon regulatory factor-1; GAS, gamma-activated sequence; ISREa-b, interteronstimulated response element-a and -b.

From Marette A (133). Mediators of cytokine-induced insulin resistance in obesity and other inflammatory settings. Current opinion in clinical nutrition and metabolic care 2002;**5**:377-83.

4 Intestinal homeostasis and obesity-linked diseases

The role of the intestine in metabolic control was object of research in the past (140, 141). In the last decade, however, our notion on the relevance of this complex organ to obesity-linked diseases has grown exponentially, fueling a paradigm shift from an "adipocentric" to an "enterocentric" view point. The intestine harbors an extensive immune system due to the exposure to microbial and ingested antigens from the diet, and now inflammatory and immune cell changes in the bowel are being investigated in depth as a link to obesity and insulin resistance. But the intestine definitely received its patent of nobility as researchers started to unveil the influence exerted by gut microbes on host metabolism. In this section, important aspects related to diet-induced and obesity-related intestinal inflammation and its relationship with insulin resistance are discussed. The role of the gut microbiota in this process will be discussed in section 5.

4.1 Obesity-related intestinal inflammation

The intestinal innate immune system is the first line of defense against infection while also ensuring tolerance to the normal gut microbiota. This system encompasses the mucus layer (secreted by goblet cells), intestinal epithelial cells (IEC), Paneth cells (secrete antimicrobial peptides), innate lymphoid cells (ILC) and other fast responding immune cells, such as macrophages and neutrophils. The enteric innate immune system is governed by pattern recognition receptors (PRR), such as toll-like receptors (TLR) and NOD-like receptors (NLR), that bind to microbial-associated molecular patterns (MAMPs) from luminal microorganisms to regulate gut immune response. Under eubiosis (*i.e.,* a healthy equilibrium between

14

gut microbiota and host), MAMPs trigger the secretion of anti-inflammatory mediators such as IL-25, IL-33, transforming growth factor β (TGFβ) and thymic stromal lymphoprotein (TSLP) (142). However, upon an imbalance between gut microbiota and host defenses (termed dysbiosis), the typical enteric immune response is marked by the secretion of pro-inflammatory cytokines, such as INFγ, IL-1β, IL-6, IL-12, IL-18 and IL-23 (142). Some key elements involved in obesity-linked intestinal inflammation and its consequences to gut homeostasis are illustrated in figure 4.
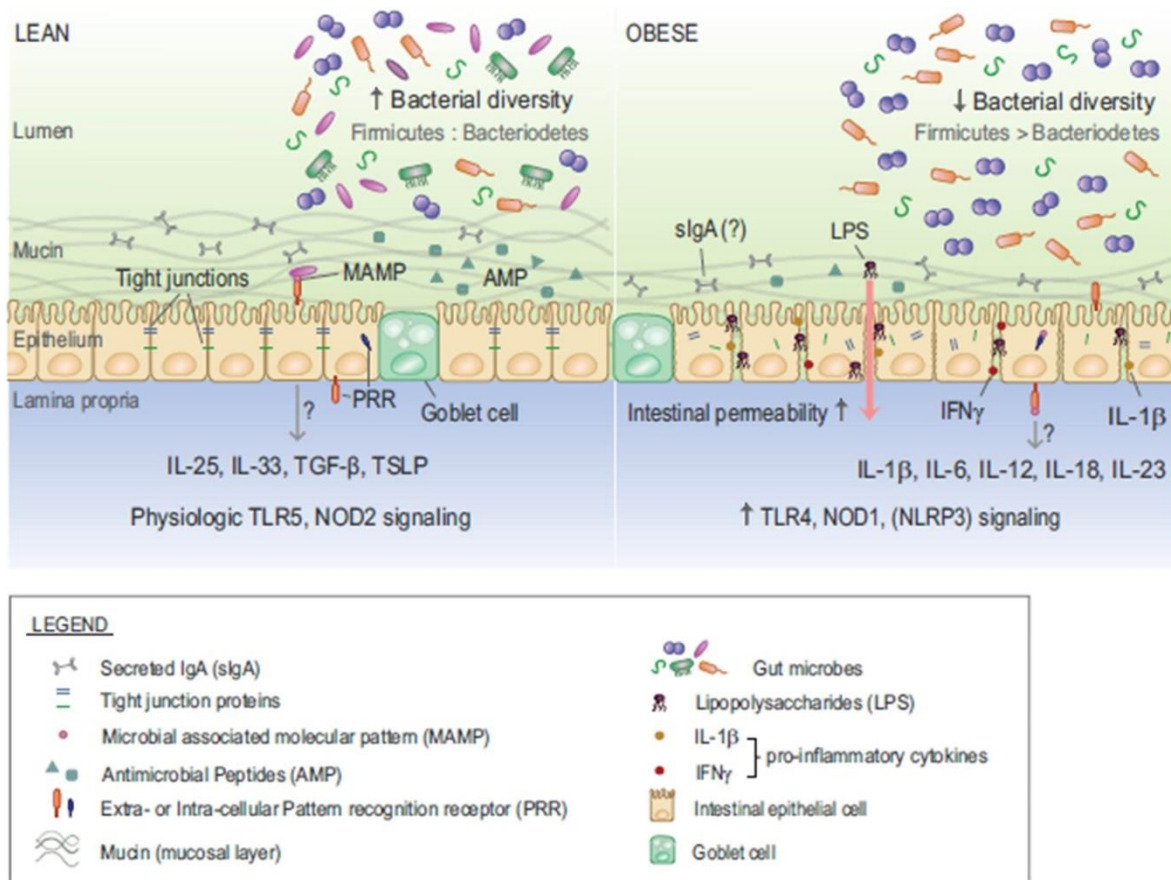
Figure 4: Changes to intestinal physiology during obesity.

During eubiosis, the intestinal barrier (mucus layer, antimicrobial peptides - AMPs, IgA, intestinal epithelial cells - IECs) efficiently protects the host from bacterial encroachment and excessive leakage of microbial-related molecules to circulation. Tolerogenic response is elicited upon activation of pattern recognition receptors (PRRs) by microbial-associated molecular patterns (MAMPs) from comensal bacteria. This includes IL-25, IL-33, transforming growth factor β (TGFβ) and thymic stromal lymphopoietin (TSLP). Activation of NOD2 and TLR5 are important during eubiosis. Obesity-linked gut microbial dysbiosis is marked by lower bacterial richness and higher

Firmicutes to Bacteroidetes ratio. Mucin and AMP production is reduced during obesity-induced dysbiosis, facilitating bacterial invasion. Invasive bacteria and bacterial products trigger immune responses essentially through TLR4, NOD1 and NLRP3 activation. In turn, several pro-inflammatory cytokines and chemokines are produced and released by IEC and surrounding immune cells (not represented in this figure). This includes IL1β, IL6, IL12, IL18 and INFγ. Such a pro-inflammatory milieu contributes to weaken intercellular adhesion structures within IECs by decreasing or misplacement of tight juction proteins (ZO1 and Occludin). Bacterial LPS and microbial products can leak accross the damaged gut barrier and reach circulation, causing low-grade endotoxemia and worsening metabolic diseases.

From Winer *et al.* (143) The Intestinal Immune System in Obesity and Insulin Resistance. Cell metabolism 2016;**23**:413-26.

Several studies have shown diet-induced obesity as a major driver of enhanced small bowel (144-150) and colonic (151-154) inflammation both in humans and in animal models. The tight connection between obesity and gut inflammation is also evident in the observed reduction of colonic pro-inflammatory cytokines and immune cell infiltration as obese adults lose weight and display improved glycemic control (155). Ding *et al.* demonstrated that increased mRNA expression of TNFα and activation of NFκB were both increased in HFD-fed mice, preceding and predisposing to obesity (146). Moreover, de La Serre *et al.* showed that, upon HFD feeding, only obesity prone, but not obesity-resistant, Sprague Dawley rats developed intestinal inflammation (147). Since all rats were fed a HFD, this study is particularly interesting as it provided a specific link between intestinal inflammation and obesity, but not between gut inflammation and HFD feeding alone. The contribution of intestinal inflammation to metabolic diseases is further demonstrated using KO models. Luck *et al.* fed β7 integrin KO mice a HFD. These mice display hypoplasia of gut lymphoid tissue and a drastic reduction of intestinal leukocytes. The authors showed that, besides becoming obese, HFD-fed β7 integrin KO mice were protected against metabolic diseases with alleviated adipose tissue inflammation and improved NASH (156). Similarly, the specific deletion of IEC MyD88 (a common downstream target of TLR) was enough to improve diet-induced insulin resistance (157).

Given the clear inflammatory reaction associated with obesity, several research groups started to shed light on changes in enteric immune populations in a context of diet-induced obesity. Three weeks of HFD-feeding was enough to

reduce the population of Tregs in the colon and increase the INFγ-producing Th1 and the pro-inflammatory CD8$^+$ T cells in the colon and in the small intestine of both mice (156) and humans (144, 156). Increased Th1 population was also seen after 4 weeks of HFD, which was accompanied by reduced IL17-producing Th17 populations (150, 158).

The aforementioned data position the gut as a promising target for pharmaceutical or dietary strategies aiming to alleviate obesity and insulin resistance. For instance, administration of the gut anti-inflammatory drug 5-aminosalicylic acid (mesalamine) resolved HFD-induced gut inflammation and was enough to ameliorate adipose tissue inflammation and insulin resistance in mice (156). Taken together, the current state-of-knowledge shows that diet-induced obesity alters the intestinal profile of cytokine expression and immune populations and those low-grade bowel inflammatory changes are an early manifestation of HFD feeding that precedes metabolic diseases.

4.1.1 How intestinal inflammation evolves to systemic insulin resistance?

The inflamed bowel displays a disrupted gut barrier, which facilitates the leakage of bacteria and microbial-related molecules to circulation and therefore contributes to trigger and sustain low-grade inflammation and insulin resistance in peripheral organs, such as the liver and the adipose tissue (Figure 4) (159-161). The gut barrier is formed by components of the innate immune system: mucus layer, secretory IgA, antimicrobial peptides from Paneth cells and the IEC line altogether contribute to keep luminal microorganisms at a safe distance from the host. The cohesion of the IEC line depends on tight junctions, which are formed by a network of proteins (*e.g.*, Ocln, ZO1, Claudin) that seals adjacent epithelial cells in a narrow band and limits the passage of molecules through the intercellular space (162).

As previously mentioned, IECs elicit tolerogenic responses to MAMPs via PRRs, which stimulates the secretion of anti-inflammatory mediators. Some PRR signaling pathways important to eubiotic homeostasis include TLR5 (163), NOD2

(161), TLR2 (164) and NLRP6 (165, 166), the latter being crucial to mucus secretion. HFD feeding provokes gut microbial dysbiosis, a trait linked to diminished diversity of the gut microbiota and imbalanced ratio of bacterial species (*This topic is further discussed in section 5*). HFD feeding also reduces the mucus layer thickness (167, 168), impair the secretion of anti-microbial peptides (*i.e.*, Reg3β, Reg3γ) (167) and downregulates the expression and/or misplaces tight junction proteins (*e.g.*, ZO1, Ocld) (147, 169, 170), which in turn facilitates the encroachment of bacteria closer to host cells and the penetration of bacteria and microbial-derived molecules into the circulation (159, 160, 168). Invasive bacteria and bacterial-derived molecules then activates NLR and TLR signaling via TLR4 (168, 171), NOD1 (172) and NLRP3 (173, 174), therefore stimulating a more pro-inflammatory response and promoting the release of cytokines such as IL-1β, IL-6, IL-12, IL-18 and INFγ (Figure 4). Interestingly, in a recent report to *Cell*, Wolf *et al.* demonstrated that the glycolytic enzyme hexokinase can also work as a PRR to activate a NLRP3-related pro-inflammatory response (175).

The exact mechanism by which inflammation mediates gut barrier disruption is far from being completely understood. It is known that INFγ (156) and IL-1β (176), both weaken the epithelial barrier by downregulating the expression and/or misplacing ZO1 and Ocld. Moreover, IL-22, from T regs, dampens INFγ-mediated immunity and stimulates mucin production and antimicrobial IgA (177, 178). In addition to these cytokines, there is significant evidence supporting a role for GLP2, produced by enteroendocrine L-cells, as a link between a healthy gut and a functional intestinal barrier (167, 179-181); however, how inflammation affects GLP2 secretion and how GLP2 enhances gut permeability is currently unknown. It is interesting to note that activation of the receptor GPR119 (which is particularly expressed in intestinal L-cells (182)) by the endocannabinoid analogue 2-oleoylglycerol (2-OG) has been proposed as an underlying mechanism triggering GLP2 secretion (183). The endocannabinoid system comprises several bioactive lipids, enzymes involved in the synthesis and degradation of these lipids and two main receptors, CB1 and CB2. This system has been object of intense research given the wide range of physiological processes under its regulation, such as

energy metabolism and satiety (184, 185). Moreover, alterations in the endocannabinoid system tone have been related to pain, neurological disorders, inflammation (186) and gut barrier homeostasis (187). While agonism of CB1 was associated with disruption of gut barrier and a leaky gut through disarranging the distribution of ZO1 and Ocld (187, 188), lower levels of anandamide (AEA) (157) and increased 2-arachidonoylglycerol (2-AG) (167, 189) were both associated with improved gut barrier, although the latter is controversial (190, 191). Other endocannabinoid analogues, such as 2-palmitoylglycerol (2-PG) and 2-OG, have been associated with protective effects on the gut barrier (157, 167). While further investigation is needed to clarify the role of the endocannabinoid system in the gut barrier homeostasis, this system apparently works as important crosstalk mediators between host and gut microbiota (183) and as major modulators of metabolic and immune functions (184, 185), undoubtedly constituting a fertile field of research in the near future.

Translocation of bacterial lipopolysaccharides LPS, a component of the outer membrane of Gram-negative bacteria, across the damaged gut barrier is one of the most studied links between intestinal inflammation and systemic insulin resistance. Dr Patrice Cani *et al.* were the first to demonstrate that, upon HFD feeding, the concentration of LPS in circulation increases as a consequence of disrupted intestinal permeability in mice (159). This process was termed metabolic endotoxemia (159), and his findings were later confirmed by others both in humans (192, 193) and in animal models (168, 194). Alternatively, LPS can also enter the circulation associated to chylomicrons after a HFD (195). Metabolic endotoxemia thus impair insulin sensitivity via binding of LPS to TLR4 in the adipose tissue (196), liver (197) and pancreatic β-cells (198), stimulating the secretion of TNFα, IL-6, IL-β and MCP1 (199). Activation of the innate immune system in peripheral organs by means of TLR signaling has a major impact on diet-induced insulin resistance, as demonstrated by the genetic invalidation of either TLR2 or TLR4; indeed, these mice were fully protected from obesity-driven inflammation and insulin resistance (197, 200-202). On the contrary, abrogation of TLR5 caused spontaneous colitis (203) and metabolic syndrome (163) in mice, suggesting that

some TLR are important mediators of tolerogenic responses. The adipose tissue (204), liver (205) and muscle (206) express a complete and functional TLR system, which indicates that several MAMPs, other than LPS, may potentially modulate inflammation in major metabolic organs. Mounting evidence supports that translocation of live bacteria and bacterial DNA directly contributes to metabolic syndrome (160, 161) and NAFLD (207). PRRs other than TLR are also expressed in key-metabolic organs and participate to MAMP-related control of metabolic inflammation. For instance, NOD1 and NOD2 both recognize bacterial peptidoglycan (NOD1 binds to meso-diaminopimelic acid-containing muropeptides and NOD2 detects muramyl dipeptide-containing peptidoglycan). Both receptors are expressed in adipocytes and hepatocytes (161, 172, 208, 209) and, interestingly, while NOD1 activation is associated with worsening of the metabolic profile upon HFD feeding (172, 208, 209), NOD2 activation protects from the detrimental metabolic consequences of HFD (161, 210).

4.1.2 Does the gut become insulin resistant?

Several evidence suggest that the intestine is an insulin-responsive organ and that the gut mucosa becomes insulin resistant, impairing both lipid and glucose homeostasis (211-214). While increased hepatic VLDL production and decreased clearance of triglyceride-rich lipoproteins in the liver are typically associated with insulin resistance, the insulin resistant gut contributes to dyslipidemia by an exaggerated production of chylomicrons along with increased apolipoprotein B48 biogenesis and enhanced *de novo* lipogenesis rate (211, 213, 214).

It has been known for decades that the gut can participate to the regulation of glucose homeostasis (215). Indeed, increased glucose utilization by the gut is involved in the hypoglycemic action of metformin (140, 216), one of the most prescribed anti-diabetic drugs worldwide. In the 1980's, Barrett *et al.* reported increased enterocyte glucose uptake after combined infusion of glucose and insulin in dogs (141). More recently, Honka *et al.* used ^{18}F-FDG as a radiotracer in PET experiments to show that glucose uptake to enterocytes (mostly in the small intestine) is enhanced in response to insulin, and that this process is impaired in

non-diabetic obese subjects (212). GLUT2 rapidly translocates to the brush border membrane in response to dietary glucose, whereas GLUT2 internalization is stimulated by insulin and constitutes a limiting step for glucose uptake from the lumen to circulation (217). In insulin-resistant subjects, GLUT2 has been shown to permanently locate at the apical membrane of enterocytes (217, 218). Overall these data suggest that insulin resistance impair glucose depuration from the blood to the intestine while facilitating glucose uptake from the lumen to circulation. As these observations were made in non-diabetic subjects (212), it indicates that intestinal insulin resistance is an early alteration in T2D.

Gluconeogenesis also occur in the intestine and it contributes to about 20-25% of endogenous glucose production (219). Intestinal gluconeogenesis is especially important during fasting and is rapidly abolished upon insulin stimulation (220). Interestingly, intestinal gluconeogenesis has been shown to regulate satiety through glucose-sensing by the periportal neural system (219). While protein-triggered satiety has been related to this mechanism (221), the effect of the microbial by-products of fiber fermentation butyrate and propionate on satiety and energy expenditure was also linked to intestinal gluconeogenesis-related activation of gut-brain circuitry after glucose sensing by periportal neurons (222). However, a question that persists is to what extent intestinal gluconeogenesis is beneficial in a scenario of impaired insulin-driven gluconeogenesis suppression typical of insulin resistance.

While little is known about the molecular determinants of insulin signaling in the enterocyte, this process is presumably strongly related to intestinal inflammation. In fact, a study showed that cytokines derived from activated intestinal T cells, such as IL-17A, IL-22, INFγ and TNFα modulate enterocyte insulin sensitivity *ex vivo* (144).

5. Gut microbiota

The concepts discussed in section 4 clearly points to the gut microbiota as a primary modulator of host metabolism and at the onset of the main

immunometabolic events leading to obesity-linked disease state, a conceptual model that was supported by two studies published in the late 2010s. In the first one, the authors fed germ-free mice (*i.e.*, mice devoid of any symbiotic microorganism, including gut bacteria) a HFD and showed that these animals were protected from diet-induced intestinal inflammation (146); in the other study, antibiotic treatment was used to minimize the presence of bacteria in the gut and, similarly to the previously mentioned work, the authors found that antibiotic-treated mice were protected from HFD-induced intestinal inflammation and disruption of the gut barrier (223). Although gut microbiota-related intestinal inflammation is strongly related to insulin resistance, and possibly obesity *per se* (147), the role of intestinal microbes in obesity-linked diseases goes beyond this concept, being also involved in the control of energy availability and partitioning (13, 224-226). Moreover, in addition to bacterial components such as LPS and peptidoglycan, a myriad of secreted factors and microbial metabolites can reach the circulation and exert biological effects (*e.g.*, SCFA, deconjugated and secondary bile acids).

The term "microbiota" describes all microorganisms living within or at the surface of an animal. In humans, the majority of the 100 trillion microbes inhabiting our body are part of the gut microbiota, with approximately 10^{11} of them living in the colon (227). These microorganisms are bacteria, archaea, viruses and fungi, albeit more than 99% of the microbial genes detected in the gut are bacterial genes (228). Variations in oxygen availability, pH, luminal flow and the presence of antimicrobial molecules are important drivers of quantitative and qualitative differences in gut microbial populations throughout the gastro-intestinal tract (229). The microbial density (cells/g) increases from the duodenum (10^3-10^4) to the colon (10^{11}), whereas the presence of aerobic and facultative anaerobic bacteria (*e.g.*, *Lactobacillaceae, Enterobacteriaceae*) in the small intestine is replaced by strict anaerobes in the colon (*e.g.*, *Bacteroidaceae, Prevotellaceae, Rikenellaceae, Lachnospiraceae, Ruminococcaceae*) (229). Although revised calculations showed that the ratio between bacterial cells and our own cells is around 1:1 (230), and not 10:1 as previously believed (231), the gut microbiome (*i.e.*, the genomes of all gut bacteria) still encodes 150 times more genes than our own genome,

therefore complementing host biology in a mutually beneficial fashion and providing us with major genetic and metabolic attributes (232). In fact, gut microbes are critical players in the development of the immune system, defense against pathogens and gut barrier homeostasis, being also relevant to nutrient and xenobiotic metabolism (228, 233).

The colonization of the gut occurs at the moment of birth and evolves from a poorly diverse to a richer and relatively stable adult microbiota by the age of 3–5 (234-236). Mode of delivery (C-section or vaginal delivery), nutrition and weaning have all been related to specific traits of the gut microbiota in early life and consequences to the mature gut microbiota (158, 237, 238). Importantly, while gender, age and genetics all influence gut microbial profiles (236, 239, 240), geographical location (236, 241) and other environmental features, especially dietary habits (11, 241, 242), are major determinants of community structure in the gut microbiota. Gut bacteria are distributed among a few phyla, being the most abundant ones, in descending order, Firmicutes, Bacteroidetes, Actinobacteria, Proteobacteria and Verrucomicrobia (243). The latter is represented by a single species, *Akkermansia muciniphila*, which can make up to 5% of the gut microbiota (244). Nonetheless, diversity at the species level is considerably higher: One individual harbours, at least, 160 different species out of a repertoire of approximately 1500 prevalent species identified in the human gut microbiota (228).

5.1 Diet-induced dysbiosis

As previously mentioned dysbiosis is characterized by the disruption in the equilibrium between gut microbiota and host and plays a role in diet-induced enteric inflammation, obesity and insulin resistance. Moreover, diet is the major driver of changes in the gut microbiota. But what characterizes the dysbiotic gut microbiota and how such an imbalance affects host metabolism?

5.1.1 Enterotypes

In an attempt to find microbial patterns associated with dysbiosis and eubiosis, researchers have described a "core gut microbiota", that is, the set of

species shared by the majority of the Western adult population (228, 245). From this observation, it was possible to categorize the human gut microbiota in three distinct clusters of taxa, also termed "enterotypes", claimed to be reproducible across Western adults: Enterotype 1 is dominated by *Bacteroides*, enterotype 2 by *Prevotella* and enterotype 3 by *Ruminococcus* (246). Enterotypes 1 and 3 were also proposed to be present in the mouse gut microbiota (247), however the value of this finding was questioned by the demonstration that enterotype 3, dominated by *Ruminococcus*, significantly merged with enterotype 1 (*Bacteroides*) and did not configure an individual cluster (242, 248). Some research teams have confirmed this distribution and associated enterotype 2 (*Prevotella*) with an agrarian and healthier lifestyle, which included a diet rich in complex carbohydrates, as opposed to enterotype 1 (*Bacteroides*), which was associated with typical Western habits considered triggers of dysbiosis (*i.e.*, low-fiber, animal fat/protein-rich diet) (236, 242, 249). The notion of enterotypes, however, is far from being consensual. While Huse *et al.* did not find such a categorization in a population of 200 individuals (250), recent re-analysis of the data sets of agrarian and more urbanized subjects mentioned above did not confirm the separation of these populations among enterotypes (248). Another study suggested that the categorization of the human gut microbiota in enterotypes is rather discrete (251).

The usefulness of clustering populations according to enterotypes 1 and 2 is also a matter of debate: While either short- (10 days) (242) or long-term (6 months) (252) dietary interventions failed to shift enterotypes, it is well demonstrated that changes in carbohydrate or animal fat/protein intake markedly affect gut microbial community structure and are enough to alter host metabolism (11, 253, 254). More recently, in a 26 week dietary intervention, it has been shown that obese and overweight humans with higher *Prevotella/Bacteroides* ratio are more susceptible to lose fat mass on diets high in fiber and whole grains than individuals with low *Prevotella/Bacteroides* ratio (255). While changing one person's enterotype seems an unrealistic goal, this latter study points to a role for enterotype-based population categorization in personalized nutrition.

Another issue related to the notion of enterotypes is the false idea that *Prevotella spp* are necessarily beneficial whereas *Bacteroides spp* are always detrimental. If on one hand *B. tethaiotaomicron* (256) and *B. vulgatus* (257) were both linked to obesity and insulin resistance, on the other hand *B. fragilis* is a well-recognized trigger of enteric tolerogenic responses (258). Importantly, Pedersen *et al.* showed that *Prevotella copri* was an important driver of insulin resistance in a Danish population of 277 individuals; furthermore, the authors associated this expansion of *P. copri* with increased bacterial synthesis of branched-chain amino acids (BCAA) (257), an early trait of insulin resistance (259). In addition, previous reports have associated the family *Prevotellaceae* with gut inflammation (260). In sum, while the trade-off between *Prevotella* and *Bacteroides* possibly exists (257), the use of *Prevotella-* or *Bacteroides*-dominant enterotypes as biomarkers of health and disease may lead to the overlook of important gut microbial features. Rather than arranged in clusters, the gut microbiota is more likely a continuous gradient of communities that can change within an individual over time (261-263).

5.1.2 Microbial gene richness

Gut microbiota dysbiosis is often characterized by reduced bacterial richness, and this is a common feature observed in obesity (14, 264, 265), IBD (228, 266) an aging (267). A robust demonstration of the link between gut bacterial richness and obesity-related metabolic disorders came from two studies concomitantly published in *Nature*. In the first study, Le Chatelier *et al.* showed that obese/insulin resistant patients displayed lower gut bacterial richness than lean subjects, as suggested by lower gene count (LGC) (14). The authors also showed the main taxonomic features of the gut microbiota of LGC and high gene count (HGC) patients: There was a predominance of Gram-negative Proteobacteria and Bacteroidetes in the gut microbiota of LGC, whereas HGC showed high levels of Verrucomicrobia, Actinobacteria and Euryarcheota (14). Moreover, while *Bacteroides*, *Parabacteroides*, *Ruminococcus torques*, *Ruminococcus gnavus*, *Campylobacter*, *Dialister*, *Porphyromonas*, *Staphylococcus* and *Anaerostipes* were all highly represented in the gut microbiota of LGC, *Fæcalibacterium*, *Bifidobacterium*, *Lactobacillus*, *Butyrivibrio,* *Alistipes*, *Coprococcus*,

Methanobrevibacter and *Akkermansia muciniphila* were all strongly present in HGC subjects (14). At the functional level, the gut microbiome of LGC subjects showed an enhanced capacity to handle exposure to oxygen and oxidative stress, increased mucus degradation, overexpression of bacterial genes associated with the production of deleterious metabolites (*e.g.*, β-glucuronide and aromatic compound degradation, dissimilatory nitrate reduction) and a predominance of sulfate-reduction pathways (14). In contrast, microbial pathways assigned to the production of organic acids (*i.e.,* lactate, propionate and butyrate) and hydrogen were increased in HGC subjects together with a more acetogenic/methanogenic environment (14). In the second study, Cotillard *et al.* showed that an energy restriction-based dietary intervention alleviated several features of the metabolic syndrome in obese subjects while significantly increasing bacterial richness (*i.e.* gene count) (264).

The studies aforementioned provided convincing data to support the use of markers of bacterial richness, such as gene count, as a proxy of gut microbiota dysbiosis. However, it is important to highlight that the interpretation of taxonomic profiles as markers of dysbiosis, although possible, requires caution. While the gut microbiota is extremely variable among individuals, these two papers discussed above were restricted to two Western European populations. Functional redundancy is a common trait of intestinal bacteria, which ensures that varied gut microbial arrays exert similar effects on host biology (235, 265). In this sense, observing functional alterations, in addition to taxonomic profiles, associated with health and disease is often a more informative and reproducible strategy. Finally, as several gut bacteria share common metabolic features, HGC subjects are presumably protected from dysbiosis because, upon an ecological challenge (*i.e.*, HFD), the gut microbiome repertoire is wide enough to surmount the insult without major consequences to the host. The contrary is possibly observed in a context of reduced bacterial richness, in which a poor bacterial collection cannot effectively compensate for ecological damages to the gut microbiota, resulting in a dysfunctional gut microbiome with deleterious effects to the host.

5.1.3 Short chain fatty acids

Short chain fatty acids (SCFA) are the main microbial end-products from bacterial fermentation in the murine and human large intestine, being mostly derived from the breakdown of complex polysaccharides by anaerobic bacteria. (268). SCFA are also formed from the fermentation of oligosaccharides, proteins, peptides and glycoproteins (e.g. mucins) (269). Hence, branched chain fatty acids (BCFA) can be formed from BCAA catabolism (268). The principal SCFA derived from carbohydrate and amino acids are acetate, propionate and butyrate, whereas valerate, formate and caproate are formed at a much lower extent (268). The molar ratio acetate:propionate:butyrate found in the human colon was 60:20:20 (270), showing that acetate is normally more abundant than propionate and butyrate.

There is a consistent body of literature supporting a protective role of SCFA in obesity and metabolic disturbances by modulating energy metabolism, gut barrier integrity and inflammatory responses in various organs (Figure 5) (271). SCFA supplementation has been reported to decrease weight gain by preventing fat accumulation (222, 272-274), which is corroborated by the fact that mice lacking the SCFA receptor G-coupled protein receptor 43 (GPR43) are obese on a normal diet, whereas its overexpression in the adipose tissue protects from diet-induced obesity (37). Moreover, butyrate administration was shown to increase energy expenditure by activating AMP-activated protein kinase (AMPK) in muscle (35), propionate has been reported to reduce lipid synthesis in isolated rat hepatocytes (275) and acetate was shown to reduce hepatic fat deposition, a trait related with improved glycemic control in diabetic mice (276).
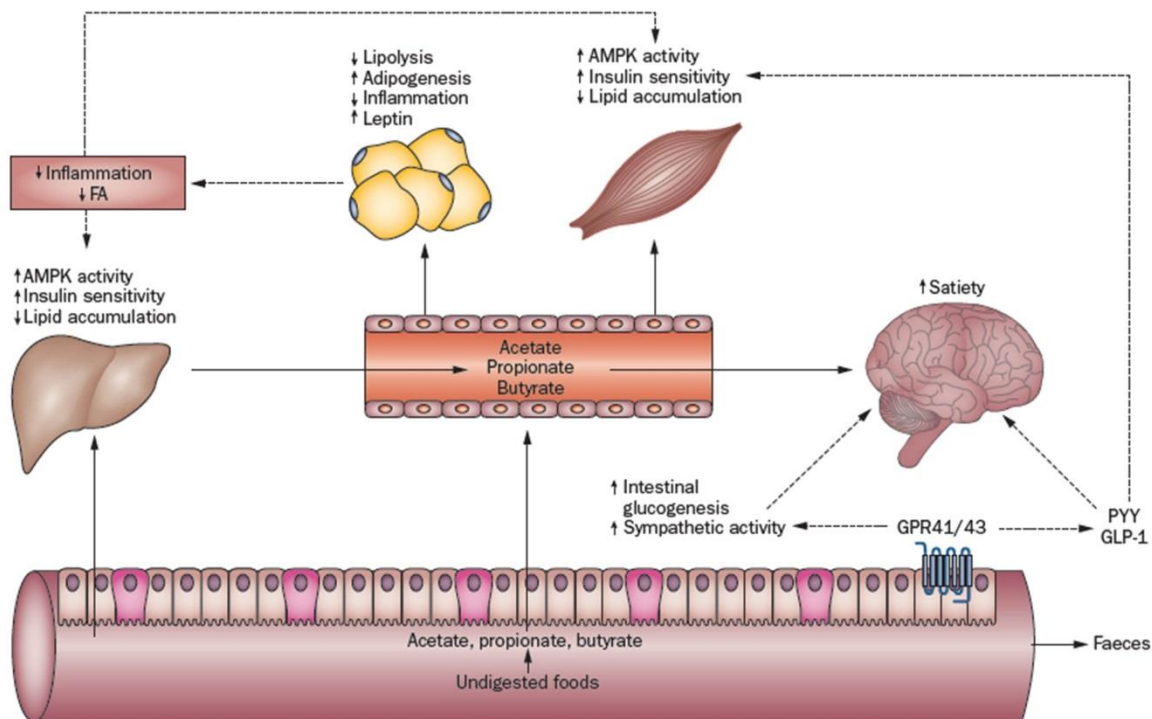
Figure 5: SCFA improve metabolic syndrome.

In the distal gut, SCFA bind to G-protein coupled receptors (GPR41) and (GPR43), which leads to the production of peptide YY (PYY) and glucagon-like peptide 1 (GLP1) and affects satiety and glucose homeostasis. Propionate and butyrate trigger intestinal gluconeogenesis, which is linked to improved glucose and energy homeostasis. Propionate, butyrate and mostly acetate reach the circulation and can affect the physiology of peripheral organs. Acetate is involved in controlling satiety by directly acting on the brain. Solid lines: direct effects of SCFA. Dashed lines: indirect effects of SCFA.

From Canfora *et al.* (277) Short-chain fatty acids in control of body weight and insulin sensitivity. Nature reviews Endocrinology 2015;**11**:577-91

SCFA are thought to display specific intestinal actions: while butyrate acts on intestinal L-cells through GPR43 to increase GLP-1 production (272, 273), propionate activates GPR41 to increase intestinal gluconeogenesis through a mechanism dependent on the portal nervous system (222), both leading to improved glucose homeostasis and increased satiety. The effect of butyrate on intestinal homeostasis is the subject of particular attention: inoculation of mice with the butyrate-producers *Clostridium* clusters IV and XIVa or butyrate administration

per se were both capable to expand the colonic population of regulatory Tregs, which increased the production of the anti-inflammatory cytokine IL-10 and reduced the colonic population of the pro-inflammatory CD4$^+$ T cells (278-281). In addition, butyrate is necessary for the maintenance of intestinal epithelium integrity (282, 283) and acts through histone deacetylase inhibition to decrease intestinal NO, IL-6 and IL-12 production by macrophages (284).

Based on the pieces of evidence relating SCFA to metabolic benefits, it is possible to hypothesize that Western diets, which are depleted from substrates enabling gut microbial synthesis of SCFA, are associated with poor availability of SCFA and therefore increased risk of intestinal inflammatory diseases and metabolic maladies. In fact, consumption of complex carbohydrates from fruits and vegetables is associated with higher microbial production of SCFA and better health status (285-287).

However, the notion of SCFA as beneficial molecules cannot be viewed in black and white. First, obese humans and genetically obese *ob/ob* mice have been shown to excrete more SCFA in the feces than lean subjects, whereas the acetate:propionate:butyrate ratio was unaltered (225, 288). This increased presence of SCFA in stool samples of obese models led to the conclusion that the "obese microbiome" could harvest more energy from the diet through increased SCFA production, thereby contributing for the obese phenotype. (*The energy harvest hypothesis is further discussed below*). Second, Singh *et al* have demonstrated that TLR5 deletion not only generates sub-chronic inflammation, gut microbioal dysbiosis and insulin resistance as it also promotes liver steatosis and increases the hepatic expression of stearoyl CoA desaturase 1 (SCD1) (289). The authours found out that TLR5 KO mice produce more oleate in the liver using SCFA as substrates, and that both increased SCFA synthesis and increased SCD1 expression are causally linked to gut microbial alteration seen in TLR5 KO mice (277, 290). While this work stresses the fact that the relevance of SCFA to host physiology involves intrincate interplay between host immune system and gut microbiota, more studies are warranted in order to better understand the role of

SCFA in health and disease. One explanation for the conflicting conclusions on the physiological role of SCFA may involve the production level of SCFA. It is possible that the gut microbiota of TLR5 KO mice generate SCFA at a much higher rate than wild-type mice. Another explanation may be related to the ratio of acetate, propionate and butyrate produced. It is possible that synergy between the specific action of these three major SCFA is key to define their metabolic influence on host metabolism.

5.1.4 A direct link between gut microbiota and obesity

In the early 2000s, a novel perspective was raised on the relationship between the trillions of microorganisms inhabiting the intestinal lumen and obesity by a series of studies carried out at Dr Jeffrey Gordon's laboratory. This new wave of research came in the setting of, and was propelled by, major advances in culture-independent techniques for gut microbial analysis (*e.g.*, 16S rRNA gene-based and whole metagenome shotgun sequencing) and a more widespread use of germ-free mice and fecal microbiota transplantation.

5.1.4.1 The energy harvest hypothesis

In 2004, Backhed *et al.* showed that conventionalization of germ-free mice (*i.e.*, colonization with the cecal microbiota of normal mice) was associated with fat mass gain and insulin resistance, being all mice in this study fed a standard chow diet (224). Mechanistically, the authors found that the gut microbiota favoured fat deposition by stimulating hepatic *de novo* lipogenesis and triglyceride storage via carbohydrate response element binding protein (ChREBP) and SREBP1 and by suppressing fasting-induced adipocyte factor (FIAF, also known as ANGPTL4), an inhibitor of adipocyte LPL (224). Backhed *et al.* also demonstrated three years later that germ free mice were resistant to HFD-induced obesity (291). In 2005, studies using leptin-deficient ob/ob mice found lower levels of Bacteroidetes and a proportional increase in Firmicutes as compared to lean wild type mice (292), and feeding a HFHS diet to wild-type rodents led to similar microbial changes, that is, an increase in the Firmicutes to Bacteroidetes (F/R) ratio (254). Ley *et al.* also reported an overrepresentation of Firmicutes coupled with reduced Bacteroides in

obese humans *versus* lean subjects; moreover, weight loss based either on a low-fat or a low-carbohydrate diet decreased the F/R ratio (293). A pivotal point in this story was the demonstration of a causal relationship between the obesity-related alterations in the gut microbiota and the obese phenotype by reconstituting germ-free mice with the fecal microbiota of ob/ob mice (225), diet-induced obese mice (254) or obese humans (12). Turnbaugh *et al.* found that higher Firmicutes in the gut microbiota of ob/ob mice paralleled to an increase of microbial enzymes for degradation of polysaccharides, higher fecal acetate and butyrate and lower stool energy loss than in lean mice (225), therefore proposing that an increased energy harvest from the diet, mainly triggered by Firmicutes, was the mechanistic link between obesity-linked alterations in the gut microbiota and enhanced fat deposition. However it is noteworthy that, while other research teams confirmed the association between increased F/R ratio and obesity (294, 295), some did not reproduce such findings (296, 297). It is now clear that genetic background (reflected by distinct strains in mouse models) (247, 298, 299), husbandry practices (300), time since importing from a vendor (300), vendor (299), diet (*e.g.*, irradiated or non-irradiated) (300) and methodological approaches (301) can all explain these variations in outcomes between different research teams and, fortunately, researchers are more and more concerned about standardizing methods in order to reduce these variations.

In synthesis, pioneer studies by Gordon's group led to the hypothesis that, in certain individuals, the gut would act as a "high-efficiency bioreactor" to therefore promote energy storage, whereas a "low-efficiency reactor" would promote leanness due to lower energy harvest from carbohydrate fermentation. Obesity would be fueled by a chronic increase in energy harvest from the diet by means of enhanced SCFA production. However, the absorption of SCFA and storage as lipids is dependent on factors such as gut transit, mucosal absorption, gut health and the symbiotic relationship between different groups of gut bacteria (302), which implies that the link between higher fecal SCFA and fat deposition is not straightforward. Furthermore, the energy harvest hypothesis seems at odds with the demonstration that acetate, via activation of Gpr43, increases energy

expenditure and suppresses fat accumulation in the adipose tissue (37). This hypothesis was also recently challenged by the demonstration that treatment of young mice with Azithromycin and Florfenicol decreased the amount of SCFA in the feces and increased fat mass accretion (303). Finally, Firmicutes are very unlikely the sole contributors to such an increase in SCFA production, as suggested by the lack of correlation between higher fecal SCFA and expansion of Firmicutes reported by some groups (304, 305). In conclusion, while the F/B ratio serves as a very general marker of dysbiosis, the actual role of the energy harvest hypothesis in obesity warrants further investigation.

5.1.4.2 The influence of the gut microbiota on energy availability and expenditure

As discussed in section 2, regulation of body weight and adiposity relies on the balance of energy intake and energy expenditure. The energy harvest hypothesis has initially diverted efforts to understand the influence of gut microbes on obesity towards the capacity of the gut microbiota to alter energy availability to the host. Only recently researchers are focusing on the role of the gut microbiota in another key component of the energy balance equation: energy expenditure. Our understanding of the gut microbiota-related mechanisms involved in controlling energy partitioning in the host is in its infancy and, up to this date, is primordially based on two elegant studies that investigated alterations in the microbiota in cold-exposed mice (13, 226). Overall, gut microbes modulate energy expenditure by three mechanisms: (i) through altering the bile acid profile and increasing bile acid pool size, which enhances BAT activity upon binding to the nuclear receptor FXR and the membrane receptor TGR5 (13) *(see section on bile acids below)*; (ii) by increasing thermogenic potential of brite adipocytes, possibly via increasing type 2 innate response of WAT-located eosinophils and M2 macrophages (13, 306); (iii) by reducing apoptosis of IEC thus increasing intestinal surface and energy absorption (226). The latter, although not directly linked to enhanced energy expenditure, was proven necessary to fueling cold tolerance, since antibiotic treatment abrogated resistance to cold in mice (226). Moreover, while major

alterations in the gut microbiota (13, 226) and bile acid profile (13) of mice were seen as early as one day after cold exposure *(i.e.*, prior to changes in adiposity), fecal microbiota transplantation partially recapitulated enhanced BAT-related thermogenic programming (13, 226), browning of WAT (226) and increased energy availability as a result of increased intestinal surface (226). Interestingly, the long-term adaptation of the gut microbiota to cold involves a general expansion of Firmicutes (*e.g.*, *Lachnospiraceae*, *Ruminococcaceae*) and reduced Bacteroidetes (e.g. S24-7, *Rikenellaceae*) (13, 226), which resembles the changes in the gut microbiota associated with obesity (225, 293). Lower presence of Deferribacteres and a drastic reduction of *A. muciniphila* were also found to be important features of gut microbial populations upon cold exposure (13, 226). A major finding in the study by Chevalier *et al.* was the demonstration that reduced energy availability as a result of increased gut absorptive surface was recapitulated in germ-free mice reconstituted with the fecal slurry of cold-exposed mice; however, this was not observed when germ-free mice were colonized with the cold-exposed microbiota amended with *A. muciniphila* (226). Interestingly, energy expenditure remained upregulated in the presence of *A. muciniphila,* which resulted in a negative energy balance in "cold-microbiota" transplanted animals (226). In agreement with these findings, the presence of *A. muciniphila* is strongly correlated with leanness and a healthy phenotype *(see section on A. muciniphila below).* Overall, these studies support a role for the energy harvest hypothesis in obesity and stress the relevance of other taxa, besides the F/R ratio, to regulate energy availability and partitioning in the host. Importantly, Chevalier *et al.* demonstrated that changes in energy availability to the host is not restricted to SCFA uptake from polysaccharide fermentation, but is rather a result of enhanced nutrient absorption rendered possible by alterations in the intestinal absorptive capacity (226).

In addition to the mechanism discussed above, gut microbial-derived SCFA may also alter energy expenditure. While acetate was shown to enhance brown adipocyte activation in vitro (307), butyrate administration has been shown to improve insulin resistance and increase enrgy expenditure in mice (35).

5.1.5 *Akkermansia muciniphila*

Akkermansia muciniphila is a Gram-negative, strict anaerobe and mucin-degrading bacterium that colonizes the guts of humans and rodents (167, 244). Although *Akkermansia* species are conserved in the gut microbiota throughout the animal kingdom (308), *A. muciniphila* represents the sole member of the Verrucomicrobia phylum identified in the human and murine intestines (309). Moreover, *A. muciniphila* thrives in the outer mucus layer in proximity to the host's cells, and it has been shown to rely preferentially on host-derived mucin as an energy source (310). *A. muciniphila* is highly abundant in the gut microbiota (possibility as a result of an ecological advantage) and represents 1–5% of all intestinal bacteria (244). Such a successful coevolution between *A. muciniphila* and its hosts clearly indicates a relevance of this genus to host gut function and physiology. Lower abundance of *A. muciniphila* has been found in the feces of children with autism (311) and in patients with inflammatory bowel disease (IBD) (312) and appendicitis (313). Importantly, while human and mouse studies have both correlated the presence of *A. muciniphila* in the gut microbiota with leanness (14, 314-316), higher gut bacterial richness (14, 316) and better glycemic control (14, 314), studies using animal models have consistently shown a causative role for *A. muciniphila* in protecting gut barrier, which was associated with increased mucus layer thickness, improved glucose homeostasis and alleviated metabolic endotoxemia (164, 167).

A general understanding of the cellular pathways potentially regulated by *A. muciniphila* was described by Derrien *et al.* (317) and Lukovac *et al.* (318); both reports clearly demonstrated that *A. muciniphila* can significantly alter intestinal gene expression pattern (317, 318). Derrien *et al.* monocolonized germ-free mice with *A. muciniphila* and demonstrated that this bacterium modulated the expression of several genes involved in tolerogenic immune response, cell survivor, proliferation and lipid metabolism (317). Lukovac *et al.* confirmed the potential of *A. muciniphila* to alter these cellular pathways by exposing mature ileal organoids to the supernatant collected from *A. muciniphila* culture (318). The fact that *A. muciniphila* was shown to modulate cell survivor and proliferation (317, 318) is in

line with the evidence that *A. muciniphila* controls apoptosis in the intestine to limit the absorptive area and reduce energy availability to the host (164, 226). Interestingly, Lukovac *et al.* compared the effect of the *A. muciniphila*-conditioned medium to the impact of propionate, butyrate and acetate on gene expression and found out that several effects of *A. muciniphila* on host cellular pathways may be mediated by propionate (318), which is released as a by-product of mucin degradation (244). Their findings pointed to an important upregulation of Hdac3 and Hdac5 that is likely dependent upon propionate and butyrate action (318). It is noteworthy that, although *A. muciniphila* does not directly produce butyrate, it can feed butyrate-producers with acetate through cross-feeding (319). Because inhibition of Hdac3 and 5 is involved in the regulation of pro-inflammatory responses in the intestine (*e.g.*, IL8, MCP1) (320) and maintenance of Paneth cells integrity (321), upregulation of these enzymes may contribute to control enteric inflammation and bacterial overgrowth. Another interesting finding reported by Lukovac *et al.* was the increased FIAF gene expression in intestinal organoids exposed to propionate and butyrate, which may reduce fat deposition in host tissues through the inhibition of LPL. Interestingly, the *A. muciniphila* conditioned medium did not alter FIAF gene expression, suggesting the presence of other bacterial-derived molecules in the medium counteracting propionate- and butyrate-linked upregulation of FIAF. However, it is possible that the contribution of *A. muciniphila*-derived propionate to stimulate FIAF gene expression *in vivo* is dependent upon additive stimuli from other symbionts (Figure 6).
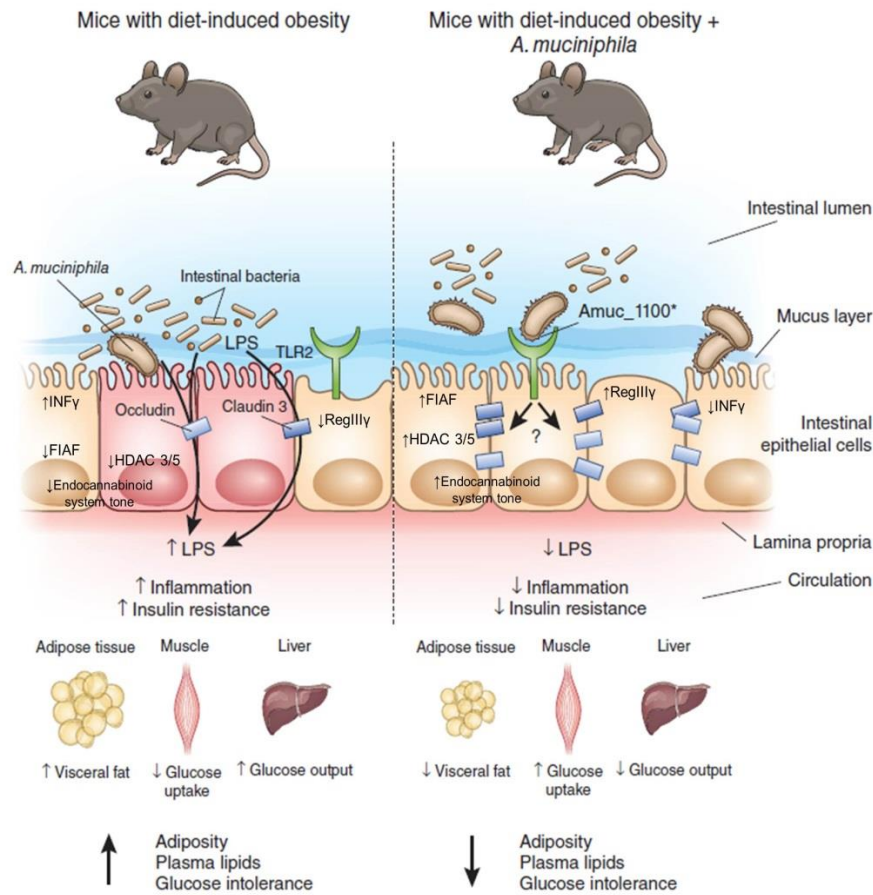
Figure 6: A. muciniphila improves gut barrier and metabolic syndrome in diet-induced obese mice.

Obesity is associated with lower abundance of *A. muciniphila* in the gut microbiota than in healthy mice (left). This promotes a dysbiotic state accompanied by gut barrier disruption and the leakage of bacterial LPS into circulation (metabolic endotoxemia). These mice display increased visceral adiposity and impaired insulin sensitivity in the muscle and liver when compared to healthy mice (left). *In vitro* studies have suggested that *A. muciniphila* enhances intestinal FIAF expression, which contributes to inhibit fat mass accretion in peripheral tissues (right); these studies also indicated that *A. muciniphila* controls the expression of HDAC3/5, which may be involved in controlling RegIIIγ secretion by Paneth cells and in the downregulation of pro-inflammatory responses in the intestine. Moreover, the inflamed gut, by secreting INFγ, may diminish *A. muciniphila* population in the lumen (left). *In vivo* administration of *A. muciniphila* to diet-induced obese mice also increased intestinal RegIIIγ expression and revealed a marked upregulation of the endocannabinoid system tone, which is relevant to the control of gut barrier homeostasis and of several other metabolic processes. *A. muciniphila* activates TLR2 upon binding of its outer

membrane protein Amuc_1100, which upregulates the expression of tight junction protein genes (Claudin3, Occludin), alleviate metabolic endotoxemia, improve glucose and lipid metabolism and reduce fat mass deposition in diet-induced obese mice. *A. muciniphila* administration to mice is also associated with increased mucus layer thickness, which contributes to prevent bacterial invasion, intestinal inflammation and the leakage of LPS to circulation.

Adapted from (322) Anhê FF, Marette A: A microbial protein that alleviates metabolic syndrome. Nature medicine 2017;23:11-12.

A whole new perspective on the role of *A. muciniphila* in controlling host metabolism was given by the group of Dr Patrice Cani. By administering *A. muciniphila* to HFD-fed mice, Everard *et al.* showed that *A. muciniphila* is important to keep gut barrier homeostasis through its ability to maintain mucus layer thickness, preventing bacterial encroachment and metabolic endotoxemia to therefore alleviate gut/systemic inflammation (167). Similar findings were reported by others (323). The effect of *A. muciniphila* treatment was accompanied by an increase in the intestinal mRNA expression of RegIIIγ, a bactericidal C-type lectin that targets Gram positive bacteria, suggesting that *A. muciniphila* controls the overgrowth of several potentially pathogenic species (167). Moreover, the maintenance of gut homeostasis after *A. muciniphila* administration to diet-induced obese mice was associated with an increase of some intestinal bioactive lipids belonging to the endocannabinoid system (*i.e.,* 2-oleoylglyceral, 2-palmitoylglycerol, 2-arachidonoylglycerol) (167). Recently, Plovier *et al.* demonstrated in a mouse model of diet-induced obesity that the beneficial impact of *A. muciniphila* on gut barrier, glucose homeostasis and obesity are mediated by the action of the outer membrane protein Amuc_1100 via TLR2 activation (164). Moreover, the authors have shown that administration of either live or non-replicative *A. muciniphila* to overweight humans for 2 weeks is safe and well tolerated, definitively raising *A. muciniphila* to the status of "next generation probiotic" (164, 322) (Figure 6).

Greer *et al.* made considerable advances in our understanding of the interaction between *A. muciniphila* and the host by showing that this bacterium integrates enteric inflammation and host metabolism in an INFγ-dependent manner

(324). The authors demonstrated that INFγ KO mice possess an expanded *A. muciniphila* population in their gut microbiota, which parallels to improved glucose tolerance (324). Moreover, INFγ administration drastically reduced *A. muciniphila* population in addition to detrimental consequences to glycemic control (324). Interestingly, depletion of the gut microbiota or *A. muciniphila* in INFγ KO mice abrogated the favourable glucose homeostasis previously observed in these mice (324) (Figure 1). The authors identified the enzyme immunity-related GTPase family M 1 (Irgm1) as a downstream target of INFγ involved in controlling *A. muciniphila* population (324). Given that metformin has been shown to reduce INFγ levels (325), these findings are particularly interesting as they confer a possible mechanistic explanation to the expansion of *A. muciniphila* population seen after metformin administration to mice (323) and humans (326, 327).

5.2 Bile acids and gut microbiota

Bile acids (BAs) are synthesized in the liver from cholesterol and stored in the gallbladder. The primary BAs produced by the human liver are chenodeoxycholic acid (CDCA) and cholic acid (CA), while rodents produce CA and muricholic acids (MCAs), predominantly βMCA (328). Prior to secretion into bile and discharge into the duodenum, BAs are amidated (*i.e.*, conjugated) with the amino acids glycine or taurine. While glycine-conjugated BAs are predominant in humans, taurine-conjugated BAs are almost exclusively produced by mice and rats (328). The gut microbiota plays a major part in shaping the BA profile by modifying the structure of liver synthesized BAs via 7α-dehydroxylation and glycine/taurine deconjugation, yielding secondary BAs. The main secondary BAs are deoxycholic acid (DCA), lithocholic acid (LCA), ωMCA (only in mice and rats) and ursodeoxycholic acid UDCA (is a secondary BA in humans but a primary BA in mice) (328). Although secondary BAs are more hydrophilic than primary BAs, a minor portion of microbial-derived unconjugated secondary BAs are absorbed from the gut through passive diffusion and may also undergo glycine/taurine conjugation in the liver. Upon ingestion of a meal, I-cells, which are mostly present in the duodenum and in the jejunum, secrete cholecystokinin (CCK); in turn, this gut hormone triggers pancreatic exocrine secretion and the discharge of BAs in the gut

lumen. BAs are amphipatic molecules with detergent-like properties, allowing the formation of micelles and therefore facilitating the absorption of dietary lipids and fat-soluble vitamins. Efficient reabsorption of BAs takes place in the terminal ileum by the apical sodium dependent bile acid transporter (ASBT, also known as IBAT), resulting in the accumulation of BA in the body (*i.e.* the BA pool). While the majority of the BA pool cycles between the liver and the intestine through the enterohepatic circulation about six times per day, a small amount can escape to the systemic circulation (ref 18670431). Moreover, approximately 5% of the BAs secreted into the gut lumen are lost in the feces, which are compensated by *de novo* BA synthesis in the liver in order to maintain the BA pool and constitute an important route for cholesterol turnover.

BAs can autoregulate their synthesis and intestinal reabsorption through the modulation of the nuclear-located farnesoid X receptor (FXR) (329). In the liver, BA-activated FXR induces the expression of small heterodimer partner (SHP), which binds to liver receptor homolog-1 (LRH-1) and inhibits cholesterol 7α-hydroxylase (Cyp7a1) gene expression, the rate-limiting enzyme involved in the synthesis of BA from cholesterol (330, 331). Ileal FXR is also activated by luminal BAs, which triggers the production of FGF15 (FGF19 in humans). FGF15/19 reaches the liver through the portal circulation, activates the FGF receptor 4 (FGFR4)/β-klotho heterodimer, which thereby provides a redundant inhibitory signal to control Cyp7a1 gene expression (332, 333). Interestingly, studies using tissue-specific FXR KO mice suggested that ileal FXR activation leads to stronger suppression of Cyp7a1 than hepatic FXR activation (334, 335). CDCA, CA and DCA are the strongest FXR activators (*i.e.*, downregulate BA synthesis), whereas UDCA and MCA are FXR antagonists (*i.e.*, upregulate BA synthesis) (336-338).

Studies using FXR KO models in order to unveil the role of this receptor in metabolic syndrome are often conflicting (339-344). Overall, FXR whole-body deletion is beneficial to diet- or genetically-induced obese mice (342-344), whereas some studies have reported hyperglycemia and hypercholesterolemia in chow-fed mice (339, 340) and enhanced atherogenesis in Apoe$^{-/-}$ mice (345) in which FXR

was knocked out . Liver-specific FXR abrogation was associated with NASH and dyslipidemia, suggesting that hepatic FXR agonism is rather protective against NAFLD (346). In fact, recent clinical trials using the semi-synthetic CDCA-derivative obeticholic acid (OCA), which potently activates FXR, have shown promising results against NASH (347, 348). As opposed to the liver, studies using intestine-specific deletion of FXR indicated that FXR antagonism in the gut protects against NASH and obesity upon HFD-feeding (349, 350).

Different dietary sources (*e.g.*, milk fat *versus* fish oil) (351) and particular gut bacterial community structures seen in mice from the same strain but from different vendors (298) have both been shown to impact BA profile and affect FXR signaling. Interestingly, recent studies using germ-free mice and antibiotic treatment revealed that the gut microbiota controls energy partitioning through FXR signaling by altering adipose tissue inflammation and hepatic lipid uptake (343, 350). The authors revealed that a gut microbial-related drop in the circulating levels of the FXR antagonist TβMCA is an important driver of weight gain in conventionalized germ-free mice (343), whereas the same group reported that high levels of conjugated primary BAs (including TβMCA) are associated with increased thermogenesis upon cold-exposure (13). In sum, while there is an intricate interplay between gut microbiota, BAs and FXR signaling, this relationship is markedly influenced by differences in the gut microbiota, tissue-specific role of FXR and diet. Importantly, if on one hand mouse studies generally point to intestinal FXR antagonism (349, 350) and hepatic FXR agonism (346) as protective against features of the metabolic syndrome, on the other hand more studies are warranted in order to decipher the role of FXR in human metabolism.

TGR5 (also known as Gpbar1) is a plasma membrane-bound G protein coupled receptor with high expression in gallbladder, liver, intestine, BAT and WAT and constitutes another bile acid-responsive receptor involved in host metabolism (352-354). TGR5 is activated mainly by the secondary bile acids LCA and DCA (353, 355), which positions this receptor as an important mediator between the trialogue BA-gut microbiota-host metabolism. Watanabe *et al.* demonstrated that

TGR5 activation promotes intracellular thyroid hormone activity thereby increasing BAT thermogenesis (33). The authors reported that diet-induced obesity and fat accumulation in BAT was fully reversed by dietary CA supplementation, initially suggesting a FXR-linked mechanism (33). However, further experiments excluded this hypothesis since the highly active synthetic FXR ligand GW4064 did not reproduce the effects of CA administration (33). The authors then found out that the weak TGR5 agonist CA was metabolized to the stronger TGR5 agonist DCA by the gut microbiota and was the main driver of enhanced BAT activity (33). In line with these findings, upregulation of TGR5 signaling was shown to improve glucose homeostasis by increased BAT and muscle thermogenesis and by increased GLP-1 release in intestinal L cells (356). Moreover, the TGR5-specific agonist INT-777 ameliorated hepatic steatosis, obesity and insulin sensitivity in diet-induced obese mice (356). Taken together, TGR5 activation by secondary BAs improve several features of the metabolic syndrome in mice and are strongly associated with thermogenic control. However, similarly to FXR, the impact of TGR5 signaling in human physiology deserves further investigation. A summary of the trialogue between bile acids, gut microbiota and host metabolism is presented in figure 7.
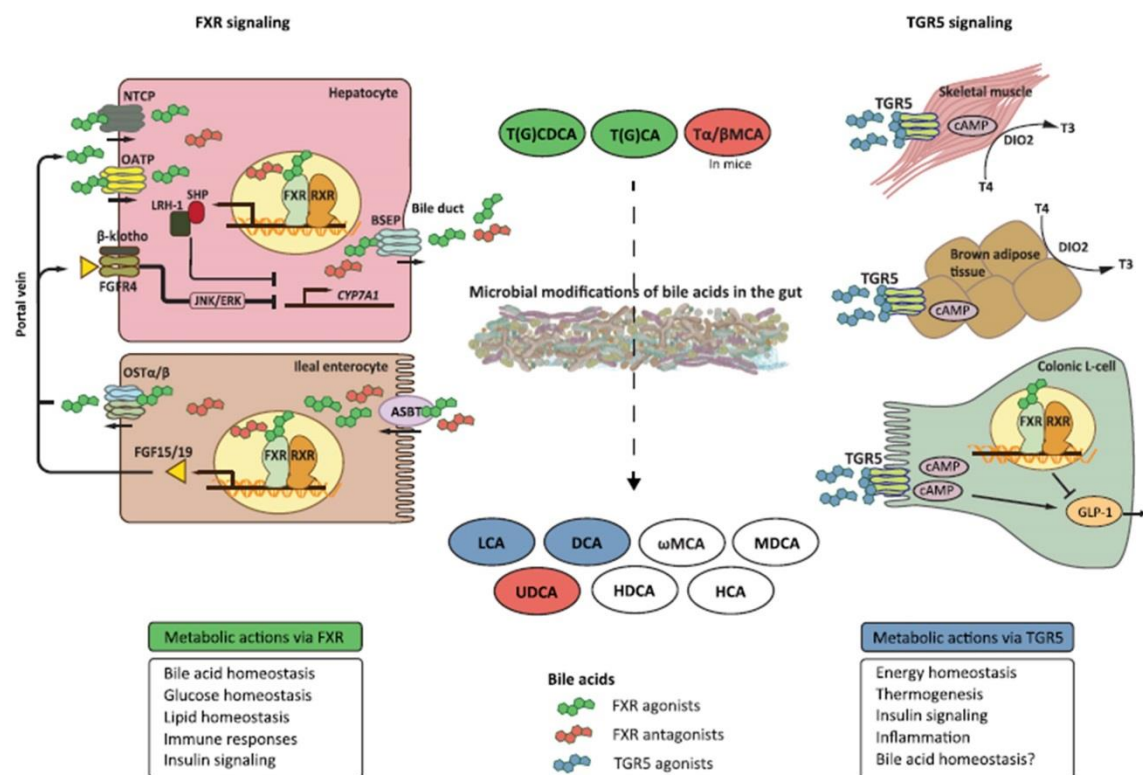
Figure 7: Bile acids are modified by the gut microbiota and influence host metabolism through FXR and TGR5.

Primary bile acids (BAs) T(G)CDCA, T(G)CA, and Tα/βMCA (in mice) are synthesized and conjugated in the liver and transported from the hepatocytes into the bile duct by bile salt export pump (BSEP). Primary BAs are therefore converted to secondary BAs by gut microbial enzymes. BAs (primary and secondary) are then transported from the gut back to the liver via the enterohepatic circulation by several active transporters on ileal enterocytes (ASBT, organic solute transporter alpha/beta - OSTα/β) and hepatocytes (sodium taurocholate cotransporting polypeptide -NTCP and organic anion-transporting polypeptide - OATP). BAs signal via the nuclear BA receptor FXR and the plasma membrane receptor TGR5. FXR is activated mainly by the primary bile acids CDCA and CA (green), while the most potent ligands for TGR5 are LCA and DCA (blue). OtherBAs, such as Tα/βMCA and UDCA, have shown FXR inhibitory activity (red). In ileal enterocytes, activation of FXR leads to transcription of FGF15/19, which is secreted into the portal vein and binds to the FGFR4/b-klotho receptor complex on hepatocytes. The FGFR4/b-klotho complex activates JNK/ERK signaling that inhibits expression of CYP7A1. In colonic L-cells, FXR activation inhibits the synthesis of GLP-1, whereas TGR5 activation in colonic L cells increases synthesis and release of GLP-1. TGR5 in skeletal muscle and brown adipose tissue increases energy expenditure by promoting the conversion of inactive thyroxine (T4) into active thyroid hormone (T3).

The interaction between the gut microbiota and BAs is bidirectional. Besides modifications in the molecular structure of BAs by bacterial enzymes, the presence of BAs in the gut lumen exert a selective pressure that favours BA-metabolizing (or BA-resistant) bacteria while inhibiting the growth of BA-sensitive bacteria. This antimicrobial effect is either direct (*i.e.*, dependent on detergent properties of BAs) or indirect (*i.e.*, related to a FXR-mediated stimulation of enteric immune responses, such as iNOS and IL8 stimulation) (358). Diet is the main driver of changes in the gut microbial profile and this is partially linked to specific BA signatures. For example, mice fed a milk fat-based diet, but not a polyunsaturated fat-rich diet, displayed high circulating levels of tauro-cholic acid (TCA) and expansion of *Bilophila wadsworthia,* a BA-tolerant sulphite-reducing bacterium linked to intestinal inflammation (351)*.* Interestingly, omega-3 fatty acid supplementation reduced the abundance of *B. wadsworthia* in parallel to altered BA composition (351). In addition to *B wadsworthia*, other bile-tolerant bacteria, such as *Alistipes putredinis* and *Bacteroides spp.* increased within days in the gut microbiota of humans together with a significant build up of BAs in the feces after the consumption of an animal-based diet, whereas the levels of bacteria that metabolize plant polysaccharides (*e.g.*, *Roseburia, Eubacterium rectale, Ruminococcus bromii*) decreased (11). If, on one hand, diet can rapidly alter the gut microbiota to increase host susceptibility to intestinal and metabolic diseases, on the other hand, it is reasonable to assume that certain dietary molecules particularly abundant in healthy regimens can do the opposite, that is, protect against the development of diseases by improving the relationship between microbiota and host.

6 Polyphenols

Polyphenols, also known as flavonoids, were first described by the 1937 Nobel Prize awardee Dr Albert Szent-Györgyi. Originally looking for a cure for scurvy (359), Dr Szent-Györgyi prepared an extract from lemons, which

successfully helped a friend who had that problem. The effect was then attributed to vitamin C (also discovered by Dr Szent-Györgyi). However, when he gave to his friend a purified version of the extract (enriched in vitamin C), the effect was lost. Dr Szent-Györgyi analyzed the fraction he had removed from the purified extract and found out they were rich in molecules he then named vitamin P. The extract enriched in vitamin P alleviated his friend's bleeding gums, which led Dr Szent-Györgyi to conclude that vitamin P was important for vascular health and a remedy for petechia (i.e., bleeding and bruising caused by the breakdown of capillaries) (360). Further research demonstrated that vitamin P was a non-essential phytonutrient, which prompted its withdrawal from the list of vitamins and the change of its denomination to polyphenols or flavonoids.

Since the first discoveries by Dr Szent-Györgyi, much attention has been devoted to the particular impact of phenolic phytochemicals on health. This was in great measure fueled by several epidemiological studies showing an inverse correlation between the intake of polyphenol-rich foods and the incidence of diseases, such as CVD, T2D and cancer (361-365). I*n vitro* and *in vivo* studies have demonstrated putative mechanisms associated with the health benefits of polyphenols, with a particular focus on isolated molecules at pharmacological doses (*this topic is discussed below*). However, the exact role of dietary polyphenols is not yet completely understood.

6.1 Classification of polyphenols

Phenolic phytochemicals, generally referred to as polyphenols, occur as products of plant secondary metabolism in response to biotic and abiotic stress (366, 367) and can exist as simple phenolic acids (*i.e.* hydroxybenzoic acids or hydroxycinnamic acids) or as flavonoids: C6-C3-C6 molecules with two aromatic rings (rings A and B) linked by three carbons usually arranged as an oxygenated heterocycle (ring C). Flavonoids are classified according to the degree of oxidation of ring C into anthocyanins, flavonols, flavones, flavanols (also named catechins), flavanones and isoflavones; they also occur as oligomers and polymers (*i.e.* tannins), classified as condensed tannins (also known as proanthocyanidins or

procyanidins) or hydrolysable tannins (368, 369) (Figure 8). While proanthocyanidins are polymers of catechins, and their structure is dependent both on the kind of monomer and the type of linkage between monomers, hydrolysable tannins consist of a central core constituted by a polyol (*e.g.* flavonoid, sugar) and a phenolic carboxylic acid esterifying the core molecule. Stilbenoids (*e.g.* resveratrol) and lignans comprise two other classes of non-flavonoid polyphenols. Most flavonoids are present in nature as O-glycosides and other conjugates (catechins are an exception), which contribute to their complexity and the large number of individual molecules that have been identified (>5000).
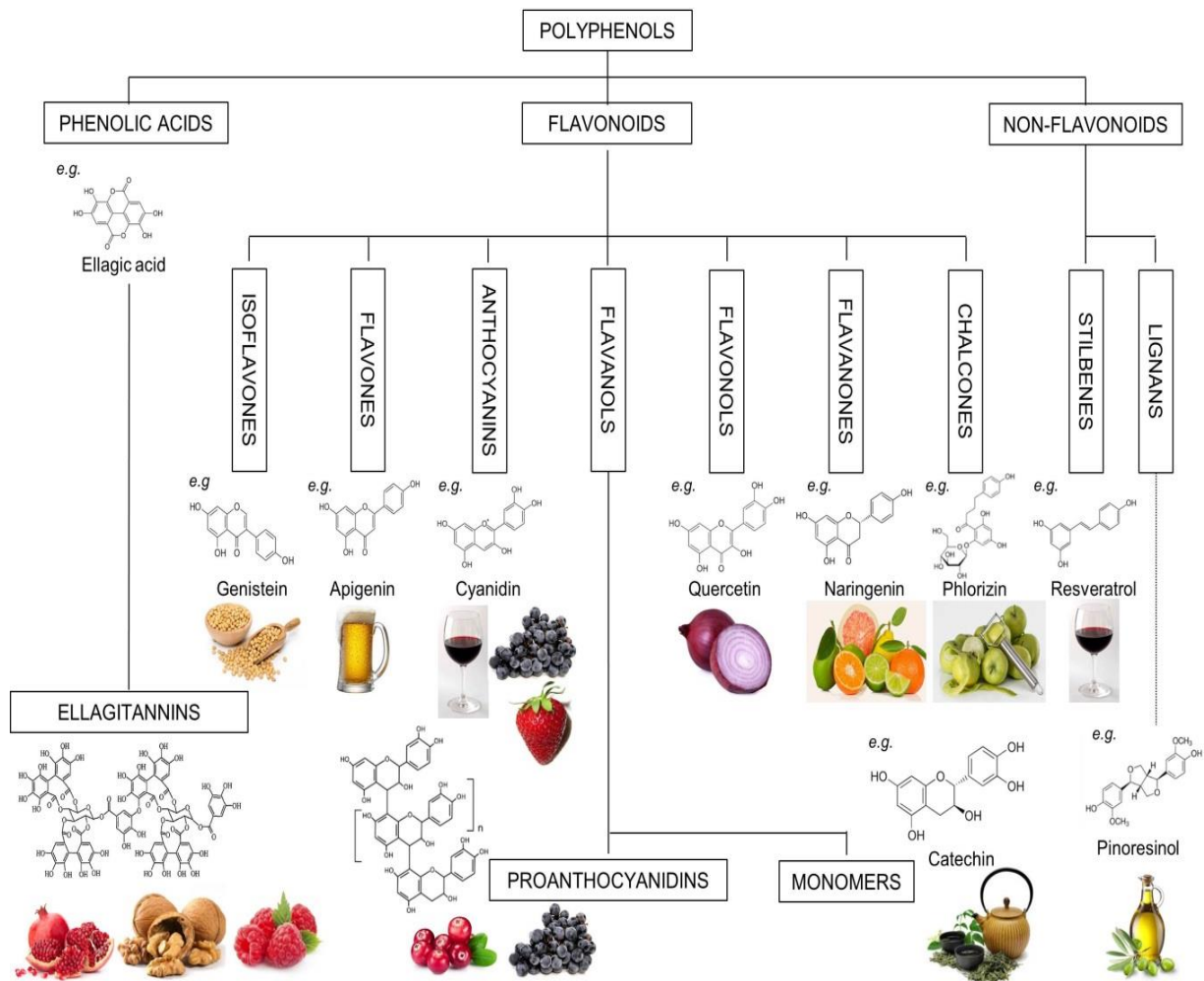
Figure 8: Classification of polyphenols.

6.2 Bioavailability of polyphenols

Once ingested, plant phenolics are partially absorbed in the stomach and small intestine (369), and hydrolysis of the glycoside moiety seems to be a requisite step for absorption at this level. Moreover, type and position of the sugar linked to flavonoids and the degree of polymerization or galloylation of flavanols (catechins) importantly impact bioavailability. The multidrug resistance protein (MRP), member of the ATP-binding cassette transporter superfamily, together with intestinal SGLT1, have been implicated in flavonoid absorption (371). The endogenous β-glucosidases, located at the intestinal brush border, lactase phloridzin hydrolase (LPH) and cytosolic-β-glucosidase (CBG) are capable of hydrolyzing flavonoids to generate more lipophilic, thus absorbable, aglycones (372, 373). As CBG is a cytosolic enzyme, SGLT1 transport seems to be a pre requisite for its action (374). The majority of dietary polyphenols (~95%) escapes absorption in the small intestine and builds up in the colon, where they are metabolized by gut bacteria yielding a complex series of end-products (375). Indeed, the gut microbiota exhibits a much richer and distinct repertoire of metabolizing enzymes, thus being capable of promoting O- and C-deglycosylation, ester and amide hydrolysis, deglucuronidation of large flavonoids and fermentation of the flavonoid backbone. Fermentation leads to the breakage of aromatic rings followed by the release of phloroglucinol, hydroxylated forms of phenylpropionate and phenylacetate, short-chain fatty acids, lactate, succinate, oxaloacetate, ethanol, CO_2 and H_2 (375) (Figure 9). It is noteworthy that the best absorbed polyphenols are, in descending order, gallic acid, isoflavones, catechins, flavanones and quercetin glucosides. Moreover, while gallic acid, quercetin glucosides, catechins, free hydroxycinnamic acids and anthocyanins are mostly absorbed in the stomach and small intestine, flavanones are highly dependent on the release of aglycones by the gut microbiota prior to absorption. After absorption, polyphenols undergo extensive biotransformation by enterocytes and hepatocytes, a necessary step to increase hydrophilicity and favour urinary excretion. Sulfation, glucuronidation, methylation and glycine-conjugation are the most common biotransformation reactions (375).
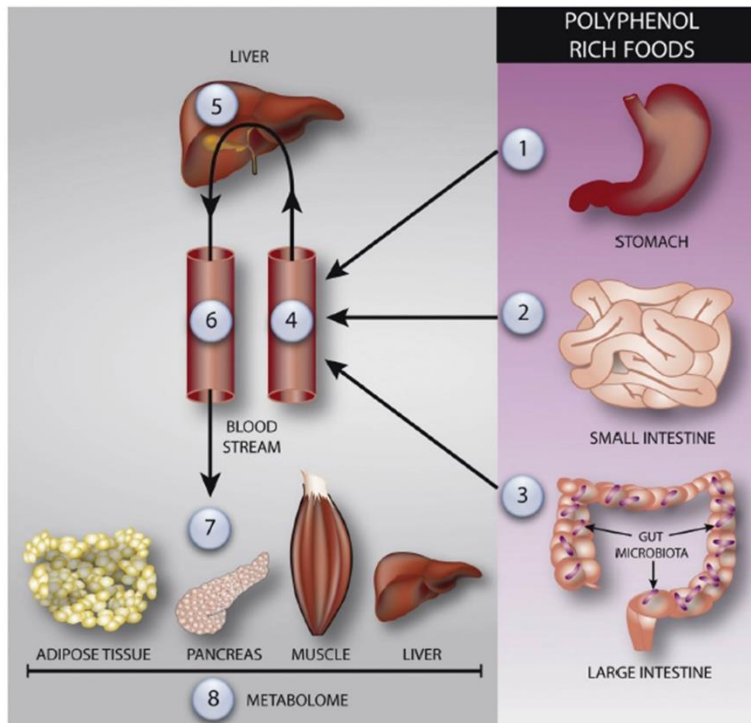
Figure 9: Body distribution of dietary polyphenols.

A small fraction of dietary polyphenols are directly absorbed through the stomach and small intestine (1,2). Gut microbes in the small intestine are not represented in this figure. The majority of dietary polyphenols reach the large intestine, thereafter undergoing intensive gut microbial metabolization prior to absorption (3). Polyphenols coming from microbial transformation and direct absorption through the stomach and intestinal mucosa reach the liver through the enterohepatic circulation (4), where they undergo phase I and II biotransformation (5). Polyphenol metabolites derived from liver metabolization reach the blood stream (6) to be thereafter distributed through peripheral tissues, where they may exert relevant biological effects (7). The thorough investigation of polyphenolic metabolites present in the peripheral blood and in the tissues (*i.e.* that integrates the metabolome) is crucial in order to clarify the relevance of phenolic phytonutrients to human health (8). Because a considerable amount of dietary polyphenols exhibit limited bioavailability, it is likely that intestinal- and gut microbial-related effects mediate the health benefits of polyphenols.

From Anhê FF *et al.* (376). Polyphenols and type 2 diabetes: A prospective review. PharmaNutrition 2013;1:105-114.

6.3 How do polyphenols improve features of the metabolic syndrome?

The health benefits of polyphenols are generally attributed to both non-specific mechanisms, dependent upon a broad anti-oxidant activity, and specific

mechanisms, which involves the interaction of polyphenols with key signaling proteins (377). Interestingly, non-specific mechanisms are apparently fomented by the induction of cellular antioxidant defenses, as suggested by the stimulation of glutathione synthesis and activation of antioxidation enzymes, such as glutathione-S-transferase, thioreductases and peroxidases after the consumption of polyphenol-rich foods (378-380). More specific mechanisms by which polyphenols improve metabolic health involve a great number of physiological processes. For instance, polyphenols have been suggested to ameliorate fasting and postprandial hyperglycemia by inhibiting disaccharidases (*i.e.* α-amylase and α-glucosidase) and competing with glucose for SGLT1 in the intestinal lumen (381), which limits post-prandial hyperglycemia, and by stimulating hepatic glucokinase activity, therefore reducing hepatic glucose output (381). In addition to effects on glycemic control, polyphenols are thought to protect pancreatic β-cells from glucotoxicity while exerting marked anti-inflammatory effect (382-397). Interestingly, some phenolic phytochemicals are thought to exert anti-obesity effects by augmenting energy expenditure. Catechins, abundantly present in green tea, are thought to inhibit catechol-o-methyl transferase (COMT), an enzyme that degrades norepinephrine (NE), therefore increasing the presence of NE within the synaptic cleft and leading to prolongation of NE-induced thermogenesis and fat oxidation in BAT. In fact, ingestion of green tea catechins is related to increased energy expenditure, a shift from carbohydrate to fat oxidation and increased urinary excretion of NE (40, 398-401). Moreover, while resveratrol administration induced brown-like adipocyte formation in white fat depots in mice through activation of AMPK (52) and enhanced mitochondrial activity in primary cultured brown adipocytes (402), genistein (a soybean isoflavone) (403-405) and a mix of apigenin/naringenin (41) have both been shown to increase BAT activity *in vivo* and *ex vivo* respectively.

Polyphenols may alter cellular pathways through modulation of Sirtuin1 (SIRT1), a type III protein deacetylase implicated in anti-aging and anti-inflammatory effects (406). Over the last decade, resveratrol, a non-flavonoid polyphenol abundant in grapes and red wine, has been shown to directly activate

SIRT1 *in vivo* to exert calorie restriction-like benefits (407-409). On the other hand, recent data suggest that resveratrol is not a direct activator of SIRT1, but rather a positive regulator of AMPK, a master regulator of glucose and lipid metabolism. It is noteworthy that a SIRT1-dependent PPARγ deacetylation has been proposed to selectively modulate PPARγ, leading to induction of BAT activity and repression of visceral WAT genes associated with insulin resistance (410). Other polyphenols, such as quercetin, catechin, butein, piceatannol and myricetin have also been shown to activate SIRT1 (406, 411-413), possibly as a result of AMPK regulation. In sum, polyphenols may potentially alter cell biology via AMPK, SIRT1 and PPARγ to promote a great number of metabolic benefits.

7. Problem statement

While the epidemiological evidence for the benefit of consuming polyphenol-rich foods is very strong, the bioavailability of dietary phenolic phytochemicals is paradoxically generally low (369). Moreover, our understanding of the mode of action of polyphenols is highly based on experiments performed *in vitro* or in animal models by using concentrations much higher than the usual dietary intake, therefore providing putative mechanistic explanation that often lacks relevance when translated to human physiology. Another issue relies on the fact that several *in vitro* mechanistic studies tested the effect of polyphenol aglycones or its sugar conjugated rather than their metabolites that actually reaches target cells *in vivo*.

The pieces of evidence discussed throughout the introduction of this thesis stress (*i*) the clear impact of the gut and its colonizing bacteria on several features of the metabolic syndrome, (*ii*) the major role of diet in modelling gut microbial community structure, (*iii*) the unequivocal health benefits of dietary polyphenols and (*iv*) the low bioavailability of phenolic phytochemicals. The observation of these major points leads to the working hypothesis that the gut and its colonizing microbes are mechanistically involved in the metabolic health benefits of dietary polyphenols.

8. Objectives

The principal aim of this thesis was to investigate, using a mouse model of high fat-high sucrose- (HFHS) induced obesity, the metabolic impact of daily oral treatment with polyphenol-rich berry extracts at a nutrionally relevant dose (200 mg of extract/kg of body weight). The studies presented herein focus on how the metabolic outcomes linked to the administration of polyphenol-rich extracts are related to changes in intestinal homeostasis, with a particular attention to the gut microbiota. The secondary objective of this work was to unveil polyphenolic subclasses and bacterial groups with potential therapeutic application against obesity and its related comorbidities.

In chapter I, the objective was to investigate the preventive effects of a polyphenol-rich cranberry extract on features of the metabolic syndrome in order to test the hypothesis that cranberry polyphenols protect against obesity in association with important changes in gut bacterial communities. The same cranberry extract and mouse model was used in chapter II in order to investigate whether cranberry polyphenols are able to reverse diet-induced obesity and associated diseases. The main hypothesis in this chapter was that cranberry polyphenols reverse diet-induced dysbiosis, intestinal and liver inflammation and insulin resistance without affecting body weight gain.

In chapter III we aimed to analyze the effects of polyphenolic extracts from five Arctic berries in a model of diet-induced obesity. In this chapter we tested the hypothesis that extracts with particular polyphenolic signatures are more effective in preventing features of metabolic syndrome, and that dietary polyphenols primarily act on the gut-liver axis to alleviate gut inflammation, metabolic endotoxemia, insulin sensitivity and chronic hyperinsulinemia.

In chapter IV we aimed to assess the effect of a crude extract of camu camu (*Myrciaria dubia*) on obesity and associated immunometabolic disorders in high fat/high sucrose (HFHS)-fed mice. We tested the hypothesis that this raw extract prevents diet-induced obesity by enhancing brown adipose tissue activation, which

is mechanistically linked to changes in gut microbial community structure and in the circulating bile acid profile.

CHAPTER I

A polyphenol-rich cranberry extract protects from diet-induced obesity, insulin resistance and intestinal inflammation in association with increased *Akkermansia spp.* population in the gut microbiota of mice.

Fernando F. Anhê[1,2], Denis Roy[2], Geneviève Pilon[1,2], Stéphanie Dudonné[2], Sébastien Matamoros[2], Thibault V. Varin[2], Carole Garofalo[3], Quentin Moine[3], Yves Desjardins[2], Emile Levy[3,4] and André Marette[1,2]

[1]Department of Medicine, Faculty of Medicine, Cardiology Axis of the Quebec Heart and Lung Institute, [2] Institute of Nutrition and Functional Foods, Laval University, Quebec, Canada, [3] Research Centre, Sainte-Justine Hospital, Montreal, Quebec, Canada, [4] Department of Nutrition, Faculty of Medicine, University of Montreal, Montreal, Quebec, Canada

Résumé

Objectif: L'augmentation croissante de la prévalence de l'obésité et du diabète de type 2 (DT2) démontre l'échec des traitements conventionnels à contrer ces désordres métaboliques.D'autre part, le microbiote intestinal est présenté comme un acteur clé dans la pathophysiologie du (DT2), et la diète représente un facteur majeur dans la modulation de ces populations microbiennes intestinales. Puisque la consommation de la canneberge (*Vaccinium macrocarpon* Aiton) est associée à plusieurs effets bénéfiques sur la santé, nous avons étudié l'impact métabolique d'un extrait de canneberge (CE) chez des souris nourries à une diète riche en gras et en sucrose (HFHS). Nous avons aussi déterminé si les effets positifs du CE chez ces souris étaient liés à des modulations du microbiote intestinal.Méthodes: Des souris C57BL/6J ont été nourries soit avec une diète standard (Chow) ou une diète HFHS et traitées quotidiennement avec le véhicule (eau) ou le CE (200 mg/kg) pendant 8 semaines. La composition du microbiota intestinal a été évaluée en analysant les séquences de gènes 16S ARNr par 454 pyrosequençage. Résultats: Le traitement au CE a prévenu le gain de poids et l'obésité viscérale induits par la diète HFHS. Le traitement a également diminué le poids du foie, l'accumulation de triglycérides, les niveaux de stress oxydatif etd'inflammation hépatique. L'administration de CE a aussi amélioré la sensibilité à l'insuline, révélée par une meilleure tolérance à l'insuline, une réduction de l'indice HOMA-IR et une diminution de l'hyperinsulinémie lors d'un test oral de tolérance au glucose. Le traitement avec le CE a réduit de mannière importante la teneur en triglycérides intestinaux, tout en atténuant l'inflammation intestinale et le stress oxydatif. Fait intéressant, le traitement avec le CE a occasionné une augmentation marquée de la proportion de la bactérie *Akkermansia muciniphila* dans le microbiote fécal des souris.Conclusions: Le CE exerce des effets métaboliques bénéfiques en améliorant des caractéristiques typiques du syndrome métabolique en association à une augmentation proportionnelle d' *Akkermansia muciniphila* dans le microbiote intestinal.

Abstract

Objective: The increasing prevalence of obesity and type 2 diabetes (T2D) demonstrates the failure of conventional treatments to curb these diseases. The gut microbiota has been put forward as a key player in the pathophysiology of diet-induced T2D. Importantly, cranberry (*Vaccinium macrocarpon* Aiton) is associated with a number of beneficial health effects. We aimed to investigate the metabolic impact of a cranberry extract (CE) on high fat/high sucrose (HFHS)-fed mice and to determine whether its consequent antidiabetic effects are related to modulations in the gut microbiota. Design: C57BL/6J mice were fed either a Chow or a HFHS diet. HFHS-fed mice were gavaged daily either with vehicle (water) or CE (200 mg/kg) for 8 weeks. The composition of the gut microbiota was assessed by analyzing 16S rRNA gene sequences with 454 pyrosequencing. Results: CE treatment was found to reduce HFHS-induced weight gain and visceral obesity. CE treatment also decreased liver weight and triglyceride accumulation in association with blunted hepatic oxidative stress and inflammation. CE administration improved insulin sensitivity, as revealed by improved insulin tolerance, lower HOMA-IR and decreased glucose-induced hyperinsulinemia during an oral glucose tolerance test. CE treatment was found to lower intestinal triglyceride content and to alleviate intestinal inflammation and oxidative stress. Interestingly, CE treatment markedly increased the proportion of the mucin-degrading bacterium *Akkermansia* in our metagenomic samples. Conclusions: CE exerts beneficial metabolic effects through improving HFHS diet-induced features of the metabolic syndrome, which is associated with a proportional increase in *Akkermansia spp*. population.

Introduction

Type 2 diabetes (T2D) and cardiovascular diseases (CVD) are well known consequences of a combination of pathological conditions defined as the metabolic syndrome, which comprises obesity, hyperglycemia, glucose intolerance, dyslipidemia, insulin resistance and hypertension (414). T2D is characterized by a complex interplay between genetic background and environmental influences, such as dietary habits, which leads to an insulin-resistant state (2-4). The molecular mechanisms underlying insulin resistance and the onset of associated metabolic alterations are related to a low-grade subclinical inflammation, triggered by an increased release and action of proinflammatory cytokines, which can impede insulin receptor signaling in skeletal muscle, liver, intestine and adipose tissue (5-10). Moreover, the intestinal epithelium, along with its colonizing bacteria, represents a first site of interactions between diet and the host immune system. Such an interaction can impact on the composition of the gut microbiota (11), which in turn directly affects the gut-immune homeostasis and intestinal permeability (12). The intestine and its microbial flora are therefore a potential source of proinflammatory molecules that can affect whole-body metabolism, possibly representing an early event that precedes and predisposes to obesity and insulin resistance (13).

Growing evidence supports that the gut microbiota plays a decisive role in energy homeostasis through modulating energy balance (14; 15), glucose metabolism (16-18) and the chronic inflammatory state associated with obesity (16; 19-21). The gut microbiota-derived lipopolysaccharide (LPS), a potent inducer of inflammation, plays an important role in the onset and progression of inflammation and related metabolic diseases (17). For instance, high-fat diet intake has been shown to be associated with elevated portal and systemic circulating levels of LPS (*i.e.* metabolic endotoxemia) (17; 22). These findings suggest a link between the gut microbiota-derived endotoxin and the pathogenesis of non-alcoholic fatty liver disease (NAFLD), thereby evidencing a key role for the intestinal microbiota as an orchestrator of the gut-liver axis. Metabolic endotoxemia is driven by increased

intestinal permeability to LPS because of the disruption of the gut barrier function (16; 17; 23) and/or enhanced LPS transport via chylomicrons particles in response to fat feeding (24; 25).

High fat diet has been reported to reshape the gut microbiota, particularly by increasing the proportion of *Firmicutes* in relation to *Bacteroidetes* (22; 26)*,* which is thought to play a key role in the pathogenesis of obesity-induced metabolic diseases (16; 19; 27). Furthermore, growing evidence indicates that increased intestinal abundance of *Akkermansia* spp. can protect against obesity-linked metabolic syndrome (28) and contributes to the beneficial metabolic effects of gastric bypass surgery and of the anti-diabetic drug metformin (29; 30). *Akkermansia* is a Gram-negative, strict anaerobe and mucin-degrading bacterium that lives in the mucus layer of the intestine and represents 1-3% of the total gut microbiota (31). Despite steady advances in understanding the complex pathophysiology of metabolic disorders, obesity and T2D have grown to worrisome pandemic proportions, therefore urging the search for new therapeutic approaches.

American cranberry (*Vaccinium macrocarpon Aiton*) is an important source of phytochemicals, especially polyphenols (32), and is widely consumed in North America. Its high polyphenol content is related to an important antioxidant activity (33; 34), which is particularly relevant in the context of the gastro-intestinal physiology (35). Interestingly, cranberry proanthocyanidins (PAC) have been recently shown to improve the gut mucus layer morphology in mice (36). Moreover, cranberries are also related to anticarcinogenic (37; 38), anti-inflammatory (39-41) and antimicrobial effects, the latter being mainly due to changes in the surface hydrophobicity and biofilm formation of P-fimbriated *Escherichia coli*, a species related to urinary tract infection (UTI) (42; 43). Interestingly, cranberry administration has been reported to ameliorate dyslipidemia, hyperglycemia and oxidative stress in individuals with the metabolic syndrome (44-46). However, the underlying mechanisms of the beneficial effects of cranberry consumption remain largely unknown. The main goal of the present study was to define the metabolic

influence of a cranberry extract (CE) on high fat/high sucrose (HFHS)-fed mice and to determine whether its potential health effects are related to the modulation of the gut microbiota.

Material and methods

Animals. Eight-week-old C57Bl/6J male mice (n=36, Jackson, USA) were bred, two animals per cage in the animal facility of the Quebec Heart and Lung Institute. Animals were housed in a controlled environment (12 hours daylight cycle, lights off at 18:00) with food and water *ad libitum*. After two weeks of acclimation (week 0 and week 1) on a normal-chow diet (Teklad 2018, Harlan), mice were fed either a chow or a high-fat high-sucrose (HFHS) diet containing 65% lipids, 15% proteins and 20% carbohydrates. Animals were randomly divided in three groups of 12 mice, and one group (assigned as CE) received daily doses (200 mg/kg) of cranberry extract (CE) by gavage, whereas the other two groups (assigned as Chow and HFHS) received the vehicle (water). Feces were collected by the end of weeks 0, 1, 5 and 9 for subsequent metagenomic analysis (Figure S1). Body weight gain and food intake were assessed twice a week. After 8 weeks of HFHS feeding, animals were anesthetized in chambers saturated with isoflurane and then sacrificed by cardiac puncture. Blood was drawn in EDTA-treated tubes and immediately centrifuged in order to separate plasma from cells. Subcutaneous and visceral fat pads were carefully collected along with gastrocnemius muscle, liver and intestine. All procedures were previously approved by the Laval University Animal Ethics Committee.

Cranberry extract. Cranberry powdered extract was obtained from Nutra Canada (Quebec, Canada). Its phenolic characterization is shown in Table 1. Cranberry extract (CE) was diluted in water at a concentration of 40 mg of CE powder per mL. The detailed methodology used to perform the phenolic characterization of the cranberry extract is described in the online supplementary methods.

Glucose homeostasis. At week 7*,* animals were 6 hours fasted and an insulin tolerance test (ITT) was performed after an intraperitoneal injection of insulin (0.75 UI/kg body weight). Blood glucose concentrations were measured with an Accu-Check glucometer (Bayer) before (0 min) and after (5, 10, 15, 20, 25, 30 and 60 min) insulin injection. At the end of the week 8, mice were fasted overnight and an oral glucose tolerance test (OGTT) was performed after gavage with glucose (1 g/kg body weight). Blood was collected before (0 min) and after (15, 30, 60, 90 and 120 min) glucose challenge for glycemia determination. Additionally, blood samples (~30µL) were collected at each time point during OGTT for insulinemia and C-peptide determination.

Analytical methods. Plasma insulin and C-Peptide concentrations were measured using an ultra-sensitive ELISA kit (Alpco, Salem, USA). The homeostasis model assessment of insulin resistance (HOMA-IR) index was calculated based on the following formula: fasting insulinemia (µUI/mL) x fasting glycemia (mM)/22.5. Liver and jejunal triglyceride (TG) as well as cholesterol content was assessed after chloroform-methanol extraction and enzymatic reactions with commercial kits (Randox Laboratories, Crumlin, UK). Phospholipids were measured by the Bartlett technique as described previously (47). Lipid peroxidation was estimated by measuring the production of free malondialdehyde (415) in jejunal and hepatic tissues using HPLC with fluorescence detection as described previously (10; 48). Briefly, proteins were first precipitated with a 10% sodium tungstate solution (Sigma). The protein-free supernatants was then reacted with an equivalent volume of 0.5% (wt/v) thiobarbituric acid solution (Sigma) at 95°C for 60 min. After cooling to room temperature, the pink chromogene thiobarbituric acid 2-MDA was extracted with 1-butanol and dried over a stream of nitrogen at 37°C. The dry extract was then resuspended in a potassium dihydrogen phosphate-methanol mobile phase (70:30, pH 7.0) before MDA determination. For the assessment of the endogenous antioxidant defense, tissue samples were homogenized in a buffer (50 mM Tris-HCl and 0.1 mM EDTA-Na$_2$ pH 7.8),

centrifuged at 10,000 x g for 5 min at 4°C and the supernatants were collected. The activities of superoxide dismutase (262) and glutathione peroxidase (GPx) were determined as described previously (10). Total SOD activity was determined as described by McCord et al (49) while SOD2 activity was examined in the presence of sodium diethyldithiocarbamate (1 mM) that allows defining the contribution of MnSOD activity. For GPx activity, hepatic or jejunal tissue homogenates were added to a PBS buffer (pH 7.0) containing 10 mM GSH, 0.1 U of G-Red, and 2 mM NADPH with 1.5% H_2O_2 to initiate the reaction. Absorbance was monitored every 30 s at 340 nm for 5 min. Plasma LPS concentration was determined using a kit based on a Limulus amebocyte extract (LAL kit endpoint-QCL1000, Lonza, Switzerland).

Metagenomic analysis. The methods used to analyze the bacterial taxonomic profiles of the murine gut microbiome are described in the online supplementary methods.

Statistical Analyses. Data are expressed as mean ± SEM. Statistical analysis was performed using one-way ANOVA with a post-hoc Bonferroni multiple comparison test (GraphPad, USA). Body weight gain and energy intake curves were statistically compared using two-way repeated measures ANOVA with a Student-Newman-Keuls posthoc-test (Sigmaplot, USA). All results were considered statistically significant at $P < 0.05$.

Results

Effects of cranberry extract on body weight gain, plasma lipid profile and liver homeostasis. As depicted in Figure 1A-B, CE administration to HFHS-fed animals prevented weight gain and this effect was seen as early as 7 days post-CE treatment. Although this was associated with a small reduction in total energy intake, this effect became significant only from the 24th day onwards (Figures 1C, 1D). Additionally, CE administration to HFHS-fed mice significantly reduced the ratio of weight gain/energy intake in comparison with untreated HFHS animals

(Figure 1G), suggesting that the preventive effect of CE on weight gain is mostly related to a decrease in energy efficiency. Interestingly, the CE-induced effect on weight gain was particularly evident in visceral adipose tissue (Figure 1E), whereas no significant difference in subcutaneous fat mass was found between HFHS-fed control mice and CE-treated animals (Figure 1F). Moreover, CE administration reduced liver weight (Figure 2C) while concomitantly lowering hepatic triglyceride accumulation (Figure 2D) and ameliorating HFHS-induced hypertriglyceridemia (Figure 2A) and hypercholesterolemia (Figure 2B) in these animals. CE also decreased liver oxidative stress as indicated by a complete prevention of HFHS-mediated malondialdehyde (MDA, Figure 2E) and by improvements of antioxidant defense mechanisms, as revealed by restoration of superoxide dismutase 2 (SOD2, Figure 2G) along with a tendency to improve glutathione peroxidase (GPx, Figure 2H) and superoxide dismutase (SOD, Figure 2F) activity in the liver of HFHS-fed mice. Inflammation was also decreased in the liver of CE-treated HFHS-fed mice, as revealed by normalization of the transcription factor NFκB/IκB ratio (Figure 2K). This was not explained by reduced TNF-α levels in the liver (Figure 2J), whereas COX2 protein synthesis was neither affected by the dietary or CE treatments (Figures 2I).

Impact of cranberry extract on diet-induced insulin resistance. We next determined the impact of CE treatment on glucose homeostasis and insulin sensitivity. Although CE-treated HFHS-fed mice did not display improved fasting glycemia, these animals showed significant lower fasting insulinemia when compared to untreated HFHS-fed animals (Figures 3A-3B), suggesting that CE improved insulin sensitivity in these animals. We next performed insulin and oral glucose tolerance tests in order to further examine the effect of CE on insulin sensitivity and glucose homeostasis. CE-treated HFHS mice displayed improved insulin sensitivity in comparison to HFHS controls as revealed by insulin tolerance tests (Figures 3C, 3D). Although CE administration did not improve HFHS-induced glucose intolerance (Figures 3E, 3F), the lower plasma insulin and c-peptide levels measured during the oral glucose tolerance tests further confirmed that CE

treatment improves insulin sensitivity (Figures 3G-3J). This conclusion is also supported by the lower HOMA-IR index values of the CE-treated HFHS-fed mice as compared to their vehicle-treated HFHS controls (Figure 3K).

Influence of cranberry extract administration on diet-induced intestinal inflammation and metabolic endotoxemia. Diet-induced obesity has been previously reported to cause metabolic endotoxemia, oxidative stress and low-grade inflammation that is associated with increased intestinal permeability, as revealed by elevated circulating LPS levels (16; 17). In accordance with previous studies, eight weeks of HFHS feeding produced a 2-fold increase in circulating LPS which was fully prevented by CE administration. (Figure 4A). This finding was associated with a CE-induced reduction in jejunal triglycerides (Figure 4B). To further assess the impact of CE administration on intestinal oxidative stress and inflammation, we investigated lipid peroxidation and the expression of key inflammatory modulators in the jejunum of Chow, HFHS and CE-treated HFHS animals. No significant changes were noted in MDA and SOD among groups (Figures 4C and 4D). However, CE treatment was found to prevent the decrease in SOD2 activity by HFHS (Figures 4E) without any effects on GPx (Figures 4F). Importantly, CE administration fully prevented HFHS diet-induced intestinal inflammation, as evidenced by the reduced COX2 and TNFα protein expression as well as by the normalization of NFκB/IκB ratio (Figures 4G-4E).

Effects of cranberry extract administration on the gut microbiota. The overall composition of the bacterial community in the different groups was assessed by analyzing the degree of bacterial taxonomic similarity between metagenomic samples at the genus level. Bacterial communities were clustered using principal component analysis (PCA), which distinguished microbial communities based both on diet/treatment and time of fecal sampling (weeks 0, 1, 5 and 9). As shown in Figure 5A, PCA disclosed that distinct diets promoted the main alterations in the gut microbiota of mice. From week 5 onwards, chow-fed mice metagenomes clustered very distinctly from those of HFHS-fed animals. On the other hand, after

61

5 and 9 weeks of CE administration, samples from CE-treated HFHS-fed mice formed a cluster that was different from metagenomes derived from untreated HFHS-fed animals. These results indicate that CE administration had a substantial effect on the gut microbial composition of HFHS-fed mice. Further analysis at the *phylum* level revealed that the proportion of sequences assigned to *Firmicutes* was significantly increased in metagenomes of HFHS-fed animals, whereas reads assigned to *Bacteroidetes* were reduced in these samples. A similar trend observed for the *Bacteroidetes phylum* in metagenomes from untreated HFHS-fed animals was found in samples from CE-treated HFHS-fed mice. Furthermore, the relative abundance of *Verrucomicrobia* was significantly higher at week 9 compared to week 1 in metagenomes of CE-treated mice (Figure 5B and S2). Finally, pre-treatment with CE (*i.e.* one week before day 0 of HFHS feeding, see Figure S1) was not associated with specific changes in the baseline metagenome (week 1) of CE mice when compared with untreated groups (Figure S4).

The HFHS diet-induced rise in the relative abundance of *Firmicutes* was mostly explained by an increase of reads assigned to species from the genus *Oscillibacter* (Figure 5C), whereas the decreased proportion of *Bacteroidetes* found at week 9 was associated with a reduction in sequences assigned to the *Barnesiella* genus and other unclassified members of the *Porphyromonadaceae* family. Importantly, CE administration was associated with a striking 30% increase in the relative abundance of *Akkermansia* in the CE-treated mice metagenome at week 9 (Figure 5C).

Discussion

There is growing evidence that the consumption of fruits and plant-derived foods is inversely correlated with several features of the metabolic syndrome, thus reducing the risk of T2D and CVD (50-53). Despite the positive health effects possibly arising from the presence of vitamins, minerals and dietary fibers in fruits, there is a growing body of literature now supporting a key role for polyphenols in the protection against obesity-related diseases (54; 55). Given that cranberry is

one of the fruits with the highest phenolic content (56), which includes a remarkable amount of proanthocyanidins (PAC) (32; 57), we have elected to explore its impact on several components of the metabolic syndrome. We found that CE administration prevents HFHS-induced weight gain and reduced visceral adiposity. Moreover, the effect on weight gain was observed before any difference in caloric intake was noticed, and was mostly linked to reduced energy efficiency. CE gavage fully prevented the development of fatty liver disease, as revealed by reduced triglyceride accumulation and blunted hepatic inflammation, which was associated with restoration of antioxidant defense mechanisms. These preventive effects on visceral obesity and liver steatosis were associated with improved insulin sensitivity, as revealed by lower fasting and post-glucose insulinemia, improved insulin tolerance and a lower HOMA-IR index in CE-treated HFHS-fed mice. Glucose tolerance *per se* was not improved by CE treatment, but this may be explained by the high glucose challenge during the OGTT, which is quite important as compared to the glucose load generated by a complex meal, thus possibly overwhelming the tissues' ability to uptake more glucose, even in the context of an improved insulin sensitivity.

Phenolic phytochemicals are generally poorly absorbed, and this has been put forward to suggest that these compounds are possibly acting primarily at the level of intestinal absorption (58; 59). Furthermore, several reports have demonstrated that the gut microbiota has a causal role in the pathogenesis of obesity and T2D (12; 28; 30; 60;). This prompted us to investigate the impact of CE administration on the gut microbiota in the present study. Our results show that HFHS feeding induced a dramatic shift in the gut microbiota of mice by increasing the proportion of *Firmicutes* and decreasing the proportion of *Bacteroidetes*. This diet-induced reshape in the microbial community of HFHS-fed mice is a typical characteristic of obesity-driven dysbiosis, and is in agreement with previous publications (11; 60; 61; 62), as was the finding of an increased presence of the genus *Oscillibacter* in obese mice (63).

The beneficial effects of CE treatment on metabolic phenotypes were associated with a robust modulation in the relative abundance of *Akkermansia* spp., as suggested by the higher representation (30%) of reads assigned to this genus in CE metagenome at week 9 in comparison with week 1*.* To the best of our knowledge, this is the first report of a fruit extract exerting such a major effect on the presence of *Akkermansia* in the intestinal microbiota of an animal model of diet-induced obesity. Interestingly, administration of green tea polyphenols to high fat-fed mice has also been recently associated with an increase in the proportion of *Akkermansia* (64), whereas Kemperman *et* al. showed that complex polyphenols from black tea and from a grape juice/red wine mixture, in the context of a simulator of the human intestinal microbial ecosystem *(i.e.* SHIME), increased the relative proportion of *Akkermansia* (65). Moreover, the metabolic benefits of gastric bypass surgery and of the antidiabetic drug metformin have been also linked to an increased intestinal abundance of this bacterium (29; 30). We found that the CE-mediated increase in the relative abundance of *Akkermansia* was associated with the prevention of the HFHS-induced rise in circulating LPS and abrogation of intestinal inflammation in these animals. Although we have not directly established the causal relationship between CE-induced increase in the relative proportion of *Akkermansia* population and the improved features of the metabolic syndrome in CE-treated HFHS-fed mice, it has been already reported that oral administration of *Akkermansia* (*i.e.* as a probiotic) reverses high fat diet-induced metabolic disorders (28) and could also mimic the antidiabetic effects of metformin in diabetic mice (30). Importantly, our results further suggest that the CE-related increase in *Akkermansia* population might be sufficient to prevent the negative metabolic phenotype associated with obesity-driven dysbiosis without major modifications in the proportions of *Firmicutes* and *Bacteroidetes*.

Hepatic triglyceride accumulation is a measure of steatosis, which in combination with oxidative stress and inflammation may lead to NAFLD, the most important cause of liver disease in western countries that usually develops in the setting of insulin resistance and obesity (66). LPS derived from the gut microbiota

reaches the portal circulation and thus can access the liver to affect host metabolic physiology in critical ways (67). Elevated levels of circulating LPS in obese individuals have been shown to be a consequence of nutrient overload and high-fat-induced changes in the gut microbiota (17). Furthermore, metabolic endotoxemia (*i.e.* increased circulating LPS after an obesogenic diet) is explained by the transport of LPS from the gut lumen by newly synthesized chylomicrons from enterocytes in response to fat feeding (24; 25) and by a gut microbiota-dependent disruption of the gut barrier, thus favoring LPS leakage (16; 17; 23). Interestingly, besides the fact that *Akkermansia* utilizes mucins as a food supply, it seems to be crucial for the mucus layer integrity (28; 68). *Akkermansia* administration as a probiotic was reported to reduce systemic LPS levels in high-fat fed mice, which is possibly associated with the ability of *Akkermansia* to preserve the mucus layer thickness, therefore reducing gut permeability and LPS leakage (28). Taken together, these observations suggest that CE, by increasing the presence of *Akkermansia*, may reduce intestinal permeability and LPS leakage, therefore ameliorating insulin resistance in diet-induced obese mice. Accordingly, the ability of CE to blunt circulating LPS levels may be accounted for the reduced hepatic triglyceride accumulation and protection from hepatic oxidative stress and inflammation in HFHS-fed mice.

Intestinal inflammation is growingly recognized to play a major role in the early deterioration of glucose and lipid metabolism in models of obesity and insulin resistance (13). Remarkably, CE administration was found to completely suppress NFκB activation in the intestine of HFHS-fed mice. NFκB is a central regulator of metabolic inflammation and controls the production of several pro-inflammatory cytokines, including TNFα. CE treatment reduced the amount of TNFα in the intestine and also decreased COX2 protein expression, an enzyme crucial for the synthesis of several pro-inflammatory molecules. Additionally, CE administration was found to increase the activity of SOD2, suggesting that it could exert some of its effects through promoting oxidant defense mechanisms in the intestine. It has been suggested that interactions between diet and enteric bacteria are necessary

for inducing inflammatory changes in the intestine and to impact on diet-induced obesity and insulin resistance (13). Therefore, our observations suggest that CE treatment, acting as a prebiotic, may be a novel strategy against intestinal inflammation and the prevention of the metabolic syndrome.

The mechanisms by which phenolic phytochemicals may exert prebiotic effects and reshape the gut microbiota with benefits to the host are still unclear. It has been suggested that *Akkermansia* can display a rapid growth rate in order to monopolize the resources when competition is low following an important ecological disruption (*e.g.* gastric bypass surgery, caloric restriction, antibiotic therapy) (69). CE is very rich in polyphenols, particularly phenolic acids, flavan-3-ols (*e.g.* catechin, epicatechin) and PAC (Table 1). These molecules have been shown to possess remarkable antibacterial activity (43; 70; 71), and can potentially reshape the gut microbiota ecology of obese mice. One explanation is that this latter effect could be associated with a reduction in the abundance of species capable of holding *Akkermansia* in check, thus favoring a rise in its proportion. In fact, a polyphenol extract of wine and grapes stimulated the growth of *Akkermansia* while exerting profound antimicrobial activity in the transversal colon of a gut biofermentor model (65). Moreover, this hypothesis is supported by the fact that broad-spectrum antibiotic treatment increases the proportion of *Akkermansia* in humans (72). Another explanation is that CE, through their high PAC content, influences the production of mucin and thereby provides ample trophic resources for *Akkermansia* to thrive. Indeed, cranberry PAC have been shown to increase the differentiation of goblet cells and to preserve the production of luminal Mucin 2 (Muc2) in mice fed through elemental enteral nutrition, a treatment known to decrease the mucosal barrier (36). Conversely, we found that CE administration is associated with increased Kruppel-like factor 4 (Klf4) – a marker of goblet cells – and Muc2 mRNA expression in the proximal colon (Figure S3), which supports the hypothesis that these condensed tannins are able to stimulate mucus production and therefore create an ecological niche for the mucus-eating bacterium *Akkermansia*. Importantly, since it has been reported that *Akkermansia* administration, *per se*, can reestablish the mucus layer integrity in diet-induced

obese mice (28), it is possible that a direct trophic effect of CE on *Akkermansia* precedes the positive effects found on the mucus layer integrity. Finally, *Akkermansia* contributes to the restoration of antimicrobial peptides such as Regenerating islet-derived protein 3 gamma (RegIIIγ) (28). Although our results did not show a statistically significant modulation of Reg3g by CE treatment, we did observe a trend for modulation of this antimicrobial marker that would suggest that CE stimulates the induction of antimicrobial defenses, which is possibly linked with higher *A. muciniphila* abundance in these animals. Further investigations are definitely warranted in order to better understand the prebiotic effects of CE on *Akkermansia*.

The use of *Akkermansia* as a probiotic in humans, although a promising strategy, may find some barriers. Its *in vitro* culture is technically complex and time-consuming, suggesting that the production of *Akkermansia* as a commercial-scale probiotic may be costly. Therefore, finding alternative methods to increase the presence of *Akkermansia* spp. in the gut microbiota seems a valid, safe and likely more cost-effective approach. In addition, given the fact that cranberries are already highly consumed (especially in North America), using CE as a prebiotic might be an interesting strategy to ease adherence to the treatment when compared to the introduction of a novel probiotic strain. Moreover, the dose used in this study in mice may represent a feasible dose in humans. By applying the US Food and Drug Administration's guidelines to establish the human equivalent dose based on body surface area (73), we found that a 16 mg/kg dose would be the human equivalent of a 200 mg/kg dose in mice. This is perfectly achievable by supplementation or by incorporating CE in other food products.

While our study provides evidence for the beneficial metabolic effects of CE treatment, some limitations must be acknowledged. First, while we have found that the CE treatment improves insulin sensitivity, based on ITT analysis, HOMA-IR and fasting and post-glucose insulin levels, future studies that uses the euglycemic clamp technique together with isotopic tracers could be performed to further confirm this effect of CE and to determine the contribution of the liver and

peripheral tissues to this phenotype. Moreover, we acknowledge that the pooling of samples used to analyse the metagenomic bacterial diversity of the mice constitutes another limitation of this study, but allowed us to focus on the shifts occurring within the dominant phylotypes due to the different treatments.

In summary, we found that CE treatment protects from diet-induced obesity, liver steatosis and insulin resistance in HFHS-fed mice. This effect was associated with alleviation of metabolic endotoxemia and intestinal inflammation. Our study further suggests that the ability of CE administration to raise the relative proportion of *Akkermansia* is playing a key role in this protective effect, leading us to propose that fruit polyphenols may prevent obesity and the metabolic syndrome through a prebiotic effect on the gut microbiota.

Competing interests: The authors declare no conflict of interest.

References

1. Eckel R, Grundy S, Zimmet P: The metabolic syndrome. Lancet 2005;365:1415-1428

2. Hossain P, Kawar B, El Nahas M: Obesity and diabetes in the developing world--a growing challenge. The New England journal of medicine 2007;356:213-215

3. Doria A, Patti ME, Kahn CR: The emerging genetic architecture of type 2 diabetes. Cell Metab 2008;8:186-200

4. Walley AJ, Asher JE, Froguel P: The genetic contribution to non-syndromic human obesity. Nat Rev Genet 2009;10:431-442

5. Marette A: Mediators of cytokine-induced insulin resistance in obesity and other inflammatory settings. Current opinion in clinical nutrition and metabolic care 2002;5:377-383

6. Freedman A, Freeman G, Rhynhart K, Nadler L: Selective induction of B7/BB-1 on interferon-gamma stimulated monocytes: a potential mechanism for amplification of T cell activation through the CD28 pathway. Cellular immunology 1991;137:429-437

7. Wellen K, Hotamisligil G: Inflammation, stress, and diabetes. The Journal of clinical investigation 2005;115:1111-1119

8. Weisberg S, McCann D, Desai M, Rosenbaum M, Leibel R, Ferrante A: Obesity is associated with macrophage accumulation in adipose tissue. The Journal of clinical investigation 2003;112:1796-1808

9. Xu H, Barnes G, Yang Q, Tan G, Yang D, Chou C, Sole J, Nichols A, Ross J, Tartaglia L, Chen H: Chronic inflammation in fat plays a crucial role in the development of obesity-related insulin resistance. The Journal of clinical investigation 2003;112:1821-1830

10. Veilleux A, Grenier E, Marceau P, Carpentier AC, Richard D, Levy E: Intestinal Lipid Handling: Evidence and Implication of Insulin Signaling Abnormalities in Human Obese Subjects. Arterioscler Thromb Vasc Biol 2014;

11. Cotillard A, Kennedy SP, Kong LC, Prifti E, Pons N, Le Chatelier E, Almeida M, Quinquis B, Levenez F, Galleron N, Gougis S, Rizkalla S, Batto JM, Renault P, Dore J, Zucker JD, Clement K, Ehrlich SD: Dietary intervention impact on gut microbial gene richness. Nature 2013;500:585-588

12. Arpaia N, Campbell C, Fan X, Dikiy S, van der Veeken J, deRoos P, Liu H, Cross JR, Pfeffer K, Coffer PJ, Rudensky AY: Metabolites produced by commensal bacteria promote peripheral regulatory T-cell generation. Nature 2013;504:451-455

13. Ding S, Chi MM, Scull BP, Rigby R, Schwerbrock NM, Magness S, Jobin C, Lund PK: High-fat diet: bacteria interactions promote intestinal inflammation which precedes and correlates with obesity and insulin resistance in mouse. PloS one 2010;5:e12191

14. Backhed F, Ding H, Wang T, Hooper LV, Koh GY, Nagy A, Semenkovich CF, Gordon JI: The gut microbiota as an environmental factor that regulates fat storage. Proceedings of the National Academy of Sciences of the United States of America 2004;101:15718-15723

15. Turnbaugh PJ, Ley RE, Mahowald MA, Magrini V, Mardis ER, Gordon JI: An obesity-associated gut microbiome with increased capacity for energy harvest. Nature 2006;444:1027-1031

16. Cani PD, Bibiloni R, Knauf C, Waget A, Neyrinck AM, Delzenne NM, Burcelin R: Changes in gut microbiota control metabolic endotoxemia-induced inflammation in high-fat diet-induced obesity and diabetes in mice. Diabetes 2008;57:1470-1481

17. Cani PD, Amar J, Iglesias MA, Poggi M, Knauf C, Bastelica D, Neyrinck AM, Fava F, Tuohy KM, Chabo C, Waget A, Delmee E, Cousin B, Sulpice T, Chamontin B, Ferrieres J, Tanti JF, Gibson GR, Casteilla L, Delzenne NM, Alessi MC, Burcelin R: Metabolic endotoxemia initiates obesity and insulin resistance. Diabetes 2007;56:1761-1772

18. Cani PD, Neyrinck AM, Maton N, Delzenne NM: Oligofructose promotes satiety in rats fed a high-fat diet: involvement of glucagon-like Peptide-1. Obesity research 2005;13:1000-1007

19. Cani PD, Possemiers S, Van de Wiele T, Guiot Y, Everard A, Rottier O, Geurts L, Naslain D, Neyrinck A, Lambert DM, Muccioli GG, Delzenne NM: Changes in gut microbiota control inflammation in obese mice through a mechanism involving GLP-2-driven improvement of gut permeability. Gut 2009;58:1091-1103

20. Rabot S, Membrez M, Bruneau A, Gerard P, Harach T, Moser M, Raymond F, Mansourian R, Chou CJ: Germ-free C57BL/6J mice are resistant to high-fat-diet-induced insulin resistance and have altered cholesterol metabolism. FASEB J 2010;24:4948-4959

21. Geurts L, Lazarevic V, Derrien M, Everard A, Van Roye M, Knauf C, Valet P, Girard M, Muccioli GG, Francois P, de Vos WM, Schrenzel J, Delzenne NM, Cani PD: Altered gut microbiota and endocannabinoid system tone in obese and diabetic leptin-resistant mice: impact on apelin regulation in adipose tissue. Frontiers in microbiology 2011;2:149

22. Cani PD, Neyrinck AM, Fava F, Knauf C, Burcelin RG, Tuohy KM, Gibson GR, Delzenne NM: Selective increases of bifidobacteria in gut microflora improve high-fat-diet-induced diabetes in mice through a mechanism associated with endotoxaemia. Diabetologia 2007;50:2374-2383

23. Muccioli GG, Naslain D, Backhed F, Reigstad CS, Lambert DM, Delzenne NM, Cani PD: The endocannabinoid system links gut microbiota to adipogenesis. Molecular systems biology 2010;6:392

24. Vreugdenhil AC, Rousseau CH, Hartung T, Greve JW, van 't Veer C, Buurman WA: Lipopolysaccharide (LPS)-binding protein mediates LPS detoxification by chylomicrons. J Immunol 2003;170:1399-1405

25. Ghoshal S, Witta J, Zhong J, de Villiers W, Eckhardt E: Chylomicrons promote intestinal absorption of lipopolysaccharides. J Lipid Res 2009;50:90-97

26. Hildebrandt MA, Hoffmann C, Sherrill-Mix SA, Keilbaugh SA, Hamady M, Chen YY, Knight R, Ahima RS, Bushman F, Wu GD: High-fat diet determines the composition of the murine gut microbiome independently of obesity. Gastroenterology 2009;137:1716-1724 e1711-1712

27. Everard A, Lazarevic V, Derrien M, Girard M, Muccioli GG, Neyrinck AM, Possemiers S, Van Holle A, Francois P, de Vos WM, Delzenne NM, Schrenzel J, Cani PD: Responses of gut microbiota and glucose and lipid metabolism to

prebiotics in genetic obese and diet-induced leptin-resistant mice. Diabetes 2011;60:2775-2786

28. Everard A, Belzer C, Geurts L, Ouwerkerk JP, Druart C, Bindels LB, Guiot Y, Derrien M, Muccioli GG, Delzenne NM, de Vos WM, Cani PD: Cross-talk between Akkermansia muciniphila and intestinal epithelium controls diet-induced obesity. Proceedings of the National Academy of Sciences of the United States of America 2013;

29. Liou AP, Paziuk M, Luevano JM, Jr., Machineni S, Turnbaugh PJ, Kaplan LM: Conserved shifts in the gut microbiota due to gastric bypass reduce host weight and adiposity. Science translational medicine 2013;5:178ra141

30. Shin NR, Lee JC, Lee HY, Kim MS, Whon TW, Lee MS, Bae JW: An increase in the Akkermansia spp. population induced by metformin treatment improves glucose homeostasis in diet-induced obese mice. Gut 2013;

31. Derrien M, Collado MC, Ben-Amor K, Salminen S, de Vos WM: The Mucin degrader Akkermansia muciniphila is an abundant resident of the human intestinal tract. Applied and environmental microbiology 2008;74:1646-1648

32. Blumberg JB, Camesano TA, Cassidy A, Kris-Etherton P, Howell A, Manach C, Ostertag LM, Sies H, Skulas-Ray A, Vita JA: Cranberries and their bioactive constituents in human health. Adv Nutr 2013;4:618-632

33. Neto CC: Cranberry and blueberry: evidence for protective effects against cancer and vascular diseases. Mol Nutr Food Res 2007;51:652-664

34. He X, Liu RH: Cranberry phytochemicals: Isolation, structure elucidation, and their antiproliferative and antioxidant activities. Journal of agricultural and food chemistry 2006;54:7069-7074

35. Denis MC, Furtos A, Dudonne S, Montoudis A, Garofalo C, Desjardins Y, Delvin E, Levy E: Apple peel polyphenols and their beneficial actions on oxidative stress and inflammation. PloS one 2013;8:e53725

36. Pierre JF, Heneghan AF, Feliciano RP, Shanmuganayagam D, Roenneburg DA, Krueger CG, Reed JD, Kudsk KA: Cranberry proanthocyanidins improve the gut mucous layer morphology and function in mice receiving elemental enteral nutrition. JPEN Journal of parenteral and enteral nutrition 2013;37:401-409

37. Deziel B, MacPhee J, Patel K, Catalli A, Kulka M, Neto C, Gottschall-Pass K, Hurta R: American cranberry (Vaccinium macrocarpon) extract affects human prostate cancer cell growth via cell cycle arrest by modulating expression of cell cycle regulators. Food & function 2012;3:556-564

38. Neto CC, Amoroso JW, Liberty AM: Anticancer activities of cranberry phytochemicals: an update. Mol Nutr Food Res 2008;52 Suppl 1:S18-27

39. Madrigal-Carballo S, Rodriguez G, Sibaja M, Reed JD, Vila AO, Molina F: Chitosomes loaded with cranberry proanthocyanidins attenuate the bacterial lipopolysaccharide-induced expression of iNOS and COX-2 in raw 264.7 macrophages. Journal of liposome research 2009;19:189-196

40. Kim MJ, Ohn J, Kim JH, Kwak HK: Effects of freeze-dried cranberry powder on serum lipids and inflammatory markers in lipopolysaccharide treated rats fed an atherogenic diet. Nutrition research and practice 2011;5:404-411

41. Kivimäki AS, Ehlers PI, Siltari A, Turpeinen AM, Vapaatalo H, Korpela R: Lingonberry, cranberry and blackcurrant juices affect mRNA expressions of

inflammatory and atherothrombotic markers of SHR in a long-term treatment. Journal of Functional Foods 2012;4:496-503

42. Foo LY, Lu Y, Howell AB, Vorsa N: A-Type proanthocyanidin trimers from cranberry that inhibit adherence of uropathogenic P-fimbriated Escherichia coli. Journal of natural products 2000;63:1225-1228

43. Uberos J, Iswaldi I, Belmonte RR, Segura-Carretero A, Fernández-Puentes V, Molina-Carballo A, Muñoz-Hoyos A: Cranberry (Vaccinium macrocarpon) changes the surface hydrophobicity and biofilm formation of E. coli. Microbiology Insights 2011;4:21-27

44. Shidfar F, Heydari I, Hajimiresmaiel SJ, Hosseini S, Shidfar S, Amiri F: The effects of cranberry juice on serum glucose, apoB, apoA-I, Lp(a), and Paraoxonase-1 activity in type 2 diabetic male patients. Journal of research in medical sciences : the official journal of Isfahan University of Medical Sciences 2012;17:355-360

45. Lee IT, Chan YC, Lin CW, Lee WJ, Sheu WH: Effect of cranberry extracts on lipid profiles in subjects with Type 2 diabetes. Diabetic medicine : a journal of the British Diabetic Association 2008;25:1473-1477

46. Basu A, Lyons TJ: Strawberries, blueberries, and cranberries in the metabolic syndrome: clinical perspectives. Journal of agricultural and food chemistry 2012;60:5687-5692

47. Spahis S, Vanasse M, Belanger SA, Ghadirian P, Grenier E, Levy E: Lipid profile, fatty acid composition and pro- and anti-oxidant status in pediatric patients with attention-deficit/hyperactivity disorder. Prostaglandins, leukotrienes, and essential fatty acids 2008;79:47-53

48. Levy E, Trudel K, Bendayan M, Seidman E, Delvin E, Elchebly M, Lavoie JC, Precourt LP, Amre D, Sinnett D: Biological role, protein expression, subcellular localization, and oxidative stress response of paraoxonase 2 in the intestine of humans and rats. American journal of physiology Gastrointestinal and liver physiology 2007;293:G1252-1261

49. McCord JM, Fridovich I: Superoxide dismutase. An enzymic function for erythrocuprein (hemocuprein). The Journal of biological chemistry 1969;244:6049-6055

50. Morimoto A, Ohno Y, Tatsumi Y, Mizuno S, Watanabe S: Effects of healthy dietary pattern and other lifestyle factors on incidence of diabetes in a rural Japanese population. Asia Pacific journal of clinical nutrition 2012;21:601-608

51. Bauer F, Beulens JW, van der AD, Wijmenga C, Grobbee DE, Spijkerman AM, van der Schouw YT, Onland-Moret NC: Dietary patterns and the risk of type 2 diabetes in overweight and obese individuals. European journal of nutrition 2013;52:1127-1134

52. Eshak ES, Iso H, Mizoue T, Inoue M, Noda M, Tsugane S: Soft drink, 100% fruit juice, and vegetable juice intakes and risk of diabetes mellitus. Clin Nutr 2013;32:300-308

53. Chan HT, Yiu KH, Wong CY, Li SW, Tam S, Tse HF: Increased dietary fruit intake was associated with lower burden of carotid atherosclerosis in Chinese patients with Type 2 diabetes mellitus. Diabetic medicine : a journal of the British Diabetic Association 2013;30:100-108

54. Corder R, Mullen W, Khan NQ, Marks SC, Wood EG, Carrier MJ, Crozier A: Oenology: red wine procyanidins and vascular health. Nature 2006;444:566

55. Anhê FF, Desjardins Y, Pilon G, Dudonné S, Genovese MI, Lajolo FM, Marette A: Polyphenols and type 2 diabetes: A prospective review. PharmaNutrition 2013;1:105-114

56. Vinson JA, Su X, Zubik L, Bose P: Phenol antioxidant quantity and quality in foods: fruits. Journal of agricultural and food chemistry 2001;49:5315-5321

57. Grace MH, Massey AR, Mbeunkui F, Yousef GG, Lila MA: Comparison of health-relevant flavonoids in commonly consumed cranberry products. Journal of food science 2012;77:H176-183

58. Manach C, Williamson G, Morand C, Scalbert A, Remesy C: Bioavailability and bioefficacy of polyphenols in humans. I. Review of 97 bioavailability studies. The American journal of clinical nutrition 2005;81:230S-242S

59. Cardona F, Andres-Lacueva C, Tulipani S, Tinahones FJ, Queipo-Ortuno MI: Benefits of polyphenols on gut microbiota and implications in human health. The Journal of nutritional biochemistry 2013;24:1415-1422

60. Caricilli AM, Picardi PK, de Abreu LL, Ueno M, Prada PO, Ropelle ER, Hirabara SM, Castoldi A, Vieira P, Camara NO, Curi R, Carvalheira JB, Saad MJ: Gut microbiota is a key modulator of insulin resistance in TLR 2 knockout mice. PLoS biology 2011;9:e1001212

61. Ley RE, Backhed F, Turnbaugh P, Lozupone CA, Knight RD, Gordon JI: Obesity alters gut microbial ecology. Proceedings of the National Academy of Sciences of the United States of America 2005;102:11070-11075

62. Ley RE, Turnbaugh PJ, Klein S, Gordon JI: Microbial ecology: human gut microbes associated with obesity. Nature 2006;444:1022-1023

63. Lam YY, Ha CW, Campbell CR, Mitchell AJ, Dinudom A, Oscarsson J, Cook DI, Hunt NH, Caterson ID, Holmes AJ, Storlien LH: Increased gut permeability and microbiota change associate with mesenteric fat inflammation and metabolic dysfunction in diet-induced obese mice. PloS one 2012;7:e34233

64. Axling U, Olsson C, Xu J, Fernandez C, Larsson S, Strom K, Ahrne S, Holm C, Molin G, Berger K: Green tea powder and Lactobacillus plantarum affect gut microbiota, lipid metabolism and inflammation in high-fat fed C57BL/6J mice. Nutrition & metabolism 2012;9:105

65. Kemperman RA, Gross G, Mondot S, Possemiers S, Marzorati M, Van de Wiele T, Doré J, Vaughan EE: Impact of polyphenols from black tea and red wine/grape juice on a gut model microbiome. Food Research International 2013;53:659-669

66. Gariani K, Philippe J, Jornayvaz FR: Non-alcoholic fatty liver disease and insulin resistance: From bench to bedside. Diabetes Metab 2012;

67. Vajro P, Paolella G, Fasano A: Microbiota and gut-liver axis: their influences on obesity and obesity-related liver disease. Journal of pediatric gastroenterology and nutrition 2013;56:461-468

68. Belzer C, de Vos WM: Microbes inside--from diversity to function: the case of Akkermansia. The ISME journal 2012;6:1449-1458

69. Cox LM, Blaser MJ: Pathways in microbe-induced obesity. Cell metabolism 2013;17:883-894

70. Rastmanesh R: High polyphenol, low probiotic diet for weight loss because of intestinal microbiota interaction. Chemico-biological interactions 2011;189:1-8

71. Feldman M, Grenier D: Cranberry proanthocyanidins act in synergy with licochalcone A to reduce Porphyromonas gingivalis growth and virulence properties, and to suppress cytokine secretion by macrophages. Journal of applied microbiology 2012;113:438-447

72. Dubourg G, Lagier JC, Armougom F, Robert C, Audoly G, Papazian L, Raoult D: High-level colonisation of the human gut by Verrucomicrobia following broad-spectrum antibiotic treatment. International journal of antimicrobial agents 2013;41:149-155

73. Reagan-Shaw S, Nihal M, Ahmad N: Dose translation from animal to human studies revisited. FASEB J 2008;22:659-661

Tables

Table 1: Chemical characterization of CE

	Extract content (g/100g dry weight)	Relative polyphenol content * (%)	Dailt intake (mg/kg body weight)
Total polyphenols	37.4 ±0.2		74.8 ±0.5
Phenolic acids	3.1 ±0.0	12.0 ±0.1	6.2 ±0.0
Flavonols	9.4 ±0.1	36.5 ±0.6	18.8 ±0.2
Total anthocyanins	3.3 ±0.0	12.6 ±0.0	6.6 ±0.0
Total proanthocyanidins	10.0 ±0.2	38.9 ±0.7	20.0 ±0.4
DP 1-3	6.1 ±0.2		12.2 ±0.2
DP > 3	3.9 ±0.2		7.8 ±0.4
Sugars	6.2 ±0.2		12.4 ±0.4
Glucose	4.9 ±0.1		9.8 ±0.1
Fructose	1.2 ±0.2		2.4 ±0.4
Fibers	2.5		5

* The relative polyphenol content has been calculated on the basis of the individually measured polyphenol content. Extract of cranberry (CE). Degree of polymerization (DP). The results are expressed as mean ± SD.

Figure legends

Figure 1. Effects of CE administration on body composition. Mice were fed either a chow or a high-fat/high sucrose (HFHS) diet for 8 weeks. HFHS-fed animals were treated with daily oral doses of CE (200 mg/kg). Chow- and HFHS-fed control mice were gavaged with vehicle (water). (A) Weight gain curves; (B) Total weight gain; (C) Energy intake curves; (D) Total energy intake; (E) Visceral and (F) Subcutaneous fat mass; (G) Energy efficiency (*i.e.* ratio between body weight gain and energy intake). n=11-12 (A, B, E and F); n=6-7 (D and E). Data are expressed as the mean ±SEM. *$p<0.05$ vs. Chow controls; #$p<0.05$ vs. HFHS controls.

Figure 2. **Effect of CE administration on plasma and liver lipid profiles, hepatic inflammation and oxidative stress.** CE administration to HFHS-fed mice prevented diet-induced increase in plasma triglycerides (A) and total cholesterol (B), whereas liver weight (C) and hepatic triglyceride accumulation (D) were reduced after CE treatment. Moreover, CE decreased liver oxidative stress as indicated by a complete prevention of HFHS-mediated malondialdehyde levels (E) and by improvements of antioxidant defense mechanisms, as revealed by restoration of superoxide dismutase 2 (G) and a tendency to improve glutathione peroxidase (H) and superoxide dismutase (F) activity in the liver of HFHS-fed mice. A trend towards lessening cyclooxygenase-2 protein expression (I) and a significant reduction in the NFκB/IκB ratio (K) were found after CE treatment. CE administration did not affect TNFα protein synthesis (J) in the liver. n=11-12 (A-D); n=6-7 (E-K). Data are expressed as the mean ±SEM. *$p<0.05$ vs. Chow controls; #$p<0.05$ vs. HFHS controls.

Figure 3. CE administration increases insulin sensitivity, alleviates diet-induced hyperinsulinemia and improves insulin resistance in HFHS-fed mice. Mice were 12 hours fasted for fasting glycemia (A) and fasting insulinemia (B) determination. Mice were 6 hours fasted and an insulin tolerance test (C) was performed after an intraperitoneal injection of insulin (0.75 UI/kg body weight). (D) Area under the curve for insulin tolerance tests. Animals were fasted overnight (12

h) and an oral glucose tolerance test (E) was performed after gavage with glucose (1 g/kg body weight). (F) Area under the curve for oral glucose tolerance tests. Blood samples were collected at each time point during OGTT for insulinemia (G, H) and C-peptide (I, J) determination. (K) Homeostasis model assessment of insulin resistance (HOMA-IR) index. n=11-12 (A, E and F); n=7-8 (B-D, G-K). Data are expressed as the mean ±SEM. *p<0.05 vs. Chow controls; #p<0.05 vs. HFHS controls.

Figure 4. **CE administration reduced circulating LPS and ameliorated oxidative stress and inflammation in the jejunum.** CE-treated mice displayed reduced circulating LPS levels in comparison with untreated HFHS-fed mice (A). Jejunal triglyceride accumulation (B) were lessened in CE-treated mice, however no changes were detected in malondialdehyde levels (C). CE administration increased superoxide dismutase 2 activity (E), whereas superoxide dismutase (D) and glutathione peroxidase (F) activities were unchanged after CE treatment. Cylooxygenase-2 (G) and TNFα (H) protein expression, as well as the NFκB/IκB ratio (I), were significantly reduced in CE-treated mice as compared to HFHS controls. n=6-7 (A-I). Data are expressed as the mean ±SEM. *p<0.05 vs. Chow controls; #p<0.05 vs. HFHS controls.

Figure 5. Metagenomic analysis. Feces were harvested at the end of the two first weeks of adaptation (week 0 and week 1), when all groups were pre-fed a Chow diet. Feces were also collected at the end of week 5 and week 9, representing respectively 4 and 8 weeks of HFHS feeding for HFHS and CE mice. Chow animals were fed a normal-chow diet throughout the study (see supplementary Figure S1 for further details). **(A) Principal component analysis of gut microbiota metagenomes.** The PCA analysis focus on grouping sampled fecal communities with respect to diet/treatment (Chow, HFHS, CE) and time of stool sampling (week 0, 1, 5, or 9) using principal components. This plot shows the degree of bacterial taxonomic similarity between metagenomic samples at the genus level; the closer the spatial distance between samples, the more similar they are with respect to both axes (PC1 and PC2). Chow: green dots; HFHS: yellow

triangles; CE: red squares. Samples with the highest taxonomic similarity are clustered together and illustrated in the plot by a grey circle. Samples representing the most dissimilar bacterial communities in comparison with the cluster of metagenomes included in the grey circle are identified by a yellow (HFHS) or red (CE) circle. **(B) Relative abundance distribution of OTU sequences (97% level).** Percentages of total OTU sequences taxonomically assigned to bacterial phyla from fecal metagenomes of Chow, HFHS or CE mice at weeks 0, 1, 5, and 9**. (C) Statistical comparisons of gut metagenomic profiles at the genus level.** Plots showing significant differences in abundance of reads assigned to a given bacterial genus between week 1 and week 9 for Chow, HFHS and CE diets. The bar graphs on the left side display the mean proportion of sequences assigned to each genus. The dot plots on the right side display the difference in mean proportions between week 1 and week 9 with associated q-value. Error bars on both sides of dots represent the 95% confidence intervals. Only features (genus) with a q-value of >0.05 and a difference between proportions value >1 were considered.

Figures

Figure 1: Effects of CE administration on body composition.
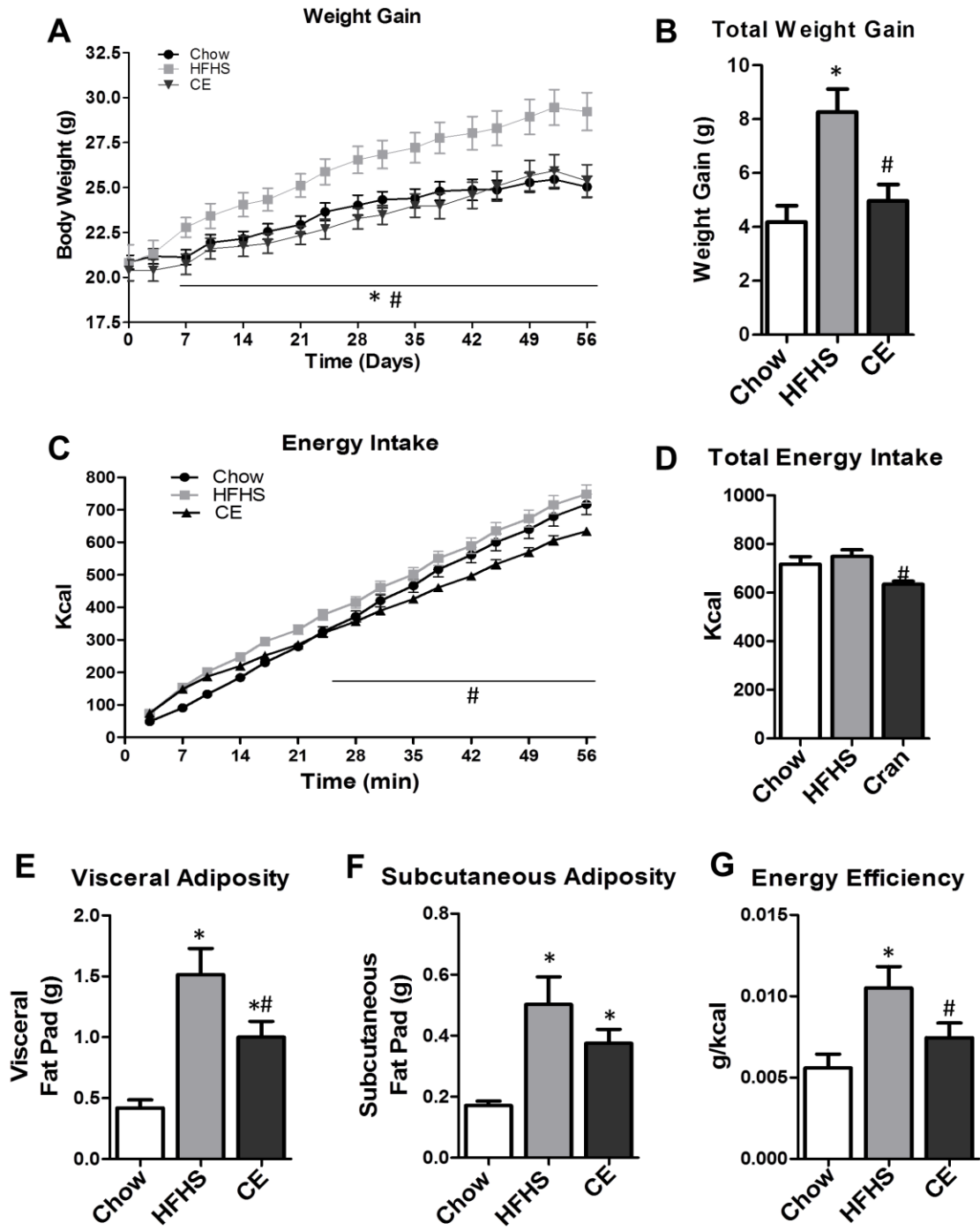
Figure 2: Effects of CE administration on plasma and liver lipid profiles, hepatic inflammation and oxidative stress.
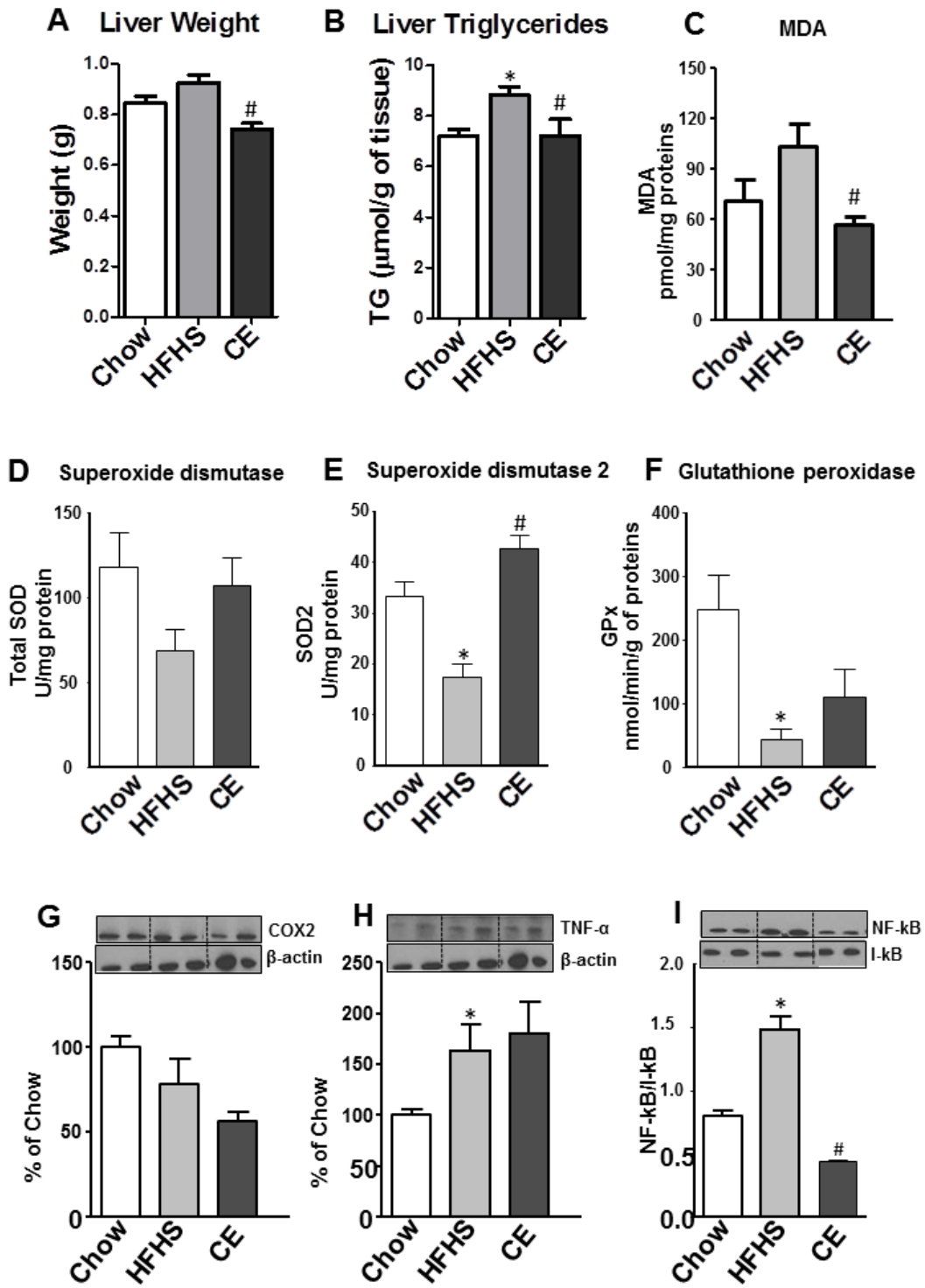
Figure 3: CE administration increases insulin sensitivity, alleviates diet-induced hyperinsulinemia and improves insulin resistance in HFHS-fed mice.
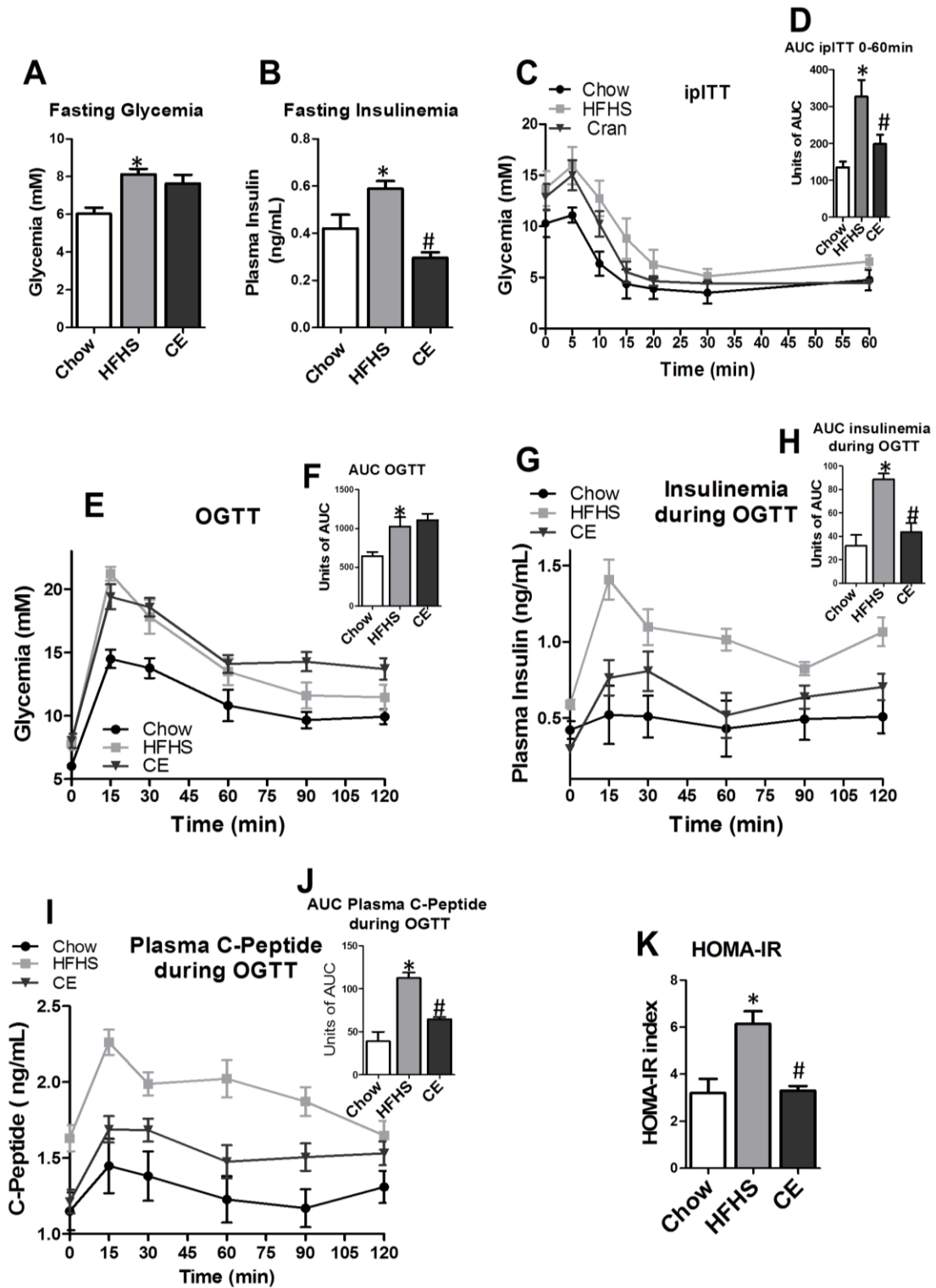
Figure 4: CE administration reduced circulating LPS and ameliorated oxidative stress and inflammation in the jejunum.
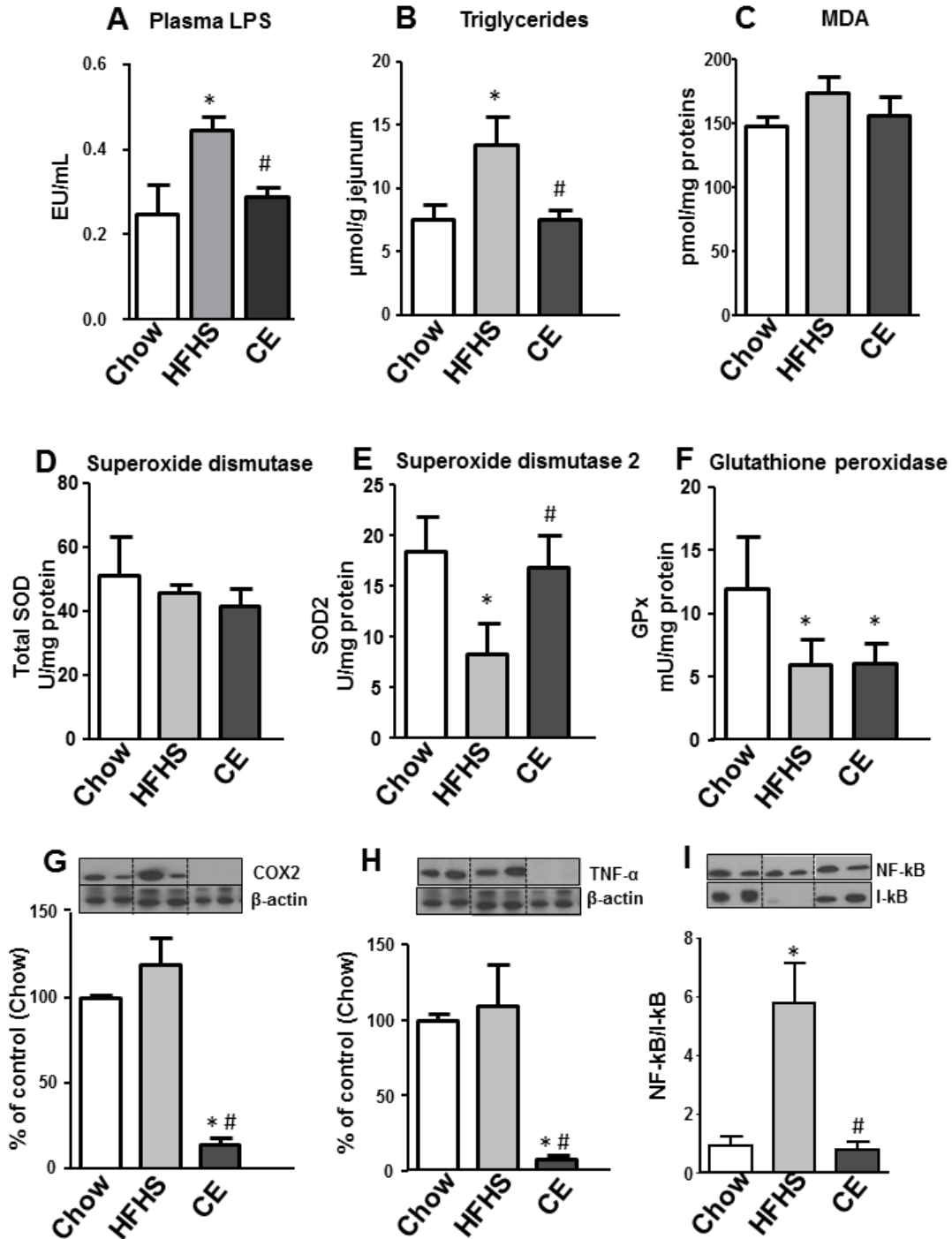
Figure 5: Metagenomic analysis.
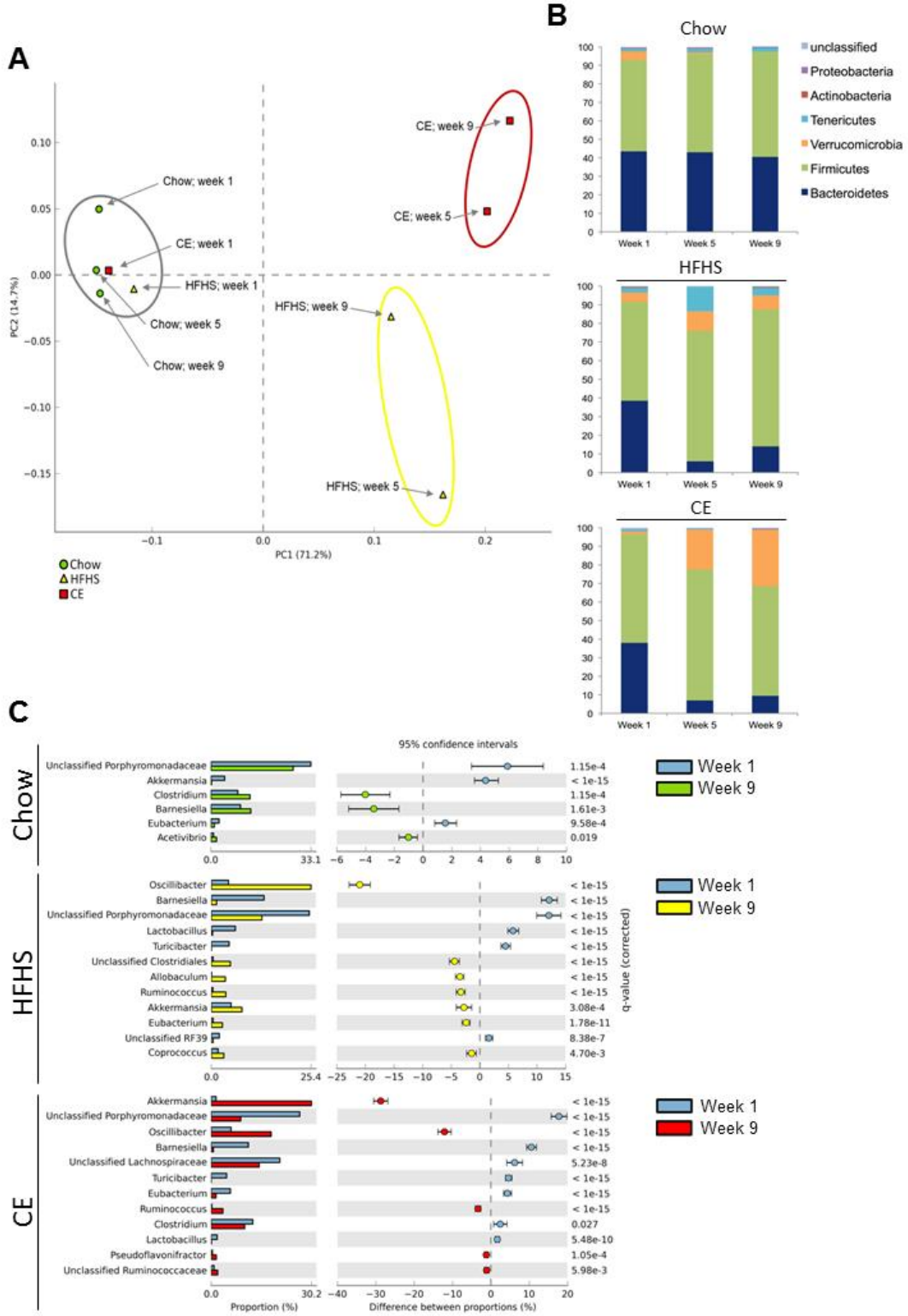
Supplemental material

Supplemental Figure S1. Experimental Design. Eight-week-old C57Bl/6J male mice (n=36, Jackson, USA) were bred two animals per cage in a controlled environment with food and water *ad libitum*. After two weeks of acclimation (week 0 and week 1) on a normal-chow diet (Teklad 2018, Harlan), mice were fed either a chow or a high-fat high-sucrose (HFHS) diet containing 65% lipids, 15% proteins and 20% carbohydrates. Animals were randomly divided in three groups of 12 mice, and one group (assigned as CE) started to receive daily doses (200 mg/kg) of cranberry extract (CE) by gavage, whereas the other two groups (assigned as Chow and HFHS) received the vehicle (water). Feces were collected by the end of weeks 0, 1, 5 and 9 for subsequent metagenomic analysis. Body weight gain and food intake were assessed twice a week. After 8 weeks of HFHS feeding, animals were anesthetized in chambers saturated with isoflurane and then sacrificed by cardiac puncture. Tissues and blood were collected for subsequent analysis.

Supplemental Figure S2. Statistical comparisons of gut metagenomic profiles at the phylum level. Plots showing significant differences in abundance of reads assigned to a given bacterial phylum between week 1 and week 9 for Chow, HFHS and CE mice. The bar graphs on the left side display the mean proportion of sequences assigned to each phylum. The dot plots on the right side display the difference in mean proportions between the week 1 and week 9 with associated q-value. Error bars on both sides of dots represent the 95% confidence intervals. Only features (genus) with a q-value of >0.05 and a difference between proportions value >1 were considered.

Supplemental Figure S3. Muc2, Klf4 and Reg3g mRNA expression in the jejunum and proximal colon. Mucin 2 (Muc2), Kruppel-like factor 4 (Klf4) and Regenerating islet-derived 3 gamma (Reg3g) mRNA expressions were analysed by qPCR. Total RNA was extracted from jejunum and proximal colon and used for cDNA synthesis. Hprt (hypoxanthine guanine phosphoribosyl transferase) was used as the housekeeping gene. Data were calculated according to the $2^{-\Delta\Delta Ct}$

method. Primer sequences for targeted mouse gene are available in Table S3. n=6-8. Data are expressed as the mean ±SEM. *$p<0.05$ vs. Chow controls; #$p<0.05$ vs. HFHS controls.

Supplemental Figure S4. Statistical comparisons of gut metagenomic profiles during adaptation period (week 0 and week 1). Plots showing significant differences in abundance of reads assigned to a given bacterial genus between week 0 and week 1 for Chow, HFHS and CE groups. The bar graphs on the left side display the mean proportion of sequences assigned to each genus. The dot plots on the right side display the difference in mean proportions between week 0 and week 1 with associated q-value. Error bars on both sides of dots represent the 95% confidence intervals. Only features (genus) with a q-value of >0.05 and a difference between proportions value >1 were considered.

Supplemental figures

Supplemental Figure S1: Experimental Design

Figure S1

Experimental Design
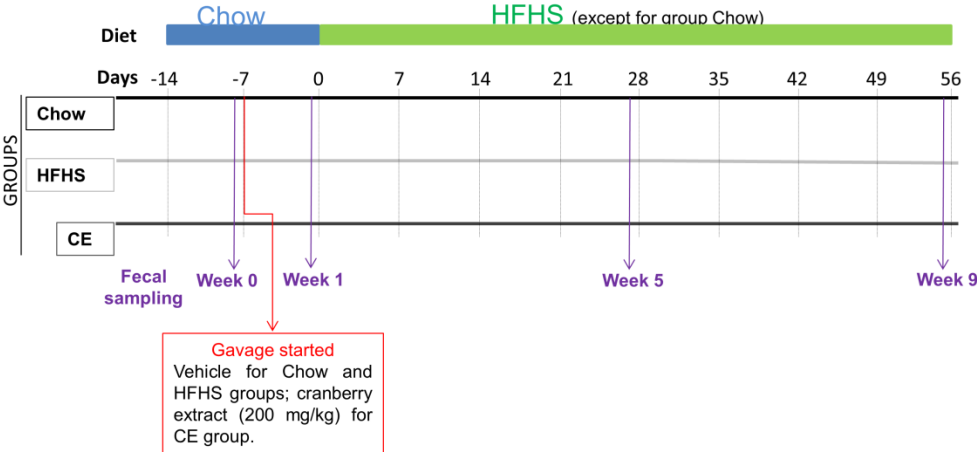
Supplemental Figure S2: Statistical comparisons of gut metagenomic profiles at the phylum level.

Figure S2
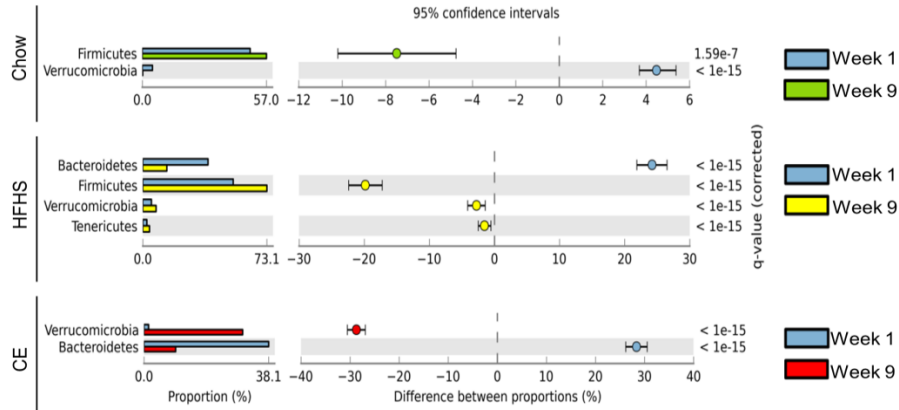
Supplemental Figure S3: Muc2, Klf4 and Reg3g mRNA expression in the jejunum and proximal colon.

Figure S3
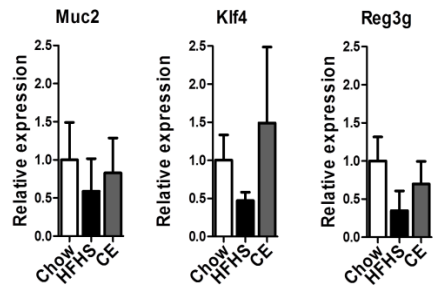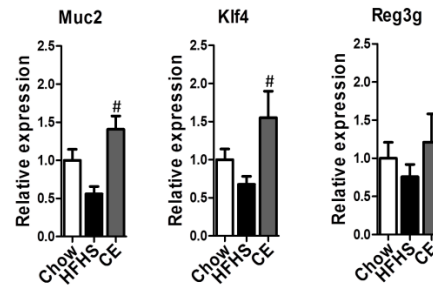
Supplemental Figure S4: Statistical comparisons of gut metagenomic profiles during adaptation period (week 0 and week 1).

Figure S4
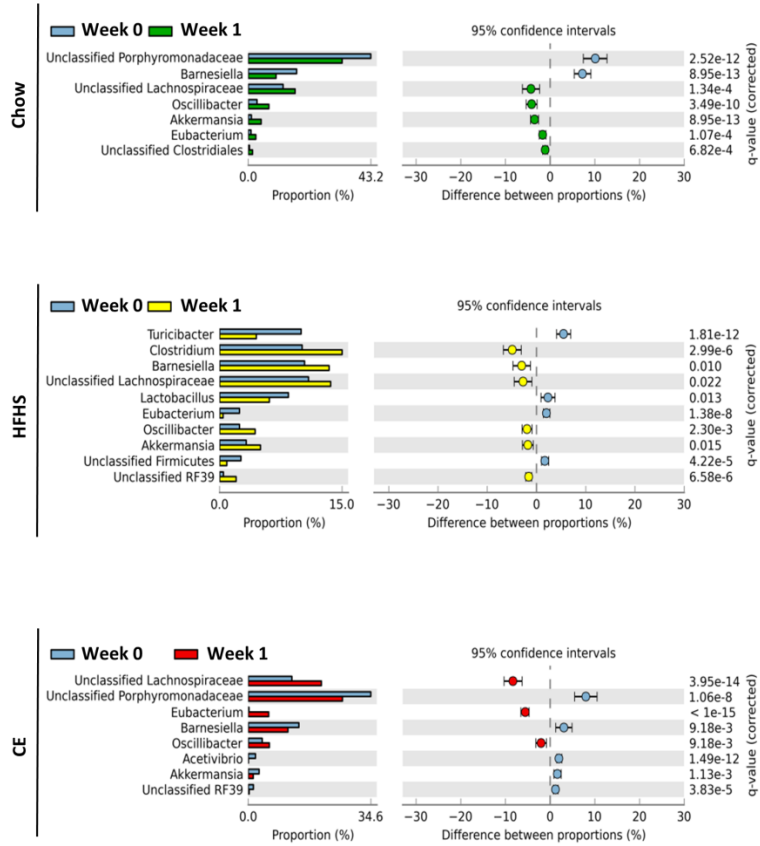
Table S1: Relative abundance of genera in CHOW, HFHS and CE groups.

		Relative abundance (%)											
Treatment		**CHOW**				**HFHS**				**CE**			
Taxon	**Week**	**0**	**1**	**5**	**9**	**0**	**1**	**5**	**9**	**0**	**1**	**5**	**9**
Phylum	**Genus***												
Actinobacteria	*Propionibacterium*	0,00	0,00	0,08	0,00	0,00	0,00	0,00	0,04	0,00	0,00	0,00	0,04
Actinobacteria	*Adlercreutzia*	0,04	0,12	0,16	0,08	0,39	0,19	0,12	0,51	0,19	0,16	0,23	0,23
Bacteroidetes	*Phocaeicola*	0,08	0,00	0,00	0,00	0,00	0,00	0,00	0,00	0,00	0,04	0,00	0,00
Bacteroidetes	*Barnesiella*	17,07	9,82	20,03	13,21	10,52	13,45	1,44	1,36	14,30	11,22	1,44	0,70
Bacteroidetes	*unclassified*	43,22	33,09	22,92	27,28	27,01	24,90	4,64	12,82	34,65	26,66	5,53	8,85
Bacteroidetes	*unclassified*	0,31	0,19	0,00	0,04	0,16	0,04	0,00	0,04	0,16	0,08	0,00	0,16
Bacteroidetes	*unclassified*	0,19	0,23	0,00	0,00	0,04	0,04	0,04	0,00	0,00	0,04	0,04	0,00
Firmicutes	*Bacillus*	0,00	0,00	0,00	0,00	0,00	0,00	0,00	0,00	0,00	0,00	0,00	0,08
Firmicutes	*Staphylococcus*	0,00	0,00	0,00	0,00	0,00	0,00	0,00	0,00	0,00	0,00	0,04	0,00
Firmicutes	*Melissococcus*	0,00	0,00	0,04	0,00	0,00	0,00	0,00	0,00	0,00	0,00	0,00	0,00
Firmicutes	*Lactobacillus*	1,71	2,30	2,49	2,96	8,46	6,12	1,05	0,31	2,65	1,79	1,33	0,12
Firmicutes	*unclassified*	0,00	0,00	0,04	0,00	0,00	0,00	0,00	0,00	0,00	0,08	0,00	0,00
Firmicutes	*Turicibacter*	3,66	2,34	0,94	3,55	10,17	4,29	0,31	0,04	4,83	4,56	0,00	0,00
Firmicutes	*unclassified*	0,04	0,00	0,00	0,00	0,00	0,00	0,00	0,00	0,00	0,00	0,00	0,00
Firmicutes	*unclassified*	0,00	0,16	0,47	0,74	0,39	0,12	0,12	0,12	0,58	0,51	0,58	0,90
Firmicutes	*Clostridium*	0,00	0,00	0,04	0,04	0,12	0,35	1,75	0,19	0,12	0,00	0,00	0,00
Firmicutes	*Acidaminobacter*	0,00	0,00	0,00	0,00	0,00	0,00	0,00	0,00	0,00	0,00	0,00	0,00
Firmicutes	*Anaerovorax*	0,00	0,00	0,00	0,00	0,00	0,00	0,00	0,00	0,00	0,00	0,00	0,00
Firmicutes	*Eubacterium*	0,82	2,38	1,29	1,05	2,14	0,23	0,19	0,35	0,08	5,81	0,19	0,27
Firmicutes	*Dehalobacterium*	0,00	0,00	0,16	0,12	0,12	0,00	0,00	0,12	0,19	0,00	0,08	0,16
Firmicutes	*Eubacterium*	0,16	0,19	0,04	0,12	0,27	0,19	0,16	2,49	0,12	0,00	0,39	1,17
Firmicutes	*Anaerostipes*	0,00	0,00	0,16	0,12	0,00	0,16	0,04	0,00	0,12	0,00	0,00	0,00
Firmicutes	*Bacteroides*	0,08	0,08	0,19	0,08	0,00	0,00	0,00	0,00	0,04	0,08	0,00	0,00
Firmicutes	*Blautia*	0,04	0,16	0,16	0,08	0,00	0,12	0,00	0,08	0,00	0,00	0,04	0,00

Firmicutes	Clostridium	7,56	8,61	9,24	12,2	9,47	13,7	7,60	5,18	9,74	12,5	6,27	5,85
Firmicutes	Coprococcus	0,58	1,44	1,64	1,33	2,42	1,79	0,78	3,08	1,40	1,01	3,20	1,60
Firmicutes	Lachnobacterium	0,00	0,08	0,08	0,16	0,00	0,12	0,08	0,19	0,08	0,04	0,27	0,35
Firmicutes	Lachnospira	0,12	0,08	0,12	0,66	0,82	0,27	0,00	0,00	0,16	0,23	0,00	0,00
Firmicutes	Lactonifactor	0,27	0,19	0,51	0,62	0,31	0,35	0,04	0,04	0,16	0,00	0,12	0,00
Firmicutes	Marvinbryantia	0,16	0,04	0,12	0,12	0,04	0,00	0,00	0,00	0,04	0,00	0,00	0,00
Firmicutes	Oscillibacter	2,84	5,42	3,59	4,25	1,75	3,39	10,8	21,4	1,95	3,66	16,4	14,8
Firmicutes	Parasporobacterium	0,23	0,00	0,00	0,04	0,00	0,00	0,12	0,00	0,00	0,08	0,27	0,08
Firmicutes	Robinsoniella	0,04	0,08	0,04	0,08	0,04	0,00	0,08	0,08	0,00	0,00	0,00	0,08
Firmicutes	Roseburia	0,00	0,00	0,00	0,00	0,00	0,00	0,00	0,00	0,00	0,00	0,00	0,12
Firmicutes	Ruminococcus	0,00	0,08	0,16	0,27	0,23	0,19	10,6	3,55	0,08	0,04	2,30	3,47
Firmicutes	Sporobacterium	0,08	0,16	0,00	0,08	0,12	0,08	0,00	0,00	0,19	0,16	0,00	0,00
Firmicutes	Syntrophococcus	0,04	0,08	0,04	0,16	0,00	0,00	0,00	0,08	0,00	0,23	0,08	0,00
Firmicutes	unclassified	12,3	16,8	21,3	15,9	10,5	13,7	11,5	13,6	12,4	20,4	17,9	14,4
Firmicutes	Dehalobacter	0,00	0,00	0,00	0,00	0,00	0,00	0,00	0,00	0,00	0,00	0,00	0,00
Firmicutes	Clostridium	0,35	0,16	0,12	0,27	0,47	0,31	11,5	6,31	0,27	0,00	7,01	3,04
Firmicutes	Peptostreptococcus	0,00	0,00	0,00	0,00	0,00	0,00	0,00	0,04	0,00	0,00	0,00	0,00
Firmicutes	unclassified	0,00	0,00	0,00	0,00	0,00	0,00	0,12	0,16	0,00	0,00	0,19	0,08
Firmicutes	Acetanaerobacterium	0,00	0,00	0,00	0,00	0,00	0,00	0,00	0,00	0,00	0,00	0,00	0,00
Firmicutes	Acetivibrio	0,47	0,82	1,05	1,79	1,29	0,97	1,29	0,39	2,07	0,08	0,23	0,08
Firmicutes	Anaerotruncus	0,04	0,00	0,04	0,04	0,16	0,19	0,23	0,27	0,16	0,16	0,04	0,16
Firmicutes	Bacteroides	0,08	0,19	0,00	0,08	0,04	0,00	0,12	0,12	0,00	0,16	0,04	0,16
Firmicutes	Butyricicoccus	0,00	0,00	0,08	0,00	0,00	0,00	0,00	0,00	0,00	0,00	0,00	0,00
Firmicutes	Clostridium	0,43	0,16	0,31	0,90	0,23	0,62	3,35	1,33	0,47	0,19	0,62	1,40
Firmicutes	Eubacterium	0,04	0,08	0,00	0,04	0,00	0,00	0,00	0,00	0,00	0,04	0,00	0,00
Firmicutes	Flavonifractor	0,00	0,00	0,04	0,00	0,00	0,12	0,23	0,12	0,00	0,00	0,12	0,39
Firmicutes	Hydrogenoanaerobacterium	0,08	0,00	0,00	0,00	0,00	0,00	0,00	0,00	0,00	0,00	0,00	0,00
Firmicutes	Oscillibacter	0,66	1,71	2,49	2,92	0,78	1,05	2,49	3,86	1,87	2,34	4,48	3,12
Firmicutes	Oscillospira	0,94	1,05	1,75	1,64	1,75	1,64	1,17	1,56	0,82	1,13	1,29	1,99
Firmicutes	Papillibacter	0,00	0,00	0,00	0,00	0,08	0,00	0,00	0,04	0,00	0,00	0,19	0,00
Firmicutes	Pseudoflavonifrac	0,27	1,17	0,74	1,25	1,05	0,62	1,29	1,68	0,94	0,35	2,26	1,44

Firmicutes	*Ruminococcus*	0,04	0,04	0,47	0,39	0,19	0,16	0,19	0,04	0,39	0,16	0,04	0,00
Firmicutes	*Sporobacter*	0,00	0,00	0,00	0,00	0,00	0,00	0,00	0,00	0,08	0,00	0,00	0,00
Firmicutes	unclassified*	0,82	1,33	1,21	1,01	0,47	0,66	0,66	1,48	0,94	0,82	2,22	1,75
Firmicutes	unclassified*	0,43	1,56	1,60	0,94	0,62	0,31	1,91	4,60	0,86	1,09	2,18	1,75
Firmicutes	unclassified*	0,04	0,04	0,12	0,16	0,00	0,16	0,04	0,08	0,08	0,00	0,00	0,00
Firmicutes	unclassified*	1,05	0,51	0,23	0,70	2,49	1,17	0,04	0,08	1,01	0,90	0,19	0,12
Proteobacteria	*Methylobacterium*	0,00	0,00	0,00	0,04	0,00	0,00	0,00	0,00	0,00	0,00	0,04	0,00
Proteobacteria	*Enterobacter*	0,00	0,00	0,00	0,00	0,00	0,08	0,00	0,00	0,00	0,00	0,00	0,39
Proteobacteria	unclassified*	0,00	0,00	0,00	0,00	0,00	0,00	0,00	0,00	0,00	0,00	0,00	0,08
Proteobacteria	*Acinetobacter*	0,00	0,00	0,00	0,00	0,00	0,00	0,00	0,00	0,00	0,00	0,00	0,00
Proteobacteria	*Pseudomonas*	0,00	0,00	0,00	0,00	0,00	0,00	0,00	0,00	0,00	0,00	0,00	0,04
Tenericutes	*Allobaculum*	0,04	0,00	0,08	0,04	0,00	0,08	12,1	3,51	0,04	0,00	0,00	0,00
Tenericutes	*Clostridium*	0,00	0,00	0,00	0,00	0,00	0,00	0,08	0,00	0,04	0,00	0,00	0,00
Tenericutes	*Coprobacillus*	0,00	0,00	0,00	0,00	0,00	0,00	0,04	0,00	0,00	0,00	0,08	0,00
Tenericutes	unclassified*	0,04	0,00	0,00	0,04	0,04	0,08	0,12	0,00	0,12	0,04	0,00	0,08
Tenericutes	*Anaeroplasma*	0,08	1,01	1,21	0,74	0,08	0,27	0,04	0,00	0,39	0,47	0,04	0,00
Tenericutes	unclassified*	0,90	0,78	0,97	1,13	0,47	2,03	0,27	0,43	1,48	0,27	0,04	0,04
Verrucomicrobia	*Akkermansia*	1,09	4,56	0,78	0,19	3,27	5,03	10,6	7,76	3,08	1,44	21,5	30,1
unclassified	unclassified	0,43	0,70	0,70	0,23	0,94	0,58	0,55	0,39	0,55	0,94	0,35	0,27

[a]Taxa marked with asterisk could not be assigned to any of the genera and are shown at the lowest common taxon

Table S2: Proportion of sequences assigned to bacterial taxa.

Treatment	Genus[*]	Proportion (%)	
		Week 1	Week 9
Chow	Unclassified *Porphyromonadaceae*[*]	43,2	27,2
	Unclassified *Lachnospiraceae*[*]	12,3	16,8
	Clostridium	8,7	12,9
	Barnesiella	17,1	13,3
	Oscillibacter	3,1	6,8
	Acetivibrio	0,5	1,9
	Lactobacillus	1,7	3,0
	Pseudoflavonifractor	0,2	1,2
HFHS	*Oscillibacter*	2,5	25,4
	Unclassified *Porphyromonadaceae*[*]	27,0	12,9
	Turicibacter	10,0	0,04
	Barnesiella	10,4	1,3
	Lactobacillus	8,5	0,3
	Akkermansia	3,3	7,8
	Unclassified *Clostridiales*[*]	0,5	4,8
	Allobaculum	0,0	3,5
	Ruminococcus	0,4	3,7
	Clostridium	10,1	13,3
	Unclassified *Firmicutes*[*]	2,6	0,1
CE	*Akkermansia*	3,1	30,2
	Unclassified *Porphyromonadaceae*[*]	34,6	8,9
	Oscillibacter	3,9	18,0
	Barnesiella	14,3	0,7
	Turicibacter	4,7	0
	Ruminococcus	0,5	3,5
	Lactobacillus	2,7	0,1
	Acetivibrio	2,1	0,1
	Unclassified RF39 (*Mollicutes*)[*]	1,5	0,04
	Eubacterium	0,2	1,4
	Unclassified *Firmicutes*[*]	1,3	0,1
	Oscillospira	0,8	2,0

[*]Taxa marked with asterisk could not be assigned to any of the genera and are shown at the lowest common taxon

Table S3: Primer sequences

Gene	Forward sequence	Reverse sequence
Hprt	CCCCAAAATGGTTAAGGTTGC	AACAAAGTCTGGCCTGTATCC
Muc2	ACGTGTCATATTTGCACCTCT	TCAACATTGAGAGTGCCAACT
Klf4	GTAGTGCCTGGTCAGTTCATC	AACCTATACCAAGAGTTCTCATCTC
Reg3g	TTCCTGTCCTCCATGATCAAA	CATCCACCTCTGTTGGGTTC

Supplemental methods

Metagenomic analysis

Bacterial DNA extraction. DNA is extracted as described in (414) using a combination of physical cell-disruption (Bead-beater) and silica column purification using QIAamp DNA Stool Mini Kit (QIAGEN, Missisauga, ON, Canada) (414). Briefly, approximately 100 mg of feces are manually crushed in ASL buffer (QIAGEN) and mixed with 0.4 g of 0.1 mm zirconium beads. Homogenisation is carried out in a MiniBeadBeater (Biospec Products, Bartlesville, OK, USA) to break bacterial cells. After centrifugation (1 min, 20 000 *g*), supernatant is treated with an InhibitEx reagent (QIAGEN) in order to remove PCR inhibitors present in large quantities in the feces. RNA and proteins are degraded using RNAse (Roche Diagnostics, Indianapolis, IN, USA) and proteinase K (QIAGEN). DNA Purification is then carried out using QIAamp DNA Stool Mini Kit (QIAGEN) according to supplier's recommendations. Total extracted DNA is quantified with a ND-1000 Nanodrop (Nanodrop Technologies, Wilmington, DE, USA). All extracted DNA samples were pooled according to dietary/treatment conditions (Chow, HFHS, and CE) and time of sampling (weeks 0, 1, 5 and 9) which resulted in a total of 12 DNA samples.

16S rRNA gene amplification and purification. For each pooled DNA sample, a fragment of the V6-V8 hypervariable region of the bacterial 16S rRNA gene was amplified by PCR with bar-coded primers adapted from existing rRNA primers as described in Comeau *et* al. (2). The PCR reaction mixture contained 1 μL of template DNA, 200 μM of each dNTP (Feldan Bio), 1X HF polymerase buffer (NEB), 0.2 μM of each 454 primer (Invitrogen), 0.4 mg/mL BSA (Fermentas), 1 U of Phusion High-Fidelity DNA polymerase (NEB). The PCR program was as follows: an initial cycle at 98°C during 30 s, followed by 30 cycles of denaturation at 98°C for 10 s, annealing at 55°C for 30 s, extension at 72°C for 30 s, with a final extension of 72°C during 5 min. PCR products were purified using the QIAquick PCR purification kit (QIAGEN). The concentration of the samples was evaluated

spectrophotometrically using a NanoDrop ND-1000 (Thermo scientific). Final amplicon mean length varied between 497-507 bp for all samples.

454 pyrosequencing. Sequencing of the 12 bar-coded amplicons was conducted using 1/8th plate on a single run of Roche 454 GS-FLX Titanium platform at the IBIS (Institut de Biologie Intégrative et des Systèmes - Université Laval). The pyrosequencing run yielded 132611 sequences with numbers of reads varying between 4560 and 8745 per sample.

Raw sequence pre-processing quality control and re-sampling. After de-multiplexing of the raw 454 reads by the Roche MID (multiplex identifier) script, a series of sequence processing was carried out with Mothur (3) to remove low quality. Briefly, reads were filtered using the following restrictions: presence of one or more uncertain bases (N); too short (<150 bp after adaptor and bar-code removal) or too long reads (greater than expected amplicon size); sequences that begin with low quality (incorrect F primer) or containing homopolymers longer than 8 nucleotides. All bases beyond the R primer were trimmed. According to Huse *et* al., those quality control steps have shown to reduce reads 454 sequencing error rates <0.2% (4). Mothur was used to identify and eliminate chimeric reads and sequences considered as contaminants (with mitochondrial or chloroplastidial origin). Reads that passed the above quality filter were then aligned against SILVA reference alignments using the k size= 9 parameter. Then, aligned reads were manually screened to remove all misaligned sequences. All aligned reads were randomly re-sampled according to their respective bar-code to equalize the number of reads between all samples. After re-sampling, each of the 12 samples contained 2566 reads which was equal to the smallest amount of sequences originally found in the bar-coded samples.

OTU detection. Sequences that successfully passed pre-processing and filtering steps were used in Mothur to generate a pair wise distance matrix from which reads were then clustered into OTUs (Operational Taxonomic Units) using the furthest-neighbor algorithm and specifying a distance cutoff value of 0.03. The sequence identity threshold of 97% allows reasonable discrimination of sequences

at the species- or at least genus-level (5-7). The choice of a clustering distance of 0.03 is also judicious considering that the intragenomic distance between 16S rRNA gene copies is typically less than 0.03, and thereby avoiding classifying replicate 16S rRNA gene sequences from the same genome into different OTUs (8). Singletons (OTUs with a unique sequence occurring only once among all reads) were discarded at this step.

OTU identification. Taxonomical classification of OTUs was carried out in Mothur with the Wang method (9) and a 50% bootstrap cut-off value. This strategy has been shown to be ≥95% accurate at the genus level on real and simulated pyrosequencing reads (4; 10; 11), even for much shorter sequences (around 80 pb) than those produced in this study (10). As described in Comeau *et* al., representative sequences of each OTU were taxonomically assigned comparing them to a customized collection of reference sequences based on the Greengenes (2; 12) and the RDP databases (13), and trimmed to the V6-V8 region.

Statistical comparisons of metagenomic samples. We employed the Statistical Analysis of Metagenomic Profiles (STAMP; version 2.0.0) statistical probability model to identify biologically relevant differences between metagenomic communities (14). This model allows choosing appropriate statistical methods to evaluate differences in the proportions of sequences assigned to different taxonomic groups between metagenomes, while considering effect sizes and confidence intervals in assessing biologically relevant differences. Statistically significant differences between taxonomic profiles (at the genus-level) of multiple metagenomic samples obtained after different dietary and temporal conditions were calculated from Principal Component Analysis (PCA), using ANOVA model combined with the Tukey-Kramer method as Post-hoc test, and the Storey's false-discovery-rate (FDR) or Benjamini-Hochberg FDR method as a multiple-hypothesis test correction. Two-way comparisons of taxonomic distributions (at the genus-level) between metagenomic samples (e.g. HFHS0 vs HFHS9) were tested within STAMP, using the Fisher's exact test associated with the Newcombe-Wilson method for calculating confidence intervals (nominal coverage of 95%). To indicate

the percentages of false positives (reported by q values) that should be expected among all significant taxonomic units illustrated on extended error bar plots, a Storey or Benjamini-Hochberg FDR approach was employed. Two filters were applied to all analyses performed with STAMP to remove features with a q value of >0.05 or an effect size <1.

Cranberry extract and phenolic characterization

Plant material and chemicals. Standardized cranberry (*Vaccinium macrocarpon* L.) extract was provided by Nutra Canada (Quebec, Canada). The phenolic standards were obtained from Sigma-Aldrich (MO, USA) except for cyanidin 3-glucoside, which was purchased from Extrasynthèse (France).

Total phenolic content determination. The total phenolic content of cranberry extract was determined using Folin-Ciocalteu method, using gallic acid as standard. In a 96-well plate, 100 µl of a water-diluted Folin-Ciocalteu reagent (1/10) and 80 µl of sodium carbonate solution (75 g/l) were added to 20 µl of a 20% MeOH 0.1% TFA solution of the extract. After incubation for 1h at room temperature, the absorbance was measured at 765 nm using a BMG Labtech Fluostar Omega microplate reader.

Characterization of anthocyanins and procyanidins. Anthocyanins were characterized by reverse-phase analytical HPLC using an Agilent 1100 series system equipped with a diode array detector. The separation was performed on a Phenomenex Develosil C18 reverse-phase column (250 mm x 4 mm, 5 µm particle size), protected with an Ultrasep C18 guard column, using a previously described methodology (15). Anthocyanins were quantified using cyanidin 3-glucoside as standard. Procyanidins were characterized by normal-phase analytical HPLC using an Agilent 1260/1290 infinity system equipped with a fluorescence detector. The separation was performed at 35°C on a Phenomenex Develosil Diol column (250 mm x 4.6 mm, 5 µm particle size), protected with a Cyano SecurityGuard column, using a published methodology (16). The fluorescence was monitored at excitation and emission wavelengths of 230 and 321 nm. Procyanidins with degrees of

polymerization (DP) from 1 to >10 were quantified using external calibration curve of epicatechin, taking into account their relative response factors in fluorescence (17).

Characterization of phenolic acids and flavonoids. Phenolic acids and flavonoids were analyzed using a Waters Acquity UHPLC-MS/MS equipped with an H-Class quaternary pump system, a flow through needle (FTN) sample manager system, a column manager and a TQD mass spectrometer equipped with a Z-spray electrospray interface. The separation was achieved at 40°C on an Agilent Plus C18 column (2.1 mm x 100 mm, 1.8 µm) with a flow rate of 0.4 ml/min. The mobile phase consisted of 0.1% formic acid in ultrapure water and acetonitrile (solvent A and B respectively) was used with following gradient conditions: 0-4.5 min, 5-20% B; 4.5-6.45 min, 20% B; 6.45-13.5 min, 20-45% B; 13.5-16.5 min, 45-100% B; 16.5-19.5 min, 100% B; 19.5-19.52 min, 100-5% B; 19.52-22.5 min, 5% B. The MS/MS analyses were carried out in negative mode using following electrospray source parameters: electrospray capillary voltage: 2.5 kV, source temperature: 140°C, desolvation temperature: 350°C, cone and desolvation gas flows: 80 l/h and 900 l/h respectively. Data were acquired through multiple reaction monitoring (MRM) using Waters Masslynx V4.1 software. Phenolic standards were analyzed using the same parameters and used for the quantification.

Characterization of simple sugars and fibers. Sugars were extracted from cranberry extract using 80% ethanol. After heating at 70°C for 10 minutes, the solution was centrifuged (5 minutes, 3000 rpm, 4°C), evaporated and resuspended in ultrapure water. The characterization was achieved by HPLC using a Waters 600 system equipped with a LKB Bromma 2142 refractometer. The separation was performed on a Waters Sugar Pak column (300 mm x 6.5 mm, 10 µm particle size) with an isocratic elution with EDTA 5 mg/l at a flow rate of 0.5 ml/min. Total dietary fibers were determined using the AOAC 985.29 procedure.

Data analysis. All phenolic characterizations were carried out in triplicate and results were expressed as mean ± standard deviation (SD).

Immunoblot Analysis. Tissues were frozen with liquid nitrogen and then crushed in order to obtain homogeneous powdered samples. Proteins were denatured in a buffer containing SDS and ß-mercaptoethanol, separated on a 7.5% SDS-PAGE and electroblotted onto Hybond nitrocellulose membranes (Amersham, Canada). Bradford assay (Bio-Rad, Ontario, Canada) was used to determine the protein concentration of each sample. Signals were detected with an enhanced chemiluminescence system for antigen-antibody complexes. Unspecific binding sites in the membranes were blocked by defatted milk proteins. Membranes were then incubated with the following primary antibodies: 1:1000 polyclonal anti-COX-2 (70 kDa; Novus, Canada); 1:10000 polyclonal anti-NF-kB (65 kDa; Santa Cruz Biotechnology, USA); 1:5000 polyclonal anti-IkB (39 kDa; Cell Signaling, USA); 1/5000 polyclonal anti-tumor necrosis factor (TNF)-α (26 kDa; R&D, Canada) and 1:40000 monoclonal anti-β-actin (42 kDa; Sigma, USA). The relative amount of primary antibody was detected with specie-specific horseradish peroxidase-conjugated secondary antibody (Jackson, USA). Blots were developed and the protein mass was quantitated by densitometry using an HP Scanjet scanner equipped with a transparency adapter and the UN-SCAN-IT gel 6.1 software.

References (supplemental methods)

1. Savard P, Lamarche B, Paradis ME, Thiboutot H, Laurin E, Roy D: Impact of Bifidobacterium animalis subsp. lactis BB-12 and, Lactobacillus acidophilus LA-5-containing yoghurt, on fecal bacterial counts of healthy adults. International journal of food microbiology 2011;149:50-57
2. Comeau AM, Li WK, Tremblay JE, Carmack EC, Lovejoy C: Arctic Ocean microbial community structure before and after the 2007 record sea ice minimum. PloS one 2011;6:e27492
3. Schloss PD, Westcott SL, Ryabin T, Hall JR, Hartmann M, Hollister EB, Lesniewski RA, Oakley BB, Parks DH, Robinson CJ, Sahl JW, Stres B, Thallinger GG, Van Horn DJ, Weber CF: Introducing mothur: open-source, platform-independent, community-supported software for describing and comparing microbial communities. Applied and environmental microbiology 2009;75:7537-7541
4. Huse SM, Huber JA, Morrison HG, Sogin ML, Welch DM: Accuracy and quality of massively parallel DNA pyrosequencing. Genome biology 2007;8:R143

5. Lozupone CA, Knight R: Species divergence and the measurement of microbial diversity. FEMS microbiology reviews 2008;32:557-578

6. Quince C, Curtis TP, Sloan WT: The rational exploration of microbial diversity. The ISME journal 2008;2:997-1006

7. Fraser C, Alm EJ, Polz MF, Spratt BG, Hanage WP: The bacterial species challenge: making sense of genetic and ecological diversity. Science 2009;323:741-746

8. Schloss PD, Handelsman J: Toward a census of bacteria in soil. PLoS computational biology 2006;2:e92

9. Wang Q, Garrity GM, Tiedje JM, Cole JR: Naive Bayesian classifier for rapid assignment of rRNA sequences into the new bacterial taxonomy. Applied and environmental microbiology 2007;73:5261-5267

10. Claesson MJ, O'Sullivan O, Wang Q, Nikkila J, Marchesi JR, Smidt H, de Vos WM, Ross RP, O'Toole PW: Comparative analysis of pyrosequencing and a phylogenetic microarray for exploring microbial community structures in the human distal intestine. PloS one 2009;4:e6669

11. Sundquist A, Bigdeli S, Jalili R, Druzin ML, Waller S, Pullen KM, El-Sayed YY, Taslimi MM, Batzoglou S, Ronaghi M: Bacterial flora-typing with targeted, chip-based Pyrosequencing. BMC microbiology 2007;7:108

12. DeSantis TZ, Hugenholtz P, Larsen N, Rojas M, Brodie EL, Keller K, Huber T, Dalevi D, Hu P, Andersen GL: Greengenes, a chimera-checked 16S rRNA gene database and workbench compatible with ARB. Applied and environmental microbiology 2006;72:5069-5072

13. Cole JR, Wang Q, Cardenas E, Fish J, Chai B, Farris RJ, Kulam-Syed-Mohideen AS, McGarrell DM, Marsh T, Garrity GM, Tiedje JM: The Ribosomal Database Project: improved alignments and new tools for rRNA analysis. Nucleic acids research 2009;37:D141-145

14. Parks DH, Beiko RG: Identifying biologically relevant differences between metagenomic communities. Bioinformatics 2010;26:715-721

CHAPTER II

A polyphenol-rich cranberry extract reverses insulin resistance and hepatic steatosis independently of body weight loss.

Fernando F. Anhê[1,2], Renato T. Nachbar[1], Thibault V. Varin[2], Vanessa Vilela[1], Stéphanie Dudonné[2], Geneviève Pilon[1,2], Maryse Fournier[3], Marc-André Lecours[3],Yves Desjardins[2], Denis Roy[2], Emile Levy[3] and André Marette[1,2*]

[1]Department of Medicine, Faculty of Medicine, Cardiology Axis of the Québec Heart and Lung Institute, [2]Institute of Nutrition and Functional Foods, Laval University, Québec, Canada, [3]Research Centre, Sainte-Justine Hospital, Montréal, Québec, Canada

Résumé

Les canneberges sont de riches sources de polyphénols et nous avons démontré l'effet préventif d'un extrait de canneberge enrichi en polyphénols (CE) sur l'inflammation intestinale, l'homéostasie hépatique et la résistance à l'insuline chez des sourissur régime obésogène. Dans la présente étude, nous avons étudié le potentiel du CE pour renverser l'obésité chez des souris ainsi que son interaction avec différents régimes alimentaires. Les souris ont d'abord été nourries soit à une diète saine (Chow) ou à un régime de haute teneur en gras et en sucrose (HFHS) pendant 13 semaines. Par la suite, les souris ont été traitées avec le CE (200 mg/kg, Chow+CE, HFHS+CE) ou le véhicule (Chow, HFHS) pendant 8 semaines supplémentaires. Le traitement avec le CE n'a pas renversé le gain de poids ou l'accumulation de masse grasse chez des souris nourries avec une diète Chow ou HFHS. Cependant, nous avons constaté une nette amélioration de la stéatose hépatique, une meilleure tolérance à l'insuline et au glucose et une amélioration de la résistance à l'insuline chez des souris HFHS+CE *versus* des souris HFHS traitées au véhicule. Des souris nourries avec un régime chow et traitées avec CE ont démontré un métabolisme de glucose similaire par rapport aux souris témoins chow traitées au véhicule. Le microbiote intestinal des souris HFHS+CE a été caractérisé par une diminution du rapport Firmicutes/Bacteroidetes, une expansion drastique d'*Akkermansia muciniphila* et, dans une moindre mesure, une augmentation de l'abondance relative du genre *Barnesiella*. Chez les souris Chow+CE, nous avons constaté une altération moins prononcée de la communauté intestinale associée principalement à une expansion de certaines *Clostridiales* et *Lachnospiraceae* non classées. L'expansion d'*A. muciniphila* et *Barnesiella* a également été trouvée dans le microbiota intestinal de souris chow+CE, mais dans une moindre mesure par rapport à ce qui fut observé dans le microbiote des souris HFHS+CE. L'ensemble de nos résultats soulignent l'axe intestin-foie comme étant une cible principale du CE qui,en association avec l'augmentation d'*A. muciniphila* dans le microbiota intestinal, est suffisant pour améliorer l'homéostasie glycémique et la résistance à l'insuline.

Abstract

Objective: Previous studies have reported that polyphenol-rich extracts from various sources can prevent obesity and associated gastro-hepatic and metabolic disorders in diet-induced obese (DIO) mice. However, whether such extracts can reverse obesity-linked metabolic alterations remains unknown. In the present study, we aimed to investigate the potential of a polyphenol-rich extract from cranberry (CE) to reverse obesity and associated metabolic disorders in DIO-mice. **Methods:** Mice were pre-fed either a Chow or a High Fat-High Sucrose (HFHS) diet for 13 weeks to induce obesity and then treated either with CE (200 mg/kg, Chow+CE, HFHS+CE) or vehicle (Chow, HFHS) for 8 additional weeks. **Results:** CE did not reverse weight gain or fat mass accretion in Chow- or HFHS-fed mice. However, HFHS+CE fully reversed hepatic steatosis and this was linked to upregulation of genes involved in lipid catabolism (eg, PPARα) and downregulation of several pro-inflammatory genes (eg, COX2, TNFα) in the liver. These findings were associated with improved glucose tolerance and normalization of insulin sensitivity in HFHS+CE mice. The gut microbiota of HFHS+CE mice was characterized by lower Firmicutes to Bacteroidetes ratio and a drastic expansion of *A. muciniphila* and, to a lesser extent, of *Barnesiella spp*, as compared to HFHS controls. **Conclusions:** Taken together, our findings demonstrate that CE, without impacting on body weight or adiposity, can fully reverse HFHS diet-induced insulin resistance and hepatic steatosis while triggering *A. muciniphila* blooming in the gut microbiota, thus underscoring the gut-liver axis as a primary target of cranberry polyphenols.

Introduction

Obesity has reached pandemic proportions worldwide, significantly contributing to reduce life quality and lifespan [1]. This condition is characterized by abnormal and excessive fat accumulation and is influenced by both genetic and environmental determinants. While several genetic loci have been associated with obesity, they explain only a fraction of the total variance within populations; moreover, genes deemed obesity-predisposing interact with environmental factors to regulate, for instance, satiety and energy expenditure [2]. Among the environmental determinants of obesity and its associated dysmetabolic conditions, dietary habits play a central role. Diet also strongly influences our "other genome" (*i.e.*, the metagenome), modelling gut microbial community structure [3] and impacting host metabolism and energy partitioning [4]. Research conducted throughout the last decade has revealed a clear association between obesity and gut microbial dysbiosis, which is generally characterized by a reduction in bacterial richness and by major taxonomic and functional changes [5].

The consumption of fiberless diets rich in simple sugars and saturated fat (often referred to as Western diets) generates well-known detrimental metabolic consequences, leading to insulin resistance and glucose intolerance in the early-term, which later evolves to overt obesity, type 2 diabetes and cardiovascular complications. NAFLD and NASH are highly prevalent diseases often occurring in the setting of obesity and type 2 diabetes; they may eventually progress to hepatocellular carcinoma and importantly contribute to dysregulate glucose and lipid homeostasis [6]. The gut exerts major influences on liver physiology, first as both organs are anatomically and functionally connected by means of the portal circulation, but also since bacteria and bacteria-derived molecules can translocate from the gut to the liver and contribute to diet-induced insulin resistance and liver disease [7, 8].

Plant-rich diets are abundant in fruits and vegetables and strongly linked to lean and healthy phenotypes [9], which prompts the search for bioactive phytonutrients to treat or prevent obesity and its related dysmetabolic conditions.

The use of polyphenol-rich fruit extracts or isolated polyphenols as strategies to alleviate obesity-linked diseases have been demonstrated in humans [10, 11] and in animal models [12, 13], but the mechanisms of action are not yet fully elucidated. Several dietary polyphenols are generally poorly bioavailable and build up in the colon, where they are modified by gut microbial enzymes and, in turn, reshape gut microbial communities [14]. We have previously demonstrated that a polyphenol-rich cranberry extract prevents diet-induced obesity in high fat high sucrose-fed mice, and these findings were linked to improved gut-liver homeostasis and expansion of *Akkermansia muciniphila* population in the gut microbiota [12]. Similar effects were reported by others using a polyphenol-rich extract of concord grape [15] and apple proanthocyanidins [16], but no studies have yet tested whether polyphenols can reverse an already established obesity and more severe metabolic alterations, including hepatic steatosis and inflammation. In the present study, we investigated the potential of a polyphenol-rich cranberry extract to reverse an already established obesity, insulin resistance and NAFLD, and whether such effects may be linked to the reshaping of the gut microbiota and blooming of *Akkermansia muciniphila*, a well-known target of food polyphenols.

Material and methods

Animals. All animal experiments reported in this manuscript comply with the Animal Research: Reporting of *In Vivo* experiments (ARRIVE) guidelines. Eight week-old C57Bl/6J male mice (Jackson, USA) were housed 2-3 animals per cage, kept on Sani-chips bedding and in controlled environment (12 hours daylight cycle, lights off at 18:00) with food and water *ad libitum* in the animal facility of the Québec Heart and Lung Institute (Québec, Canada). After two weeks of acclimatization, mice were pre-fed either a healthy Chow (Teklad 2018, Harlan) or a High-Fat/High-Sucrose (HFHS) diet for 21 weeks. Diet composition was previously published [12] and, although the abbreviation HFHS particularly refers to the enriched presence of saturated fat and simple sugars, it is important to stress

that the lack of soluble fibers is a major obesogenic component of this diet [17]. During the last 8 weeks of the study (ie, from the beginning of week 13 to the beginning of week 21), control groups (Chow, n=8 and HFHS, n=8) were orally administered the animal facility's drinking water whereas the treated groups (Chow+CE, n=11 and HFHS+CE, n=10) received a cranberry extract (CE, 200 mg/kg, Nutra Canada, Québec, Canada). The polyphenolic profile of CE was published elsewhere [12, 18]. Body weight gain and food intake were assessed twice weekly. At week 21, animals were anesthetized in chambers saturated with isoflurane and then sacrificed by cardiac puncture. Organs and tissues were carefully collected and blood was drawn in tubes containing 2 IU of heparin and immediately centrifuged in order to separate plasma from cells. All interventions were carried out during the animals' light cycle. All procedures strictly followed the National Institutes of Health (NIH)'s Guide for the Care and Use of Laboratory Animals and were previously approved by the Laval University Animal Ethics Committee.

Glucose homeostasis. At week 17, mice were fasted for 6 hours and insulin tolerance tests (ITT) were performed after intraperitoneal injections of insulin (0.75 UI/kg body weight). Glycemia was measured with an Accu-Check glucometer (Bayer) before (0 min) and after (10, 20, 30, 60 and 90 min) insulin injection. At the end of week 19, mice were fasted overnight (12 h) and oral glucose tolerance tests were carried out (OGTT, 1 g of glucose/kg body weight). Blood was collected before (0 min) and after (15, 30, 60, 90 and 120 min) glucose challenge for glycemia determination. Blood samples (~30μL) were collected at each time point during OGTT and insulinemia was determined using an ultra-sensitive ELISA kit (Alpco, USA). The homeostasis model assessment of insulin resistance (HOMA-IR) index was calculated based on the following formula: fasting insulinemia (μUI/mL) x fasting glycemia (mM)/22.5.

Oil red O staining. During necropsies, mouse livers were embedded in Tissue-Tek® OCT, immediately snap-frozen in liquid nitrogen and stored at -80 °C. Staining of neutral lipids was based on the methods described by Mehlem *et al.*

107

with some adaptations [19]. Briefly, 12 µm liver sections were allowed to equilibrate at room temperature for 5 minutes and then post-fixed with a Formalin (10%)/Calcium (2%) solution for 15 minutes. The sections were then incubated with oil red O (ORO) working solution at room temperature for 5 minutes, followed by a 5- minute clearing in 60% isopropyl alcohol and a counterstaining of 15 seconds with Mayer's hematoxylin.

Q-PCR and antioxidant enzymes. Gene mRNA expression analysis by q-PCR and quantification of antioxidant enzymes were carried out as previously described [12]. Primer sequences used were: (5'→ 3') PPARα F- CGACCTGAAAGATTCGGAAA, R- GGCCTTGACCTTGTTCATGT; PPARγ F- CAGGCCTCATGAAGAACCTT, R- GCATCCTTCACAAGCATGAA; SREBP1c F- GACCCTACGAAGTGCACACA, R- TCATGCCCTCCATAGACACA; SREBP2 F- CGACCAGCTTTCAAGTCCTG, R- CCTGTACCGTCTGCACCTG; LXRα F- GGAGTGTCGACTTCGCAAAT, R- CTTGCCGCTTCAGTTTCTTC; LXRβ F- AAACGATCTTTCTCCGACCA, R- ATGGCTAGCTCGGTGAAGTG; COX2 F- GCTGTACAAGCAGTGGCAAA, R- CCCCAAAGATAGCATCTGGA; TNFα F- GAACTGGCAGAAGAGGCACT, R- AGGGTCTGGGCCATAGAACT; NFκB F- AGCTTCACTCGGAGACTGGA, R- ACGATTTTCAGGTTGGATGC; IκB F- TGGCCAGTGTAGCAGTCTTG, R- GACACGTGTGGCCATTGTAG.

Cecal mucin determination. Cecal contents were collected at week 21, snap-frozen in liquid nitrogen and stored at -80 °C. Cecal feces were freeze-powdered and the presence of mucins was determined using a fluorometric assay kit (Cosmo Bio, Japan) that discriminates *O*-linked glycoproteins (mucins) from N-linked glycoproteins.

Fecal samples. Fecal samples were freshly collected at baseline (week 13) and week 21 and immediately stored at -80 °C. Bacterial genomic DNA was extracted from approximately 50 mg of fecal material collected from each cage. Samples were resuspended in lysis buffer containing 20 mg/ml lysozyme and incubated for 30 minutes at 37°C. Further lysis was performed by adding 10% SDS and proteinase K to 350 µg/ml followed by incubation for 30 minutes at 60°C.

Samples were homogenized using a bead beater and 0.1mm zirconium beads and then processed using a DNA extraction kit (DNeasy, Qiagen). DNA yield was assessed using a NanoDrop ND-1000 spectrophotometer (Thermo Scientific). Extracted DNA was stored at -20 °C until use. Each DNA sample was subsequently used for 16S amplification of the V3-V4 region using the primers 341F (5'-CCTACGGGNGGCWGCAG-3') and 805R (5'-GACTACHVGGGTATCTAATCC-3') adapted to incorporate the transposon-based Illumina Nextera adapters (Illumina, USA) and a sample barcode sequence allowing multiplexed paired-end sequencing. Constructed 16S metagenomic libraries were purified using 35 µL of magnetic beads (AxyPrep Mag PCR Clean up kit; Axygen Biosciences, USA) per 50 µL PCR reaction. Library quality control was performed with a Bioanalyzer 2100 using DNA 7500 chips (Agilent Technologies, USA). An equimolar pool was obtained and checked for quality prior to further processing. The pool was quantified using picogreen (Life Technologies, USA) and loaded on a MiSeq platform using 2 x 300 bp paired-end sequencing (Illumina, USA). High-throughput sequencing was performed at the IBIS (Institut de Biologie Intégrative et des Systèmes - Université Laval).

16S rRNA gene-based gut microbial analysis. Generated and demultiplexed sequences were analyzed using the QIIME software package (version 1.9.1). Paired-end sequences were merged with at least a 50-bp overlap using fastq-join . Resulting sequences containing ambiguous or low quality reads (Phred score ≤ 25) were removed from the dataset. Forward and reverse primers were trimmed from the filtered sequences; reads with at least one reverse primer mismatch or where the reverse primer was not found were discarded. Chimera checking and filtering was performed using UCHIME ([4](#)). OTU (Operational Taxonomic Units)-picking from post-filtering reads was performed using USEARCH 61 version 6.1.544 [20] with an open-reference methodology, which consisted of clustering sequences *de novo* at 97% identity threshold if they did not hit the reference sequence collection. Representative OTU sequences were assigned taxonomy against the Greengenes reference database (August 2013 release) [21] using the RDP-classifier [22]. Singleton OTUs and OTUs with a number of

sequences < 0.005% of total number of sequences were discarded at this step [23]. Unclassified OTUs at the genus level against Greengenes were further investigated with the RDP classifier against the RDP database (version September 30, 2016) [24] using a minimum bootstrap cutoff of 50% [25].

Statistical analysis. Two-way ANOVA with a Student-Newman-Keuls was used to assign significance to the comparisons between groups (Sigmaplot, USA). The significance of the differences between time points was calculated using two-way repeated measures ANOVA with a Student-Newman-Keuls post hoc test (Sigmaplot, USA). Data are expressed as mean ± SEM. All results were considered statistically significant at $P< 0.05$.

In order to illustrate β-diversity of metagenomic samples, weighted UniFrac distance matrix was calculated at the genus level based on taxa having at least 1% of total relative abundance. PCoA (Principal Coordinates Analysis) was performed on the resulting distance matrix using the 'phyloseq' R package (version 1.16.2). The statistical significance of differentially abundant and biologically relevant taxonomical biomarkers between two distinct biological conditions was measured using a linear discriminant analysis (LDA) effect size (LEfSe) [26]. Only taxa meeting an LDA significant threshold of 2.5 were considered. A P-value < 0.05 was considered to indicate statistical significance for the factorial Kruskal–Wallis rank-sum test.

Results

CE administration throughout 8 weeks did not reverse body weight gain in both Chow- and HFHS-fed mice (Figures 1A). Accordingly, we found similar energy intake and fat mass accumulation when comparing Chow *versus* Chow+CE and HFHS *versus* HFHS+CE (Figures 1B, C). The livers of CE-treated HFHS-fed mice tended to be lighter than those of untreated HFHS-fed mice (Figure 2A) and, during necropsies, we noted that the livers of untreated HFHS-fed mice were pale and clearly steatotic whereas those of HFHS+CE mice displayed a reddish healthy aspect (Figure 2C, top panel). Accordingly, quantification of liver triglycerides and

ORO staining revealed massive triglyceride accumulation in the livers of HFHS mice, which was fully reversed in HFHS+CE mice (Figures 2B-D). CE administration did not reduce triglyceride levels in the liver of healthy Chow-fed mice (Figures 2B-D) and fasting plasma triglycerides were not affected by diet or treatment (Figure 2E).

Liver MDA levels were reduced in HFHS+CE mice when compared with vehicle-treated HFHS mice (Figure 2F), suggesting lower lipid peroxidation. Conversely, levels of superoxide dismutase (SOD, SOD2), glutathione peroxidase (GPx) and catalase, all important constituents of the cell's anti-oxidant defense, were not affected by diet, treatment or the interaction of both (Figures 2F). Interestingly, CE administration reversed the HFHS-induced mRNA overexpression of cyclooxygenase-2 (COX2), tumor necrosis factor-α (TNFα), nuclear factor κ-light-chain-enhancer of activated B cells (NFκB) and NFκB inhibitor (IκB), suggesting a broad resolution of diet-induced hepatic inflammation in HFHS-fed CE-treated mice (Figures 2G). Consistent with improved hepatic steatosis we found higher mRNA levels of peroxisome proliferator-activated receptor α (PPARα) and lower levels of both sterol regulatory element-binding protein 1 and 2 (SREBP1/2) transcripts in the livers of HFHS+CE mice *versus* HFHS mice (Figures 2H). Unexpectedly, the mRNA expression of PPARγ and liver X receptor α and β (LXRα/β), all nuclear factors linked to lipid anabolism, was upregulated in HFHS+CE in comparison with vehicle-treated HFHS-fed mice (Figures 2H).

We then sought to investigate whether glucose homeostasis and insulin sensitivity were affected by CE administration in diet-induced obese mice. We found lower glycemia 10 and 15 minutes after insulin injection (Figure 3A) and lower area under the ipITT curves (Figure 3B) in CE-treated *versus* vehicle-treated HFHS-fed mice. Despite lower glycemia 5 minutes after insulin injection in Chow+CE as compared with Chow mice (Figure 3A), the overall insulin response was not different between these two groups as suggested by similar area under the ipITT curves (Figure 3B). We found lower glucose excursions 30, 90 and 120 minutes after oral glucose challenge (Figure 3C) and reduced area under the

OGTT curves (Figure 3D) in HFHS+CE *versus* HFHS mice. Importantly, determination of insulinemia during OGTT revealed that improved glucose tolerance in HFHS+CE mice was achieved despite lower basal and 15 minutes insulin levels post-glucose challenge (Figure 3E), which is in agreement with improved insulin sensitivity in these animals. Glucose tolerance and insulinemia during OGTT were not different between CE-treated and vehicle treated mice on the Chow diet (Figure 3C-E).

Fecal DNA was extracted and 16S rRNA-based microbial profiling was performed in order to investigate whether the phenotypic traits of Chow, Chow+CE, HFHS and HFHS+CE were associated with changes in gut microbial community structure. β-diversity was generally assessed by means of principal component analysis (PCoA) on weighted unifrac distances and revealed a clear diet-induced separation in the microbial composition of Chow- and HFHS-fed mice (PCo1, 57,1%) (Figure 4A). Treatment also importantly influenced the gut microbiota (PCo2, 21,3%) and separated vehicle- and CE-treated microbial communities of both Chow- and HFHS-fed mice (Figure 4A). β-diversity changes between HFHS and HFHS+CE were accompanied by a drop in the Firmicutes to Bacteroidetes ratio in HFHS+CE mice *versus* vehicle-treated HFHS-fed mice (Figure 4B). LEfSe analysis disclosed that obesity-driven dysbiosis was mostly explained by a reduction in the populations of *Barnesiella*, *Bifidobacterium*, *Turicibacter*, *Anaerostipes* and *Clostridium* and an expansion of Peptostreptococcaceae, Clostridiales, *Oscillospira*, *Oscillibacter*, Clostridiaceae and *Anaerotruncus* (Figure 4C). Administration of CE to Chow-fed mice was associated with an increase of Clostridiales, Lachnospiraceae and *Akkermansia muciniphila* (Figure 4D and Supplemental figure 1), whereas in HFHS-fed mice CE-treatment was related to expansion of *A. muciniphila*, *Coprobacillus* and *Barnesiella* (Figure 4E and Supplemental figure 1).

Because the presence of *A. muciniphila* in the gut microbiota has been linked to improved intestinal barrier and mucus layer integrity [27, 28], we assessed fecal mucin as a readout of mucus layer thickness. We found a reduction

in fecal mucin in HFHS-fed mice as compared to Chow-fed mice, which tended to be reversed in HFHS+CE (P=0.06, HFHS *vs* HFHS+CE; two-way ANOVA with Student-Newman-Keuls post hoc test) (Figure 5).

Discussion

We and others have previously shown that treatment with polyphenol-rich extracts for 8 weeks significantly protected against diet-induced obesity and also resulted in reduced hepatic steatosis and intestinal inflammation, traits linked to a drastic expansion of *A. muciniphila* in the gut microbiota [12, 15]. In these studies, however, it was not possible to determine to what extent the preventive effects of such extracts were secondary to lower body weight gain and reduced fat mass accretion. In the present study, we now document that CE can protect against two major metabolic complications of obesity, insulin resistance and NAFLD, independently from changes in body weight or adiposity.

The marked reduction of fat deposition in the livers of CE-treated mice was accompanied by reduced hepatic inflammation, as suggested by downregulation of COX2, TNFα, NFκB and IκB mRNA expression. Conversely, enzymatic components of the cellular antioxidant machinery (*i.e.* SOD1, SOD2, GPx, catalase) were unaltered in the liver of HFHS+CE mice, and similar results were found in *db/db* mice supplemented with a cranberry powder [29]. Importantly, lower hepatic levels of MDA indicate that lipid peroxidation is decreased in HFHS+CE mice. This is possibly explained by the lower availability of triglycerides in the liver of HFHS+CE. In addition, CE may counter ROS-induced lipid peroxidation by alleviating inflammation, which may contribute to tone down ROS formation. Moreover, since CE did not alter the amount of antioxidant enzymes in the liver, it is also plausible that CE polyphenols directly neutralize ROS, which would further contribute to reduce lipid peroxidation.

Consistent with augmented lipid catabolism in the liver, we found higher mRNA levels of PPARα and lower amount of mRNA transcripts of SREBP1 and SREBP2 in HFHS+CE mice when compared with untreated HFHS-fed mice.

However, in apparent contradiction with lower hepatic steatosis, CE treatment was associated with higher mRNA expression of PPARγ and upregulation of LXRα and LXRβ mRNA in HFHS-fed mice. PPARα is a key nuclear receptor to steatogenesis, being highly expressed in the liver and the principal activator of PPAR-responsive elements (PPREs) in this organ [30, 31, 32]. It is conceivable that PPARα-related activation of β-oxidation genes likely overcomes PPARγ-driven stimulation of lipogenesis in the liver of HFHS-fed CE treated mice. Moreover, PPARγ and LXR are both highly expressed in Kupffer cells (liver resident macrophages), where their activation is linked to anti-inflammatory effects [33, 34]. Macrophage PPARγ and LXRα/β may account for the increased hepatic expression of these nuclear receptors in HFHS+CE mice *versus* HFHS mice, and may also contributed to alleviate hepatic inflammation in HFHS-fed CE treated mice. Interestingly, since activation of hepatic PPARγ and LXR are both linked to reduced hepatic glucose output [30, 35, 36], our results also point to a role of these two nuclear receptors in the CE-related benefits to glucose homeostasis. Taken together, our findings suggest that CE alleviates steatogenesis by targeting PPARα, which, in parallel to PPARγ and LXRα/β upregulation, enhances hepatic immune-metabolic status while sustaining increased lipid catabolism in the liver. It is noteworthy that the massive lipid deposition observed in the liver of HFHS-fed mice did not result in dyslipidemia in our model, as suggested by similar levels of fasting plasma triglycerides found among groups. While this is presumably linked to the fact that, as opposed to humans, mice have a low LDL/high HDL cholesterol profile, which might favor hepatic lipid storage and limit dyslipidemia in diet-induced obese mice [37], this observation indicates that the marked effect of CE on hepatic triglyceride accretion is not a consequence of increased lipid mobilization to the plasma, which is in accordance with enhanced lipid oxidation being the main mechanism of reduced liver fat accumulation in HFHS+CE mice.

Because gut microbial factors are increasingly recognized as key drivers of hepatic metabolism [7, 8, 38], and CE has been previously linked to major gut microbial changes [12], we sought to investigate intestinal bacterial profiles in CE- and vehicle-treated mice. Similarly to our previous report using a preventive

approach [12], we found that CE administration to already obese mice triggered a remarkable bloom of *A. muciniphila* in the gut microbiota of HFHS-fed mice. This effect of CE treatment was also observed in Chow-fed mice, albeit to a lesser extent. *A. muciniphila* is a Gram-negative mucin degrading bacterium strongly correlated with healthy and lean phenotypes [5, 39], and its administration as a probiotic was shown to reverse diet-induced obesity in mice [27, 40]. Previous studies have demonstrated a particular association between higher *A. muciniphila* and better glycemic control, which was independent of reduced visceral fat mass deposition [41, 42]. These findings suggest that the interaction between *A. muciniphila* and host metabolism is context-specific, being likely dependent on factors such as gut community structure, the severity of the dysmetabolic condition and the host's genetic background. Indeed, Shin et al showed that the metformin-like effects of *A. muciniphila* on glucose tolerance were only achieved with doses higher than $4\text{x}10^7$ CFU in diet-induced obese mice [28]. Our results revealed that, upon a 21-week long HFHS regimen, the CE-related increase in *A. muciniphila* population was not linked to lower fat accumulation, but it was rather associated with improved glucose metabolism and alleviated hepatic steatosis.

Despite the fact that LEfSe analysis did not classify *A. muciniphila* as a key-phylotype of Chow+CE mice, we found a small, yet significant, increase in this taxon in Chow-fed CE-treated mice *versus* vehicle-treated Chow-fed mice by applying a distinct statistical approach. Because Chow-fed mice are metabolically healthy, this finding was not associated with major changes in glucose homeostasis or weight gain. However, this result is of great relevance as it suggests that CE may still favor an expansion of *A. muciniphila* in healthy individuals, which might be protective in the long-term. Moreover, Lachnospiraceae and Clostridiales were both ranked as important discriminative taxa between Chow+CE and vehicle-treated Chow-fed mice. This may be related to the capacity of certain species within the family Lachnospiraceae and the order Clostridiales to resist to the antimicrobial effect of CE and/or utilize CE-polyphenols as substrates. More studies are warranted to further explore the gut microbial-related protective role of CE polyphenols in healthy mice.

Cranberry polyphenols have been shown to improve mucus layer and villi morphology in mice receiving elemental enteral nutrition [43]. Moreover, dietary polyphenols increased the amount of mucin in the feces of high fat-fed mice [44]. We therefore hypothesized that CE may create a favorable environment for *A. muciniphila* to thrive by boosting mucus secretion [12, 45]. In accordance with this hypothesis, we found a strong trend ($P = 0.06$) towards higher mucin concentration in the cecum of CE-treated HFHS-fed mice. Consistently, enhanced mucus layer thickness was previously observed in DIO-mice treated with live *A. muciniphila* [27]. Our data suggest that the benefits of CE to gut barrier and hepatic homeostasis are tightly linked to expansion of *A. muciniphila* in the gut microbiota.

Polyphenols possess antimicrobial activity [46] and, because Gram-negative bacteria are generally more resistant to this effect [47], *A. muciniphila* may find a competitive advantage in the gut environment of CE-treated mice. Similar mechanism might favor the presence of *Barnesiella spp* in the gut microbiota of HFHS+CE mice. While little is known about the relevance of *Barnesiella spp* to the host, our data stress its beneficial impact on host metabolism as they classified this taxon as the main discriminative feature of Chow mice when compared with HFHS mice. Moreover, it has been suggested that *Barnesiella spp.* confer resistance to intestinal growth and bloodstream infection with vancomycin-resistant *Enterococcus* [48], which supports a beneficial interaction between host and *Barnesiella*. *Coprobacillus* was ranked a key-feature of HFHS+CE mice, however its abundance is much lower than 1% and its relevance to host metabolism might be minor in this study.

Lower Firmicutes to Bacteroidetes ratio is often considered as a key feature of the "obese gut microbiota" [49, 50]. In our model, however, we found lower Firmicutes to Bacteroidetes ratio in association with improved glucose and insulin tolerance in HFHS+CE mice, traits that were unrelated with changes in body weight and fat mass accumulation. While suggesting that CE-driven gut microbial remodeling is primarily linked to hepatic homeostasis and the regulation of glucose metabolism/insulin sensitivity, our findings also indicate that lower Firmicutes to

Bacteroidetes ratio seems to influence host glucose homeostasis prior to affect host fat mass accretion. Indeed, lower Firmicutes to Bacteroidetes ratio has been particularly associated with better glycemic control in humans [41], and reconstitution of germ-free mice with the fecal slurry of mice fed on a high-fat diet for 10 weeks rendered them glucose intolerant but not obese [51]. Future studies are warranted to determine whether CE administration for a longer period of time, therefore more chronically exposing the host to lower Firmicutes to Bacteroidetes ratio and higher *A. muciniphila*, would affect host fat mass storage.

The dose of CE used in this study (200 mg of extract/kg, 75 mg of polyphenols/kg) is equivalent to the consumption of approximately 120 g of fresh cranberries/day by a 60 kg individual [18]. The translation of this dose to humans, however, is probably not straightforward. Considering the US Food and Drug Administration's guidelines to calculate the human equivalent dose based on body surface area [52] we found that a 16 mg of extract/kg (6 mg of polyphenols/kg) dose would be the human equivalent of a 200 mg/kg dose in mice. Based on this, we estimated that obtaining 360 mg of polyphenols/60 kg from a cranberry juice cocktail (a very popular form of consuming cranberries) would require the daily consumption of 206.8 mL of this product (considering a cocktail containing 54% of cranberry juice and 1.74 mg of polyphenols/mL [53]) . It is, however, important to stress that while the polyphenolic composition of cranberry juices or cranberry juice cocktails may be different from that of the extract, these preparations often contain added sugars and/or artificial sweeteners [53], which may contribute to metabolic disease. We believe that other sources of cranberry polyphenols, such as capsuled cranberry extract or unsweetened dried cranberries, are likely better options in order to target metabolic diseases.

As a prospect, changes in the bile acid profile may be investigated as a mechanism behind the metabolic benefits of CE. Bile acids can regulate their own synthesis and ileal re-uptake via binding to the nuclear receptor farnesoid-X-receptor (FXR). Furthermore, the role of bile acids goes beyond aiding lipid digestion and extends to regulation of glucose/lipid homeostasis and energy

metabolism [54]. Interestingly, while changes in bile acid profile have been associated with NASH in clinical studies [55], pre-clinical analyses using mouse models of obesity have revealed that FXR agonism is protective against liver steatosis and insulin resistance [56, 57]. Since dietary polyphenols have been shown to bind to bile acids and alter their re-uptake (and possibly their ability to signal through FXR) [58, 59], it is possible that CE treatment changes the bile acid profile, which may in turn contribute to improve liver steatosis and insulin resistance. Bile acids are modified by the gut microbiota, yielding secondary bile acids. Since CE importantly affects gut microbial populations, it may also affect the microbial capacity to transform bile acids, which would further contribute to modify the bile acid profile and potentially modulate metabolic status. It is noteworthy that the ability of *A. muciniphila* and *Barnesiella*, the two best representative taxa of HFHS+CE, to modify or resist to bile acids is currently unknown.

Conclusion

Our findings shed light on novel mechanisms by which CE improves metabolic health. Using a reversal experimental design allowed us to demonstrate that CE polyphenols strongly target the liver, where it modulates key hepatic nuclear factors and genes involved in the modulation of steatogenesis and inflammation, thus markedly improving liver homeostasis. This was associated with improvements in glucose tolerance and full restoration of insulin sensitivity despite the maintenance of obesity in these animals. Our data also put forward *A. muciniphila* and *Barnesiella spp.* as potential microbial contributors to the effect of CE and that the abundance of these bacteria in the gut microbiota is not phenotypically linked to changes in obesity. Finally, while supporting the regular consumption of cranberries to help counteracting obesity-related diseases, our data provide the fundamental bases for future human trials with CE or CE-related products as a strategy against diet-induced NAFLD/NASH and metabolic syndrome.

Acknowledgements

Duality of interest. The authors declare no conflict of interest.

References

1   Finucane MM, Stevens GA, Cowan MJ, Danaei G, Lin JK, Paciorek CJ, *et al.*, 2011. National, regional, and global trends in body-mass index since 1980: systematic analysis of health examination surveys and epidemiological studies with 960 country-years and 9.1 million participants. Lancet 377:557-567.

2   Locke AE, Kahali B, Berndt SI, Justice AE, Pers TH, Day FR, *et al.*, 2015. Genetic studies of body mass index yield new insights for obesity biology. Nature 518:197-206.

3   David LA, Maurice CF, Carmody RN, Gootenberg DB, Button JE, Wolfe BE, *et al.*, 2014. Diet rapidly and reproducibly alters the human gut microbiome. Nature 505:559-563.

4   Zietak M, Kovatcheva-Datchary P, Markiewicz LH, Stahlman M, Kozak LP, Backhed F, 2016. Altered Microbiota Contributes to Reduced Diet-Induced Obesity upon Cold Exposure. Cell metabolism 23:1216-1223.

5   Le Chatelier E, Nielsen T, Qin J, Prifti E, Hildebrand F, Falony G, *et al.*, 2013. Richness of human gut microbiome correlates with metabolic markers. Nature 500:541-546.

6   Margini C, Dufour JF, 2016. The story of HCC in NAFLD: from epidemiology, across pathogenesis, to prevention and treatment. Liver international : official journal of the International Association for the Study of the Liver 36:317-324.

7   Cani PD, Amar J, Iglesias MA, Poggi M, Knauf C, Bastelica D, *et al.*, 2007. Metabolic endotoxemia initiates obesity and insulin resistance. Diabetes 56:1761-1772.

8   Amar J, Chabo C, Waget A, Klopp P, Vachoux C, Bermudez-Humaran LG, *et al.*, 2011. Intestinal mucosal adherence and translocation of commensal bacteria at the early onset of type 2 diabetes: molecular mechanisms and probiotic treatment. EMBO molecular medicine 3:559-572.

9   Wang X, Ouyang Y, Liu J, Zhu M, Zhao G, Bao W, *et al.*, 2014. Fruit and vegetable consumption and mortality from all causes, cardiovascular disease, and cancer: systematic review and dose-response meta-analysis of prospective cohort studies. BMJ : British Medical Journal 349.

10   Bozzetto L, Annuzzi G, Pacini G, Costabile G, Vetrani C, Vitale M, *et al.*, 2015. Polyphenol-rich diets improve glucose metabolism in people at high cardiometabolic risk: a controlled randomised intervention trial. Diabetologia 58:1551-1560.

11   Cases J, Romain C, Dallas C, Gerbi A, Cloarec M, 2015. Regular consumption of Fiit-ns, a polyphenol extract from fruit and vegetables frequently consumed within the Mediterranean diet, improves metabolic ageing of obese volunteers: a randomized, double-blind, parallel trial. International journal of food sciences and nutrition 66:120-125.

12   Anhe FF, Roy D, Pilon G, Dudonne S, Matamoros S, Varin TV, *et al.*, 2015. A polyphenol-rich cranberry extract protects from diet-induced obesity, insulin resistance and intestinal inflammation in association with increased Akkermansia spp. population in the gut microbiota of mice. Gut 64:872-883.

13	Thaiss CA, Itav S, Rothschild D, Meijer M, Levy M, Moresi C*, et al.*, 2016. Persistent microbiome alterations modulate the rate of post-dieting weight regain. Nature 540:544-551.

14	Manach C, Scalbert A, Morand C, Remesy C, Jimenez L, 2004. Polyphenols: food sources and bioavailability. The American journal of clinical nutrition 79:727-747.

15	Roopchand DE, Carmody RN, Kuhn P, Moskal K, Rojas-Silva P, Turnbaugh PJ*, et al.*, 2015. Dietary Polyphenols Promote Growth of the Gut Bacterium Akkermansia muciniphila and Attenuate High-Fat Diet-Induced Metabolic Syndrome. Diabetes 64:2847-2858.

16	Masumoto S, Terao A, Yamamoto Y, Mukai T, Miura T, Shoji T, 2016. Non-absorbable apple procyanidins prevent obesity associated with gut microbial and metabolomic changes. Scientific reports 6:31208.

17	Chassaing B, Miles-Brown J, Pellizzon M, Ulman E, Ricci M, Zhang L*, et al.*, 2015. Lack of soluble fiber drives diet-induced adiposity in mice. American journal of physiology Gastrointestinal and liver physiology 309:G528-541.

18	Dudonné S, Varin TV, Forato Anhê F, Dubé P, Roy D, Pilon G*, et al.*, 2015. Modulatory effects of a cranberry extract co-supplementation with Bacillus subtilis CU1 probiotic on phenolic compounds bioavailability and gut microbiota composition in high-fat diet-fed mice. PharmaNutrition 3:89-100.

19	Mehlem A, Hagberg CE, Muhl L, Eriksson U, Falkevall A, 2013. Imaging of neutral lipids by oil red O for analyzing the metabolic status in health and disease. Nature protocols 8:1149-1154.

20	Edgar RC, 2010. Search and clustering orders of magnitude faster than BLAST. Bioinformatics 26:2460-2461.

21	DeSantis TZ, Hugenholtz P, Larsen N, Rojas M, Brodie EL, Keller K*, et al.*, 2006. Greengenes, a chimera-checked 16S rRNA gene database and workbench compatible with ARB. Applied and environmental microbiology 72:5069-5072.

22	Wang Q, Garrity GM, Tiedje JM, Cole JR, 2007. Naive Bayesian classifier for rapid assignment of rRNA sequences into the new bacterial taxonomy. Applied and environmental microbiology 73:5261-5267.

23	Bokulich NA, Subramanian S, Faith JJ, Gevers D, Gordon JI, Knight R*, et al.*, 2013. Quality-filtering vastly improves diversity estimates from Illumina amplicon sequencing. Nature methods 10:57-59.

24	Cole JR, Wang Q, Fish JA, Chai B, McGarrell DM, Sun Y*, et al.*, 2014. Ribosomal Database Project: data and tools for high throughput rRNA analysis. Nucleic acids research 42:D633-642.

25	Claesson MJ, O'Sullivan O, Wang Q, Nikkila J, Marchesi JR, Smidt H*, et al.*, 2009. Comparative analysis of pyrosequencing and a phylogenetic microarray for exploring microbial community structures in the human distal intestine. PloS one 4:e6669.

26	Segata N, Izard J, Waldron L, Gevers D, Miropolsky L, Garrett WS*, et al.*, 2011. Metagenomic biomarker discovery and explanation. Genome biology 12:R60.

27	Everard A, Belzer C, Geurts L, Ouwerkerk JP, Druart C, Bindels LB*, et al.*, 2013. Cross-talk between Akkermansia muciniphila and intestinal epithelium

controls diet-induced obesity. Proceedings of the National Academy of Sciences of the United States of America 110:9066-9071.

28   Shin NR, Lee JC, Lee HY, Kim MS, Whon TW, Lee MS, *et al.*, 2014. An increase in the Akkermansia spp. population induced by metformin treatment improves glucose homeostasis in diet-induced obese mice. Gut 63:727-735.

29   Kim MJ, Chung JY, Kim JH, Kwak HK, 2013. Effects of cranberry powder on biomarkers of oxidative stress and glucose control in db/db mice. Nutrition research and practice 7:430-438.

30   Larsen TM, Toubro S, Astrup A, 2003. PPARgamma agonists in the treatment of type II diabetes: is increased fatness commensurate with long-term efficacy? Int J Obes Relat Metab Disord 27:147-161.

31   Brocker CN, Yue J, Kim D, Qu A, Bonzo JA, Gonzalez FJ, 2017. Hepatocyte-specific PPARA expression exclusively promotes agonist-induced cell proliferation without influence from nonparenchymal cells. American journal of physiology Gastrointestinal and liver physiology 312:G283-G299.

32   Montagner A, Polizzi A, Fouche E, Ducheix S, Lippi Y, Lasserre F, *et al.*, 2016. Liver PPARalpha is crucial for whole-body fatty acid homeostasis and is protective against NAFLD. Gut 65:1202-1214.

33   Ahmadian M, Suh JM, Hah N, Liddle C, Atkins AR, Downes M, *et al.*, 2013. PPARgamma signaling and metabolism: the good, the bad and the future. Nature medicine 19:557-566.

34   Beaven SW, Wroblewski K, Wang J, Hong C, Bensinger S, Tsukamoto H, *et al.*, 2011. Liver X receptor signaling is a determinant of stellate cell activation and susceptibility to fibrotic liver disease. Gastroenterology 140:1052-1062.

35   Ding L, Pang S, Sun Y, Tian Y, Yu L, Dang N, 2014. Coordinated Actions of FXR and LXR in Metabolism: From Pathogenesis to Pharmacological Targets for Type 2 Diabetes. International journal of endocrinology 2014:751859.

36   Tanaka N, Aoyama T, Kimura S, Gonzalez FJ, 2017. Targeting nuclear receptors for the treatment of fatty liver disease. Pharmacology & therapeutics.

37   Yin W, Carballo-Jane E, McLaren DG, Mendoza VH, Gagen K, Geoghagen NS, *et al.*, 2012. Plasma lipid profiling across species for the identification of optimal animal models of human dyslipidemia. J Lipid Res 53:51-65.

38   Lelouvier B, Servant F, Paisse S, Brunet AC, Benyahya S, Serino M, *et al.*, 2016. Changes in blood microbiota profiles associated with liver fibrosis in obese patients: A pilot analysis. Hepatology 64:2015-2027.

39   Dao MC, Everard A, Aron-Wisnewsky J, Sokolovska N, Prifti E, Verger EO, *et al.*, 2016. Akkermansia muciniphila and improved metabolic health during a dietary intervention in obesity: relationship with gut microbiome richness and ecology. Gut 65:426-436.

40   Plovier H, Everard A, Druart C, Depommier C, Van Hul M, Geurts L, *et al.*, 2017. A purified membrane protein from Akkermansia muciniphila or the pasteurized bacterium improves metabolism in obese and diabetic mice. Nature medicine 23:107-113.

41   Ciubotaru I, Green SJ, Kukreja S, Barengolts E, 2015. Significant differences in fecal microbiota are associated with various stages of glucose tolerance in African American male veterans. Translational research : the journal of laboratory and clinical medicine 166:401-411.

42   de la Cuesta-Zuluaga J, Mueller NT, Corrales-Agudelo V, Velasquez-Mejia EP, Carmona JA, Abad JM*, et al.*, 2017. Metformin Is Associated With Higher Relative Abundance of Mucin-Degrading Akkermansia muciniphila and Several Short-Chain Fatty Acid-Producing Microbiota in the Gut. Diabetes care 40:54-62.

43   Pierre JF, Heneghan AF, Feliciano RP, Shanmuganayagam D, Roenneburg DA, Krueger CG*, et al.*, 2013. Cranberry proanthocyanidins improve the gut mucous layer morphology and function in mice receiving elemental enteral nutrition. JPEN Journal of parenteral and enteral nutrition 37:401-409.

44   Taira T, Yamaguchi S, Takahashi A, Okazaki Y, Yamaguchi A, Sakaguchi H*, et al.*, 2015. Dietary polyphenols increase fecal mucin and immunoglobulin A and ameliorate the disturbance in gut microbiota caused by a high fat diet. J Clin Biochem Nutr 57:212-216.

45   Anhe FF, Pilon G, Roy D, Desjardins Y, Levy E, Marette A, 2016. Triggering Akkermansia with dietary polyphenols: A new weapon to combat the metabolic syndrome? Gut microbes 7:146-153.

46   Cardona F, Andrés-Lacueva C, Tulipani S, Tinahones FJ, Queipo-Ortuño MI, 2013. Benefits of polyphenols on gut microbiota and implications in human health. The Journal of nutritional biochemistry 24:1415-1422.

47   Puupponen-Pimia R, Nohynek L, Hartmann-Schmidlin S, Kahkonen M, Heinonen M, Maatta-Riihinen K*, et al.*, 2005. Berry phenolics selectively inhibit the growth of intestinal pathogens. Journal of applied microbiology 98:991-1000.

48   Ubeda C, Bucci V, Caballero S, Djukovic A, Toussaint NC, Equinda M*, et al.*, 2013. Intestinal microbiota containing Barnesiella species cures vancomycin-resistant Enterococcus faecium colonization. Infection and immunity 81:965-973.

49   Ley RE, Backhed F, Turnbaugh P, Lozupone CA, Knight RD, Gordon JI, 2005. Obesity alters gut microbial ecology. Proceedings of the National Academy of Sciences of the United States of America 102:11070-11075.

50   Turnbaugh PJ, Backhed F, Fulton L, Gordon JI, 2008. Diet-induced obesity is linked to marked but reversible alterations in the mouse distal gut microbiome. Cell host & microbe 3:213-223.

51   Rabot S, Membrez M, Blancher F, Berger B, Moine D, Krause L*, et al.*, 2016. High fat diet drives obesity regardless the composition of gut microbiota in mice. Scientific reports 6:32484.

52   Reagan-Shaw S, Nihal M, Ahmad N, 2008. Dose translation from animal to human studies revisited. FASEB J 22:659-661.

53   Flammer AJ, Martin EA, Gossl M, Widmer RJ, Lennon RJ, Sexton JA*, et al.*, 2013. Polyphenol-rich cranberry juice has a neutral effect on endothelial function but decreases the fraction of osteocalcin-expressing endothelial progenitor cells. European journal of nutrition 52:289-296.

54   Kuipers F, Bloks VW, Groen AK, 2014. Beyond intestinal soap--bile acids in metabolic control. Nature reviews Endocrinology 10:488-498.

55   Puri P, Daita K, Joyce A, Mirshahi F, Santhekadur PK, Cazanave S*, et al.*, 2017. The presence and severity of nonalcoholic steatohepatitis is associated with specific changes in circulating bile acids. Hepatology [Epub ahead of print].

56   Liu X, Xue R, Ji L, Zhang X, Wu J, Gu J*, et al.*, 2014. Activation of farnesoid X receptor (FXR) protects against fructose-induced liver steatosis via inflammatory inhibition and ADRP reduction. Biochem Biophys Res Commun 450:117-123.

57   Zhang S, Wang J, Liu Q, Harnish DC, 2009. Farnesoid X receptor agonist WAY-362450 attenuates liver inflammation and fibrosis in murine model of non-alcoholic steatohepatitis. Journal of hepatology 51:380-388.

58   Han Y, Haraguchi T, Iwanaga S, Tomotake H, Okazaki Y, Mineo S, *et al.*, 2009. Consumption of some polyphenols reduces fecal deoxycholic acid and lithocholic acid, the secondary bile acids of risk factors of colon cancer. Journal of agricultural and food chemistry 57:8587-8590.

59   Ngamukote S, Makynen K, Thilawech T, Adisakwattana S, 2011. Cholesterol-lowering activity of the major polyphenols in grape seed. Molecules 16:5054-5061.

Legend to figures

Figure 1: Impact of CE on body features of Chow- and HFHS-fed mice. Mice were pre-fed a standard Chow diet or a high fat/high sucrose diet throughout 13 weeks and treated either with a cranberry extract (CE) or the vehicle for 8 additional weeks. (A) Weight gain and final body weight; (B) energy intake; (C) weight of visceral and subcutaneous fat pads. Two-way repeated measures RM-ANOVA with a Student-Newman-Keuls post hoc test was used to assign significance to the differences between time points within different groups. Two-way ANOVA with a Student-Newman-Keuls post hoc test was applied to calculate the significance of the differences between groups. Data are expressed as the mean ±SEM; n = 8-11; *P< 0.05, **P< 0.01 and ***P< 0.001.

Figure 2: CE reverses hepatic steatosis and alleviated liver inflammation. (A) Liver weight, (B) hepatic triglyceride accumulation, (C) representative images of hepatic lipid accumulation by oil red O (ORO) staining, (D) quantification of ORO-positive area and (E) plasma triglycerides. (F) Hepatic quantification of [MDA] malondialdehyde, [SOD] superoxide dismutase, [GPx] glutathione peroxidase and catalase. (G) Liver mRNA expression of [COX2] cyclooxygenase 2, [TNFα] tumor necrosis factor α, [NFκB], nuclear factor κ-light-chain-enhancer of activated B cells, [IκB] NFκB inhibitor. (H) Liver mRNA expression of [PPARα/γ] peroxisome proliferator-activated receptor α and γ, [SREBP1c/2] sterol regulatory element-binding protein 1c and 2 and [LXRα/β] liver X receptor α and β. Two-way ANOVA with a Student-Newman-Keuls post hoc test was applied to calculate the

significance of the differences between groups. Data are expressed as the mean ±SEM; n = 8-11; *P< 0.05, **P< 0.01 and ***P< 0.001.

Figure 3: CE improves glucose homeostasis and insulin sensitivity in diet-induced obese mice. At week 17, mice were fasted for 6 hours and (A,B) insulin tolerance tests (ipITT) were carried out after intraperitoneal insulin injections (ipITT, 0.65 IU/kg). At week 19, mice were fasted overnight (12 hours) and submitted to (C,D) oral glucose tolerance tests (OGTT). (E) Blood was collected during OGTT and used to assess insulinemia after glucose challenge. (A,C,E) Two-way repeated measures ANOVA with a Student-Newman-Keuls post hoc test was used to assign significance to the differences between time points within groups. *P< 0.05, **P< 0.01 and ***P< 0.001 for Chow vs HFHS; [#]P< 0.05, [##]P< 0.01; [###]P< 0.001 for HFHS vs HFHS+CE; [&]P< 0.05 for Chow vs Chow+CE. (B,D,F) Two-way ANOVA with a Student-Newman-Keuls post hoc test was applied to calculate the significance of the differences between groups. *P< 0.05, **P< 0.01 and ***P< 0.001; n = 8-11; Data are expressed as the mean ±SEM.

Figure 4: **CE administration alters the taxonomic profile of Chow- and HFHS-fed mice.** Genomic DNA was extracted from feces collected at week 21 and subsequent 16S rRNA-based gut microbial profiling was performed. Feces from mice housed in the same cage were pooled and considered as one biological sample (Chow n=3; Chow+CE n=4; HFHS n=3 and HFHS+CE n=4). (A) β-diversity among groups was initially observed by means of principal component analysis (PCoA) on weighted unifrac distances and the (B) Firmicutes to Bacteroidetes ratio was calculated as a general index of obesity-driven dysbiosis. Linear discriminant analysis (LDA) effect size (LEfSe) was calculated in order to explore the taxa that more strongly discriminate between the gut microbiota of (C) Chow $vs.$ HFHS, (D) Chow vs Chow+CE and (E) HFHS vs HFHS+CE. (B) Two-way ANOVA with a Student-Newman-Keuls post hoc test was applied to calculate the significance of the differences between groups. *P< 0.05, **P< 0.01 and ***P< 0.001.

Figure 5: **Fecal mucin quantification.** Cecal contents were collected at week 21, snap-frozen in liquid nitrogen and stored at -80 °C. Cecal feces were freeze-

powdered and the presence of mucins was determined using a fluorometric assay kit that discriminates *O*-linked glycoproteins (mucins) from N-linked glycoproteins. Two-way ANOVA with a Student-Newman-Keuls post hoc test was applied to calculate the significance of the differences between groups; n = 8-11; *P< 0.05, **P< 0.01 and ***P< 0.001.

Figures

Figure 1: Impact of CE on body features of Chow- and HFHS-fed mice.
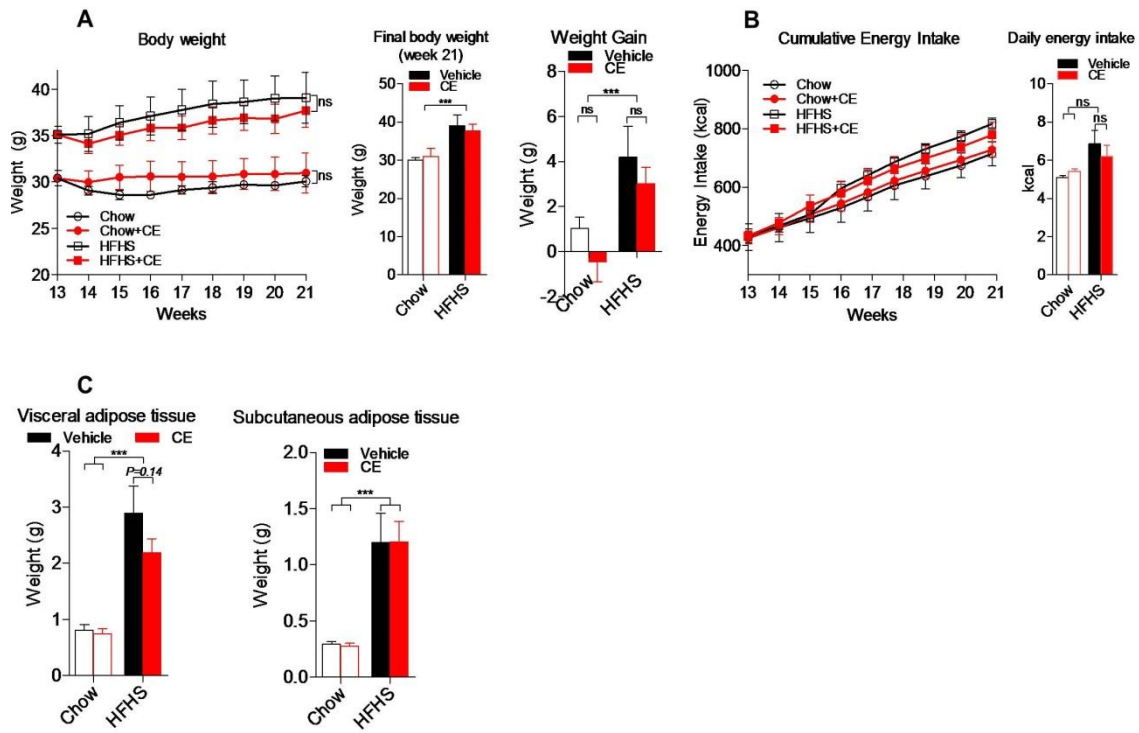
Figure 2: CE reverses hepatic steatosis and alleviates liver inflammation.
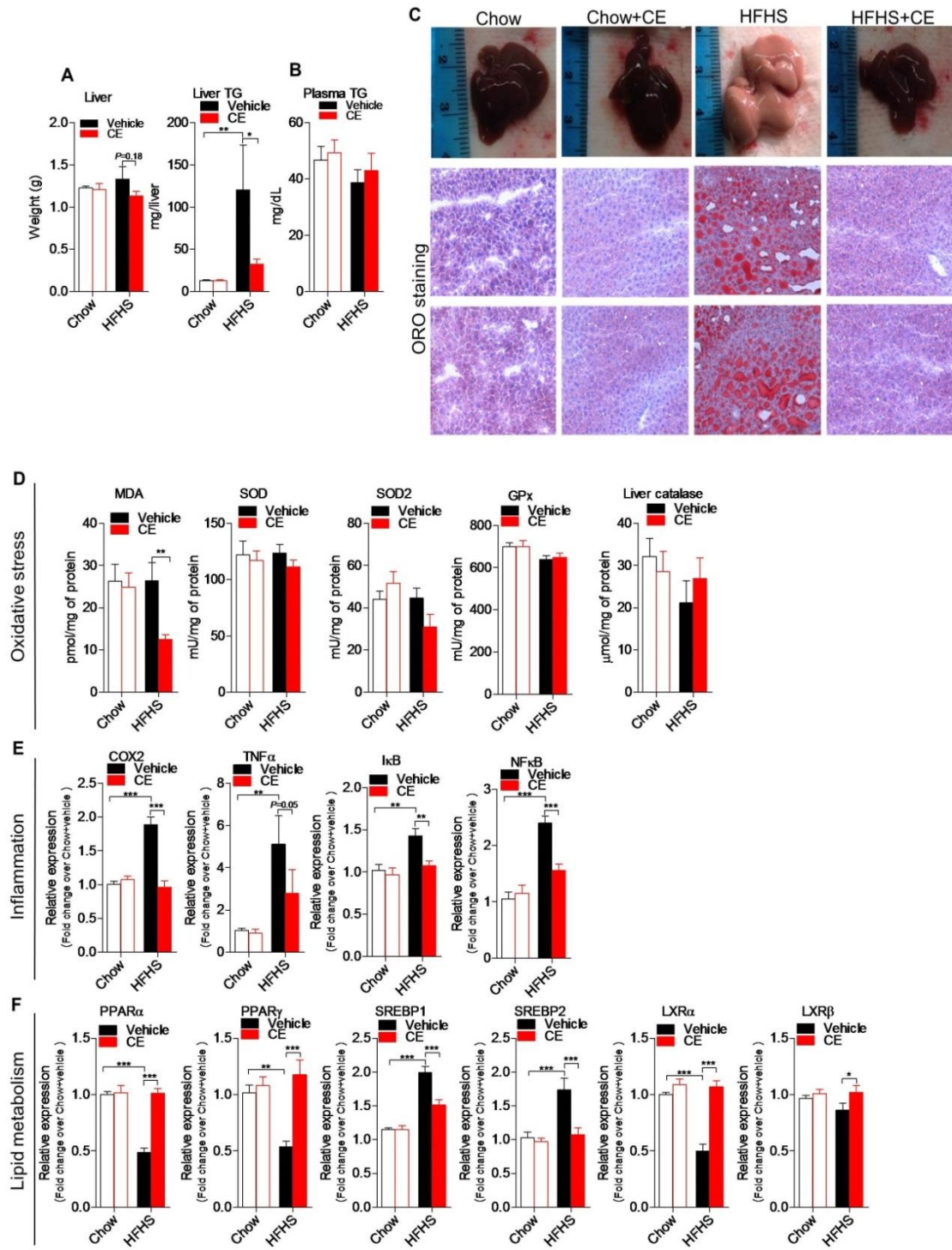
Figure 3: CE improves glucose homeostasis and insulin sensitivity in diet-induced obese mice.
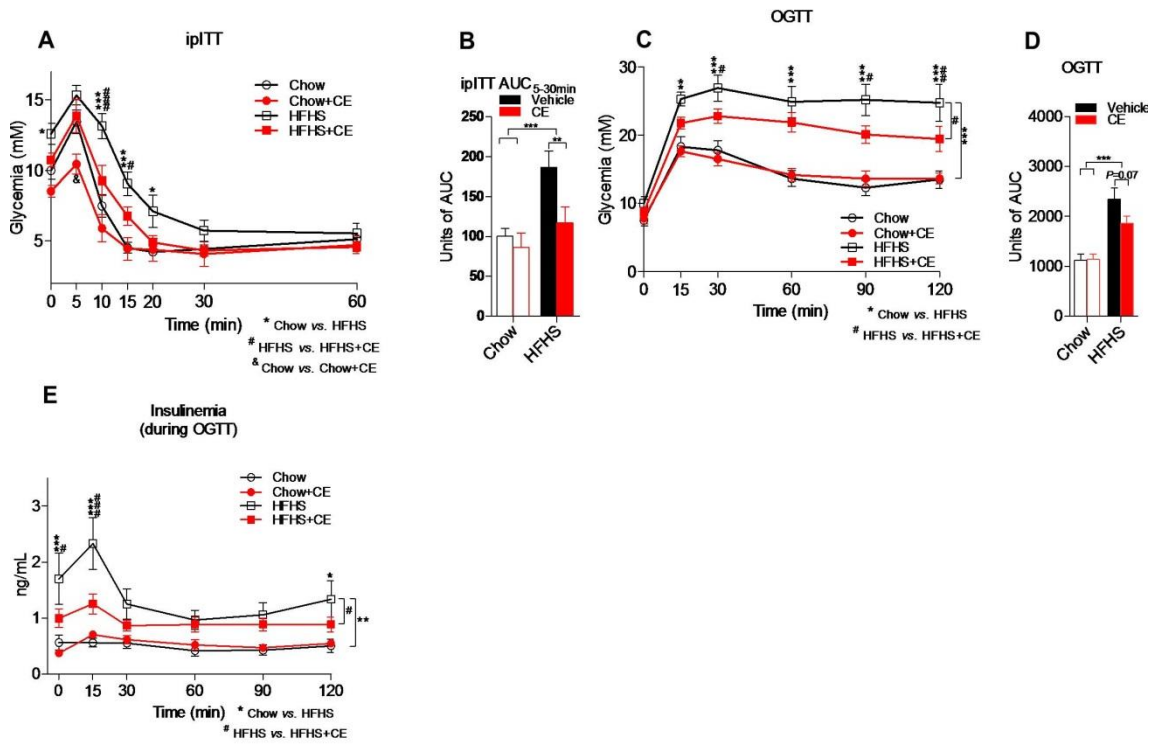
Figure 4: CE administration alters the taxonomic profile of Chow- and HFHS-fed mice.
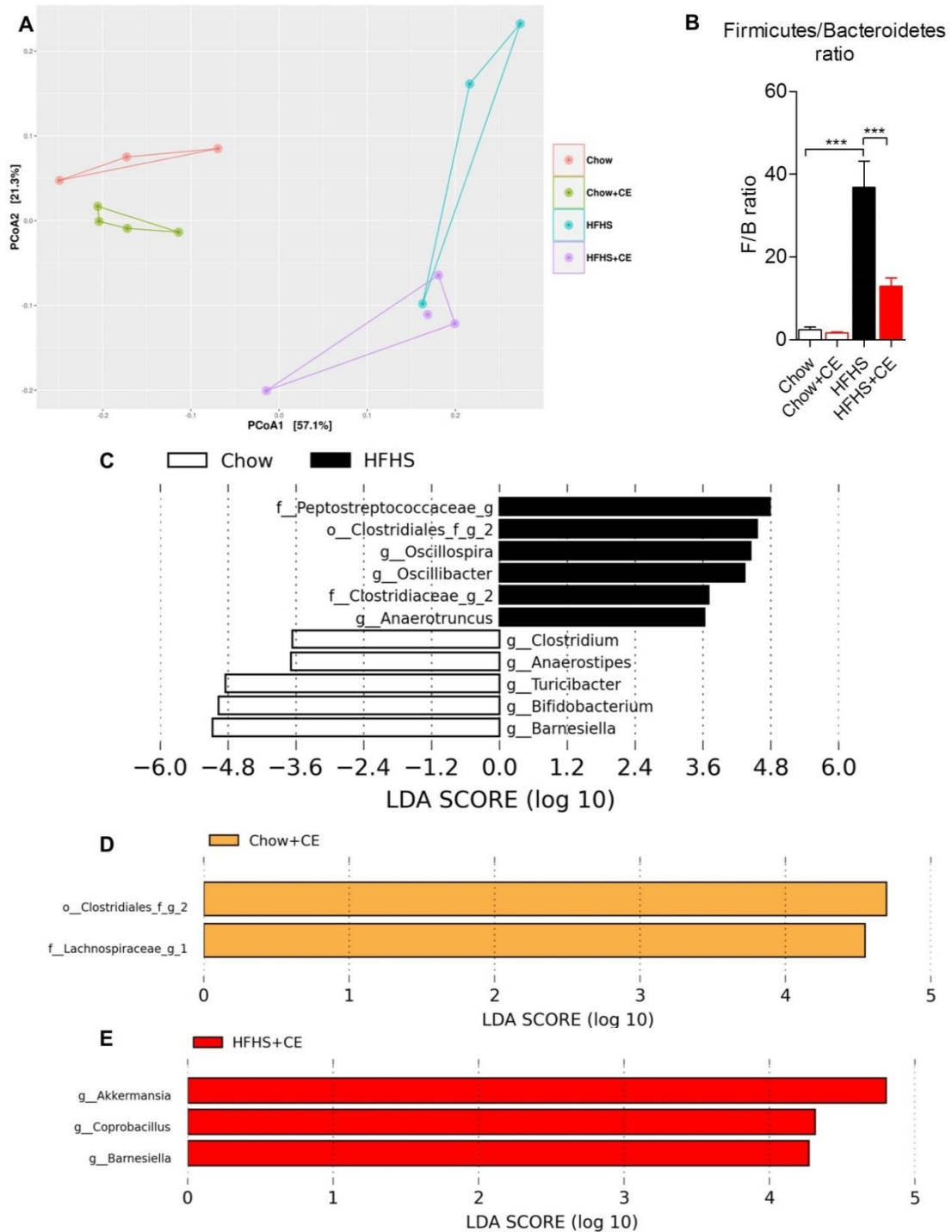
Figure 5: Fecal mucin quantification.
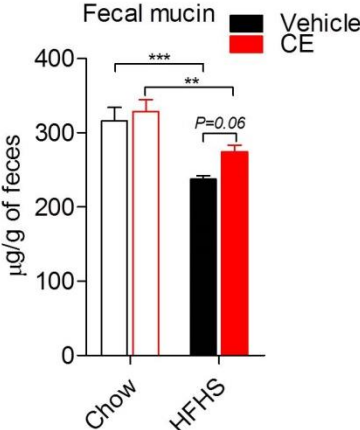
Supplemental material

Supplemental Figure 1: Gut microbial profile at genus level. In order to eliminate the putative influence of baseline (week 13) gut microbiota, the Δ relative abundance week21- relative abundance week13 was calculated. Chow n=3; Chow+CE n=4; HFHS n=3 and HFHS+CE n=4. Significance was calculated using Mann-Whitney *U* test with a Monte Carlo permutation test, *P< 0.05, **P< 0.01 and ***P< 0.001.

Supplemental Figure 1: Gut microbial profile genus level.
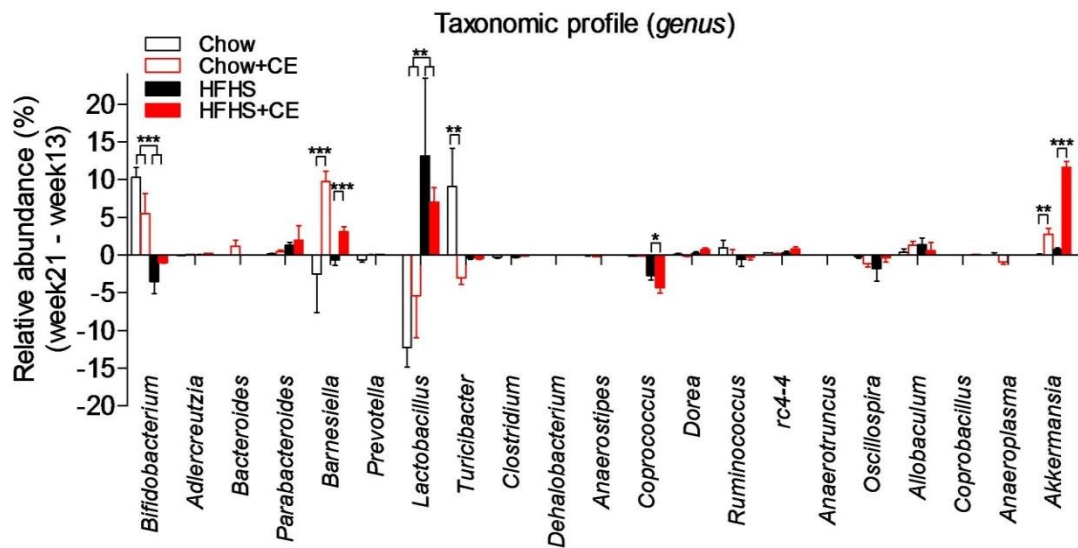
CHAPTER III

Arctic berry extracts target the gut-liver axis to alleviate metabolic endotoxemia, insulin resistance and hepatic steatosis in diet-induced obese mice

Fernando F. Anhê[1,2], Thibault V. Varin[2], Mélanie Le Barz[1,2], Geneviève Pilon[1,2], Stéphanie Dudonné[2], Philippe St-Pierre[1], Cory S. Harris[4], Michel Lucas[3], Mélanie Lemire[3], Éric Dewailly[3†], Yves Desjardins[2], Denis Roy[2] and André Marette[1,2]

[1]Department of Medicine, Faculty of Medicine, Cardiology Axis of the Québec Heart and Lung Institute, Laval University (Québec, Canada); [2]Institute of Nutrition and Functional Foods, Laval University (Québec,Canada); [3]Axe Santé des populations et pratiques optimales en santé, Centre de recherche du CHU de Québec - Département de médecine sociale et préventive, Université Laval (Québec, Canada); [4]Department of Biology, University of Ottawa (Ottawa, Canada).

[†] deceased 17 June 2014.

Résumé

Objectif: De plus en plus d'évidences indiquent que les polyphénols de fruits exercent des effets bénéfiques pour contrer le syndrome métabolique, mais les mécanismes sous-jacents demeurent encore mal compris. Dans la présente étude, nous avons analysé les effets d' extraits riches en polyphénols de cinq baies Arctiques chez un modèle de souris sur diète obésogène. Méthodes: Des souris mâles C57Bl/6J ont été nourries avec un régime riche en gras et en sucrose (HFHS) et traitées par voie orale avec des extraits de cinq différentes baies (200 mg / kg) pendant 8 semaines. Résultats: Les traitements avec des extraits de cloudberry, alpine bearberry et lingonberry, mais pas de ceux de bog blueberry ni de crowberry, ont amélioré la résistance à l'insuline et l'hyperinsulinémie post-prandiale chez des souris sur diète HFHS. Ces résultats ont été associés à une réduction du dépôt de triglycérides hépatiques et une nette amélioration de la clairance hépatique de l'insuline. Chez ces mêmes souris, au niveau intestinal, nous avons constaté une réduction de l'inflammation et de l'endotoxémie métabolique, soit une diminution des lipopolysaccharides circulants. Ces caractéristiques bénéfiques ont été associées à des modifications importantes au niveau taxonomique et fonctionnel du microbiote intestinal, favorisant principalement une représentation plus importante d'*A. muciniphila*. Conclusions: Nos résultats ont révélé de nouveaux mécanismes par lesquels les extraits riches en polyphénols d'alpine bearberry, lingonberry et surtout de cloudberry ciblent l'axe intestin-foie et protègent contre l'endotoxémie métabolique, la résistance à l'insuline et la stéatose hépatique. Ces résultats appuient les avantages potentiels de ces baies Arctiques et leur intégration dans des programmes de santé afin d'atténuer l'inflammation chronique et les troubles métaboliques liés à l'obésité.

Abstract

Aim/hypothesis: There is growing evidence that fruit polyphenols exert beneficial effects on the metabolic syndrome but the underlying mechanisms remain poorly understood. In the present study, we aimed to analyse the effects of polyphenolic extracts from five Arctic berries in a model of diet-induced obesity. *Methods:* C57Bl/6J male mice were fed a high fat/high sucrose diet and orally treated with extracts of bog blueberry (BBE), cloudberry (CLE), crowberry (CRE), alpine bearberry (ABE), lingonberry (LGE) or the vehicle (HFHS) for 8 weeks. An additional group of chow-fed vehicle-treated mice was included as a reference control for diet-induced obesity. Oral (OGTT) and insulin (ITT) tolerance tests were conducted, and both plasma insulin and c-peptide were assessed throughout OGTT. Q-PCR, western blot analysis and enzyme-linked immunosorbent assays were used to assess enterohepatic immunometabolic features. Fæcal DNA was extracted and 16S rRNA gene-based analysis was used to profile the gut microbiota. *Results*: Treatment with CLE, ABE and LGE, but not BBE or CRE, prevented fasting (Chow 67.2 ±12.3, HFHS 153.9 ±19.3, BBE 114.4 ±14.3, CLE 82.5 ±13.0, CRE 152.3 ±24.4, ABE 90.6 ±18.0, LGE 95.4 ±10.5; pmol/l) and post-prandial (Chow 14.3 ±1.4, HFHS 31.4 ±3.1, BBE 27.2 ±4.0, CLE 17.7 ±2.2, CRE 32.6 ±6.3, ABE 22.7 ±18.0, LGE 23.9 ±2.5; AUC pmol/l x min) hyperinsulinæmia. Neither of the treatments affected c-peptide levels or body weight gain. While hepatic p-AKT serine was 2.6, 2.5 and 2.2 times higher in CLE, ABE and LGE respectively, hepatic CEACAM-1 tyrosine phosphorylation was 1.6, 1.7 and 1.9 times increased in these mice when compared with vehicle-treated HFHS-fed mice. These findings were associated with reduced liver triacylglycerol deposition, lower circulating endotoxin, alleviated hepatic and intestinal inflammation and major gut microbial alterations (*eg*, bloom of *Akkermansia muciniphila*, *Turicibacter* and *Oscillibacter*) in CLE, ABE and LGE mice. *Conclusions*: Our findings reveal novel mechanisms by which polyphenolic extracts from alpine bearberry, lingonberry and especially cloudberry target the gut-liver axis to protect from metabolic endotoxæmia, insulin resistance and hepatic steatosis, which importantly improves hepatic insulin clearance. These results support the potential benefits of

these Arctic berries and their integration into health programs to help attenuate obesity-related chronic inflammation and metabolic disorders.

Introduction

Obesity has reached pandemic proportions, increasing the rates of CVD and type 2 diabetes [1]. Excessive accumulation of visceral fat promotes metabolic alterations triggered and sustained by a low-grade chronic inflammatory state [2]. While features of the metabolic syndrome have been associated with major taxonomic and functional changes in the gut microbiota [3, 4], DIO has been linked to gut barrier disruption and the leakage of microbial-derived endotoxin to circulation (ie, metabolic endotoxæmia) [5], which contributes to the onset and progression of insulin resistance. Metabolic endotoxæmia also plays a role in the development of NAFLD, which stems from the functional connection between gut and liver through the enterohepatic circulation [6].

There is compelling epidemiological evidence that diets rich in fruits and vegetables are strongly associated with better health and reduced all-cause mortality [7, 8]. While several studies using animal models have confirmed the positive impact of polyphenols on metabolic health [9], pharmacological doses with little nutritional relevance are often tested. Here we analyse the effect of five polyphenol-rich extracts of Arctic berries (*i.e.,* Bog Blueberry, Cloudberry, Crowberry, Alpine Bearberry and Lingonberry), at nutritionally relevant doses, against intestinal inflammation, metabolic endotoxæmia and features of the metabolic syndrome in a murine model of DIO.

Metagenome-wide association studies have revealed that the consumption of fruits and other polyphenol-rich foods (*e.g.*, dark chocolate, red wine, coffee, tea) are amongst the strongest factors explaining alterations in gut microbial communities in humans [10, 11]. Accordingly, we and others have previously reported that berry polyphenols have a marked impact on the gut microbiota [12-15]. We therefore applied 16S rRNA-based analysis in order to investigate the potential role of the gut microbiota in the effects of Arctic berry extracts.

Material and methods

Animals. Eight week-old C57Bl/6J male mice (Jackson, USA) were bred in the animal facility of the Institute of Nutrition and Functional Foods. Mice were housed two per cage in a controlled environment (12 hours daylight cycle, lights off at 18:00) with food and water *ad libitum*. Mice were randomly divided into 6 groups (n=12) and fed a HFHS diet (ESM Table 1). Treatment started concomitantly with the introduction of HFHS diet and consisted of daily oral doses (200 mg of powdered extract/kg of body weight) of resuspended extracts of Bog Blueberry (BBE, *Vaccinium uliginosum* L.), Cloudberry (CLE, *Rubus chamaemorus* L.), Crowberry (CRE, *Empetrum nigrum* L.), Alpine Bearberry (ABE, *Arctostaphylos alpine* L. Spreng.) or Lingonberry (LGE, *Vaccinium vitis-idaea* L.) or the vehicle used to resuspend these extracts (i.e., animal facility's drinking water) throughout 8 weeks. An additional group (n=12) of chow-fed (Teklad 2018, Envigo, UK, Cambridgeshire) vehicle-treated mice was included as a reference control for HFHS-induced obesity. Body weight gain and food intake were assessed twice a week. At week 8, animals were anesthetized in chambers saturated with isoflurane and then sacrificed by cardiac puncture. Tissues were harvested and blood was drawn in tubes containing 2 IU of heparin and immediately centrifuged in order to separate plasma from cells. This study followed the *guide for the care and use of laboratory animals* and all procedures were previously approved by the Laval University Animal Ethics Committee.

Extract of Arctic berries. Bog blueberries, cloudberries, crowberries, alpine bearberries and lingonberries (refer to Table 1 for a complete list of names) were harvested in Nunavik (Northern Québec, Canada) and stored frozen (–20 °C). After grinding, fresh frozen berries were extracted twice with 100% ethanol; the obtained solution was then filtered, rotoevaporated and freeze-dried. The phenolic profile of the extracts studied herein is described in Table 2. Harvest sites along with a more detailed phenolic profile of the berries used in this study were published elsewhere [16].

Glucose homeostasis. Insulin (ipITT) and glucose (OGTT) tolerance tests were performed as previously described [12]. Blood samples were collected at each time point during OGTT for insulinæmia and c-peptide determination.

Analytical methods. Plasma insulin and c-peptide concentrations were measured using an ultra-sensitive ELISA kit (Alpco, USA, New Hampshire). Liver triacylglycerol was assessed after chloroform-methanol extraction and enzymatic reactions with a commercial kit (Randox Laboratories, Crumlin, UK). Plasma endotoxin (LPS) concentration was determined using a kit based on a reaction with Limulus amebocyte lysate (LAL kit endpoint-QCL1000, Lonza, USA, New Jersey) as in [12]. Plasma BCAA (leucine, isoleucine and valine) were determined using a colorimetric assay kit (BioVision, USA, California). Fæcal SCFA and BCFA were assessed by GC as previously described [17]. Fæcal pellets collected at week 6 were dried and gross energy density was determined using adiabatic bomb calorimetry (Parr Instruments, Moline, IL). Plasma bile acids were assessed as previously described [18].

Western blot. Analysis of total CEACAM-1, total AKT, tyrosine-phosphorylated CEACAM-1 and p-AKT (serine 473) were performed as previously described [19, 20]. Immunoblotting was carried out using anti-CEACAM-1(#3759, 1:1000, Beauchemin Lab, McGill University, Montréal, Canada), a cocktail of monoclonal anti-phosphotyrosine antibodies (rabbit #9411, 1:1000, Cell Signalling, USA, MA and clone 4G10, 1:1000, Millipore, USA, IL), anti-AKT (rabbit #9272S, 1:1000, Cell Signalling, USA, MA) and anti-p-AKT serine 473 (rabbit #9271L, 1:1000 Cell Signalling, USA, MA). Anti-ACTIN was used as loading control (mouse sc-8432, 1:5000, Santa Cruz Biotechnology, USA, CA).

Messenger RNA quantification by real time PCR. Sections of jejunum and colon (approximately 0.5 cm) and freeze-powdered livers were homogenized in 1 ml of TRIzol reagent (Thermo Fisher Scientific, USA, MA) and total RNA was purified using a RNeasy mini kit (Qiagen, Germany). After RNA reverse transcription, real time PCR was performed using a SYBR Green Jump-Start Gene Expression Kit (Sigma-Aldrich, USA, Missouri) or with commercially available

Taqman primers and probe sets and Taqman Mastermix (Life Technologies, USA, CA). *Acaca, Adgre1, Cd11c, Cox2, Gcg, Il1b, Klf4, Marco, Nos2, Ocln, Ppara, Reg3g, Tjp1, Tlr4* and *Tnfa* gene expression was assessed by the $\Delta\Delta_{Ct}$ method and *Actb* or *Hprt* were used as reference genes. Primer sequences are available under request.

Bacterial genomic DNA extraction and 16S rRNA gene-based gut microbial analysis. Fæcal samples were freshly collected at week 8 and immediately stored at -80 °C. Bacterial genomic DNA was extracted as in [12]. 16S rRNA gene-based profiling of the fæcal microbiota was carried out as previously described [21]. All raw sequences were deposited in the public European Nucleotide Archive server under accession number PRJEB19783.

Functional prediction of gut bacterial communities. Prediction of the functional genes was performed using PICRUSt (Phylogenetic Investigation of Communities by Reconstruction of Unobserved States) ([11]). Briefly, from 16S rRNA sequencing data and from the Kyoto encyclopedia of genes and genomes (KEGG) reference genomes, PICRUSt was used to estimate gene family abundance based on an extended ancestral-state reconstruction algorithm and then to produce a predicted metagenome functional content for each sample. This software was also used to determine OTU contribution to a given KEGG pathway.

Statistical analysis. Data are expressed as mean ± SEM. One-way ANOVA with a post-hoc Student-Newman-Keuls test and unpaired student t-test were used to assign significance to the comparisons between HFHS-fed controls *versus* Arctic berry-treated groups and Chow- *versus* HFHS-fed controls respectively (GraphPad, USA). Time points within different groups were compared using two-way repeated measures ANOVA with a Student-Newman-Keuls post-test (Sigmaplot, USA). All results were considered statistically significant at $p < 0.05$.

Weighted UniFrac distance matrix was calculated at the genus level based on taxa having at least 1% of total relative abundance. PCoA (Principal Coordinates Analysis) was performed on the resulting distance matrix using the

'phyloseq' R package (version 1.16.2). The statistical significance of differentially abundant and biologically relevant taxonomical and functional biomarkers between groups was measured using a linear discriminant analysis (LDA) effect size (LEfSe) with a threshold of 2 or 2.5. A *p*-value < 0.05 was considered to indicate statistical significance for the factorial Kruskal–Wallis rank-sum test.

Results

Administration of the Arctic berry extracts had no impact on HFHS-induced weight gain, fat mass accretion (table 3) or elevated fasting blood glucose (figure 1A). However, CLE, ABE and LGE mice had lower plasma insulin levels than vehicle-treated HFHS-fed controls (figure 1B). The glucose-lowering effect of insulin measured during insulin tolerance tests (ipITT) was improved at the 10 and 90 min time points in CLE and LGE mice as compared to vehicle-treated animals, indicating an insulin sensitizing effect (figure 1D). C-peptide levels were increased by HFHS feeding but not affected by any of the berry extracts (figure 1C), suggesting that changes in insulin clearance, and not in insulin secretion, may underlie the reduced fasting hyperinsulinæmia in CLE, ABE and LGE mice.

We next sought to investigate the dynamic glycemic/insulinemic responses. None of the extracts improved HFHS-induced glucose intolerance, and blood glucose was slightly higher in ABE- (90 min time point) and LGE- (90 and 120 time points) mice post-glucose challenge (figure 2A), although this was not enough to promote glucose intolerance based on calculation of the areas under the glucose curves (insert figure 2A). Plasma insulin during OGTT in CLE-treated mice was lower than in vehicle-treated HFHS control mice, reaching the level of significance at the 15 and 30 minutes time points and also when calculating the total area under the insulin curve. ABE (30 and 90 min) and LGE (30 and 120 min) treatments also lowered insulin levels at specific time points, albeit this was not enough to significantly impact the overall areas under the insulin curves (figure 2B). Similarly to fasting state, there were no differences in glucose-induced insulin secretion as revealed by the c-peptide responses during OGTT (figure 2C), again suggesting that these three berry extracts, especially CLE, reduced hyperinsulinæmia through

an effect on insulin clearance rather than on insulin secretion. Consistent with improved hepatic insulin sensitivity, we found increased AKT phosphorylation at serine 473 in the liver of CLE-, ABE- and LGE-treated mice as compared with vehicle-treated controls (Figure 2D).

Tyrosine phosphorylation of CEACAM-1 is a key event involved in receptor-mediated insulin endocytosis and degradation in the hepatocyte [22] and a major pathway for hepatic insulin clearance *in vivo* [19, 20]. Despite no changes in total CEACAM-1 content (figure 2E), CLE, ABE and LGE mice displayed higher tyrosine phosphorylation of CEACAM-1 in comparison with HFHS-fed controls (figure 2F). Taken together, our findings suggest that those three berry extracts prevented DIO-induced hyperinsulinæmia by protecting the liver from the detrimental consequences of HFHS feeding, therefore improving the hepatic capacity to clear insulin out of circulation.

Treatment with CLE, ABE and LGE significantly reduced HFHS-induced hepatic triacylglycerol accumulation and triacylglycerolemia in comparison with vehicle-treated HFHS-fed controls (figure 2G,H). These findings suggest increased lipid oxidation in the liver, rather than decreased lipid uptake, as an important driver of the benefits of CLE, ABE and LGE to liver homeostasis. Consistent with increased lipid catabolism, the mRNA expression of *Ppara* and *Acaca* (Acetyl-CoA carboxylase) was higher and lower, respectively, in the liver of CLE-, ABE- and LGE-treated mice *versus* HFHS-fed controls (Figure 2I).

To investigate the inflammatory profile in the liver of CLE, ABE and LGE-treated mice we measured the mRNA expression of several genes involved in immune regulation. While the mRNA expression of *Adgre1* (encodes F4/80) and *Cd11c* (both markers of macrophages) was unchanged, CLE, ABE and LGE treatment markedly downregulated *Marco* and upregulated *Klf4* mRNA expression (Figure 2I). Since *Marco* and *Klf4* are markers of polarization towards M1 and M2 population [23, 24], respectively, these findings suggest that these three extracts did not alter the number of macrophages but triggered their polarization towards a less pro-inflammatory activity. Accordingly, CLE, ABE and LGE mice expressed

142

lower levels of *Il1b* transcripts and non-significantly expressed less *Tnfa* than vehicle-treated HFHS-fed mice (Figure 2I). *Cox2* mRNA expression was not altered in CLE-, ABE- and LGE-treated mice, but since HFHS-fed mice did not show higher *Cox2* mRNA expression than Chow-fed mice, it suggests that this enzyme is not particularly regulated at the transcriptional level in our model. The mRNA expression of *Tlr4* was lower in CLE, ABE and LGE-treated mice when compared with vehicle-treated HFHS-fed mice (Figure 2I), suggesting that a reduction in the activation of the hepatic innate immune response by microbial-associated molecular patterns contributes to alleviate inflammation in the liver of CLE, ABE and LGE mice.

Consistent with our previous observations, CLE, ABE and LGE administration significantly blunted metabolic endotoxæmia (figure 3A), suggesting improved intestinal barrier integrity. The mRNA expression of *Nos2* (encodes iNOS), was decreased in the jejunum of CLE and LGE mice and was non-significantly lower in ABE mice as compared to HFHS controls (figure 3B). In the colon, the HFHS-induced increase in *Nos2* expression was significantly prevented by CLE, ABE and LGE treatment (figure 3J). The mRNA expression of *Tnfa* was decreased in the jejunum of LGE mice (figure 3C) and in the colon of CLE, ABE and LGE mice (figure 3K) *versus* vehicle-treated HFHS controls. We found lower mRNA expression of *Adgre1* in the jejunum and a non-significant reduction in *Adgre1* expression in the colon of CLE, ABE and LGE mice (figures 3D, L). Similarly, the mRNA expression of *Cd11c* (also present in macrophages) was non-significantly reduced in the jejunum and was significantly lower in the colon of CLE-, ABE- and LGE-treated mice (Figures 3E, M). No significant changes in the mRNA expression of *Tjp1* and *Ocln* were found in the jejunum and in the colon, although a non-significant increase in *Tjp1* gene expression was found in the colon of CLE, ABE and LGE mice (figure 3F,G,N,O). Furthermore, while CLE, but not ABE and LGE treatment, prevented the HFHS-induced decrease in the mRNA expression of the antimicrobial peptide *Reg3g* (figure 3H,P), the mRNA expression of the proglucagon gene *Gcg* was not altered by either of the extracts (figure 3I,Q).

We next explored the impact of CLE, ABE and LGE administration on the gut-liver axis by applying 16S rRNA gene-based analysis of fæcal DNA samples. Principal component analysis (PCoA) on weighted UniFrac distances showed a separation between the gut microbiota of Chow and HFHS-fed mice (figure 4A). CLE, ABE and, to a lesser extent, LGE microbial communities clustered apart from those of HFHS-fed controls (figure 4A), indicating altered β-diversity in CLE, ABE and LGE mice *versus* vehicle-treated HFHS-fed mice. The Firmicutes to Bacteroidetes (F/B) ratio was drastically increased in HFHS- *versus* Chow-fed mice, whereas CLE, ABE and LGE administration attenuated this feature (ESM Table 3). Gut microbial communities of CLE mice were discriminated from that of HFHS-fed control mice by an increased presence of Peptostreptococcaceae, *A. muciniphila* and *Turicibacter* and by a lower representation of taxa assigned to the genera *Lactobacillus* and *Bifidobacterium* in the fæcal microbiota (Figure 4C). Overrepresentation of *Oscillibacter* and *A. muciniphila* were identified as the main features discriminating ABE from vehicle-treated HFHS-fed mice metagenomes (Figure 4D), whereas increased presence of *Oscillibacter* and *Turicibacter* were characteristic gut microbial features of LGE mice *versus* vehicle-treated HFHS mice (Figure 4E). Relative abundances are described in ESM Tables 2-6.

We applied the PICRUSt method to predict functional alterations in the gut microbiome of HFHS mice treated with CLE, ABE and LGE. As previously reported [14, 25], functions related to cell motility (*i.e.*, bacterial motility, flagellar assembly, bacterial chemotaxis) were more represented in the gut microbiota of HFHS-fed mice than in Chow-fed mice (Figure 5A). Our analysis revealed an overall increase in functional pathways related to cofactor and vitamin metabolism (*e.g.*, folate, riboflavin and biotin metabolism) and metabolism of terpenoids (e.g., limonene, pinene and geraniol degradation) in CLE, ABE and LGE mice *versus* HFHS controls (Figures 5B-D). Increased amino acid, fatty acid, carbohydrate (*e.g.*, TCA cycle) and energy metabolism were functions overrepresented in CLE, ABE and LGE gut microbiota (Figures 5B-D). Microbial pathways assigned to valine, isoleucine and leucine (BCAA) degradation were increased in CLE and ABE-treated mice *versus* vehicle-treated HFHS-fed animals (Figures 5B-D). Altogether,

PICRUSt analysis highlighted important adaptations in the intestinal microbiome in response to phytochemicals and points to a general impact of CLE, ABE and LGE administration on bacterial substrate utilisation.

We next assessed key metabolome components involved in the gut microbiota-host interaction. Neither of the extracts significantly affected the profile or the total amount of fæcal SCFA (ESM Figure 1A) and plasma bile acids (ESM Figure 2). Interestingly, fæcal energy density was found to be lower in CLE-, ABE- and LGE-treated mice *versus* HFHS-fed vehicle-treated controls (ESM Figure 1C). Moreover, the concentration of branched-chain short chain fatty acids (BCFA), which are by-products of microbial BCAA degradation, were non-significantly higher in the fæces of CLE-treated mice (ESM Figure 1B), indicating lower BCAA availability to the host. We therefore assessed the circulating levels of BCAA and found a non-significant (P=0.06) decrease in circulating BCAA in CLE mice *versus* vehicle-treated HFHS-fed mice (ESM Figure 1D).

Discussion

Our work shows that the daily administration of CLE, ABE and LGE alleviates HFHS-induced intestinal inflammation and metabolic endotoxæmia, which was found to be independent of an anti-obesity effect and associated with improved liver function, ameliorated hepatic insulin sensitivity and attenuated hyperinsulinæmia in DIO mice. Our data also provide evidence for an adaptive response of intestinal bacterial communities to the presence of CLE, ABE and LGE, leading to altered taxonomic and functional profiles.

In line with our findings, the administration of lingonberry extracts to DIO mice has been previously associated with attenuated hyperinsulinæmia, reduced liver steatosis [26, 27], alleviated circulating lipopolysaccharide binding protein (LBP) and major taxonomic and functional alterations in the gut microbiota, such as bloom of *A. muciniphila* and increased microbial pathways linked to substrate utilisation [14]. While in this latter study treatment with a lingonberry extract has been shown to prevent HF-induced obesity [14], in our model LGE did not affect

fat mass accretion. This is possibly explained by three major factors: (i) differences in the composition of the extracts, (ii) differences in the diet used and (iii) by the mode of administration of the extracts (gavage *versus* mixing the extract to the diet). Interestingly, the same group has shown that lingonberry extracts from different batches exert distinct effects on body fat accumulation [14]; in agreement with our results, the batch that did not affect obesity still improved hepatic steatosis, liver inflammation and plasma LBP [14]. Importantly, our study further demonstrates that the obesity-independent benefits of LGE involves better hepatic insulin sensitivity, improved insulin clearance and alleviated metabolic endotoxæmia.

By assessing c-peptide secretion and hepatic CEACAM-1 activation our study provides novel mechanistic insight to the metabolic benefits of LGE, CLE and ABE, where improved hepatic insulin clearance is likely the key mechanism underlying lower hyperinsulinæmia in these mice. Since liver-specific CEACAM-1 overexpression in HFHS-fed mice was shown to prevent hyperinsulinæmia, insulin resistance and hepatic lipid accumulation by increasing hepatic β-oxidation [28], it is possible that CLE, ABE and LGE target CEACAM-1 to improve both insulin clearance and hepatic steatosis. It is also conceivable that alleviation of HFHS-induced intestinal inflammation and LPS leakage in CLE, ABE and LGE mice contributes to reduce the pro-inflammatory load reaching the liver to therefore improve hepatic metabolism. While CLE, ABE and LGE administration were not associated with improved glucose tolerance, as determined from an OGTT, the glucose-induced insulinemic responses were reduced and accompanied by increased hepatic insulin clearance whereas pancreatic insulin secretion remained unchanged. It is possible that an 8-week long treatment with CLE, ABE and LGE exert beneficial effects that are more restricted to the gut-liver axis, resulting in a milder impact on the muscle's ability to uptake glucose while predominantly improving hepatic insulin resistance and limiting chronic hyperinsulinæmia. This is in line with the concept that hyperinsulinæmia is an early event leading to type 2 diabetes [29].

Our results clearly indicate that the effectiveness of polyphenolic extracts against features of the metabolic syndrome varies considerably. Ellagitannins were present only in CLE (538.7 µg/kg) and ABE (523.1 µg/kg), while low amounts of free ellagic acid were present in CLE (21.6 µg/kg), ABE (2.1 µg/kg) and LGE (22.8 µg/kg). The bioactivity of ellagic acid and its hydrolysable polymeric form (*i.e.*, ellagitannins) is dependent on gut microbial hydrolysis of ellagitannins (yielding ellagic acid) and processing of ellagic acid into urolithins [30]. While urolithin A has been implicated in mitophagy and prolonged lifespam in *C. elegans* [31], ellagic acid administration has been shown to improve metabolic health in HFHS-fed rats [32]. LGE is particularly rich in proanthocyanidins (PACs) with degree of polymerization (DP) ranging from 2 to 10 and in polymeric PACs (DP >10). PACs are poorly bioavailable and were linked to major gut microbial changes, blunted gut inflammation and enhanced metabolism in obese mice [12, 33]. However, other subclasses of polyphenols, non-flavonoid secondary metabolites, vitamins, minerals and soluble fibres were also present in the Arctic berry extracts and may potentially account for the effects seen.

A. muciniphila is a Gram-negative mucin-degrading bacterium highly associated with better health status [11], causally implicated in the improvement of diet-induced insulin resistance [34, 35] and closely associated with the intake of polyphenol-rich fruit extracts [36]. *A. muciniphila* utilises ellagic acid as a substrate [37], which may partially explain the higher presence of *A. muciniphila* in the gut microbiota of CLE and ABE mice. The effect of PACs on *A. muciniphila* still warrants further investigation, but it has been hypothesised to be a response to a PAC-stimulated increase in mucus production, which creates a propitious environment for *A. muciniphila* to thrive [36]. CLE-, but not ABE and LGE-treated mice, showed a marked upregulation of *Reg3g* mRNA expression in both jejunum and colon. REG3γ is an antimicrobial peptide and an important component of the intestinal barrier. In agreement with previous works showing a tight relationship between *A. muciniphila* and the expression of *Reg3g* [34], CLE treated mice displayed the highest abundance of this bacterium (ESM Table 6). However, since *A. muciniphila* is not a major coloniser in the jejunum, CLE may enhance REG3γ

secretion in the proximal bowel likely by mechanisms independent of *A. muciniphila*. It is noteworthy that as ABE- and LGE-treated mice showed improved gut barrier, as suggested by lower endotoxæmia in these mice, it is plausible that factors beyond REG3γ play a part in the benefits of ABE and LGE to intestinal homeostasis.

None of the extracts affected the profile or the total amount of fæcal SCFA and plasma bile acids. While our results suggest that the effects of CLE-, ABE- and LGE- on the gut microbiota and on host physiology are independent of major alterations in the synthesis of SCFA and in the BA profile, we cannot rule out the relevance of these molecules to the phenotype of CLE-, ABE- and LGE-treated mice. Further analysis of SCFA in plasma and tissues (e.g., liver) and a broader profile of bile acids (fæces, gallbladder and plasma) are both warranted.

Lower energy density in the fæces of CLE, ABE and LGE mice coupled with PICRUSt analysis suggested increased bacterial amino acid, fatty acid and carbohydrate utilisation. However, gut transit was not taken into account in our study and it is a key variable in the energy excretion equation. Importantly, since neither of the treatments significantly affected weight gain and there were no differences in energy intake between groups, it is reasonable to conclude that bacterial utilisation of dietary substrates was not modified to an extent that impacted energy availability to the host.

Microbial BCAA degradation was predicted to be overrepresented in CLE and ABE mice and similar results were found in rats supplemented with lowbush blueberries (*Vaccinium angustifolium*) [38]. Further analysis revealed a non-significant reduction in BCAA availability to the host in CLE-treated mice. This is of particular interest because increased circulating BCAA levels have been established as an early biomarker of insulin resistance, type 2 diabetes and NAFLD [39-41]. While our study does not bring definitive proof that reduced BCAA availability to the host contributes to improved insulin sensitivity and hepatic homeostasis in CLE mice, they call the attention for a promising line of investigation. For instance, our analysis revealed that *Akkermansia*, Peptostreptococcaceae and *Oscillospira*

altogether accounted for more than 50% of the predicted increase in microbial BCAA degradation in CLE mice (ESM Figure 3), constituting promising targets for future studies linking dietary polyphenols, BCAA bioavailability and insulin resistance.

Acknowledgments

References

[1]   Ng M, Fleming T, Robinson M, et al. (2014) Global, regional, and national prevalence of overweight and obesity in children and adults during 1980-2013: a systematic analysis for the Global Burden of Disease Study 2013. Lancet 384: 766-781

[2]   Marette A (2002) Mediators of cytokine-induced insulin resistance in obesity and other inflammatory settings. Current opinion in clinical nutrition and metabolic care 5: 377-383

[3]   Ridaura VK, Faith JJ, Rey FE, et al. (2013) Gut microbiota from twins discordant for obesity modulate metabolism in mice. Science 341: 1241214

[4]   Le Chatelier E, Nielsen T, Qin J, et al. (2013) Richness of human gut microbiome correlates with metabolic markers. Nature 500: 541-546

[5]   Cani PD, Amar J, Iglesias MA, et al. (2007) Metabolic endotoxemia initiates obesity and insulin resistance. Diabetes 56: 1761-1772

[6]   Li DY, Yang M, Edwards S, Ye SQ (2013) Nonalcoholic fatty liver disease: for better or worse, blame the gut microbiota? JPEN Journal of parenteral and enteral nutrition 37: 787-793

[7]   Boeing H, Bechthold A, Bub A, et al. (2012) Critical review: vegetables and fruit in the prevention of chronic diseases. European journal of nutrition 51: 637-663

[8]   Nguyen B, Bauman A, Gale J, Banks E, Kritharides L, Ding D (2016) Fruit and vegetable consumption and all-cause mortality: evidence from a large Australian cohort study. The international journal of behavioral nutrition and physical activity 13: 9

[9]   Anhê FF, Desjardins Y, Pilon G, et al. (2013) Polyphenols and type 2 diabetes: A prospective review. PharmaNutrition 1: 105-114

[10]   Zhernakova A, Kurilshikov A, Bonder MJ, et al. (2016) Population-based metagenomics analysis reveals markers for gut microbiome composition and diversity. Science 352: 565-569

[11]   Falony G, Joossens M, Vieira-Silva S, et al. (2016) Population-level analysis of gut microbiome variation. Science 352: 560-564

[12]   Anhe FF, Roy D, Pilon G, et al. (2015) A polyphenol-rich cranberry extract protects from diet-induced obesity, insulin resistance and intestinal inflammation in association with increased Akkermansia spp. population in the gut microbiota of mice. Gut 64: 872-883

[13]   Roopchand DE, Carmody RN, Kuhn P, et al. (2015) Dietary Polyphenols Promote Growth of the Gut Bacterium Akkermansia muciniphila and Attenuate High-Fat Diet-Induced Metabolic Syndrome. Diabetes 64: 2847-2858

[14]   Heyman-Linden L, Kotowska D, Sand E, et al. (2016) Lingonberries alter the gut microbiota and prevent low-grade inflammation in high-fat diet fed mice. Food & nutrition research 60: 29993

[15]   Matziouridou C, Marungruang N, Nguyen TD, Nyman M, Fak F (2016) Lingonberries reduce atherosclerosis in Apoe(-/-) mice in association with altered gut microbiota composition and improved lipid profile. Mol Nutr Food Res 60: 1150-1160

[16]   Dudonné S, Dubé P, Anhê FF, et al. (2015) Comprehensive analysis of phenolic compounds and abscisic acid profiles of twelve native Canadian berries. Journal of Food Composition and Analysis 44: 214-224

[17]   Garcia-Villalba R, Gimenez-Bastida JA, Garcia-Conesa MT, Tomas-Barberan FA, Carlos Espin J, Larrosa M (2012) Alternative method for gas chromatography-mass spectrometry analysis of short-chain fatty acids in faecal samples. Journal of separation science 35: 1906-1913

[18]   Trottier J, Perreault M, Rudkowska I, et al. (2013) Profiling serum bile acid glucuronides in humans: gender divergences, genetic determinants, and response to fenofibrate. Clinical pharmacology and therapeutics 94: 533-543

[19]   Xu E, Dubois MJ, Leung N, et al. (2009) Targeted disruption of carcinoembryonic antigen-related cell adhesion molecule 1 promotes diet-induced hepatic steatosis and insulin resistance. Endocrinology 150: 3503-3512

[20]   Dubois MJ, Bergeron S, Kim HJ, et al. (2006) The SHP-1 protein tyrosine phosphatase negatively modulates glucose homeostasis. Nature medicine 12: 549-556

[21]   Denis MC, Roy D, Yeganeh PR, et al. (2016) Apple peel polyphenols: a key player in the prevention and treatment of experimental inflammatory bowel disease. Clin Sci (Lond) 130: 2217-2237

[22]   Poy MN, Yang Y, Rezaei K, et al. (2002) CEACAM1 regulates insulin clearance in liver. Nature genetics 30: 270-276

[23]   Gensel JC, Kopper TJ, Zhang B, Orr MB, Bailey WM (2017) Predictive screening of M1 and M2 macrophages reveals the immunomodulatory effectiveness of post spinal cord injury azithromycin treatment. Scientific reports 7: 40144

[24]   Liao X, Sharma N, Kapadia F, et al. (2011) Kruppel-like factor 4 regulates macrophage polarization. J Clin Invest 121: 2736-2749

[25]   Hildebrandt MA, Hoffmann C, Sherrill-Mix SA, et al. (2009) High-fat diet determines the composition of the murine gut microbiome independently of obesity. Gastroenterology 137: 1716-1724 e1711-1712

[26]   Eid HM, Ouchfoun M, Brault A, et al. (2014) Lingonberry (Vaccinium vitis-idaea L.) Exhibits Antidiabetic Activities in a Mouse Model of Diet-Induced Obesity. Evidence-based complementary and alternative medicine : eCAM 2014: 645812

[27]   Heyman L, Axling U, Blanco N, Sterner O, Holm C, Berger K (2014) Evaluation of Beneficial Metabolic Effects of Berries in High-Fat Fed C57BL/6J Mice. Journal of nutrition and metabolism 2014: 403041

[28]   Al-Share QY, DeAngelis AM, Lester SG, et al. (2015) Forced Hepatic Overexpression of CEACAM1 Curtails Diet-Induced Insulin Resistance. Diabetes 64: 2780-2790

[29]   Mehran AE, Templeman NM, Brigidi GS, et al. (2012) Hyperinsulinemia drives diet-induced obesity independently of brain insulin production. Cell metabolism 16: 723-737

[30]   Espin JC, Larrosa M, Garcia-Conesa MT, Tomas-Barberan F (2013) Biological significance of urolithins, the gut microbial ellagic Acid-derived metabolites: the evidence so far. Evidence-based complementary and alternative medicine : eCAM 2013: 270418

[31]   Ryu D, Mouchiroud L, Andreux PA, et al. (2016) Urolithin A induces mitophagy and prolongs lifespan in C. elegans and increases muscle function in rodents. Nature medicine 22: 879-888

[32]   Panchal SK, Ward L, Brown L (2013) Ellagic acid attenuates high-carbohydrate, high-fat diet-induced metabolic syndrome in rats. European journal of nutrition 52: 559-568

[33]   Denis MC, Desjardins Y, Furtos A, et al. (2015) Prevention of oxidative stress, inflammation and mitochondrial dysfunction in the intestine by different cranberry phenolic fractions. Clin Sci (Lond) 128: 197-212

[34]   Everard A, Belzer C, Geurts L, et al. (2013) Cross-talk between Akkermansia muciniphila and intestinal epithelium controls diet-induced obesity. Proceedings of the National Academy of Sciences of the United States of America

[35]   Shin NR, Lee JC, Lee HY, et al. (2014) An increase in the Akkermansia spp. population induced by metformin treatment improves glucose homeostasis in diet-induced obese mice. Gut 63: 727-735

[36]   Anhe FF, Pilon G, Roy D, Desjardins Y, Levy E, Marette A (2016) Triggering Akkermansia with dietary polyphenols: A new weapon to combat the metabolic syndrome? Gut microbes 7: 146-153

[37]   Henning SM, Summanen PH, Lee RP, et al. (2017) Pomegranate ellagitannins stimulate the growth of Akkermansia muciniphila in vivo. Anaerobe 43: 56-60

[38]   Lacombe A, Li RW, Klimis-Zacas D, et al. (2013) Lowbush wild blueberries have the potential to modify gut microbiota and xenobiotic metabolism in the rat colon. PloS one 8: e67497

[39]   Newgard CB, An J, Bain JR, et al. (2009) A branched-chain amino acid-related metabolic signature that differentiates obese and lean humans and contributes to insulin resistance. Cell metabolism 9: 311-326

[40]   Lake AD, Novak P, Shipkova P, et al. (2015) Branched chain amino acid metabolism profiles in progressive human nonalcoholic fatty liver disease. Amino acids 47: 603-615

[41]   Wang TJ, Larson MG, Vasan RS, et al. (2011) Metabolite profiles and the risk of developing diabetes. Nature medicine 17: 448-453

Tables

Table 1: Arctic berries studied.

Scientific name	Inuktitut name	Common names
Vaccinium uliginosum L.	Kigutanginaq	Bog blueberry (BBE)[a], Bog bilberry, Blueberry, Alpine blueberry, Bog blueberry, Northern blueberry
Rubus chamaemorus L.	Arpik	Cloudberry (CLE) [a], Bakeapple, Knotberry, Lowbush salmonberry, Averin
Empetrum nigrum L.	Paurngaq	Crowberry (CRE) [a], Blackberry, Black crowberry
Arctostaphylos alpina L. Spreng.	Kallaq	Alpine bearberry (ABE) [a], Bearberry, Mountain bearberry, Black bearberry
Vaccinium vitis-idaea L.	Kimminaq	Lingonberry (LGE) [a], Redberry, Cowberry, Mountain cranberry, Partridgeberry, Red whortleberry

[a] Common names and abbreviation used throughtout the study are highlighted in bold.

Table 2: Phenolic profile of the extracts of Arctic berries.

	Daily dose (µg/kg of body weight) [a]				
	BBE	CLE	CRE	ABE	LGE
Total polyphenols	4061.7	3035.2	13937.8	14172.8	8478.6
Phenolic acids	118.0	239.7	372.9	321.8	448.4
Anthocyanins	1767.0	94.0	15487.9	3589.4	3738.6
Flavonols	1712.4	528.8	837.8	797.8	10.5
Proanthocyanidins (condensed tannins)	708.8	170.0	2162.0	2994.2	4242.5
Monomers	147.7	57.5	442.6	1860.8	690.1
Dimers	266.2	103.9	906.2	721.2	1494.8
Trimers	125.8	8.5	220.6	173.2	723.7
Tetramers	73.9		182.7	89.4	479.7
Pentamers	41.5		69.2	51.4	311.5
Hexamers	30.6		40.6	38.3	236.6
Heptamers	11.4		18.9	15.0	96.5
Octamers	5.5		12.2	8.8	61.7
Nonamers	3.0		11.4	7.4	45.3
Decamers			2.9	1.3	10.1
Polymers	3.1		254.7	27.6	92.4
Ellagitannins (hydrolysable tannins)		538.7		523.1	
Free ellagic acid		21.6		2.1	22.8

[a] The daily dose is calculated based on the amount in 200 mg of extract/kg of body weight)

Table 3: Body characteristics.

	Chow	HFHS	BBE	CLE	CRE	ABE
Total weight gain (g)	5.083 ±0.469	9.450 ±0.430†††	9.217 ±0.646	9.100 ±1.055	8.258 ±1.048	7.983 ±0.745
Total energy intake (kcal)	399.4 ±55.95	403.3 ±33.05	408.9 ±61.69	407.2 ±71.98	364.3 ±84.23	398.5 ±76.86
Visceral fat pad (g)	0.962 ±0.087	2.080 ±0.221†††	2.075 ±0.200	1.730 ±0.145	1.974 ±0.142	1.674 ±0.209
Subcutaneous fat pad (g)	0.402 ±0.038	0.755 ±0.076†††	0.825 ±0.081	0.846 ±0.136	0.911 ±0.111	0.722 ±0.088
Interscapular brown fat pad (g)	0.185 ±0.073	0.179 ±0.055	0.111 ±0.008	0.105 ±0.005	0.110 ±0.007	0.105 ±0.007
Gastrocnemius (g)	0.324 ±0.01	0.325 ±0.008	0.320 ±0.007	0.312 ±0.008	0.304 ±0.007	0.310 ±0.007
Liver (g)	1.119 ±0.043	1.037 ±0.048	1.049 ±0.045	0.994 ±0.04	0.976 ±0.048	0.973 ±0.049

Data are expressed as the mean ±SEM. BBE, bog bilberry extract - CLE, cloudberry extract - CRE, crowberry extract - ABE, al
extract - LGE, lingonberry extract. ††† $p<0.001$ *vs* Chow-fed mice

Legend to figures

Figure 1: Impact of Arctic berry extracts on fasting blood glucose, insulinæmia and plasma c-peptide and on insulin sensitivity in DIO mice. (A) Fasting blood glucose (n=12), (B) insulinæmia (n=12) and (C) c-peptide (n=9 for Chow, BBE, CRE and ABE; n=10 for HFHS, CLE and LGE). (D) At week 6, mice were 6 h fasted and insulin tolerance tests were carried out followed intraperitoneal insulin injections (ipITT, 0.65 IU/kg, n=12). Data are expressed as the mean ±SEM. In bar graphs, Chow-fed animals are represented by a reference line and the significance between Chow and HFHS was calculated using unpaired two-tailed Student's t-test (†$p < 0.05$, †† $p < 0.01$ and ††† $p < 01$). One-way ANOVA with a Student-Newman-Keuls post hoc test was used to calculate the significance between HFHS and the groups treated with the extracts of Arctic berries (*$p < 0.05$, ** $p < 0.01$ and *** $p < 01$). In line graphs, two-way repeated measures ANOVA with a Student-Newman-Keuls post hoc test was used to calculate the significance of the differences between time points (*$p < 0.05$, ** $p < 0.01$ and *** $p < 01$).

Figure 2: Impact of Arctic berry extracts on post-prandial blood glucose, insulinæmia and plasma c-peptide and on liver homeostasis in DIO mice. (A) At week 7, mice were subjected to oral glucose tolerance tests (OGTT, n=12). After overnight fasting (12h), animals were given a glucose load (1 g/kg) and blood glucose was measured before (0 min) and after (15, 30, 60, 90 and 120 min) glucose challenge. (B,C) Blood collected during OGTT was used to assess insulinæmia (n=12) and c-peptide (n=9 for Chow, BBE, CRE and ABE; n=10 for HFHS, CLE and LGE) before and after glucose challenge. (D) Mice were injected (i.v.) with saline or insulin (3.8 UI/kg) 5 min before euthanasia by cardiac puncture; aliquots of freeze-powdered livers were processed to yield total protein lysates and immunoblotted (IB) against AKT (n=12), p-AKT ser473 (n=12) and (E) carcinoembryonic antigen-related adhesion molecule-1 (CEACAM-1, n=12). (F) CEACAM-1 was immunoprecipitated (IP) from total protein lysates and immunoblotted against anti-phosphotyrosine (n=9 for Chow, n=11 for HFHS and LGE; n=12 for CLE and ABE). (G) Liver triacylglycerols. (H) Plasma

triacylglycerols. (I) Liver mRNA expression of Adhesion G protein-coupled receptor E1 (*Adgre1*), Cluster of differentiation 11c (*Cd11c*), Macrophage receptor with collagenous structure (*Marco*), Kruppel-like factor (*Klf4*), Tumor necrosis factor α (*Tnfa*), Interleukin 1β (*Il1b*), Cyclooxygenase 2 (*Cox2*), Toll-like receptor 4 (*Tlr4*), Peroxisome proliferator-activated receptor α (*Ppara*) and Acetyl-CoA carboxylase (*Acaca*). White - HFHS-fed control mice; black – CLE; grey – ABE; light grey – LGE. Chow-fed animals are represented by a reference line and the significance between Chow and HFHS was calculated using unpaired two-tailed Student's t-test (†$p < 0.05$, †† $p < 0.01$ and ††† $p < 0.001$). One-way ANOVA with a Student-Newman-Keuls post hoc test was used to calculate the significance between HFHS and the groups treated with the extracts of Arctic berries (*$p < 0.05$, ** $p < 0.01$ and *** $p < 0.001$). In line graphs, two-way repeated measures ANOVA with a Student-Newman-Keuls post hoc test was used to calculate the significance of the differences between time points (*$p < 0.05$, ** $p < 0.01$ and *** $p < 0.001$).

Figure 3: CLE, ABE and LGE improve intestinal inflammation, gut permeability and metabolic endotoxæmia in DIO mice. (A) A limulus amebocyte lysate-based assay was used to assess circulating lipopolysaccharide (LPS/endotoxin). Jejunal mRNA expression of (B) inducible nitric oxide synthase (*Nos2*), (C) tumor necrosis factor α (*Tnfa*), (D) Adhesion G protein-coupled receptor E1 (*Adgre1*), (E) Cluster of differentiation 11c (*Cd11c*), (F) Zonula occludens 1 (*Tjp1*), (G) Occludin (*Ocln*), (H) Regenerating islet-derived protein 3 γ (*Reg3g*) and (I) Proglucagon (*Gcg*). Colonic mRNA expression of (J) *Nos2*, (K) *Tnfa*, (L) *Adgre1*, (M) *Cd11c*, (N) *Tjp1*, (O) *Ocln*, (P) *Reg3g* and (Q) *Gcg.* Data are expressed as the mean ±SEM. Chow-fed animals are represented by a reference line and the significance between Chow and HFHS was calculated using unpaired two-tailed Student's t-test (†$p < 0.05$, †† $p < 0.01$ and ††† $p < 0.001$). One-way ANOVA with a Student-Newman-Keuls post hoc test was used to calculate the significance between HFHS and the groups treated with the extracts of Arctic berries (*$p < 0.05$, ** $p < 0.01$ and ***$p < 0.001$).

Figure 4: CLE, ABE and LGE administration is associated with changes in the gut microbial profile of DIO mice. Fæcal samples of Chow-fed (n=9) and HFHS-fed (n=11) mice, as well as of HFHS-fed mice orally treated with CLE (n=6), ABE (n=4) and LGE (n=7) were freshly harvested at week 8. Genomic DNA was extracted from fæces and 16S rRNA-based analysis profiling was performed. (A) β-diversity between groups was initially observed by means of principal component analysis (PCoA) on weighted Unifrac distance. Linear discriminant analysis (LDA) effect size (LEfSe) was calculated in order to explore the taxa within genus level that more strongly discriminate between the gut microbiota of (B) Chow and HFHS, (C) HFHS and CLE, (D) HFHS and ABE and (E) HFHS and LGE. Families followed by the label '_g' indicate unidentified genera. Dark grey – Chow; white - HFHS-fed control mice; black – CLE; grey – ABE; light grey – LGE.

Figure 5: CLE, ABE and LGE alter metabolic pathways in the gut microbiota of DIO mice. Prediction of the functional genes in the sampled bacterial community was performed using PICRUSt. 16S rRNA sequencing data and KEGG reference genomes were used to estimate gene family abundance based on an extended ancestral-state reconstruction algorithm and then to produce a metagenome prediction for each sample. Linear discriminant analysis (LDA) effect size (LEfSe) was calculated in order to explore the microbial functions that more strongly discriminates between the gut microbiota of (A) Chow and HFHS, (B) HFHS and CLE, (C) HFHS and ABE, (D) HFHS and LGE. Dark grey – Chow; white - HFHS-fed control mice; black – CLE; grey – ABE; light grey – LGE.

Figures

Figure 1: Impact of Arctic berry extracts on fasting glycemia, insulinemia and plasma c-peptide and on insulin sensitivity in DIO mice.
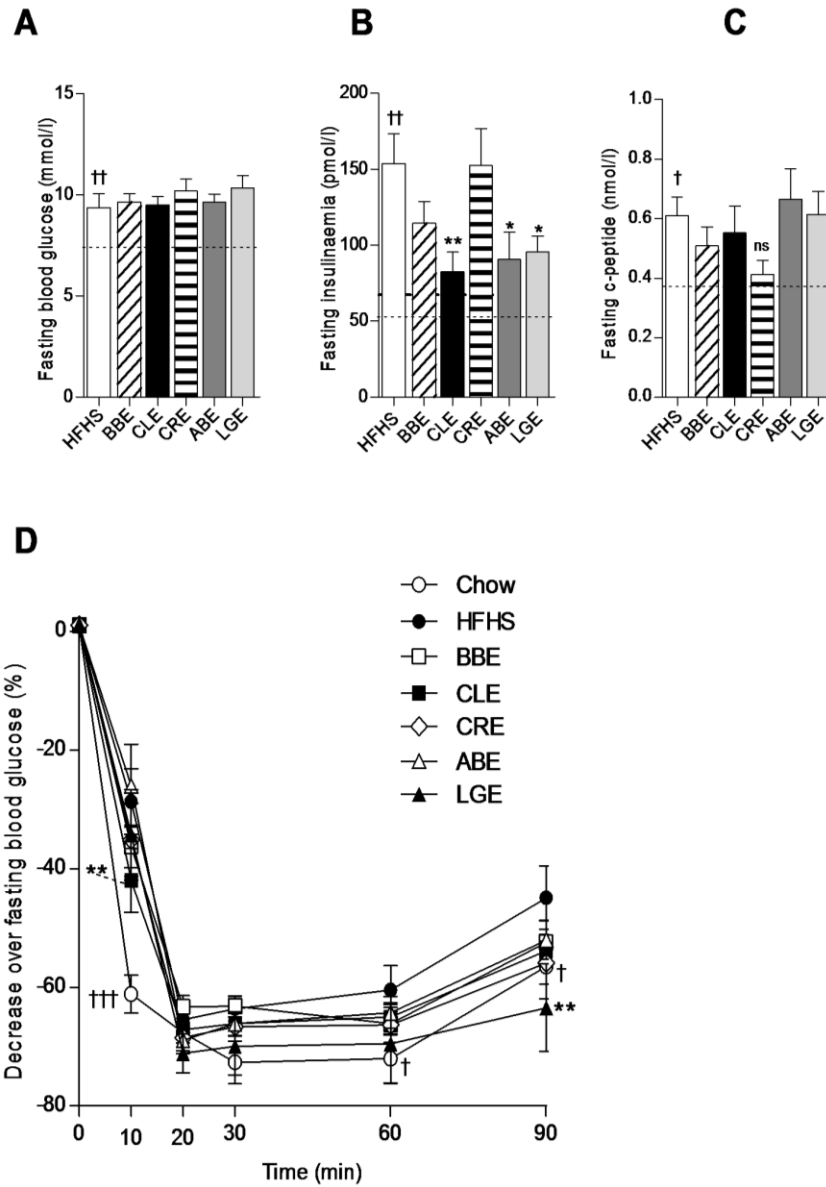
Figure 2: Impact of Arctic berry extracts on post-prandial glycemia, insulinemia and plasma c-peptide and on liver homeostasis in DIO mice.
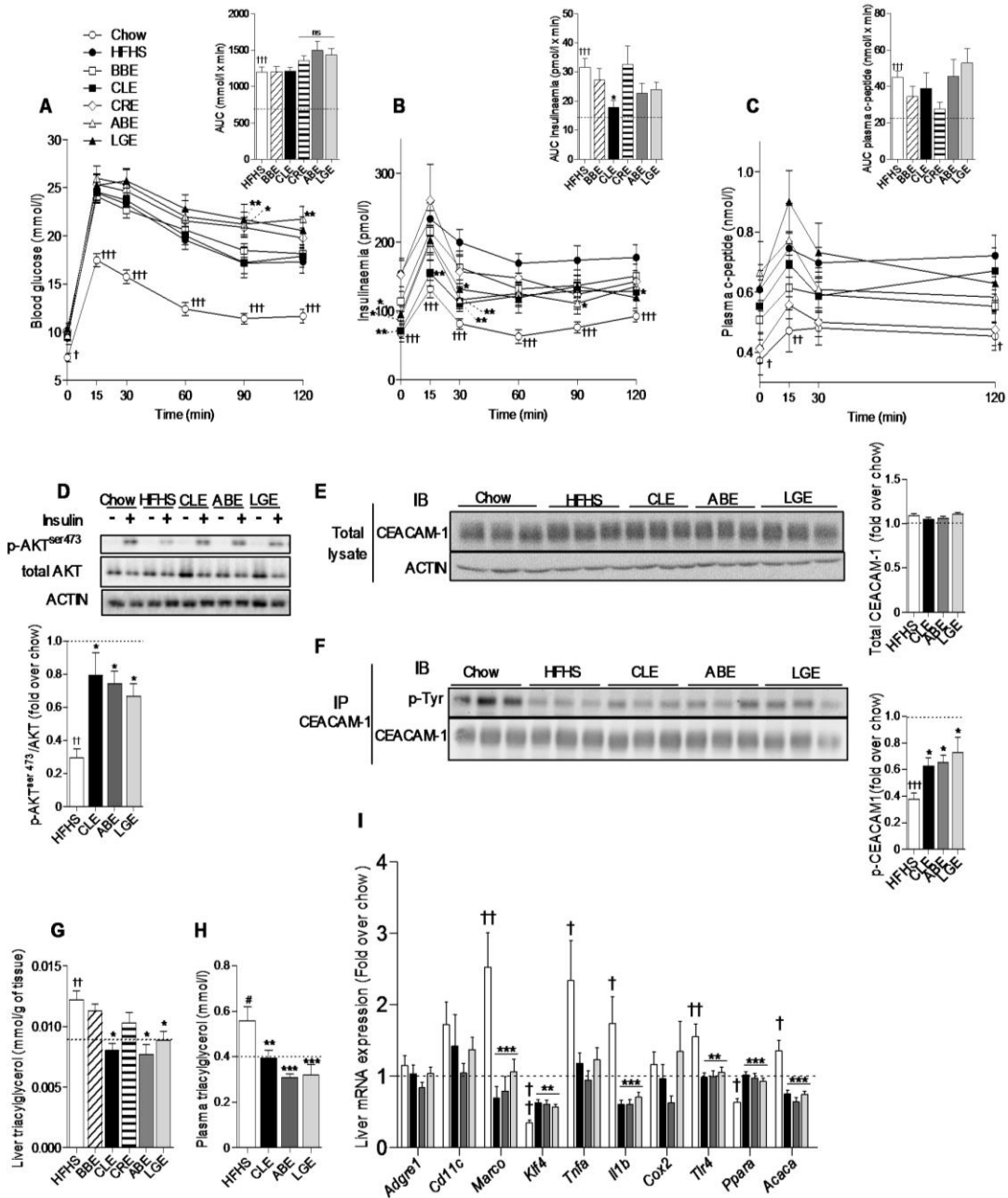
Figure 3: CLE, ABE and LGE improve intestinal inflammation, gut permeability and metabolic endotoxemia in DIO mice.
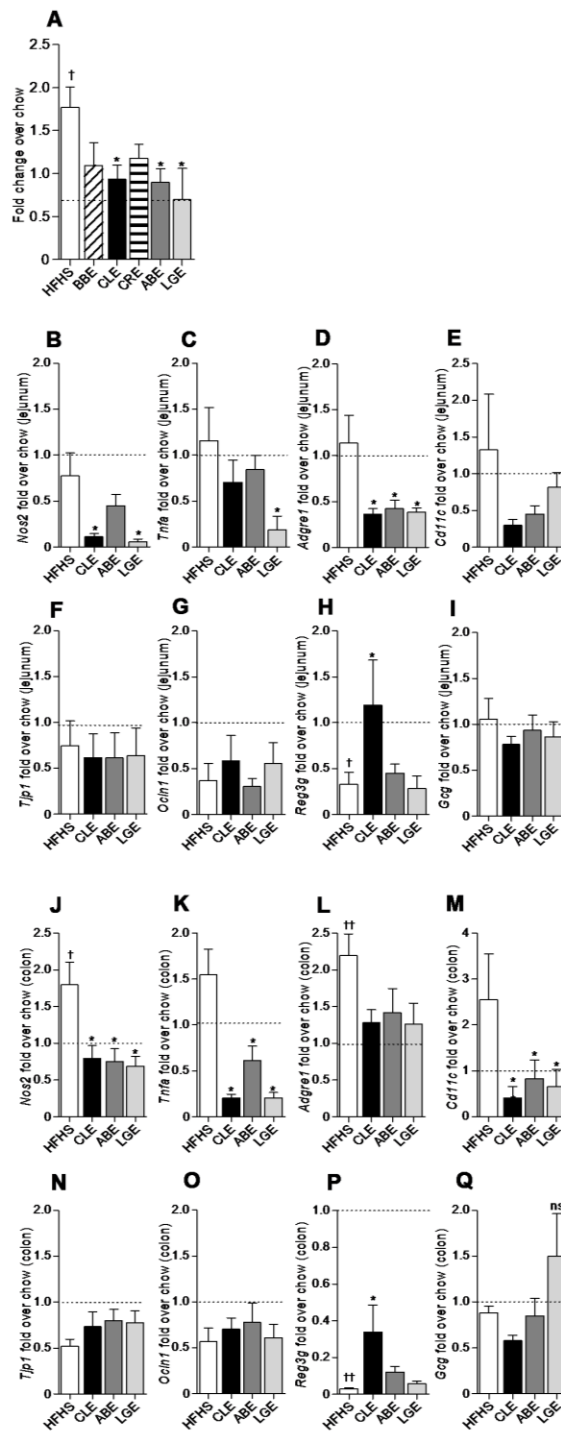
Figure 4: CLE, ABE and LGE administration is associated with changes in the gut microbial profile of DIO mice.
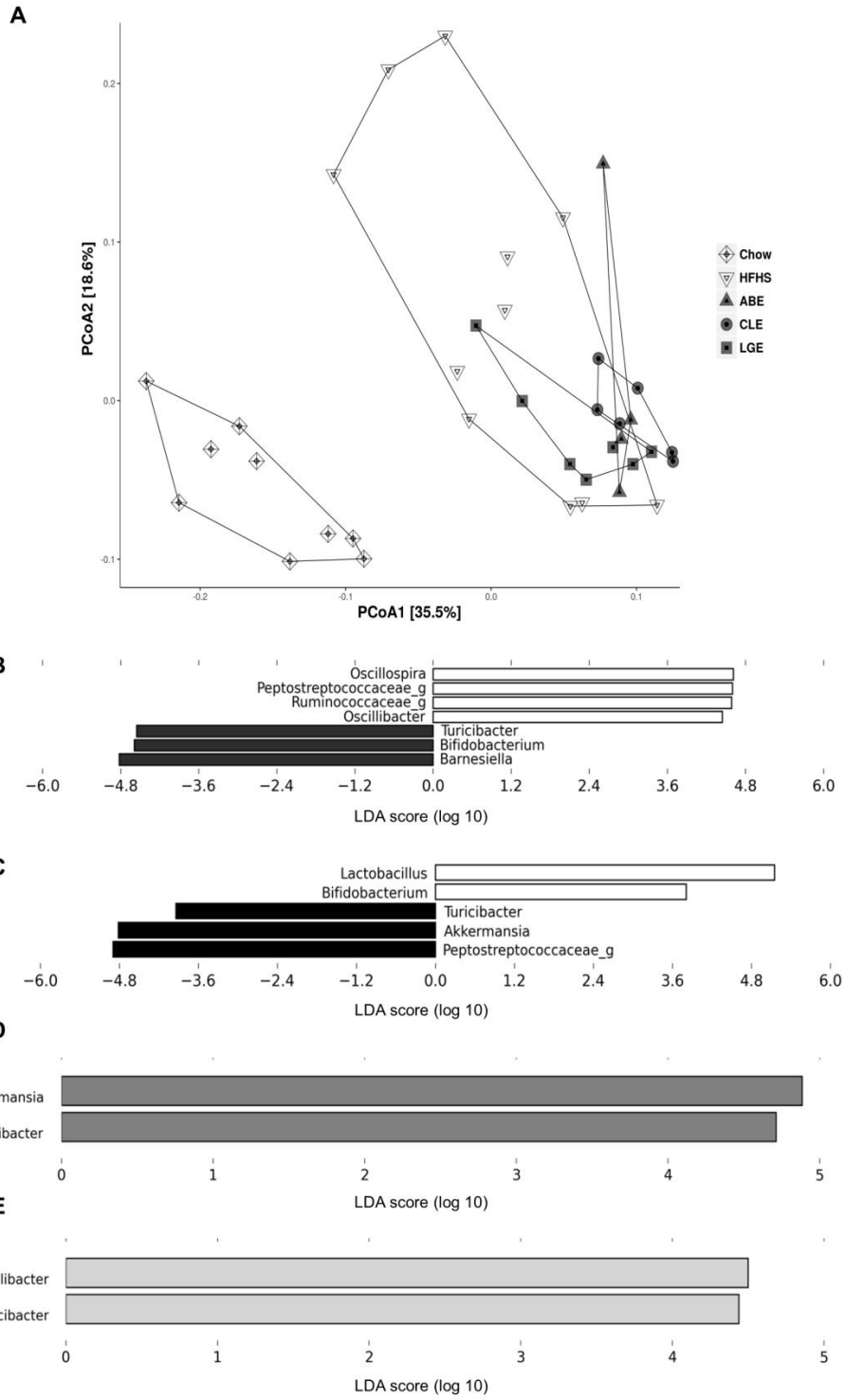
Figure 5: CLE, ABE and LGE alter metabolic pathways in the gut microbiota of DIO mice.
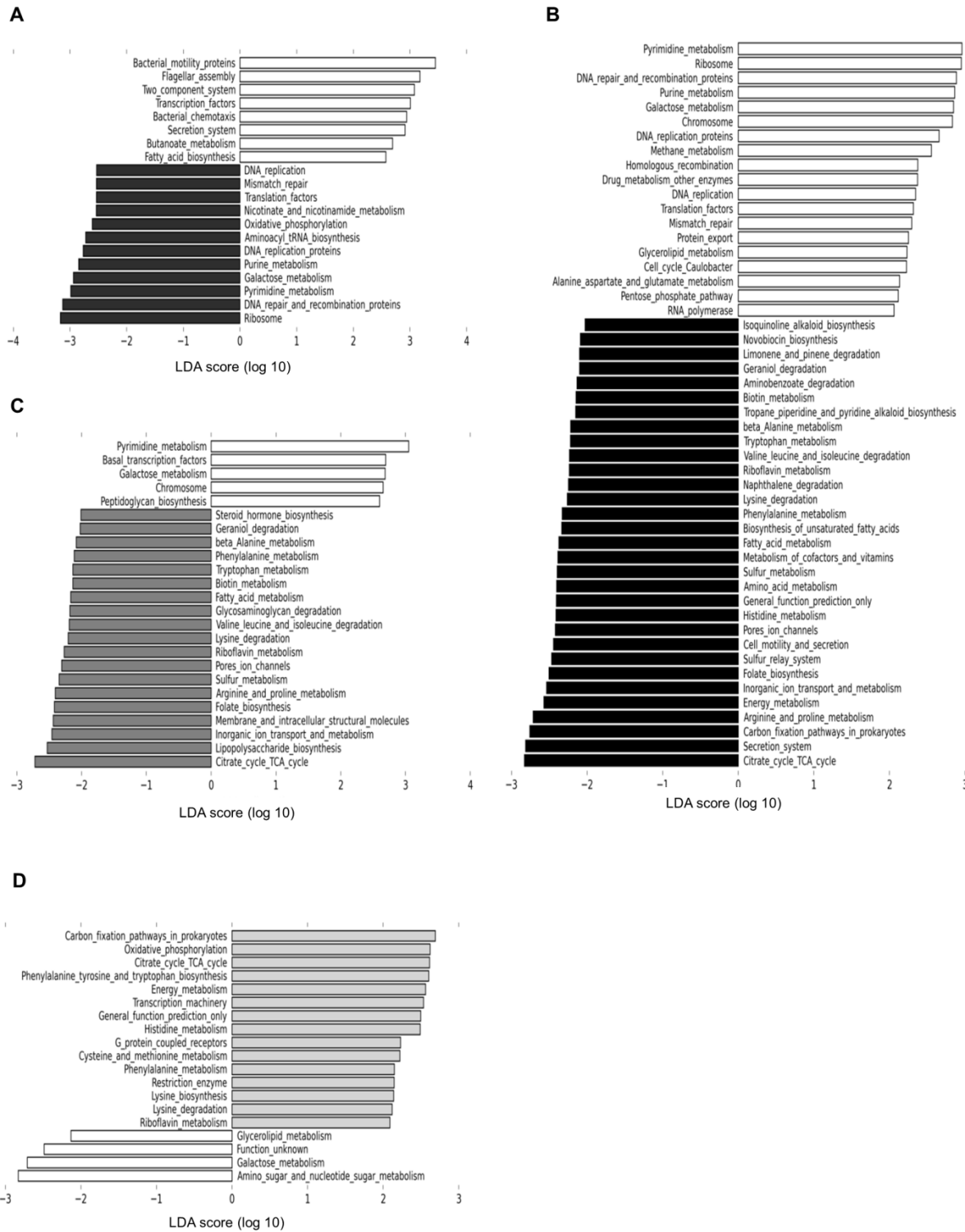
Supplemental material

ESM Figure 1: Fæcal short-chain fatty acids (SCFA), Fæcal energy density and Branched-chain amino acids (BCAA) availability. (A) Fæces were collected at week 6 and the profile of SCFA (white – acetate; black – propionate; light grey – butyrate; grey – valerate) and of (B) Branched-chain SCFA (grey – isobutyrate; light grey – isovalerate) was assessed by gas chromatography in samples collected from Chow (n=10), HFHS (n=9), BBE (n=12), CLE (n=12), CRE (n=12), ABE (n=12) and LGE (n=10) mice. (C) Gross fæcal energy was determined by adiabatic bomb calorimetry in fæcal pellets of Chow (n=6), HFHS (n=6), CLE (n=6), ABE (n=4) and LGE (n=4) mice. (D) Circulating levels of BCAA valine, isoleucine and leucine (Chow n=12; HFHS n=10; CLE n=12; ABE n=12; LGE n=12). Data are expressed as the mean ±SEM. The significance between Chow and HFHS was calculated using unpaired two-tailed Student's t-test ($^{†}p<$ 0.05, $^{††}p<$ 0.01) and $^{†††}p<$ 0.001). One-way ANOVA with a Student-Newman-Keuls post hoc test was used to calculate the significance between HFHS and the groups treated with the extracts of Arctic berries (*$p<$ 0.05, **$p<$ 0.01 and ***$p<$ 0.001). (C,D) Chow-fed animals are represented by a reference line.

ESM Figure 2: Plasma bile acid profile. Blood was collected in heparin-treated tubes from cardiac puncture after 6h fasting and immediately centrifuged. Systemic plasma was used in order to characterise the circulating bile acid profile (n=12). (A) Total bile acids; (B) quantification of Cholic acid (CA), Chenodeoxycholic acid (CDCA), Deoxycholic acid (DCA), Ursodeoxycholic acid (UDCA), Tauro-Cholic acid (TCA), Tauro-Deoxycholic acid (TDCA), Tauro-ursodeoxycholic acid (TUDCA), α-Murocholic acid (αMCA), β-Murocholic acid (βMCA), ω-Murocholic acid (ωMCA), Tauro-α-murocholic acid (TαMCA), Tauro-β-murocholic acid (TβMCA), Tauro-ω-murocholic acid (TωMCA). Data are expressed as the mean ±SEM. The significance between Chow and HFHS was calculated using unpaired two-tailed Student's t-test ($^{†}p<$ 0.05, $^{††}p<$ 0.01) and $^{†††}p<$ 0.001). One-way ANOVA with a Student-Newman-Keuls post hoc test was used to calculate the significance between HFHS and the groups treated with the extracts of Arctic berries (*$p<$ 0.05,

**p< 0.01 and ***p< 0.001). (A) Chow-fed animals are represented by a reference line.

ESM Figure 1: Fecal energy density and BCAA availability.
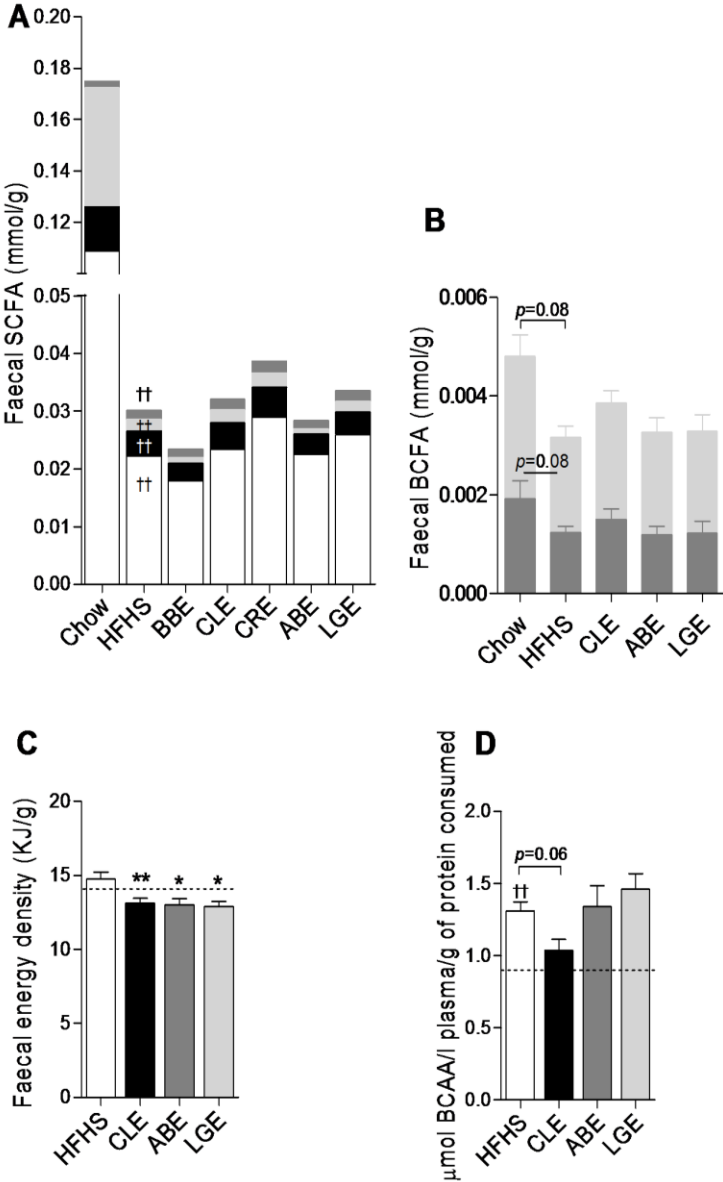
ESM Figure 2: Plasma bile acid profile.
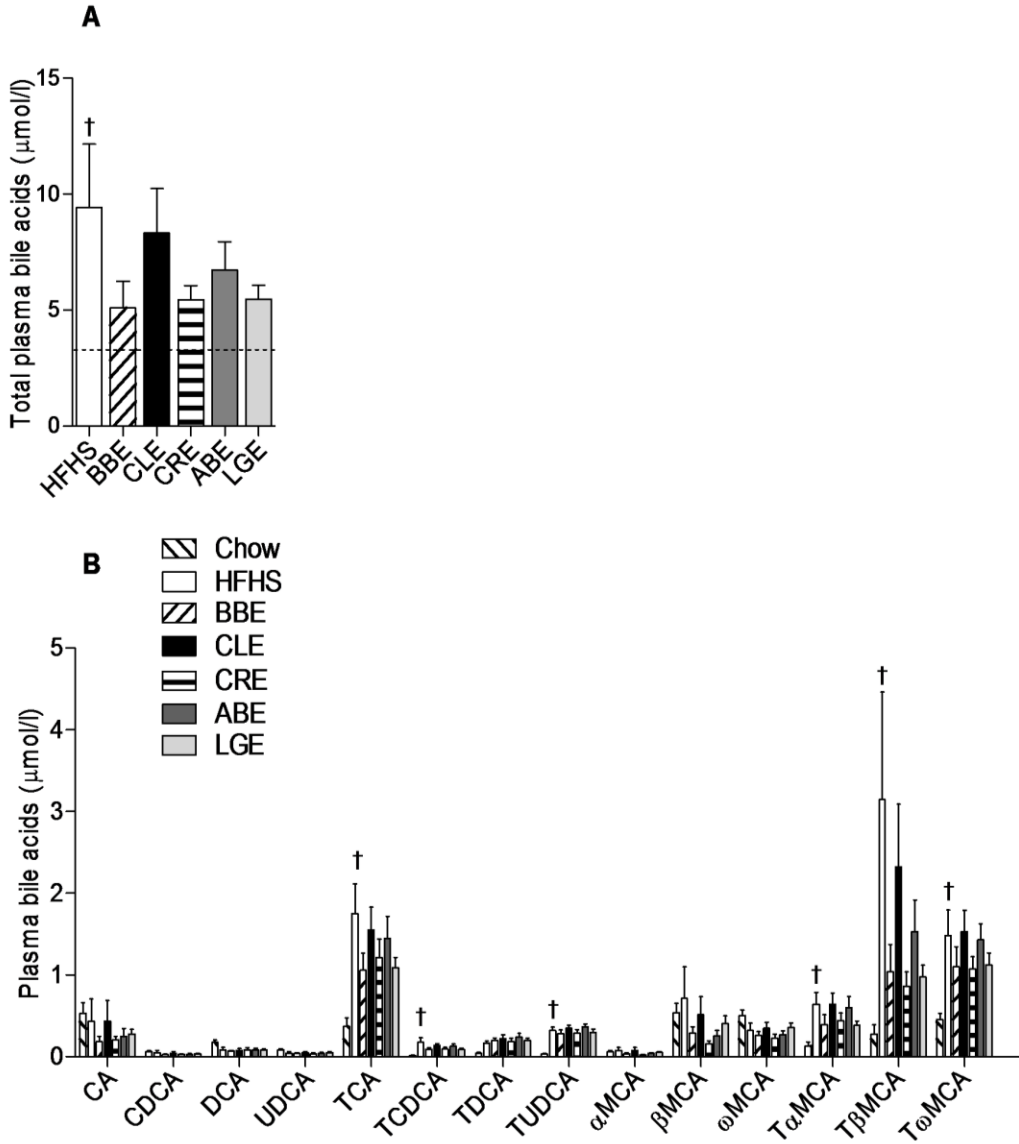
Supplemental tables

ESM Table 1: Composition of the diets.

	Chow diet (Teklad 2018, HARLAN)		HFHS diet	
Ingredients (g/100g)	Crude protein	19	Casein high nitrogen	20
	Fat (Soybean oil)	6.2	L-cysteine	0.18
	Carbohydrate	44	Sucrose FCC	26.9
	Crude fiber	3.5	Alphacel non nutritive bulk	5
	Insoluble fiber	15	Mineral mix	6.7
	Ash	5.3	Vitamin mix	1.4
			Lard	19.8
			Corn oil	19.8
			Choline bitartrate	0.2
			Tert-butylhydrytoluene (BHT)	0.03
Composition (kcal%)				
Protein		24		15
Carbohydrates		58		19.6
Lipids		18		65.4
Energy Density (kcal/g)		3.1		5.4

ESM Table 2: Abundance of taxa at phylum level.

Phylum	CHOW Mean	CHOW SEM	HFHS Mean	HFHS SEM	CLE Mean	CLE SEM	ABE Mean	ABE SEM	LGE Mean	LGE SEM
Firmicutes	75.22	±3.63	82.98	±2.50	70.40	±6.38	76.46	±2.45	75.36	±3.44
Bacteroidetes	12.34	±2.92	2.26††	±1.06	1.51	±0.72	3.73	±0.46	3.41	±1.27
Actinobacteria	9.84	±3.65	4.44	±1.22	1.88	±0.74	1.37	±0.53	2.62	±0.77
Proteobacteria	0.08	±0.02	0.16	±0.03	0.73*	±0.21	0.29	±0.12	0.35	±0.11
TM7	0.00	±0.00	0.00	±0.00	0.00	±0.00	0.00	±0.00	0.00	±0.00
Tenericutes	0.49	±0.21	0.017††	±0.01	0.01	±0.00	0.29	±0.29	0.00	±0.00
Verrucomicrobia	0.86	±0.58	3.11	±1.23	15.26	±4.71	12.05	±2.76	6.83	±2.69
F/B	29.58	±21.87	221.81††	±126.97	85.80	±21.25	21.36	±2.27	46.27	±12.51

†P< 0.05; †† P< 0.01; †††P<0.001 for HFHS vs. Chow (Mann-Whitney test). *P< 0.05; **P< 0.01; ***P<0.001 for HFHS vs. CLE, HFHS vs. ABE and HFHS vs. LGE (Kruskal-Wallis One-way ANOVA with Dunn's post-hoc test). F/B - Firmicutes/Bacteroidetes ratio

ESMTable 3: Abundance of taxa at class level.

	CHOW		HFHS		CLE		ABE		LGE	
Class	Mean	SEM	Mean	SEM	Mean	SEM	Mean	SEM	Mean	SEM
Actinobacteria	7.08	±3.54	0.87††	±0.83	0.00	±0.00	0.37	±0.22	0.90	±0.49
Coriobacteria	2.77	±0.66	3.57	±1.14	1.88	±0.74	1.00	±0.50	1.72	±0.41
Bacteroidia	12.34	±2.92	2.26††	±1.06	1.51	±0.72	3.73	±0.46	3.41	±1.27
Bacilli	37.38	±7.81	26.15	±6.12	2.00*	±0.72	9.05	±5.07	8.99	±3.59
Clostridia	38.62	±6.49	61.70††	±6.77	76.07	±4.11	72.21	±4.64	73.75	±7.28
Erysipelotrichi	0.38	±0.14	2.08††	±0.55	2.54	±0.92	0.97	±0.64	4.03	±1.66
Alphaproteobacteria	0.02	±0.01	0.00†	±0.00	0.00	±0.00	0.00	±0.00	0.00	±0.00
Betaproteobacteria	0.06	±0.02	0.16	±0.03	0.73*	±0.21	0.29	±0.12	0.33	±0.11
Gammaproteobacteria	0.00	±0.00	0.00	±0.00	0.00	±0.00	0.00	±0.00	0.02	±0.01
TM7	0.00	±0.00	0.00	±0.00	0.00	±0.00	0.00	±0.00	0.00	±0.00
Mollicutes	0.49	±0.21	0.02††	±0.01	0.01	±0.00	0.29	±0.29	0.00	±0.00
Verrucomicrobiae	0.86	±0.58	3.11	±1.23	15.26	±4.71	12.05	±2.76	6.83	±2.69

†P< 0.05; †† P< 0.01; †††P<0.001 for HFHS vs. Chow (Mann-Whitney test). *P< 0.05; **P< 0.01; ***P<0.001 for HFHS vs. CLE, HFHS vs. ABE and HFHS vs. LGE (Kruskal-Wallis One-way ANOVA with Dunn's post-hoc test).

ESM Table 4: Abundance of taxa at order level.

	CHOW		HFHS		CLE		ABE		LGE	
Order	Mean	SEM	Mean	SEM	Mean	SEM	Mean	SEM	Mean	SEM
Bifidobacteriales	7.08	±3.54	0.87††	±0.83	0.00	±0.00	0.37	±0.22	0.90	±0.49
Coriobacteriales	2.77	±0.66	3.57	±1.14	1.88	±0.74	1.00	±0.50	1.72	±0.41
Bacteroidales	12.34	±2.92	2.26††	±1.06	1.51	±0.72	3.73	±0.46	3.41	±1.27
Bacillales	0.01	±0.00	0.00††	±0.00	0.02	±0.01	0.02	±0.00	0.03	±0.01
Lactobacillales	34.04	±8.03	26.05	±6.13	1.28*	±0.65	8.82	±5.07	8.18	±3.65
Turicibacterales	3.33	±1.01	0.10†††	±0.05	0.70*	±0.13	0.22	±0.09	0.77*	±0.24
Clostridiales	38.62	±6.49	61.70††	±6.77	76.07	±4.11	72.21	±4.64	73.75	±7.28
Erysipelotrichales	0.38	±0.14	2.08††	±0.55	2.54	±0.92	0.97	±0.64	4.03	±1.66
Rickettsiales	0.02	±0.01	0.00†	±0.00	0.00	±0.00	0.00	±0.00	0.00	±0.00
Burkholderiales	0.06	±0.02	0.16	±0.03	0.73˙	±0.21	0.29	±0.12	0.33	±0.11
Enterobacteriales	0.00	±0.00	0.00	±0.00	0.00	±0.00	0.00	±0.00	0.02	±0.01
Anaeroplasmatales	0.49	±0.21	0.02††	±0.01	0.01	±0.00	0.29	±0.29	0.00	±0.00
Verrucomicrobiales	0.86	±0.58	3.11	±1.23	15.26	±4.71	12.05	±2.76	6.83	±2.69

†P< 0.05; †† P< 0.01; †††P<0.001 for HFHS vs. Chow (Mann-Whitney test). *P< 0.05; **P< 0.01; ***P<0.001 for HFHS vs. CLE, HFHS vs. ABE and HFHS vs. LGE (Kruskal-Wallis One-way ANOVA with Dunn's post-hoc test).

ESM Table 5: Abundance of taxa at family level.

Family	CHOW		HFHS		CLE		ABE		LGE	
	Mean	SEM	Mean	SEM	Mean	SEM	Mean	SEM	Mean	SEM
Bifidobacteriaceae	7.07	±3.54	0.87†	±0.83	0.00	±0.00	0.37	±0.22	0.90	±0.49
Coriobacteriaceae	2.76	±0.66	3.57	±1.14	1.88	±0.74	1.00	±0.50	1.72	±0.41
Porphyromonadaceae	12.28	±2.90	2.25†	±1.05	1.50	±0.72	3.73	±0.46	3.34	±1.23
S24-7	0.05	±0.04	0.01	±0.01	0.01	±0.00	0.00	±0.00	0.06	±0.04
Staphylococcaceae	0.00	±0.00	0.00	±0.00	0.02	±0.01	0.02	±0.00	0.03	±0.01
Enterococcaceae	0.00	±0.00	0.02†	±0.00	0.02	±0.00	0.06	±0.04	0.23	±0.12
Lactobacillaceae	34.04	±8.03	26.03	±6.14	1.26*	±0.64	8.74	±5.03	7.95	±3.71
Leuconostocaceae	0.00	±0.00	0.00	±0.00	0.00	±0.00	0.01	±0.00	0.00	±0.00
Turicibacteraceae	3.33	±1.01	0.10††	±0.05	0.69*	±0.13	0.22	±0.09	0.77*	±0.24
Christensenellaceae	0.00	±0.00	0.06	±0.05	0.46	±0.21	0.28	±0.07	0.62	±0.25
Clostridiaceae	2.32	±0.83	1.51	±0.42	1.54	±0.22	1.13	±0.22	1.96	±0.38
Dehalobacteriaceae	0.02	±0.01	0.07†	±0.01	0.03	±0.01	0.07	±0.04	0.08	±0.02
Lachnospiraceae	8.43	±2.19	8.84	±1.44	7.95	±0.95	11.55	±2.14	9.63	±1.11
Peptococcaceae	0.14	±0.07	0.20	±0.06	0.61	±0.28	0.89	±0.46	1.12	±0.56
Peptostreptococcaceae	0.04	±0.03	5.58†††	±2.48	19.43*	±4.14	10.58	±4.20	7.38	±2.27
Ruminococcaceae	8.53	±2.00	21.73††	±3.51	28.10	±4.35	23.17	±3.22	33.18	±4.54
Mogibacteriaceae	0.06	±0.03	0.03†	±0.00	0.29	±0.10	0.06	±0.01	0.11	±0.03
Erysipelotrichaceae	0.37	±0.14	2.08††	±0.55	2.54	±0.92	0.97	±0.64	4.03	±1.66
Mitochondria	0.02	±0.01	0.00†	±0.00	0.00	±0.00	0.00	±0.00	0.00	±0.00
Comamonadaceae	0.06	±0.02	0.16	±0.03	0.73*	±0.21	0.29	±0.12	0.33	±0.11
Enterobacteriaceae	0.00	±0.00	0.00	±0.00	0.00	±0.00	0.00	±0.00	0.02	±0.01
Anaeroplasmataceae	0.49	±0.21	0.02††	±0.01	0.01	±0.00	0.29	±0.29	0.00	±0.00
Verrucomicrobiaceae	0.86	±0.58	3.11	±1.23	15.26	±4.71	12.05	±2.76	6.83	±2.69

†P< 0.05; ††P< 0.01; †††P<0.001 for HFHS vs. Chow (Mann-Whitney test). *P< 0.05; **P< 0.01; ***P<0.001 for HFHS vs. CLE, HFHS vs. ABE and HFHS vs. LGE (Kruskal-Wallis One-way ANOVA with Dunn's post-hoc test).

ESM Table 6: Abundance of taxa at genus level.

	CHOW		HFHS		CLE		ABE		LGE	
Genus	Mean	SEM	Mean	SEM	Mean	SEM	Mean	SEM	Mean	SEM
Bifidobacterium	7.07	±3.54	0.87†	±0.83	0.00	±0.00	0.37	±0.22	0.89	±0.49
Adlercreutzia	0.79	±0.26	1.35	±0.39	1.87	±0.74	0.97	±0.49	1.70	±0.41
Barnesiella	12.28	±2.90	1.35††	±0.53	1.50	±0.72	1.46	±0.52	2.72	±1.22
Parabacteroides	0.00	±0.00	0.9*	±0.67	0.00	±0.00	2.26	±0.76	0.61	±0.52
Staphylococcus	0.00	±0.00	0.00	±0.00	0.01	±0.01	0.01	±0.00	0.03	±0.01
Enterococcus	0.00	±0.00	0.00	±0.00	0.00	±0.00	0.00	±0.00	0.20	±0.12
Lactobacillus	34.04	±8.03	26.02	±6.14	1.26$^{\#}$	±0.64	8.74	±5.03	7.95	±3.71
Turicibacter	3.33	±1.01	0.10†††	±0.05	0.69$^{\#}$	±0.13	0.22	±0.09	0.77$^{\#}$	±0.24
Clostridium	0.30	±0.17	0.23	±0.09	0.08	±0.03	0.06	±0.05	0.08	±0.02
Dehalobacterium	0.02	±0.01	0.07†	±0.01	0.03	±0.01	0.07	±0.04	0.08	±0.02
Anaerostipes	0.21	±0.10	0.00††	±0.00	0.00	±0.00	0.00	±0.00	0.02	±0.01
Coprococcus	0.40	±0.13	1.89	±0.67	0.97	±0.09	0.89	±0.2	0.81	±0.11
Dorea	0.99	±0.46	0.71	±0.09	0.61	±0.3	1.13	±0.5	0.61	±0.17
Roseburia	0.00	±0.00	0.02	±0.02	0.45	±0.32	0.00	±0.00	0.02	±0.01
Ruminococcus	2.57	±0.78	1.96	±0.25	1.90	±1.09	2.17	±0.32	1.68	±0.34
rc4-4	0.14	±0.07	0.20	±0.06	0.61	±0.28	0.89	±0.46	1.12	±0.56
Anaerotruncus	0.00	±0.00	0.06	±0.01	0.00$^{\#}$	±0.00	0.00$^{\#}$	±0.00	0.00$^{\#}$	±0.00
Oscillibacter	0.50	±0.17	3.40	±0.72	4.94	±0.61	7.50	±0.96	7.99	±1.28
Oscillospira	3.41	±0.94	9.33††	±1.67	10.59	±1.59	8.10	±1.37	11.34	±1.45
Ruminococcus	2.54	±0.77	1.46	±0.2	1.79	±0.46	1.18	±0.13	1.84	±0.36
Anaerovorax	0.00	±0.00	0.00	±0.00	0.11$^{\#}$	±0.03	0.02	±0.01	0.03	±0.02
Allobaculum	0.21	±0.14	1.96††	±0.53	1.47	±0.94	0.86	±0.56	3.10	±1.59
Coprobacillus	0.02	±0.02	0.02	±0.01	0.01	±0.00	0.00	±0.00	0.01	±0.00
Delftia	0.06	±0.02	0.15	±0.03	0.73$^{\#}$	±0.21	0.29	±0.12	0.33	±0.11
Anaeroplasma	0.48	±0.21	0.01††	±0.01	0.00	±0.00	0.29	±0.29	0.00	±0.00
Akkermansia	0.85	±0.58	3.10	±1.23	15.26	±4.71	12.05	±2.76	6.83	±2.69

†P< 0.05; †† P< 0.01; †††P<0.001 for HFHS vs. Chow (Mann-Whitney test). *P< 0.05; **P< 0.01; ***P<0.001 for HFHS vs. CLE, HFHS vs. ABE and HFHS vs. LGE (Kruskal-Wallis One-way ANOVA with Dunn's post-hoc test).

CHAPTER IV

Treatment with camu camu (*Myrciaria dubia*) prevents obesity by altering the gut microbiota and increasing energy expenditure in diet-induced obese mice.

Fernando F. Anhê[1,2], Mélanie Le Barz[1,2], Thibault V. Varin[2], Jocelyn Trottier[3], Stéphanie Dudonné[2], Renato T. Nachbar[1], Geneviève Pilon[1,2], Olivier Barbier [3],Yves Desjardins[2], Denis Roy[2] and André Marette[1,2]

[1]Department of Medicine, Faculty of Medicine, Cardiology Axis of the Québec Heart and Lung Institute, Laval University (Québec, Canada); [2]Institute of Nutrition and Functional Foods, Laval University (Québec,Canada); [3]CHU-Québec Research Centre, Laval University (Québec, Canada).

Résumé

La consommation de fruits est étroitement associée à une meilleure santé et à une plus grande diversité bactérienne dans le microbiota intestinal (MI). La composition du camu camu représentant parfaitement le potentiel des éléments phytochimiques pouvant agir contre les maladies immunométaboliques liées à l'obésité, nous avons évalué l'effet d'un extrait brut de ce fruit sur des caractéristiques du syndrome métabolique et sur le MI de sourissur une diète obésogène. Des souris mâles C57Bl/6J ont été nourries à une diète riche en gras et en sucrose (HFHS) et traitées quotidiennement avec le CC (200 mg/kg) ou à l'aide du véhicule (eau) pendant 8 semaines.Les souris traitées avec le CC ont vu leur prise de poids, leur graisse viscérale et leur stéatose hépatique grandement réduites par rapport à ce qui fut observé chez les souris HFHS témoins traitées à l'eau. Ces effets anti-obésité n'étaient pas liés à un dans l'apport énergétique, mais plutôt, à une augmentationde la dépense énergétique. Des analyses par qPCR du tissu adipeux brun ont révélé une expression plus élevée de l'ARNm de la protéine découplante (UCP1) chez les souris CC, des résultats fortement corrélés aux niveaux d'ARNm du récepteur d'acides biliaires (AB) TGR5. Ces résultats furent aussi associés à des changements drastiques dans le MI (i.e, de l'expansion de *Barnesiella* et d'*Akkermansia muciniphila* accompagné d'une forte réduction de *Lactobacillus*). Nous avons aussi démontré des niveaux réduits d'endotoxine circulante chez les souris CC par rapport aux souris témoins HFHS traitées à l'eau. Fait intéressant, des souris axéniques (germ-free, GF) dont le MI fut reconstitué avec le microbiote fécal des souris traitées avec le CC ont gagné moins de poids et ont eu une dépense énergétique plus élevée que les souris GF colonisées avec le MF de souris témoins. Nos résultats démontrent que le CC empêche la déposition de graisse viscérale en stimulant la dépense énergétique associé à la prévention de la dysbiose intestinale, à une amélioration de la barrière intestinale et à des changements majeurs dans le profil d'AB.

Abstract

The consumption of fruits is strongly associated with better health and higher bacterial diversity in the fecal microbiota (FM). Camu camu (*Myrciaria dubia*) is an Amazonian fruit with a unique phytochemical profile, strong antioxidant potential and purported anti-inflammatory potential. In the present study we have assessed the effect of a crude extract of camu camu (CC) on obesity and associated immunometabolic disorders in high fat/high sucrose (HFHS)-fed mice. Treatment of HFHS-fed mice with CC prevented weight gain, lowered fat accumulation and blunted metabolic inflammation and endotoxemia as compared to vehicle-treated HFHS-fed animals. CC-treated mice displayed improved glucose tolerance and insulin sensitivity and were also fully protected against hepatic steatosis. These effects were linked to increased energy expenditure and upregulation of uncoupling protein1 (UCP1) mRNA expression in the brown adipose tissue of CC-mice, which strongly correlated with the mRNA expression of the bile acid (BA) receptor TGR5. Moreover, CC-treated mice showed altered plasma BA pool and drastic changes in the GM (*e.g*, bloom of *Barnesiella* and *A. muciniphila* and a strong reduction of *Lactobacillus*). Germ-free (GF) mice reconstituted with the FM of CC-treated mice gained less weight and displayed higher energy expenditure than GF-mice colonized with the FM of HFHS controls. Our results show that CC prevents visceral and liver fat deposition through BAT activation and increased energy expenditure, a mechanism that is dependent on the GM and linked to major changes in the BA acid pool.

Introduction

The prevalence of obesity and overweight is extremely high worldwide [1] and worrisome predictions indicate that more than one billion people will be obese by 2030 [2]. Visceral obesity is crucial for the development of metabolic complications of chronic inflammatory etiology that considerably compromise life quality and reduce lifespan, such as type 2 diabetes, hepatic steatosis and cardiovascular diseases [3]. Deciphering the mechanisms leading to obesity and its associated debilitating conditions is therefore of utmost importance in order to guide the search for novel treatments and preventive strategies. Previous works by several research groups have demonstrated the role of the gastro-intestinal tract along with its colonizing bacteria in controlling host metabolism [4 5]. While diet is a major factor influencing gut microbial community structure [6], metagenome-wide association studies have revealed that the consumption of fruits and other phytonutrient-rich foods are among the strongest factors explaining alterations in the fecal microbiota of humans [7 8]. Accordingly, recent animal studies have shown that fruit extracts enriched in polyphenols can reduce body weight gain and alleviate the metabolic syndrome in association with the modulation of the gut microbiota [9 10]. However, it remains unclear to what extent the changes in the gut microbiota can contribute to the metabolic benefits. While a recent study has shown that resveratrol can impact the microbiota and thereby contribute to the metabolic benefits of this molecule [11], the dose used in these experiments far exceeds the concentration found in foods and thus is not nutritionally relevant. It is therefore still unknown whether modulation of the gut microbiota by complex mixtures of phytonutrients, such as those found in fruits, can be causally related to the prevention of body weight gain and improvement of obesity-related immunometabolic disorders.

Camu camu (*Myrciaria dubia*) is an Amazonian fruit deemed a "superfruit" for its unique phytochemical profile [12] and alleged potent antioxidant and anti-inflammatory activity [13 14]. Vitamin C is very abundant in camu camu, while the

178

concentration of flavonoids such as ellagic acid and ellagitannins is also elevated in this fruit [13 14]. As camu camu is a prolific assembly of potentially healthy phytochemicals, we sought to analyze the impact of the administration of a crude extract of camu camu (which mimics well the totality of its phytonutrients at physiologically relevant doses) on obesity and associated immunometabolic disorders, such as adipose tissue inflammation, insulin resistance and hepatic steatosis in diet-induced obese mice, and to thoroughly investigate the potential role of the gut microbiota in mediating the potential effects of this fruit on host metabolism.

Material and methods

Animals. Eight week-old C57Bl/6J male mice (Jackson, USA) were individually housed in a controlled environment (12 hours daylight cycle, lights off at 18:00) with food and water *ad libitum* in the animal facility of the Institute of Nutrition and Functional Foods. After two weeks of acclimatization on a normal-chow diet (Teklad 2018, Harlan), mice were randomly divided into 3 groups (n=12) and fed on a high-fat high-sucrose (HFHS) diet containing 65% lipids, 15% proteins and 20% carbohydrates (Supplemental Table 1). Treatment started concomitantly with the introduction of the HFHS diet and consisted of daily oral doses (200 mg/kg) of resuspended crude extract of camu camu (*Myrciaria dubia*, Sunfood, San Diego, USA), vitamin C (6.6 mg/kg, which reproduces the dose of vitamin C given within 200mg/kg of CC) or the vehicle used to resuspend the extract and vitamin C (*i.e.*, animal facility's drinking water) throughout 8 weeks. 200 mg/kg of camu camu extract is equivalent to approximately 2 g/kg of the fresh fruit (or 140 g of the fresh fruit for 70 kg individual), which consists of a nutritionally feasible dose. An additional group (n=12) of chow-fed vehicle-treated mice was included as a reference control for diet-induced obesity. The groups treated with the extract of camu camu and vitamin C are referred to as *CC* and *VitC* respectively throughout the manuscript, whereas the vehicle-treated groups are identified as *Chow* and *HFHS*. The phytochemical profile of the camu camu extract is available in Table 1. Body weight gain and food intake were assessed twice a week. At week 8, animals

were anesthetized in chambers saturated with isoflurane and then sacrificed by cardiac puncture. Blood was drawn in tubes containing 2 IU of heparin and immediately centrifuged in order to separate plasma from cells. Brown, subcutaneous and visceral fat pads were carefully collected along with gastrocnemius muscle, liver, intestine, pancreas, heart and gallbladder. All procedures were previously approved by the Laval University Animal Ethics Committee.

Germ-free mice and fecal microbiota transplants. In an additional cohort, fecal pellets of vehicle-treated and CC-treated conventional mice were harvested at week 6 and transferred to anaerobic chambers for resuspension in phosphate-buffered saline (110 mg of feces/350 µL of PBS). Fourteen 8-week old germ-free C57Bl/6J mice were purchased from Taconic, USA and, on the day of their arrival, the sterile containers were opened under a germ-free laminar flow hood and mice were immediately gavaged with freshly prepared fecal resuspensions (350 µL) made with the stool of either vehicle-treated or CC-treated HFHS-fed conventional mice. Germ-free mice reconstituted with the fecal microbiota of vehicle-treated HFHS-fed mice are referred to as HFHS-receivers (n=7) whereas those reconstituted with the fecal slurry of CC-treated HFHS-fed mice are referred to as CC-receivers (n=7) throughout the manuscript. Transplanted mice were initially housed in metabolic cages for 4 days (Columbus instruments, Columbus, OH, USA) and then transferred to ventilated sterile cages for 10 additional days and fed a low-fat diet (Research diets, D12450H) throughout the study.

Metabolic cages. At week 5, mice were individually placed in metabolic cages (Comprehensive Laboratory Animal Monitoring System, CLAMS™, Columbus Instruments, Columbus, OH, USA) for automated, non-invasive and simultaneous assessment of horizontal and vertical activity, feeding, oxygen consumption and carbon dioxide production. Room temperature for all metabolic studies was maintained at 28°C to keep mice at thermoneutrality [15 16] and with a 12-hour-light/dark cycle. The relationship between metabolic rate and body mass was normalized by using the Kleiber's interspecific mass exponent (0.75) to

calculate the metabolic body size (body weight$^{0.75}$) [17 18]. Mice were monitored over a 3-day period (1 day of acclimatization followed by 2 days of measurements). Graphs display the average of the hourly measurements during two days of monitoring.

The methods used to assess glucose homeostasis, plasma bile acids and gut microbial profile are available as supplemental material.

Statistical analysis. Data are expressed as mean ± SEM. One-way ANOVA with a Student-Newman-Keuls post hoc test (Prim GraphPad, USA) was used to compare HFHS, CC and VitC groups. In the set of experiments that did not include the VitC group, Unpaired Student's t-tests (Prim GraphPad, USA) were used to assign significance to the comparisons between CC *versus* HFHS. Because Chow-fed mice were exclusively a reference control for diet-induced obesity and the interaction between CC and different diets was out of the scope of this study, significance to the comparison Chow *versus* HFHS was also based on Unpaired Student's t-tests (Prim GraphPad, USA). Two-way repeated measures ANOVA with a Student-Newman-Keuls post-test (Sigmaplot, USA) was used when time was considered as a variable. All results were considered statistically significant at $P < 0.05$.

The statistical significance of differentially abundant and biologically relevant taxonomical and functional biomarkers between two distinct biological conditions was measured using a linear discriminant analysis (LDA) effect size (LEfSe) [26]. This tool allows for ranking by effect size the differential biomarkers using LDA. Only taxa meeting an LDA significant threshold of 2.5 were considered. A *P*-value of < 0.05 was considered to indicate statistical significance for the factorial Kruskal–Wallis rank-sum test.

Results

CC, but not vitamin C, prevents obesity and liver steatosis in DIO-mice. Daily oral administration of CC significantly prevented diet-induced weight gain from day 14 onwards (figures 1a,b), and these findings were not related to changes

in energy intake (figure 1c). The effect of CC on weight gain was explained by a significant prevention of fat accretion in all fat depots, including visceral (*ie*, epididymal, retroperitoneal and mesenteric), subcutaneous (*ie*, inguinal) and interscapular brown fat (figure 1d). The weight of gastrocnemius, pancreas, heart and caecum content as well as the intestinal length was not affected by CC administration (Supplemental figures 1a-f). Administration of vitamin C to doses equivalent to that provided in the extract of camu camu did not prevent diet-induced obesity (figures 1a-d), suggesting that other constituents in the extract are responsible for the anti-obesity observed. Liver weight was slightly, yet not significantly, reduced in CC-treated mice (figure 1e), whereas diet-induced hepatic steatosis and dyslipidemia were fully prevented in these animals, as indicated by prevention of triglyceride accumulation in both liver and circulation of CC-treated mice as compared to HFHS control mice (figures 1f,g). We found no differences in the daily energy output through the feces in CC mice *versus* vehicle-treated HFHS mice, suggesting that the anti-obesity effect of CC was not related to altered food digestion or intestinal absorption (figure 1h). Interestingly, CC administration was associated with increased energy expenditure and that was unrelated with augmented physical activity (figure 1i and supplemental figures 1g-l). This resulted in a major shift in energy partitioning with less energy available for storage in CC-treated HFHS mice in comparison with vehicle-treated HFHS control mice (figure 1j). Taken together, these results show that CC prevents diet-induced weight gain and adiposity and that this anti-obesity effect is driven by increased energy expenditure.

CC blunts adipose tissue inflammation, alleviates metabolic endotoxemia and improves glucose homeostasis in DIO-mice. CC treatment blunted many typical inflammatory markers of metabolic inflammation in the adipose tissue, leading to a strong tendency ($P = 0.06$) towards reduced interleukin-1β (IL-1β) and a significant reduction of vascular endothelial growth factor (VEGF) and monocyte chemoattractant protein-1 (MCP-1) (figure 2a-f). In accordance with lower levels of MCP-1, a key orchestrator of macrophage infiltration in the adipose tissue, we found lower mRNA expression of *Adgre* (encodes for the macrophage marker

182

F4/80) and lower crown-like structure (CLS) density in the epididymal adipose tissue of CC mice *versus* HFHS control mice (figure 2g and supplemental figures 2a-c,f). Moreover, consistent with improved adipose tissue inflammation, CC mice showed reduced adipocyte size (Supplemental figures 2a-e). CC treatment also a prevented metabolic endotoxemia, as indicated by lower levels of LPS in the plasma of CC mice *versus* vehicle-treated HFHS control mice (figure 2h). These findings show a consistent resolution of adipose tissue inflammation in CC mice linked to lower fat mass accretion and suggests that CC-driven alterations in intestinal physiology may also contribute to alleviate diet-induced metabolic inflammation in these animals.

While fasting glycemia was not different between CC-treated and HFHS control mice (figure 2i), CC administration prevented fasting hyperinsulinemia (figure 2j), resulting in improved fasting insulin resistance, as suggested by lower HOMA-IR in CC mice as compared to HFHS control mice (figure 2k). We also found improved glucose clearance (figures 2l,m) and reduced insulinemia post glucose challenge (figure 2n,o) along with ameliorated insulin sensitivity 10 min after insulin injection (figure 2p) in CC mice *versus* HFHS control mice. These results indicate that the preventive effect of CC on HFHS-induced obesity and visceral fat accumulation and inflammation resulted in improved glucose homeostasis and insulin sensitivity in these mice.

CC administration prevents obesity-driven dysbiosis and alleviates metabolic endotoxemia. Since intestinal bacterial communities play a role in host metabolism and because diet is a major driver of changes in the gut microbiota, we used 16S rRNA gene-based analysis of stool samples in order to assess the taxonomic profile of Chow, HFHS and CC mice. CC treatment fully prevented the diet-induced decrease in microbial richness (figure 3a) and the increase in the Firmicutes/Bacteroidetes ratio (figure 3b,c), two hallmarks of obesity-driven dysbiosis [19 20 21]. Fecal samples were harvested at the end of the study (*ie*, week 8) and at the end of the acclimatization period on a Chow diet (baseline, bs) in order to verify the uniformity of the microbial profile at the study beginning. CC-

treatment prevented the HFHS-driven reduction in the relative abundance of *Bifidobacterium* and *Barnesiella*, the main representatives of the phyla Actinobacteria and Bacteroidetes, respectively, affected by CC (figure 3d). Interestingly, CC drastically reduced the relative abundance of *Lactobacillus*, and this change explained most of the reduction in Firmicutes found in CC metagenomes *vs.* HFHS (figure 3d). Similarly to Chow-fed mice, CC-treated mice also showed an expansion of *Turicibacter*.

We then applied the LEfSe method in order to rank the most relevant taxonomic changes while emphasizing both statistical significance and biological representativeness of taxa. This approach ranked *Barnesiella spp.* and *Turicibacter spp.* along with a major decrease in OTUs assigned to *Lactobacillus spp.* as the main features discriminating the metagenomes of CC mice from those of HFHS control mice (figure 3e). We found a tendency of higher *Akkermansia muciniphila* in CC mice (P = 0.07, figure 3d). This bacterium deserves thorough attention since it has been previously associated with lean phenotypes [20 22] and increased in the gut microbiota of HFHS-fed mice treated with polyphenol-rich extracts [9 10]. We therefore quantified *A. muciniphila* by qPCR and found an increase in this taxon in CC-treated mice *versus* vehicle-treated HFHS-fed mice (figure 3g). OTUs assigned to the genera *Delftia*, *Roseburia*, *Anaerostipes*, *Anaerotruncus* and *Parabacteroides,* and to unclassified genera within the families *Christensenellaceae* and *Erysipelotrichaceae,* were considerably low (below 1%). We therefore decided to focus on the major CC-related effects, particularly on *Barnesiella*, *Turicibacter*, *Bifidobacterium*, *A. muciniphila* and *Lactobacillus.*

CC administration alters the plasma bile acid pool and upregulates the mRNA expression of markers of brown fat activation and browning of white adipose tissue. Since bile acids (BA) have been shown to regulate energy homeostasis and brown adipose tissue activity [23 24 25], we sought to evaluate whether changes in the bile acid pool could be linked to the phenotypic changes seen in CC-treated mice. CC administration normalized the total circulating levels of BA in HFHS-fed mice to values similar to those of Chow-fed mice (figure 4a and

supplemental figures 3a,c) and this was associated with smaller gallbladders found in CC mice *versus* HFHS control mice (figure 4c). Moreover, CC administration increased the proportion of secondary and of unconjugated bile acids in the plasma (figure 4b and supplemental figures 3b,d) as compared with vehicle-treated HFHS control mice. Relative to the total amount of BA, the taurine-conjugated form of the primary BA TαMCA (tauro-α-murocholic acid) and TβMCA (tauro-β-murocholic acid) were less abundant, while βMCA (β-murocholic acid) and ωMCA (ω-murocholic acid) were increased in the plasma of CC mice when compared with vehicle-treated HFHS mice (figure 4b). CDCA (chenodeoxycholic acid) along with the secondary BA DCA (deoxycholic acid), HDCA (hyodeoxycholic acid) and UDCA (ursodeoxycholic acid) were also increased in the plasma of CC mice *versus* HFHS control mice (figure 4b). Eight weeks of HFHS feeding increased the ileal mRNA expression of the nuclear receptor small heterodimer partner (SHP, *Nr0b2*), a pivotal downstream effector of FXR (farnesoid-X-receptor) activation (Figure 4d). As expected, this latter alteration was linked to reduced mRNA expression of the rate-limiting enzyme controlling BA synthesis cholesterol-7-hydroxylase (*Cyp7a1*) in the liver of HFHS control mice *versus* Chow-fed mice (figure 4e). *Abcb11* (bile salt export pump, Bsep), *Gpbar1* (G protein-coupled bile acid receptor 1, TGR5) and *Fgfr4* (fibroblast growth factor receptor 4) were also decreased in the liver of HFHS-fed control mice when compared with Chow-fed mice (figures 4e). Consistent with reduced BA pool size, the ileal mRNA expression of *Nr0b2* was downregulated in CC mice as compared with HFHS control mice (figure 4d), however this was not sufficient to affect the mRNA expression of *Fgf15* (fibroblast growth factor 15) and of other genes under FXR control, such as the BA transporters organic solute transporter-α (Ostα, *Slc51a*) and Ostβ (*Slc51b*), in the ileum of CC mice (figure 4d). Moreover, these latter findings were not related to changes in the mRNA expression of *Cyp7a1* in the liver of CC mice in comparison with HFHS-fed control mice (figure 4e). Taken together these results highlight drastic changes in the plasma BA pool size and composition.

As our findings pointed toward increased energy expenditure in CC-treated mice, and because BA have been suggested to regulate thermogenesis, we next evaluated markers of brown fat activity and of browning of white fat depots. Our findings revealed a significant upregulation in the mRNA levels of uncoupling protein 1 (*Ucp1*) and deiodinase 2 (*Dio2*) in both brown (BAT) and inguinal (iWAT) adipose tissues of CC-treated HFHS mice as compared with vehicle-treated HFHS mice (figures 4g,h). The mRNA expression of *Pgc1a* (peroxisome proliferator-activated receptor γ coactivator 1α) was also increased in BAT of CC mice in comparison with HFHS control mice (figure 4h). Interestingly, the mRNA expression of *Fgfr4* was upregulated in the inguinal fat of CC mice (figure 4g), but not in the epididymal fat or BAT of these mice (figures 4f,h). We found a strong correlation between *Ucp1* and *Dio2* mRNA expression in both iWAT and BAT, as well as between the mRNA expression of TGR5 (*Gpbar1*) and *Ucp1*, *Dio2* and *PGC1a* in BAT, all key genes involved in its thermogenic activation (figure 4i). Moreover, our analysis revealed that the mRNA expression of *Fgfr4* strongly correlated ($r = 0.86$) with the mRNA expression of *Dio2* in iWAT (figure 4i). We did not detect significant changes in the *Ucp1* and *Fgfr4* mRNA expression in the epididymal fat depot (eWAT) (figure 4f). Interestingly, the HFHS-induced increase in the ileal mRNA expression of fasting-induced adipose factor (*Fiaf*), a gut hormone controlling the clearance of triglycerides from plasma to tissues, was inhibited in CC mice (figure 4d), suggesting an intestinal contribution to the improved triglyceride clearance found in CC mice. *Fiaf* is also expressed in the liver and in the adipose tissue and, albeit we found higher mRNA expression of *Fiaf* in the eWAT of HFHS control mice than in Chow-fed mice, CC administration did not affect the expression of this gene in this fat tissue or in the liver (figure 4e,f). In summary, these data supports increased brown fat activation coupled with browning of subcutaneous white adipose tissue.

CC reduces weight gain and increases energy expenditure through modulation of the gut microbiota. To demonstrate the causal link between the gut microbiota of CC mice and host phenotype, we next performed fecal microbiota transplant (FMT) experiments using germ-free mice colonized with the fecal

microbiota of CC-treated donor mice to test whether this could recapitulate the effect of CC administration on weight gain and energy expenditure. Germ-free mice were gavaged with fecal resuspensions from vehicle-treated HFHS-fed and from CC-treated HFHS-fed donor mice to germ-free mice (referred to as HFHS receivers and CC receivers). Throughout days 1, 2 and 3 post-colonization HFHS receivers gained, respectively, 3%, 2% and 2.4% of their initial body weight (figure 5a). Conversely, CC receivers showed a rapid 5% body weight loss after only one day post-colonization followed by a 3.7% and a 1.4% loss of their initial body weight on days 2 and 3, respectively (figure 5a). This resulted in significant differences in weight gain between CC receivers and HFHS receivers on days 1 (P < 0.001) and 2 (P = 0.009) post-colonization and a tendency (P = 0.1) to be maintained at day 3 (figure 5a). There were no differences in energy intake or in fecal energy excretion between groups (figure 5b and supplemental figures 5a,b). Indirect calorimetry measurements performed throughout the first four days post-colonization revealed a marked increase in energy expenditure unrelated to increased physical activity on days 1 and 2 post-colonization, an effect that was markedly reduced on day 3 and completely lost on day 4 post-colonization (figure 5c and supplemental figures 5c-h). We then used qPCR to assess the abundance of key phylotypes harbored by CC-treated mice in fecal samples of HFHS-receivers and CC-receivers. On day 1 post colonization, lower Firmicutes/Bacteroidetes ratio and *Lactobacillus spp.* as well as higher abundance of *A. muciniphila* were found in the feces of CC receivers when compared with HFHS receivers (figures 5d-h). Interestingly, out of the eight key taxa explored, only *A. muciniphila* remained significantly enriched in the feces of CC receivers in comparison with HFHS receivers on day 2 post-colonization (figure 5h). The presence of *Bifidobacterium spp.*, *Barnesiella spp.*, *Allobaculum spp.* and *Turicibacter spp.* was not different between groups on days 1 and 2 post-colonization (figure 5i and supplemental figures i-k). These results show that colonization of germ-free mice with a single transplant of fecal microbiota from CC-treated donor mice transiently and partially recapitulates the phenotype of CC

mice, and point toward *A. muciniphila* as being an important driver of increased energy expenditure and reduced weight gain upon CC administration.

Discussion

In this paper we present evidence that daily treatment of HFHS-fed mice with a crude extract of camu camu containing a rich mixture of phytonutrients and fibers is sufficient to completely prevent diet-induced obesity and ameliorate several features of the metabolic syndrome in these animals. Our work further elucidates some key mechanisms underlying the beneficial action of CC treatment. First, we report that the anti-obesity effect of CC is unrelated to changes in energy intake or excretion and rather attributed to increased energy expenditure. Our data further unravel a putative role for an altered plasma BA pool size and composition that is consistent with brown fat activation and browning of subcutaneous white fat. We have also demonstrated through performing metagenomic analyses and FMT studies that major changes in the gut microbiota are causally related to key metabolic phenotypes of CC-treated mice, such as body weight gain and increased energy expenditure.

Camu camu-based products are widely marketed for their high content of vitamin C and their alleged strong anti-oxidant potential [14]. However, we showed here that mice treated daily with the same dose of vitamin C found in 200 mg/kg of CC (*ie*, 6.6 mg/kg) displayed fat mass gain comparable to vehicle-treated HFHS-fed mice, strongly suggesting that vitamin C, alone, is not involved in the anti-obesity effects of CC.

CC treatment prevented the HFHS-induced increase in BA pool size and composition. Smaller gallbladders found in CC mice *versus* HFHS control mice suggest that the effect of CC on BA pool size is linked to reduced bile acid synthesis rather than increased bile acid excretion. BA bind to FXR which in turn activates Shp to then inhibit their own synthesis in the liver and uptake in the ileum. FXR activation in the ileum also triggers the secretion of Fgf15, which contributes to the downregulation of BA synthesis in the liver through binding to Fgfr4. Our

results suggest that the reduced BA pool size found in CC-treated HFHS mice likely contributes to downregulate FXR activity in the ileum of these animals. This conclusion is based on the lower mRNA levels of Shp in the ileum of CC mice, since the mRNA expression of FXR poorly reflects its activity [26 27]. Surprisingly, the mRNA expression of the rate-limiting enzyme involved in BA synthesis, *Cyp7a1*, along with the mRNA levels of Shp were not affected by CC administration in the liver. As we found a major decrease in the abundance of FXR antagonists (*eg*, TαMCA, TβMCA) coupled with an increase in FXR agonists (*eg*, CDCA, DCA, HDCA and UDCA) in the BA pool of CC mice, we hypothesized that such a FXR-stimulatory BA profile might compensate for the inhibitory effect of a reduced BA pool size, therefore disrupting the FXR-mediated negative feedback loop controlling BA synthesis in CC mice and keeping the levels of circulating BA lower than in vehicle-treated HFHS-fed mice.

Our results also suggest that the particular plasma BA profile of CC mice may be relevant to the enhanced brown fat activation and browning of subcutaneous fat in CC mice. Indeed, CDCA and especially the secondary BA DCA, HDCA and UDCA have been shown to act through TGR5 to potentiate the response of brown adipocytes to thyroid hormone and activate non-shivering thermogenesis in this tissue [23]. In line with this previous report, we found higher abundance of secondary BA in CC mice (particularly DCA, HDCA, UDCA and ωMCA) in parallel to increased mRNA expression of genes involved in thermogenesis in both brown and subcutaneous fat depots. We also found a strong correlation between *Ucp1* mRNA expression (a key marker of brown fat activity and white fat browning) and TGR5 mRNA expression in the brown fat of CC mice. Moreover, the gut hormone Fgf15 has been shown to trigger thermogenesis and browning of white fat depots by means of Fgfr4 activation [25]. Consistently with these latter findings, we found a strong upregulation in the mRNA expression of *Fgfr4* in inguinal fat, suggesting that enhanced browning of subcutaneous white fat in CC mice is associated with increased responsiveness to Fgf15. Although the direct contribution of the altered BA pool size and composition found in CC mice to enhanced energy expenditure warrants further investigation, our study brings novel

insights into the mechanistic role of BA in the anti-obesity effects of polyphenol-rich extracts.

A direct effect of CC phytonutrients on brown and white adipocytes may also contribute to the beneficial effects of camu camu. However, while phytochemicals such as green tea polyphenols [28 29], capsaicin [29 30], naringenin [31] and resveratrol [32 33] have all been shown to trigger thermogenesis in animal models, these compounds were not detected to significant levels in CC, and they have been mostly tested at pharmacological doses and not at physiologically relevant concentrations found in foods. In the present study we tested a crude extract containing a mix of key phytochemicals that are provided at realistic concentrations and that corresponds to the consumption of feasible amounts by humans (approximately 2 g of the fresh fruit/kg of body weight). This approach allows for the discovery of mechanisms of action that more likely take place during the consumption of fruits and vegetables and may therefore guide the tailoring of diets in order to prevent or treat the metabolic syndrome. Hence, it is noteworthy that we found considerable amounts of ellagic acid and its hydrolysable polymeric form (*ie*, ellagitannins) in the camu camu extract. Hydrolysis of ellagitannins to yield ellagic acid and the conversion of this latter molecule into urolithins takes place in the gut lumen upon reaction with bacterial enzymes. Although there is strong evidence for the health supporting properties of urolithins [34], its thermogenic effect remains to be elucidated.

The microbial community structure was markedly reshaped in CC-treated mice and may be related to alteration in the plasma BA profile. Indeed, BA acids are antimicrobial molecules [35] and the altered bile acid pool observed upon high saturated fat feeding, which favors the presence of taurine-conjugated BA in the enterohepatic circulation, was found to be associated with the expansion of bile acid resistant bacteria (*eg*, *Bilophila wadsworthis* and *Lactobacillus spp.*) in the gut environment [26 36]. The reduction of BA pool size found in CC mice may therefore remove the competitive advantage of *Lactobacillus spp.* and contribute to mitigate their presence in the gut microbiota. The likely increment in the anti-

190

oxidant potential in the lumen associated with the intake of CC phytochemicals may restrain oxygen availability and further compromise the bloom of facultative anaerobe species such as lactobacilli. This latter hypothesis is supported by a major reduction in *Lactobacillus spp.* abundance observed in mice treated with the antioxidant tempol [26]. BA can reshape the gut microbiota and, in turn, microbes are able to deconjugate and dehydroxylate BA [35]. We found an expansion of unconjugated and of secondary BA in the plasma of CC mice, indicating an important influence of gut microbes on the BA profile in CC mice. Since our results suggested a role for secondary BA in brown fat activation, an interplay between gut bacteria and BA pool composition may contribute to the effect of CC on energy expenditure and weight gain. In this regard, we and others have previously shown the association between dietary polyphenols and a prebiotic-like effect on *A. muciniphila* [9 10 37], whereas the tannase activity of this bacterium (*ie*, ability to yield ellagic acid from the hydrolysis of ellagitannins) has been recently described and may bring an additional competitive advantage for *A. muciniphila* to thrive [38]. While the interaction between BA and *A. muciniphila* is currently unknown, polyphenols present in CC may thus contribute to the expansion of *A. muciniphila* population observed in metagenomes of CC mice.

Fibers are complex polysaccharides that constitute a major dietary substrate for bacterial fermentation in the gut. *Bifidobacterium spp.* possess a wide repertoire of genes encoding enzymes for the degradation of complex polysaccharides [39] and, indeed, this taxa were enriched in the gut microbiota of Chow-fed mice when compared with vehicle-treated HFHS-fed mice. *Turicibacter spp.* are not classically related to fibrolytic activity, however their identification as key phylotypes in Chow-fed mice metagenomes suggest their colonic expansion in fiber-rich environments. *Bifidobacterium spp.* and *Turicibacter spp.* were both overrepresented in CC-treated HFHS mice in comparison with HFHS control mice and this could be partly attributed to the fibers present in CC.

To demonstrate the causal link between changes in gut microbiota and the phenotype of CC mice we colonized germ-free mice with a single dose of the fecal

slurry from vehicle-treated and CC-treated donors, which revealed a significant, but transitory effect on of the transplanted microbiota from CC-treated mice on weight gain and energy expenditure. Among the key metagenomic features that were significantly different post-colonization, only *A. muciniphila* abundance was found to remain significantly higher for two consecutive days in the fecal DNA of CC receivers *versus* HFHS receivers. Our results thus demonstrate that the gut microbiota is causally-related to the anti-obesity properties of CC and suggest that an increased abundance of *A. muciniphila* as a major contributor to this effect. This is supported by previous studies showing that the oral administration of *A. muciniphila* to diet-induced obese mice counteracted obesity along with other features of the metabolic syndrome [22 40 41]. Our work thus brings a novel perspective whereby expansion of *A. muciniphila* in response to dietary phytonutrients strongly collaborates with other gut microbes to trigger a compensatory increase in energy expenditure that helps to curb fat accumulation in DIO mice.

Conclusion

We found that daily administration of a crude extract of camu camu, providing physiologically relevant doses of a unique mix of phytochemicals, prevents obesity and metabolic syndrome by impacting the gut microbiota leading to increased energy expenditure. Our findings also suggest an interplay between the BA profile and the gut microbiota to activate BAT thermogenesis in CC mice. To the best of our knowledge, this is the first demonstration of the causal role of the gut microbiota in contributing to the metabolic benefits of a fruit extract. Our data also promote the consumption of camu camu and other phytochemical-rich fruits as a safe and easily implementable nutritional strategy to trigger the expansion of *A. muciniphila* in the gut microbiota an thus alleviate several detrimental features of the metabolic syndrome.

References

1. Finucane MM, Stevens GA, Cowan MJ, Danaei G, Lin JK, Paciorek CJ, Singh GM, Gutierrez HR, Lu Y, Bahalim AN, Farzadfar F, Riley LM, Ezzati M: National, regional, and global trends in body-mass index since 1980: systematic analysis of health examination surveys and epidemiological studies with 960 country-years and 9·1 million participants. The Lancet 377:557-567
2. Kelly T, Yang W, Chen CS, Reynolds K, He J: Global burden of obesity in 2005 and projections to 2030. Int J Obes (Lond) 2008;32:1431-1437
3. Olshansky SJ, Passaro DJ, Hershow RC, Layden J, Carnes BA, Brody J, Hayflick L, Butler RN, Allison DB, Ludwig DS: A potential decline in life expectancy in the United States in the 21st century. The New England journal of medicine 2005;352:1138-1145
4. Ridaura VK, Faith JJ, Rey FE, Cheng J, Duncan AE, Kau AL, Griffin NW, Lombard V, Henrissat B, Bain JR, Muehlbauer MJ, Ilkayeva O, Semenkovich CF, Funai K, Hayashi DK, Lyle BJ, Martini MC, Ursell LK, Clemente JC, Van Treuren W, Walters WA, Knight R, Newgard CB, Heath AC, Gordon JI: Gut microbiota from twins discordant for obesity modulate metabolism in mice. Science 2013;341:1241214
5. Caesar R, Tremaroli V, Kovatcheva-Datchary P, Cani PD, Backhed F: Crosstalk between Gut Microbiota and Dietary Lipids Aggravates WAT Inflammation through TLR Signaling. Cell metabolism 2015;22:658-668
6. David LA, Maurice CF, Carmody RN, Gootenberg DB, Button JE, Wolfe BE, Ling AV, Devlin AS, Varma Y, Fischbach MA, Biddinger SB, Dutton RJ, Turnbaugh PJ: Diet rapidly and reproducibly alters the human gut microbiome. Nature 2014;505:559-563
7. Zhernakova A, Kurilshikov A, Bonder MJ, Tigchelaar EF, Schirmer M, Vatanen T, Mujagic Z, Vila AV, Falony G, Vieira-Silva S, Wang J, Imhann F, Brandsma E, Jankipersadsing SA, Joossens M, Cenit MC, Deelen P, Swertz MA, Weersma RK, Feskens EJ, Netea MG, Gevers D, Jonkers D, Franke L, Aulchenko YS,

Huttenhower C, Raes J, Hofker MH, Xavier RJ, Wijmenga C, Fu J: Population-based metagenomics analysis reveals markers for gut microbiome composition and diversity. Science 2016;352:565-569

8. Falony G, Joossens M, Vieira-Silva S, Wang J, Darzi Y, Faust K, Kurilshikov A, Bonder MJ, Valles-Colomer M, Vandeputte D, Tito RY, Chaffron S, Rymenans L, Verspecht C, De Sutter L, Lima-Mendez G, D'Hoe K, Jonckheere K, Homola D, Garcia R, Tigchelaar EF, Eeckhaudt L, Fu J, Henckaerts L, Zhernakova A, Wijmenga C, Raes J: Population-level analysis of gut microbiome variation. Science 2016;352:560-564

9. Liu J, Lee J, Salazar Hernandez MA, Mazitschek R, Ozcan U: Treatment of obesity with celastrol. Cell 2015;161:999-1011

10. Bataglion GA, da Silva FM, Eberlin MN, Koolen HH: Determination of the phenolic composition from Brazilian tropical fruits by UHPLC-MS/MS. Food chemistry 2015;180:280-287

11. Langley PC, Pergolizzi JV, Jr., Taylor R, Jr., Ridgway C: Antioxidant and associated capacities of Camu camu (Myrciaria dubia): a systematic review. J Altern Complement Med 2015;21:8-14

12. Fracassetti D, Costa C, Moulay L, Tomas-Barberan FA: Ellagic acid derivatives, ellagitannins, proanthocyanidins and other phenolics, vitamin C and antioxidant capacity of two powder products from camu-camu fruit (Myrciaria dubia). Food chemistry 2013;139:578-588

13. Feldmann HM, Golozoubova V, Cannon B, Nedergaard J: UCP1 ablation induces obesity and abolishes diet-induced thermogenesis in mice exempt from thermal stress by living at thermoneutrality. Cell metabolism 2009;9:203-209

14. Helppi J, Schreier D, Naumann R, Zierau O: Mouse reproductive fitness is maintained up to an ambient temperature of 28 when housed in individually-ventilated cages. Laboratory animals 2016;50:254-263

15. Kleiber M: Body size and metabolic rate. Physiol Rev 1947;27:511-541

16. Kim KW, Donato J, Jr., Berglund ED, Choi YH, Kohno D, Elias CF, Depinho RA, Elmquist JK: FOXO1 in the ventromedial hypothalamus regulates energy balance. J Clin Invest 2012;122:2578-2589

17. Cotillard A, Kennedy SP, Kong LC, Prifti E, Pons N, Le Chatelier E, Almeida M, Quinquis B, Levenez F, Galleron N, Gougis S, Rizkalla S, Batto JM, Renault P, Dore J, Zucker JD, Clement K, Ehrlich SD: Dietary intervention impact on gut microbial gene richness. Nature 2013;500:585-588

18. Le Chatelier E, Nielsen T, Qin J, Prifti E, Hildebrand F, Falony G, Almeida M, Arumugam M, Batto JM, Kennedy S, Leonard P, Li J, Burgdorf K, Grarup N, Jorgensen T, Brandslund I, Nielsen HB, Juncker AS, Bertalan M, Levenez F, Pons N, Rasmussen S, Sunagawa S, Tap J, Tims S, Zoetendal EG, Brunak S, Clement K, Dore J, Kleerebezem M, Kristiansen K, Renault P, Sicheritz-Ponten T, de Vos WM, Zucker JD, Raes J, Hansen T, Bork P, Wang J, Ehrlich SD, Pedersen O: Richness of human gut microbiome correlates with metabolic markers. Nature 2013;500:541-546

19. Yasir M, Angelakis E, Bibi F, Azhar EI, Bachar D, Lagier JC, Gaborit B, Hassan AM, Jiman-Fatani AA, Alshali KZ, Robert C, Dutour A, Raoult D: Comparison of the gut microbiota of people in France and Saudi Arabia. Nutrition & diabetes 2015;5:e153

20. Dao MC, Everard A, Aron-Wisnewsky J, Sokolovska N, Prifti E, Verger EO, Kayser BD, Levenez F, Chilloux J, Hoyles L, Dumas ME, Rizkalla SW, Dore J, Cani PD, Clement K: Akkermansia muciniphila and improved metabolic health during a dietary intervention in obesity: relationship with gut microbiome richness and ecology. Gut 2016;65:426-436

21. Anhe FF, Roy D, Pilon G, Dudonne S, Matamoros S, Varin TV, Garofalo C, Moine Q, Desjardins Y, Levy E, Marette A: A polyphenol-rich cranberry extract protects from diet-induced obesity, insulin resistance and intestinal inflammation in association with increased Akkermansia spp. population in the gut microbiota of mice. Gut 2015;64:872-883

22. Roopchand DE, Carmody RN, Kuhn P, Moskal K, Rojas-Silva P, Turnbaugh PJ, Raskin I: Dietary Polyphenols Promote Growth of the Gut Bacterium Akkermansia muciniphila and Attenuate High-Fat Diet-Induced Metabolic Syndrome. Diabetes 2015;64:2847-2858

23. Watanabe M, Houten SM, Mataki C, Christoffolete MA, Kim BW, Sato H, Messaddeq N, Harney JW, Ezaki O, Kodama T, Schoonjans K, Bianco AC, Auwerx J: Bile acids induce energy expenditure by promoting intracellular thyroid hormone activation. Nature 2006;439:484-489

24. Thomas C, Gioiello A, Noriega L, Strehle A, Oury J, Rizzo G, Macchiarulo A, Yamamoto H, Mataki C, Pruzanski M, Pellicciari R, Auwerx J, Schoonjans K: TGR5-mediated bile acid sensing controls glucose homeostasis. Cell metabolism 2009;10:167-177

25. Fang S, Suh JM, Reilly SM, Yu E, Osborn O, Lackey D, Yoshihara E, Perino A, Jacinto S, Lukasheva Y, Atkins AR, Khvat A, Schnabl B, Yu RT, Brenner DA, Coulter S, Liddle C, Schoonjans K, Olefsky JM, Saltiel AR, Downes M, Evans RM: Intestinal FXR agonism promotes adipose tissue browning and reduces obesity and insulin resistance. Nature medicine 2015;21:159-165

26. Wang X, Ouyang Y, Liu J, Zhu M, Zhao G, Bao W, Hu FB: Fruit and vegetable consumption and mortality from all causes, cardiovascular disease, and cancer: systematic review and dose-response meta-analysis of prospective cohort studies. BMJ 2014;349:g4490

27. Hartley L, Igbinedion E, Holmes J, Flowers N, Thorogood M, Clarke A, Stranges S, Hooper L, Rees K: Increased consumption of fruit and vegetables for the primary prevention of cardiovascular diseases. The Cochrane database of systematic reviews 2013:CD009874

28. Nguyen B, Bauman A, Gale J, Banks E, Kritharides L, Ding D: Fruit and vegetable consumption and all-cause mortality: evidence from a large Australian cohort study. The international journal of behavioral nutrition and physical activity 2016;13:9

29. Li F, Jiang C, Krausz KW, Li Y, Albert I, Hao H, Fabre KM, Mitchell JB, Patterson AD, Gonzalez FJ: Microbiome remodelling leads to inhibition of intestinal farnesoid X receptor signalling and decreased obesity. Nature communications 2013;4:2384

30. Watanabe M, Horai Y, Houten SM, Morimoto K, Sugizaki T, Arita E, Mataki C, Sato H, Tanigawara Y, Schoonjans K, Itoh H, Auwerx J: Lowering bile acid pool size with a synthetic farnesoid X receptor (FXR) agonist induces obesity and

diabetes through reduced energy expenditure. The Journal of biological chemistry 2011;286:26913-26920

31. Dulloo AG, Duret C, Rohrer D, Girardier L, Mensi N, Fathi M, Chantre P, Vandermander J: Efficacy of a green tea extract rich in catechin polyphenols and caffeine in increasing 24-h energy expenditure and fat oxidation in humans. The American journal of clinical nutrition 1999;70:1040-1045

32. Rayalam S, Della-Fera MA, Baile CA: Phytochemicals and regulation of the adipocyte life cycle. The Journal of nutritional biochemistry 2008;19:717-726

33. Varghese S, Kubatka P, Rodrigo L, Gazdikova K, Caprnda M, Fedotova J, Zulli A, Kruzliak P, Busselberg D: Chili pepper as a body weight-loss food. International journal of food sciences and nutrition 2016:1-10

34. Thaiss CA, Itav S, Rothschild D, Meijer M, Levy M, Moresi C, Dohnalova L, Braverman S, Rozin S, Malitsky S, Dori-Bachash M, Kuperman Y, Biton I, Gertler A, Harmelin A, Shapiro H, Halpern Z, Aharoni A, Segal E, Elinav E: Persistent microbiome alterations modulate the rate of post-dieting weight regain. Nature 2016;

35. Wang S, Liang X, Yang Q, Fu X, Rogers CJ, Zhu M, Rodgers BD, Jiang Q, Dodson MV, Du M: Resveratrol induces brown-like adipocyte formation in white fat through activation of AMP-activated protein kinase (AMPK) alpha1. Int J Obes (Lond) 2015;39:967-976

36. Baur JA, Pearson KJ, Price NL, Jamieson HA, Lerin C, Kalra A, Prabhu VV, Allard JS, Lopez-Lluch G, Lewis K, Pistell PJ, Poosala S, Becker KG, Boss O, Gwinn D, Wang M, Ramaswamy S, Fishbein KW, Spencer RG, Lakatta EG, Le Couteur D, Shaw RJ, Navas P, Puigserver P, Ingram DK, de Cabo R, Sinclair DA: Resveratrol improves health and survival of mice on a high-calorie diet. Nature 2006;444:337-342

37. Ryu D, Mouchiroud L, Andreux PA, Katsyuba E, Moullan N, Nicolet-Dit-Felix AA, Williams EG, Jha P, Lo Sasso G, Huzard D, Aebischer P, Sandi C, Rinsch C, Auwerx J: Urolithin A induces mitophagy and prolongs lifespan in C. elegans and increases muscle function in rodents. Nature medicine 2016;22:879-888

38. Ridlon JM, Kang DJ, Hylemon PB, Bajaj JS: Bile acids and the gut microbiome. Current opinion in gastroenterology 2014;30:332-338

39. Devkota S, Wang Y, Musch MW, Leone V, Fehlner-Peach H, Nadimpalli A, Antonopoulos DA, Jabri B, Chang EB: Dietary-fat-induced taurocholic acid promotes pathobiont expansion and colitis in Il10-/- mice. Nature 2012;487:104-108

40. Anhe FF, Varin TV, Le Barz M, Desjardins Y, Levy E, Roy D, Marette A: Gut Microbiota Dysbiosis in Obesity-Linked Metabolic Diseases and Prebiotic Potential of Polyphenol-Rich Extracts. Current obesity reports 2015;4:389-400

41. Henning SM, Summanen PH, Lee R-P, Yang J, Finegold SM, Heber D, Li Z: Pomegranate ellagitannins stimulate the growth of Akkermansia muciniphila in vivo. Anaerobe 2017;43:56-60

42. Flint HJ, Scott KP, Duncan SH, Louis P, Forano E: Microbial degradation of complex carbohydrates in the gut. Gut microbes 2012;3:289-306

43. Everard A, Belzer C, Geurts L, Ouwerkerk JP, Druart C, Bindels LB, Guiot Y, Derrien M, Muccioli GG, Delzenne NM, de Vos WM, Cani PD: Cross-talk between Akkermansia muciniphila and intestinal epithelium controls diet-induced obesity.

Proceedings of the National Academy of Sciences of the United States of America 2013;110:9066-9071

44. Plovier H, Everard A, Druart C, Depommier C, Van Hul M, Geurts L, Chilloux J, Ottman N, Duparc T, Lichtenstein L, Myridakis A, Delzenne NM, Klievink J, Bhattacharjee A, van der Ark KC, Aalvink S, Martinez LO, Dumas ME, Maiter D, Loumaye A, Hermans MP, Thissen JP, Belzer C, de Vos WM, Cani PD: A purified membrane protein from Akkermansia muciniphila or the pasteurized bacterium improves metabolism in obese and diabetic mice. Nature medicine 2017;23:107-113

45. Anhe FF, Marette A: A microbial protein that alleviates metabolic syndrome. Nature medicine 2017;23:11-12

46. Chevalier C, Stojanovic O, Colin DJ, Suarez-Zamorano N, Tarallo V, Veyrat-Durebex C, Rigo D, Fabbiano S, Stevanovic A, Hagemann S, Montet X, Seimbille Y, Zamboni N, Hapfelmeier S, Trajkovski M: Gut Microbiota Orchestrates Energy Homeostasis during Cold. Cell 2015;163:1360-1374

Tables

Table 1: Chemical characterization of the camu camu extract.

	Extract content (mg/100g dry weight)	Daily intake* (mg/kg body weight)
Total polyphenols	6550 ±140	13.10000
Anthocyanins	nd	
Proanthocyanidins	nd	
Flavanols/Flavonols	110.8 ±10	0.22160
Quercetin	33.5 ±1.25	0.06700
Quercetin-glucoside	5.6 ±0.51	0.01120
Quercetin-galactoside	2.0 ±0.83	0.00400
Quercetion-3-xyloside	3.5 ±0.96	0.00700
Quercetion-3-arabinoside	0.7 ±0.39	0.00140
Myricetin	74.3 ±1.96	0.14860
Myricetin-glucoside/galactoside	8.4 ±1.63	0.01680
Coumaroyl-glucosides	1.0 ±0.26	0.00200
Phenolic acids	100.0 ±0.001	0.20000
Ellagic acid	44.0 ±0.001	0.08800
Gallic acid	26.1 ±0.76	0.05220
4-Hydroxybenzoic acid	1.1 ±0.31	0.00220
p-Coumaric acid	4.6 ±0.30	0.00920
Ferulic acid	0.3 ±0.03	0.00060
Protocatechuic acid	0.4 ±0.12	0.00080
Gentisic acid	0.2 ±0.12	0.00040
Ellagitannins	450.0 ±110	0.90000
Saguiin H-10	11.0 ±0.35	0.02200
Saguiin H6	7.0 ±0.14	0.01400
Ellagitannin B	117.1 ±6.70	0.23420
Sugars		
Glucose	1110 ±0.08	2.22000
Fructose	1790 ±0.11	3.58000
Polysaccharides	7280 ±5.04	14.56000
Fibers	34290 ±685.8	68.58000
Insoluble	8092.44 ±161.8	16.18488
Soluble	3669.03 ±73.3	7.33806
Vitamin C	3330 ±90.8	6.66000

* Daily intake was calculated based on the 200 mg of camu camu extract/kg of body weight dose orally given to mice during 8 weeks.

Legend to figures

Figure 1: CC administration, but not vitamin C, prevents diet-induced obesity. Mice were fed either a standard chow diet (Chow, n=12) or a high fat/high sucrose (HFHS, n=12) diet and treated with daily doses of an extract of camu camu (CC, n=12) or vitamin C (VitC, n=12) throughout 8 weeks. (a,b) Body weight gain; (c) cumulative energy intake. (d) Epididymal (eWAT), retro-peritoneal (rpWAT), mesenteric (mWAT) and inguinal (iWAT) white adipose tissues along with interscapular brown adipose tissue (iBAT) were harvested and weighed during necropsies. (e) Liver weight; (f) hepatic triglyceride content; (g) circulating triglycerides (6-hour fasted mice). At week 5, mice were temporarily housed in metabolic cages and (h) fecal energy output and (i) energy expenditure were assessed. The relationship between metabolic rate and body mass was normalized by using the metabolic body size (*ie*, body mass$^{0.75}$). (j) Energy partitioning. Data are expressed as the mean ±SEM. (a, i) Two-way repeated measures ANOVA with a Student-Newman-Keuls post hoc test. (b-e) One-way ANOVA with a Student-Newman-Keuls post hoc test. (f-h) Unpaired two-tailed Student's t-test. *$P < 0.05$, **$P < 0.01$ and ***$P < 0.001$ for Chow *vs*. HFHS; [#]$P < 0.05$, [##]$P < 0.01$ and [###]$P < 0.001$ for CC *vs.* HFHS.

Figure 2: CC blunts adipose tissue inflammation, alleviates metabolic endotoxemia and improves glucose homeostasis in DIO-mice. Protein lysates from epididymal fat pads (eWAT) of Chow (n=12), HFHS (n=12) and CC (n=12) were used to quantify (a) interleukin-1β (IL-1β), (b) interleukin-6 (IL-6), (c) interferon-γ (INF-γ), (d) regulated on activation normal T cell expressed and secreted (RANTES), (e) vascular endothelial growth factor (VEGF) and (f) monocyte chemoattractant protein-1 (MCP-1). (g) qPCR analysis of *Adgre* (encodes for F4/80) mRNA expression in eWAT. (h) Circulating lipopolysaccharides (6-hour fasted mice). At week 6**,** mice (n=12) were fasted overnight (12 hours) and submitted to oral glucose tolerance tests (OGTT). CC was orally given 2 hours prior to the test, and glycemia was assessed 15 minutes

after CC administration (time point -105) to monitor possible changes in glycemia associated with sugars present in CC. (i) Fasting glycemia; (j) fasting insulinemia; (k) homeostatic model assessment for insulin resistance; (l, m) OGTT. (n, o) Blood was collected during OGTT and used in order to assess insulinemia after glucose challenge. At week 7, mice were fasted for 6 hours and (p) insulin tolerance tests were carried out after intraperitoneal insulin injections (ipITT, 0.65 IU/kg). Data are expressed as the mean ±SEM. (l, n and p) Two-way repeated measures ANOVA with a Student-Newman-Keuls post hoc test. (a-k, m and o) Unpaired two-tailed Student's t-test. $*P< 0.05$, $**P< 0.01$ and $***P< 0.001$ for Chow $vs.$ HFHS; $\#P< 0.05$, $\#\#P< 0.01$ and $\#\#\#P< 0.001$ for CC $vs.$ HFHS.

Figure 3: CC prevents obesity-driven gut microbiota dysbiosis in HFHS-fed mice. Fecal samples of Chow-fed (Chow, n=9), high fat/high sucrose-fed (HFHS, n=11) and HFHS-fed CC-treated (CC, n=11) mice were harvested at week 8. Fecal pellets were also collected during the last week of acclimatization on a Chow diet (baseline, bs), prior to the introduction of the HFHS diet or CC treatment. Genomic DNA was extracted from feces and subsequent 16S rRNA-based gut microbial profiling was performed. (a) Chao1 index of bacterial richness (at OTU level) was calculated as a measure of α-diversity. (b) Firmicutes to Bacteroidetes (F/B) ratio. Relative abundance of taxa at (c) phylum and (d) genus level. Linear discriminant analysis (LDA) effect size (LEfSe) was calculated in order to explore the taxa within genus level that more strongly discriminate between the gut microbiota of (e) Chow $vs.$ HFHS and (f) CC $vs.$ HFHS. (g) qPCR quantification of fecal $A.\ muciniphila$ normalized by total bacteria (forward P891/reverse P1033). (a) Mann-Whitney U test with a Monte Carlo permutation test. (b-d) Mann-Whitney U test. (g) Unpaired two-tailed Student's t-test.$*P< 0.05$, $**P< 0.01$ and $***P< 0.001$ Chow $vs.$ HFHS; $\#P< 0.05$, $\#\#P< 0.01$ and $\#\#\#P< 0.001$ for HFHS $vs.$ CC.

Figure 4: CC administration alters bile acid pool size and composition and upregulates the mRNA expression of genes involved in thermogenesis. (a,b) Plasma bile acids; (c) gallbladder weight. Messenger RNA extracted from (d)

ileum, (e) liver, (f) epididymal adipose tissue (eWAT), (g) inguinal adipose tissue (iWAT) and (h) brown adipose tissue (BAT) was quantified by RT-PCR. Relative expression was calculated using the ΔΔCt method with Chow mice as the group of reference and actin as the reference gene. (i) Correlation matrix between BAT and iWAT mRNA expression profiles (values outlined in bold represents statistically significant correlations; $P=0.05$ if $0.404 > r > 0.404$; $P=0.01$ if $0.515 > r > 0.515$; $P=0.001$ if $0.628 > r > 0.628$). Data are expressed as the mean ±SEM. Significance was calculated between Chow *vs*. HFHS and HFHS *vs.* CC using unpaired two-tailed Student's t-test. *$P< 0.05$, **$P< 0.01$ and ***$P< 0.001$ for Chow *vs*. HFHS; [#]$P< 0.05$, [##]$P< 0.01$ and [###]$P< 0.001$ for CC *vs.* HFHS.

Figure 5: Reconstitution of germ-free mice with the fecal microbiota of CC-treated mice recapitulates the effects of CC administration on weight gain and energy expenditure. Germ-free mice were reconstituted either with the fecal slurry of high fat/high sucrose (HFHS)-fed vehicle-treated mice (HFHS receivers, n=7) or CC-treated mice (CC receivers, n=7) and kept on a low-fat diet in metabolic cages during the initial days post-colonization. Mice were later transferred into sterile cages and kept on a low-fat diet and under specific pathogen-free (SPF) conditions. (a) Weight gain; (b) energy intake; (c) energy expenditure (the relationship between metabolic rate and body mass was normalized by using the metabolic body size, *ie*, body mass$^{0.75}$). (d-i) qPCR-based quantification of taxa in the fecal microbiota of HFHS and CC receivers. Data are expressed as the mean ±SEM. Two-way repeated measures ANOVA with a Student-Newman-Keuls post hoc test was used to calculate the significance of the differences between time points. *$P< 0.05$, **$P< 0.01$ and ***$P< 0.001$.

Figures

Figure 1: CC administration, but not vitamin C, prevents diet-induced obesity.
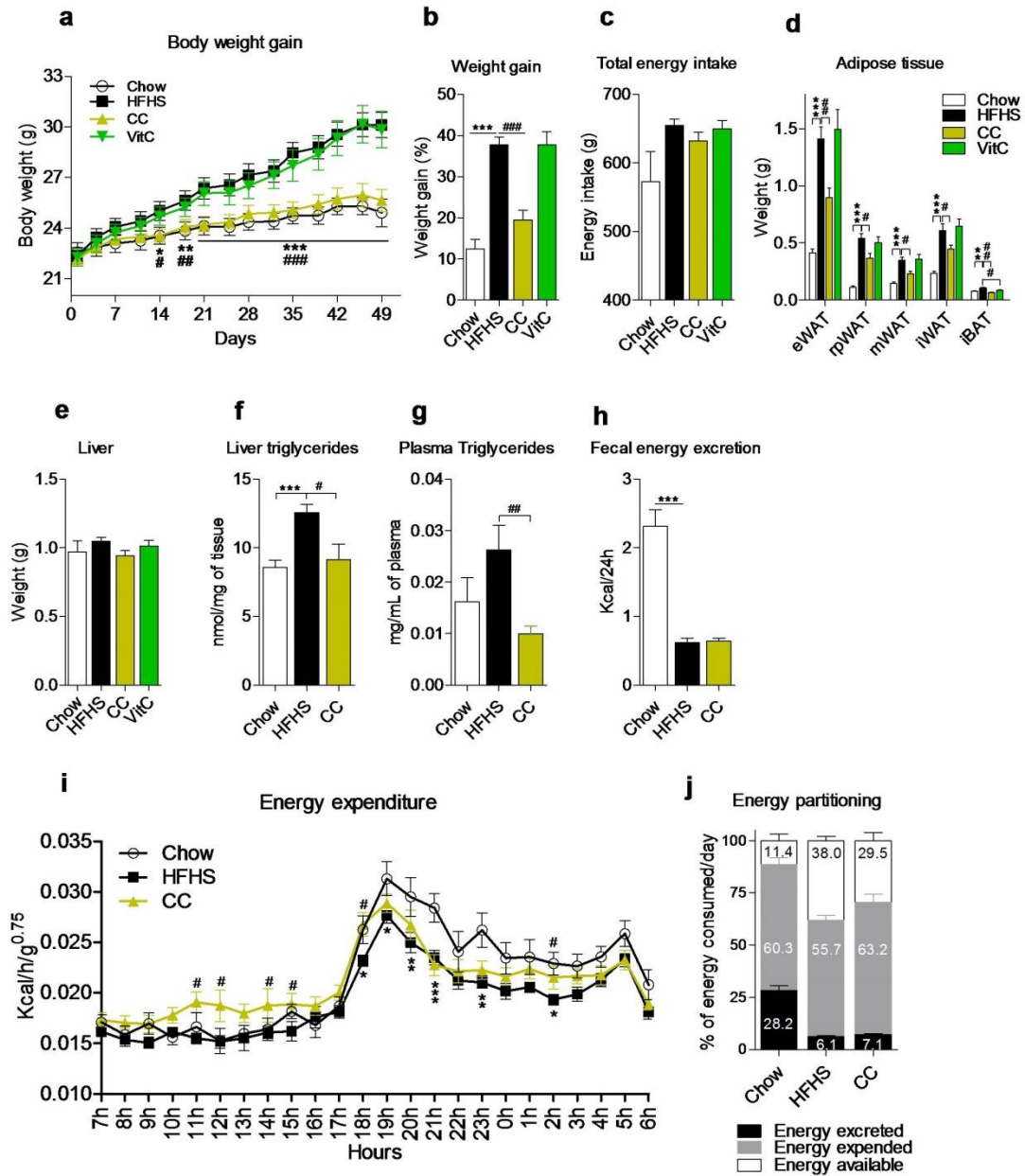
Figure 2: CC blunts adipose tissue inflammation, alleviates metabolic endotoxemia and improves glucose homeostasis in DIO-mice.
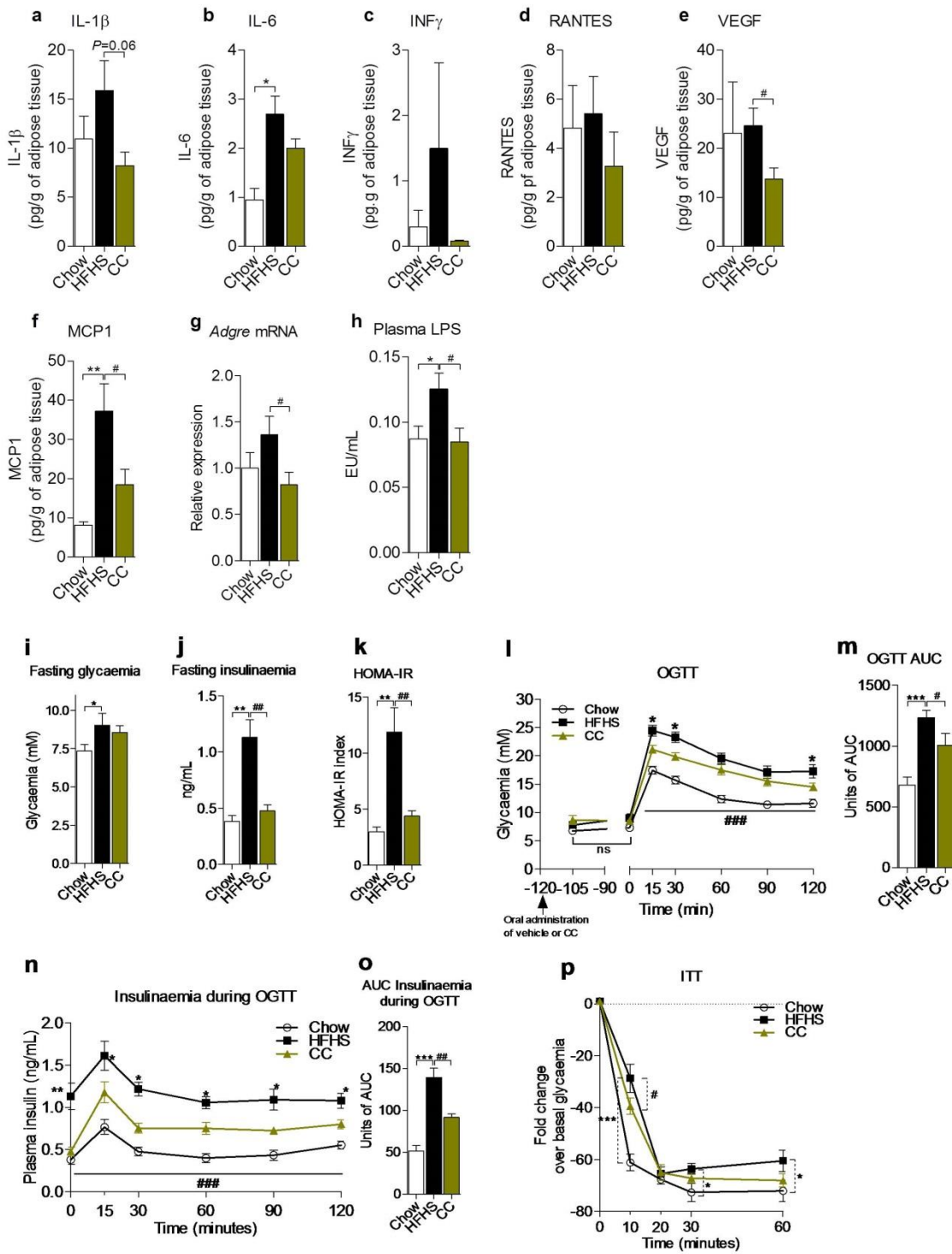
Figure 3: CC prevents obesity-driven gut microbiota dysbiosis in HFHS-fed mice.
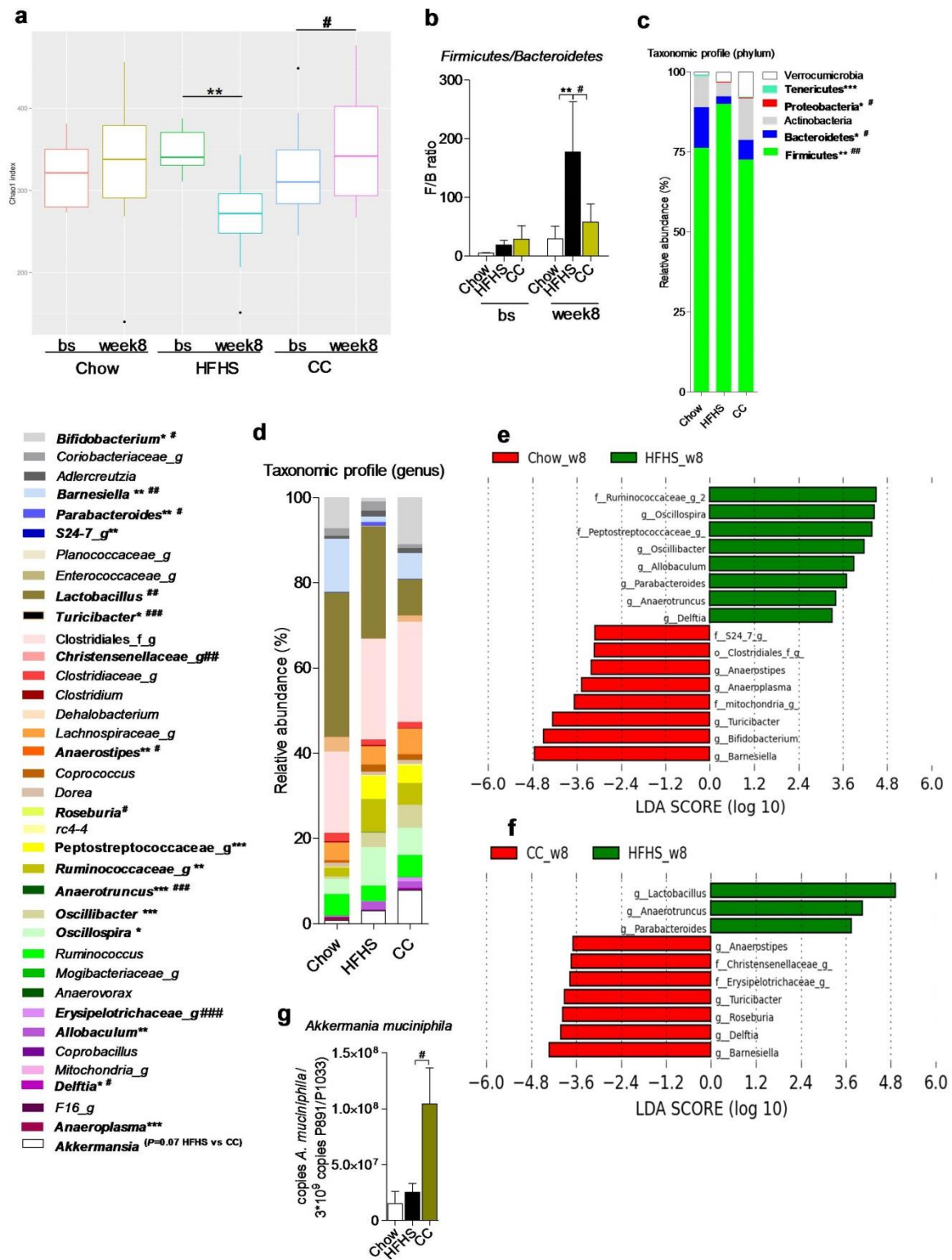
Figure 4: CC administration alters bile acid pool size and composition and upregulates the mRNA expression of genes involved in thermogenesis.
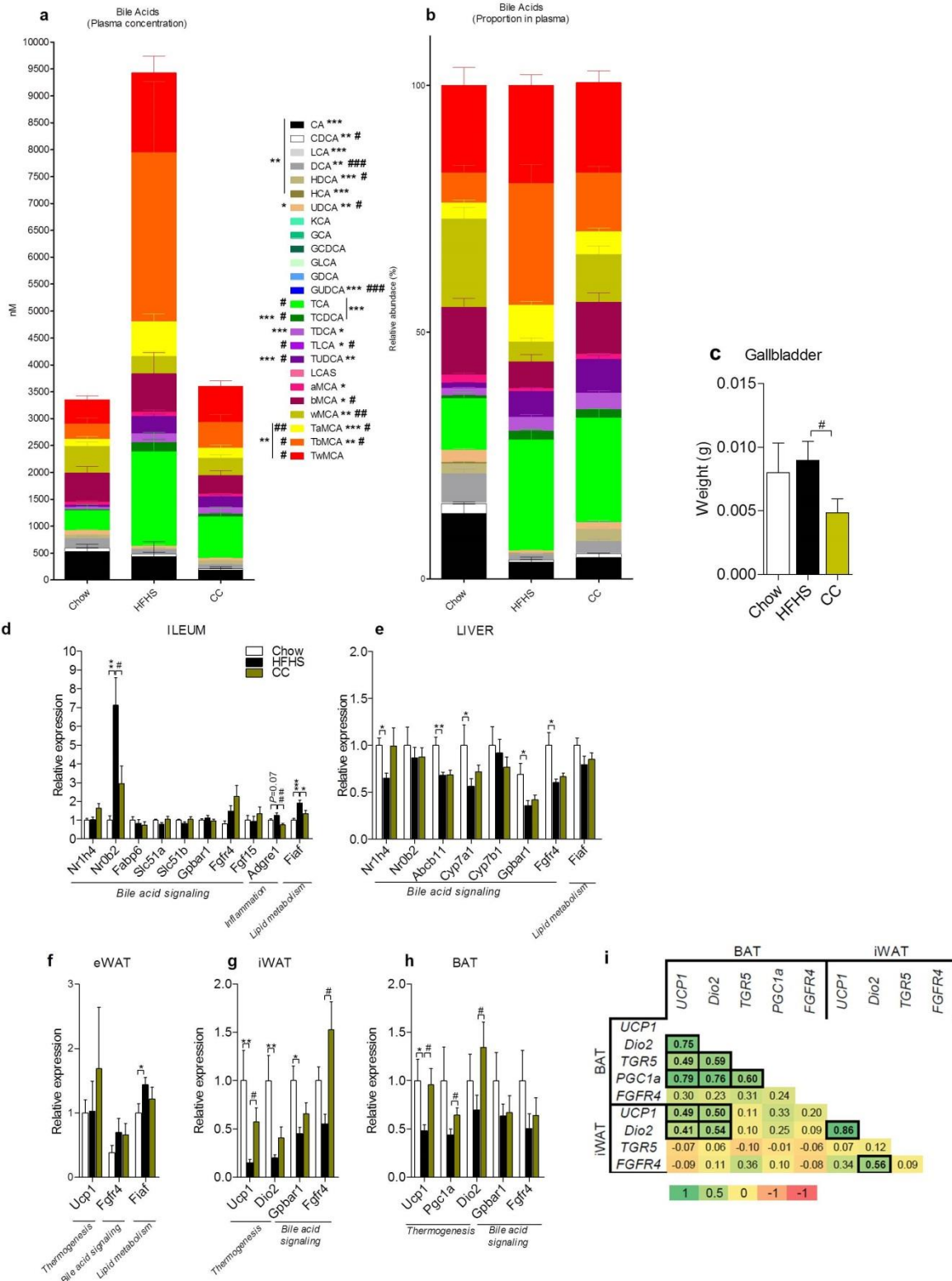
Figure 5: Reconstitution of germ-free mice with the fecal microbiota of CC-treated mice recapitulates the effects of CC administration on weight gain and energy expenditure.
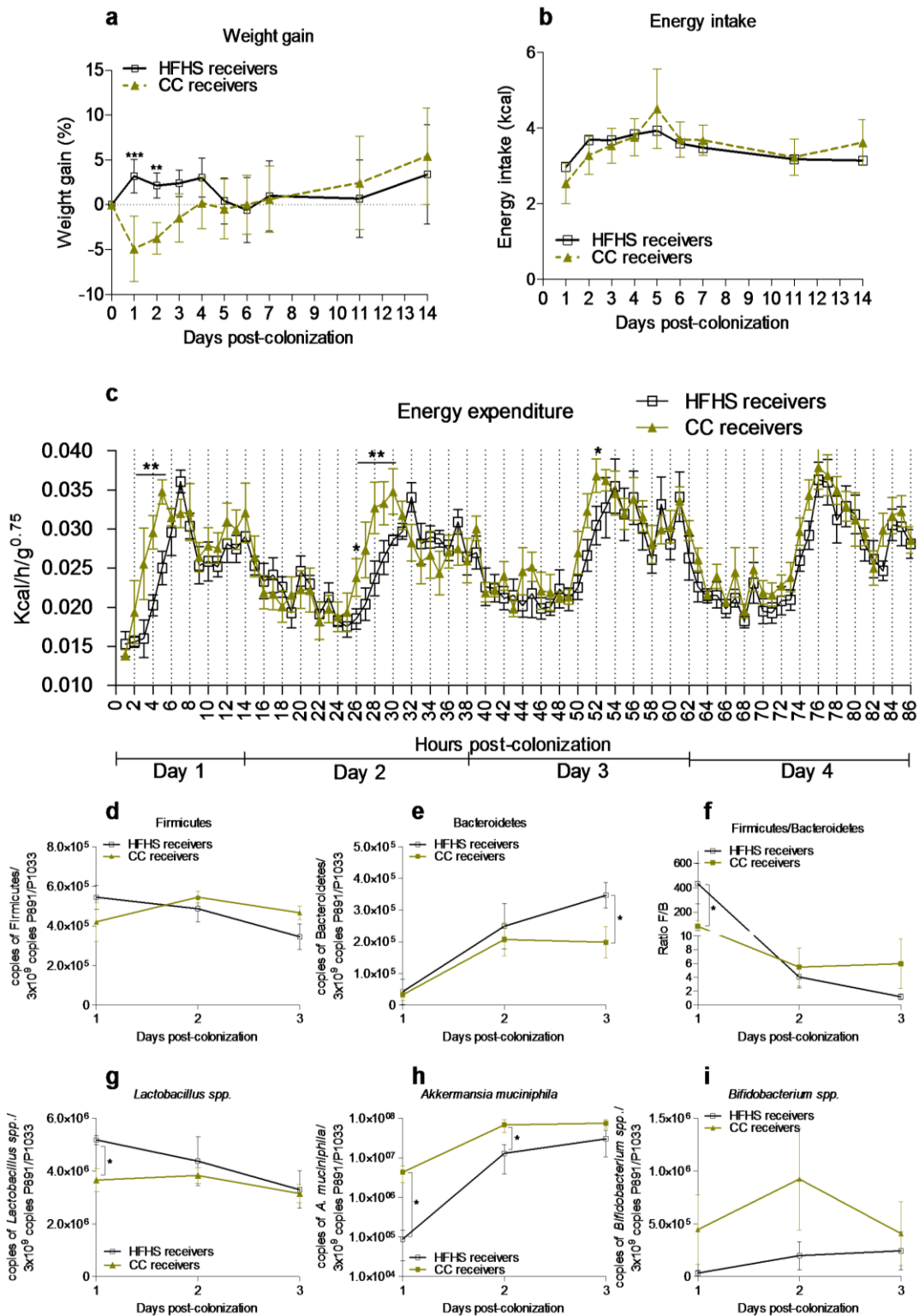
Supplemental material

Supplemental Figure 1: Tissue weight and metabolic features. Weight of (a) gastrocnemius, (b) pancreas, (c) heart and (d) caecum content. Length of the (e) small intestine and (f) colon. (g) Oxygen consumption; (h) carbon dioxide production. The relationship between metabolic rate and body mass was normalized by using the metabolic body size (*ie*, body mass$^{0.75}$). (i) Respiratory exchange ratio (CO_2 exhaled/O_2 inhaled). (j) Grooming/scratching, (k) horizontal locomotion and (l) rearing activity. Data are expressed as the mean ±SEM. (a-f) One-way ANOVA with a Student-Newman-Keuls post hoc test. (g-l) Two-way repeated measures ANOVA with a Student-Newman-Keuls post hoc test was used to calculate the significance of the differences between time points. *$P< 0.05$, **$P< 0.01$ and ***$P< 0.001$ for Chow *vs* HFHS; #$P< 0.05$, ##$P< 0.01$ and ###$P< 0.001$ for HFHS *vs* CC.

Supplemental Figure 2: Improved morphology and alleviated inflammatory features in the visceral adipose tissue of CC-treated mice. (a,b,c) Representative images of epididymal white adipose tissue (eWAT) histological sections from chow-fed (Chow, n=4), high fat/high sucrose-fed (HFHS, n=4) and high fat/high sucrose-fed CC treated (CC, n=4) mice were prepared in order to evaluate tissue morphology and immunostained against F4/80 to assess the profile of macrophage infiltration. (d) Adipocyte distribution; (e) average adipocyte size, (f) crown-like structure (CLS) density. Data are expressed as the mean ±SEM. Significance was calculated between Chow *vs*. HFHS and HFHS *vs*. CC using an unpaired two-tailed Student's t-test *$P< 0.05$, **$P< 0.01$ and ***$P< 0.001$ for Chow *vs* HFHS; #$P< 0.05$, ##$P< 0.01$ and ###$P< 0.001$ for HFHS *vs* CC.

Supplemental figure 3: Plasma bile acid profile. (a) Concentration and (b) relative proportion of primary and secondary bile acids in plasma. (c) Concentration and (d) relative proportion of conjugated and unconjugated bile acids in plasma. Data are expressed as the mean ±SEM. Significance of the differences between groups was calculated using unpaired two-tailed Student's t-test. *$P< 0.05$, **$P<$

0.01 and ***$P<$ 0.001 for Chow *vs* HFHS; [#]$P<$ 0.05, [##]$P<$ 0.01 and [###]$P<$ 0.001 for HFHS *vs* CC.

Supplemental Figure 4: Metabolic and gut microbial features of germ-free mice reconstituted with the fecal microbiota of HFHS-fed vehicle-treated or CC-treated mice. Germ-free mice were reconstituted either with the fecal slurry of high fat/high sucrose (HFHS)-fed vehicle-treated mice (HFHS receivers, n=7) or CC-treated mice (CC receivers, n=7) and kept on a low-fat diet in metabolic cages during the initial days post-colonization. Mice were later transferred into sterile cages and kept on a low-fat diet and under specific pathogen-free (SPF) conditions. (a) Energy output through the feces (kcal/day); (b) fecal energy excretion (% of energy consumed); (c) oxygen consumption; (d) carbon dioxide production. The relationship between metabolic rate and body mass was normalized by using the metabolic body size (*ie*, body mass$^{0.75}$). (e) Respiratory exchange ratio (*ie*, CO_2 exhaled/O_2 inhaled). (f) Grooming/scratching, (g) horizontal locomotion and (h) rearing activity. (i-k) Quantification of taxa by qPCR in the fecal microbiota of HFHS and CC receivers. Data are expressed as the mean ±SEM. Two-way repeated measures ANOVA with a Student-Newman-Keuls post hoc test was used to calculate the significance of the differences between time points. *$P<$ 0.05, **$P<$ 0.01 and ***$P<$ 0.001.

Supplemental Figure 1: Tissue weight and metabolic features.

Supplemental Figure 2: Improved morphology and alleviated inflammatory features in the visceral adipose tissue of CC-treated mice.

Supplemental Figure 3: Plasma bile acid profile.

a

Primary/Secondary Bile acids
(Plasma concentration)

b

Primary/Secondary Bile acids
(Proportion in plasma)

c

Conjugated/Unconjugates Bile Acids
(Plasma concentration)

d

Conjugated/Unconjugated Bile Acids
(Proportion in plasma)
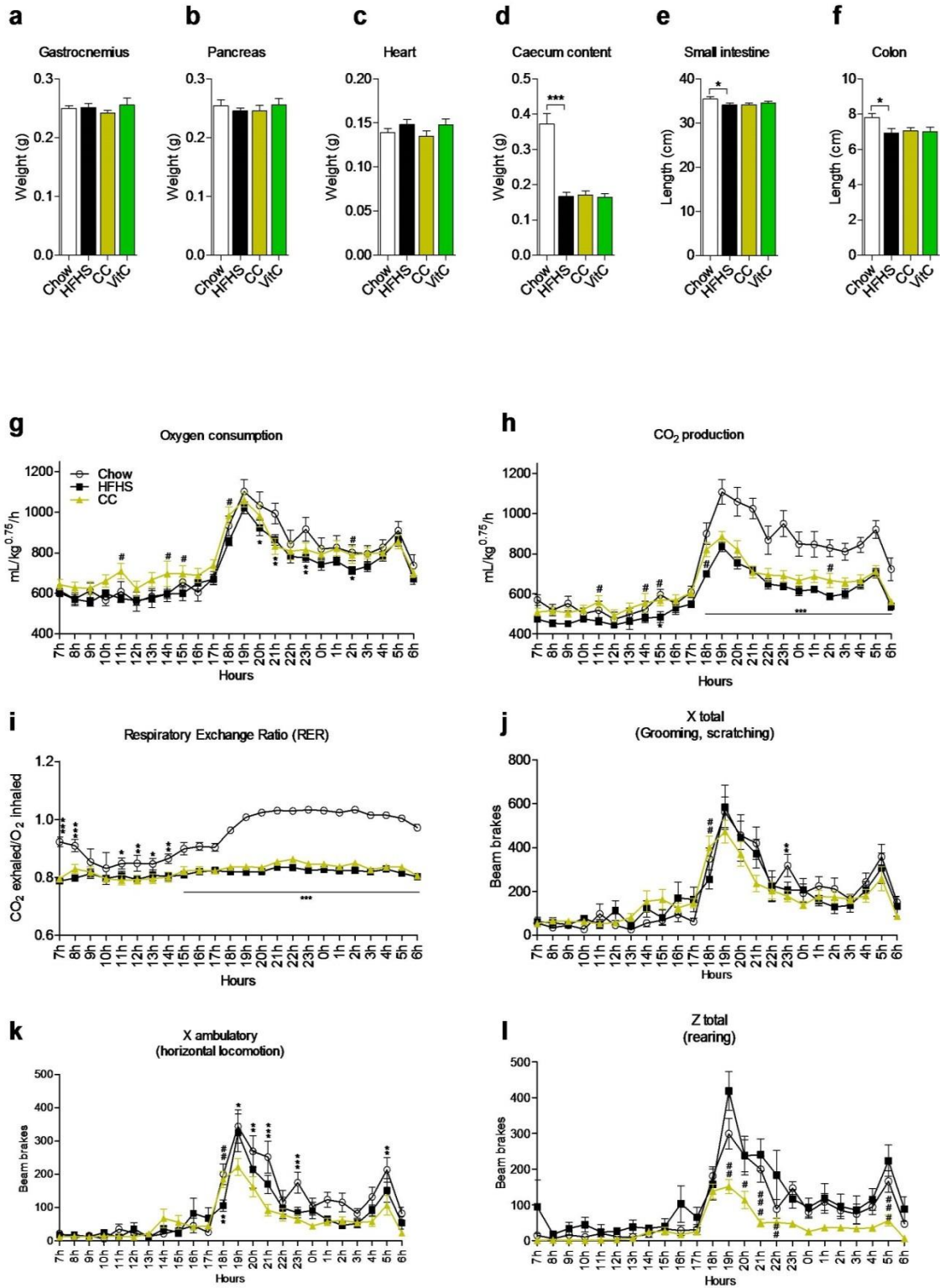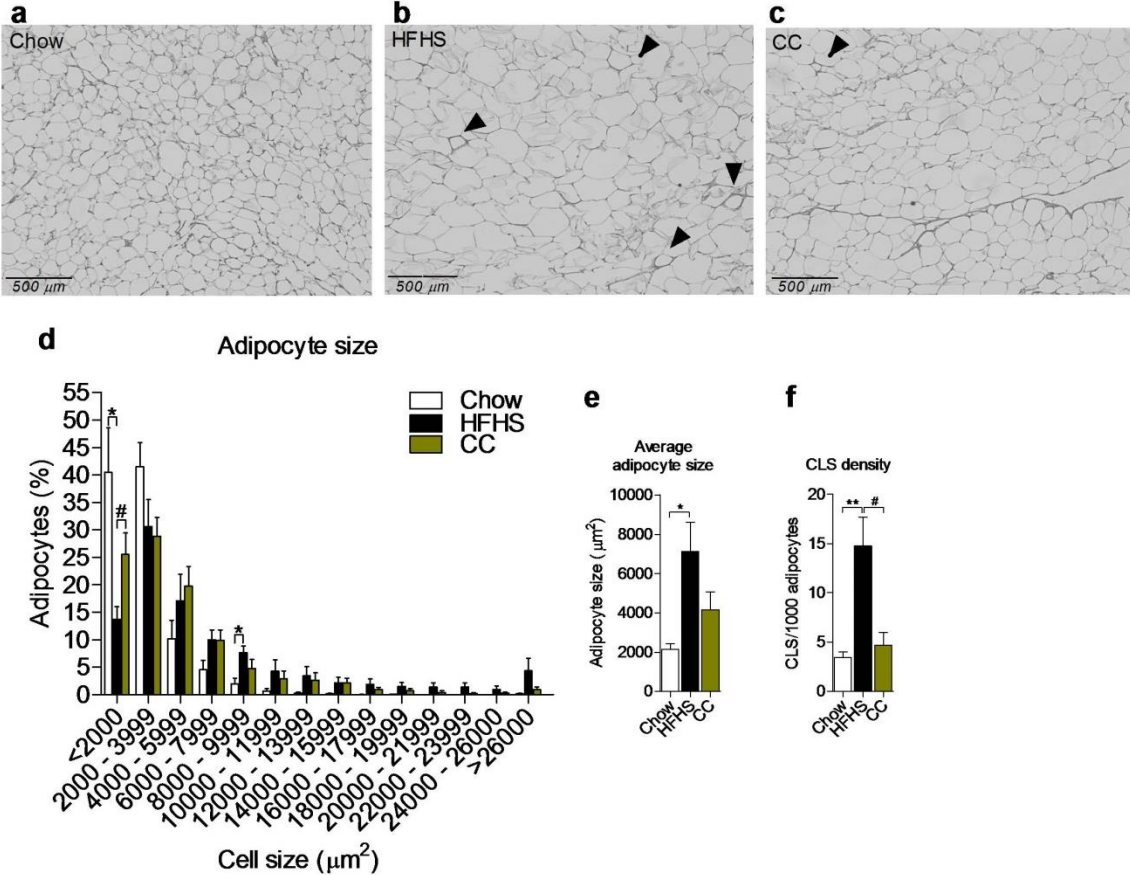
Supplemental Figure 4: Metabolic and gut microbial features of germ-free mice reconstituted with the fecal microbiota of HFHS-fed vehicle-treated or CC-treated mice.
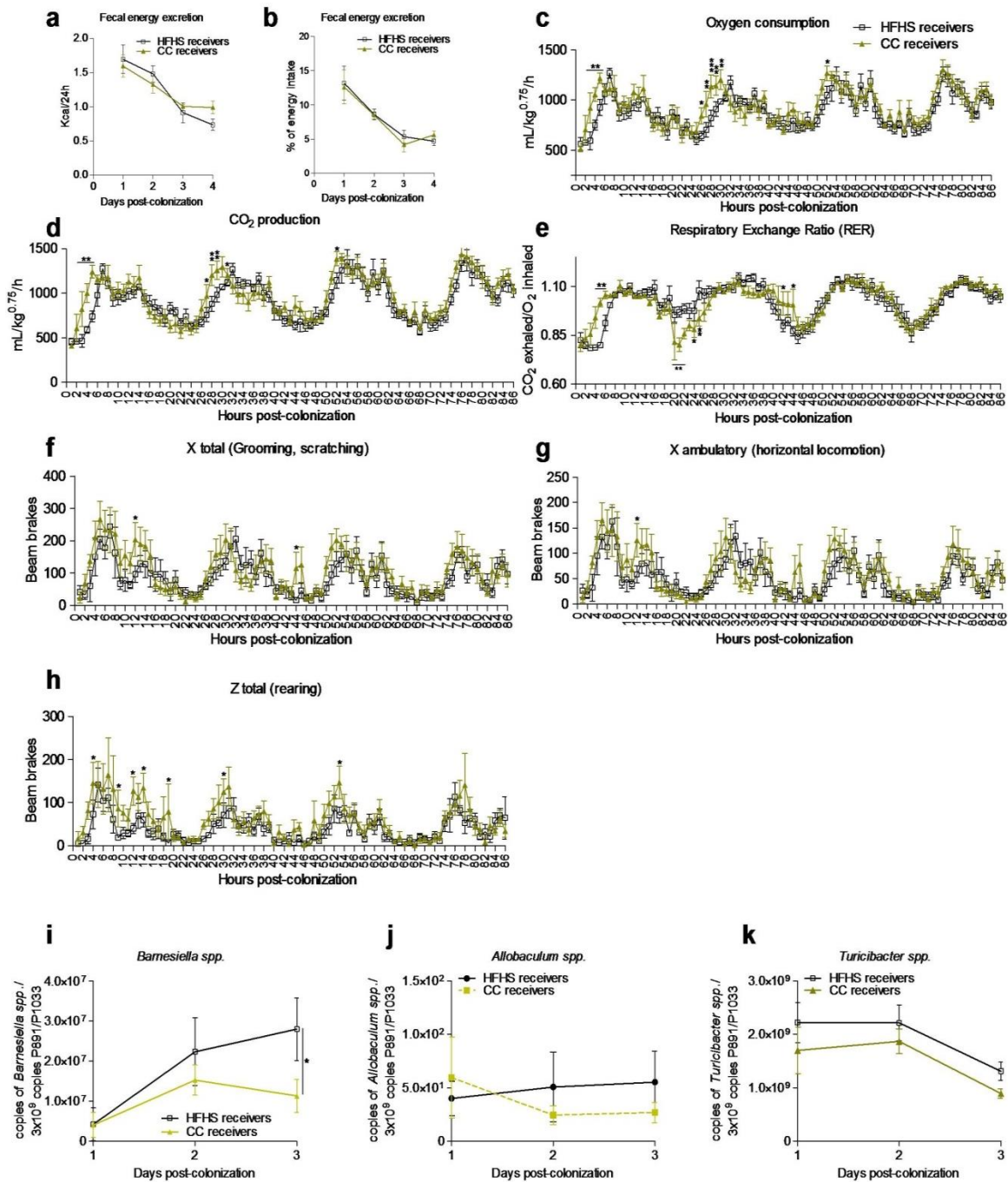
Supplemental tables

Supplemental Table 1: Composition of the diets.

	Chow diet (Teklad 2018, HARLAN)		HFHS diet	
Ingredients (g/100g)	Crude protein	19	Casein high nitrogen	20
	Fat (Soybean oil)	6.2	L-cysteine	0.18
	Carbohydrate	44	Sucrose FCC	26.9
	Crude fiber	3.5	Alphacel non nutritive bulk	5
	Insoluble fiber	15	Mineral mix	6.7
	Ash	5.3	Vitamin mix	1.4
			Lard	19.8
			Corn oil	19.8
			Choline bitartrate	0.2
			Tert-butylhydrytoluene (BHT)	0.03
Composition (kcal%)				
Protein		24		15
Carbohydrates		58		19.6
Lipids		18		65.4
Energy Density (kcal/g)		3.1		5.4

Supplemental Table 2: Primer sequences.

Gene/Taxa	Forward	Reverse
Syber Green		
Actb	CTCTAGACTTCGAGCAGGAG	AGAGTACTTGCGCTCAGGAG
Nr1h4	CTGAGACTGGGTACCAGGG	CCATTCGCGGCTTCTTTGTC
Nr0b2	ACGATCCTCTTCAACCCAGA	AGGGCTCCAAGACTTCACAC
Fabp6	GGTCTTCCAGGAGACGTGAT	ACATTCTTTGCCAATGGTGA
Slc51a	TGTTCCAGGTGCTTGTCATCC	CCACTGTTAGCCAAGATGGAGAA
Slc51b	GATGCGGCTCCTTGGAATTA	GGAGGAACATGCTTGTCATGAC
Gpbar1	CTGCTGGCTGCTTCTTCC	CACTGCCATGTAGCGTTCC
Fgfr4	GTACCCTCGGACCGCGGCACATAC	GCCGAAGCTGCTGCCGTTGATG
Fgf15	GAGGACCAAAACGAACGAAATT	ACGTCCTTGATGGCAATCG
Abcb11	AAGCTACATCTGCCTTAGACACAGAA	CAATACAGGTCCGACCCTCTCT
Cyp7a1	AGCAACTAAACAACCTGCCAGTACTA	GTCCGGATATTCAAGGATGCA
Cyp7b1	TGAGGTTCTGAGGCTGTGCTC	TCCTGCACTTCTCGGATGATG
Fiaf	CAATGCCAAATTGCTCCAATT	TGGCCGTGGGCTCAGT
Pgc1a	CTGAGACCCTCGGGGAAC	AAACGTCAGTTCACAGGGAAG
Ucp1	ACTGCCACACCTCCAGTCATT	CTTTGCCTCACTCAGGATTGG
Dio2	GTCCGCAAATGACCCCTTT	CCCACCCACTCTCTGACTTTC
891F/1033R	TGGAGCATGTGGTTTAATTCGA	TGCGGGACTTAACCCAACA
Firmicutes	CTGATGGAGCAACGCCGCGT	ACACYTAGYACTCATCGTTT
Bacteroidetes	CCGGAWTYATTGGGTTTAAAGGG	GGTAAGGTTCCTCGCGTA
Lactobacillus	TGGAAACAGRTGCTAATACCG	GTCCATTGTGGAAGATTCCC
Bifidobacterium	TCGCGTCYGGTGTGAAAG	CCACATCCAGCRTCCAC
Barnesiella	CCAAGTCGCGTGAAGGAAGA	ACGGAGTTAGCCGATGCTTT
Turicibacter	CCGCGGTAATACGTAGGTGG	ACGCATTTCACCGCTACACA
Allobaculum	TTATGGCCTGGGCTACACAC	TTCTCGGATTGGCTTGCCTT
Akkermansia muciniphila	CAG CAC GTG AAG GTG GGG AC	CCT TGC GGT TGG CTT CAG AT
TaqMan		
Actb	Mm01205647_g1	
Nos2	Mm00440483_m1	
Adgre1	Mm00802529_m1	

Supplemental methods

Glucose homeostasis. At week 6, mice were fasted for 6 hours and insulin tolerance tests (ITT) were performed after intraperitoneal injections of insulin (0.75 UI/kg body weight). Glycemia was measured with an Accu-Check glucometer (Bayer) before (0 min) and after (10, 20, 30, 60 and 90 min) insulin injection. At the end of week 7, mice were fasted overnight (12 h) and subjected to oral glucose tolerance test (OGTT, 1 g of glucose/kg body weight). Blood was collected before (0 min) and after (15, 30, 60, 90 and 120 min) glucose challenge for glycemia determination. Blood samples (~30µL) were collected at each time point during OGTT for insulinaemia determination. The homeostasis model assessment of insulin resistance (HOMA-IR) index was calculated based on the following formula: fasting insulinemia (µUI/mL) x fasting glycemia (mM)/22.5.

Analytical methods. Plasma insulin was assessed using an ultra-sensitive ELISA kit (Alpco, USA). *Liver triglyceride* (TG) was measured after chloroform-methanol extraction and enzymatic reactions with a commercial kit (Randox Laboratories, Crumlin, UK). *Chemokines and cytokines* were quantified in 25 µl of adipose tissue lysates (50 ug of protein in PBS containing 1% NP-40) using a Milliplex MAP kit (Millipore). *Plasma endotoxin (LPS)* concentration was determined using a kit based on a Limulus amebocyte extract (LAL kit endpoint-QCL1000, Lonza, USA). Samples were diluted in endotoxin-free water (Charles River, USA) and incubated at 70 °C for 15 minutes to overcome assay inhibition. Plasma bile acids were assessed as previously described (414).

RNA extraction and qPCR analysis. Sections of the ileum (approximately 0.5 cm) were homogenized in 1 ml of TRIzol reagent (Thermo Fisher Scientific) using a power homogenizer (Polytron). Freeze-powdered liver, inguinal white adipose tissue, epididymal white adipose tissue and interscapular brown adipose tissue were homogenized in 1 ml of TRIzol reagent in a bead beater. Total RNA purification was performed using a RNeasy mini kit (Qiagen). Total RNA was used for cDNA synthesis with a reverse transcription PCR kit (Applied

Biosystems). Real-time PCR was performed using the SYBR Green Jump-Start Gene Expression Kit (Sigma) with 1:25 diluted cDNA products from the reverse transcription. Gene expression was assessed by the $\Delta\Delta_{Ct}$ method and Actin was used as the reference gene. Primer sequences are available in supplemental table 2.

Fecal sample processing. Fecal samples were freshly collected at baseline and week 8 and immediately stored at -80 °C. Bacterial genomic DNA was extracted from approximately 50 mg of fecal material. Samples were resuspended in lysis buffer containing 20 mg/ml lysozyme and incubated for 30 minutes at 37°C. Further lysis was performed by adding 10% SDS and proteinase K to 350 µg/ml followed by incubation for 30 minutes at 60°C. Samples were homogenized using a bead beater and 0.1mm zirconium beads and then processed using a DNA extraction kit (DNeasy, Qiagen). DNA yield was assessed using a NanoDrop ND-1000 spectrophotometer (Thermo Scientific). Extracted DNA was stored at -20 ºC until further use. Each DNA sample was subsequently used for 16S amplification of the V3-V4 region using the primers 341F (5'-CCTACGGGNGGCWGCAG-3') and 805R (5'-GACTACHVGGGTATCTAATCC-3') adapted to incorporate the transposon-based Illumina Nextera adapters (Illumina, USA) and a sample barcode sequence allowing multiplexed paired-end sequencing. The amplification mix contained 1X Q5 buffer (NEB), 1X Q5 Enhancer (NEB), 200 µM dNTP (VWR International, Canada), 0.2 µM of forward and reverse primers (Integrated DNA Technologies, USA), 1 U of Q5 (NEB) and 1 µL of template DNA in a 50 µL reaction. Cycling condition was as follows: denaturation (30 s at 98°C), followed by a first set of 15 cycles (98°C for 10 s, 55°C for 30 s and 72°C for 30 s), then by a second step of 15 cycles (98°C for 10 s, 65°C for 30 s and 72°C for 30 s) and final elongation (2 min at 72°C).

Constructed 16S metagenomic libraries were purified using 35 µL of magnetic beads (AxyPrep Mag PCR Clean up kit; Axygen Biosciences, USA) per 50 µL PCR reaction. Library quality control was performed with a Bioanalyzer 2100 using DNA 7500 chips (Agilent Technologies, USA). An equimolar pool was

obtained and checked for quality prior to further processing. The pool was quantified using picogreen (Life Technologies, USA) and loaded on a MiSeq platform using 2 x 300 bp paired-end sequencing (Illumina, USA). High-throughput sequencing was performed at the IBIS (Institut de Biologie Intégrative et des Systèmes - Université Laval).

16S rRNA gene-based gut microbial analysis. Generated and demultiplexed sequences were analyzed using the QIIME software package (version 1.9.1). Paired-end sequences were merged with at least a 50-bp overlap. Resulting sequences containing ambiguous or low quality reads (Phred score ≤ 25) were removed from the dataset. Forward and reverse primers were trimmed from the filtered sequences; reads with at least one reverse primer mismatch or where the reverse primer was not found were discarded. Chimera checking and filtering was performed using UCHIME (4). OTU (Operational Taxonomic Units)-picking from post-filtering reads was performed using USEARCH 61 version 6.1.544 with an open-reference methodology, which consisted of clustering sequences *de novo* at 97% identity threshold if they did not hit the reference sequence collection. Representative OTU sequences were assigned taxonomy against the Greengenes reference database (August 2013 release) using the RDP-classifier. Singleton OTUs and OTUs with a number of sequences < 0.005% of total number of sequences were discarded at this step. A subsampling depth of 3159 reads (smallest amount of sequences originally found among our metagenomic samples) was chosen to rarefy the OTU tables used in the downstream analyses. Unclassified OTUs at the genus level against Greengenes were further investigated with the RDP classifier against the RDP database (version September 30, 2016) using a minimum bootstrap cutoff of 50%.

Bacterial quantification by qPCR. The presence of specific taxa in the feces of HFHS-receiver and CC-receiver mice was assessed by qPCR as previously described (2). Briefly, copy numbers of Firmicutes, Bacteroidetes, *Lactobacillus spp.*, *Akkermansia muciniphila*, *Bifidobacterium spp.*, *Barnesiella spp.*,

Allobaculum spp. and *Turicibacter spp.* per ng of fecal DNA were calculated on the basis of the *Ct* values obtained using standard curves designed for each taxon. The number of copies of each taxon was then normalized by total bacteria (primer 891F/1033R). Primers were *in silico* designed and tested by Primer-BLAST analysis and their sequences are available in supplemental table 2.

References (supplemental methods)

1. Trottier J, Perreault M, Rudkowska I, Levy C, Dallaire-Theroux A, Verreault M, Caron P, Staels B, Vohl MC, Straka RJ, Barbier O: Profiling serum bile acid glucuronides in humans: gender divergences, genetic determinants, and response to fenofibrate. Clinical pharmacology and therapeutics 2013;94:533-543
2. Riviere A, Gagnon M, Weckx S, Roy D, De Vuyst L: Mutual Cross-Feeding Interactions between Bifidobacterium longum subsp. longum NCC2705 and Eubacterium rectale ATCC 33656 Explain the Bifidogenic and Butyrogenic Effects of Arabinoxylan Oligosaccharides. Applied and environmental microbiology 2015;81:7767-7781

Conclusion

The use of a murine model of diet-induced obesity was of great value in order to explore the hypotheses and fulfill the objectives of this thesis. Polyphenols are abundantly present in the human diet, which renders difficult to assess the mechanism of action of specific polyphenol-rich extracts in human cohorts. Furthermore, murine models allow controlling dietary intake and treatment more accurately, which results in a more precise isolation of variables and in a more comprehensive mining of novel mechanisms of action. It is also noteworthy that the variability of the gut microbiota across human populations is extremely high, what would demand larger sample sizes in order to link the metabolic benefits of dietary polyphenols to changes in the gut microbiota. On the other hand, the gut microbiota of specific pathogen free inbred mice or rats is more homogenous, which eases the investigation of the trialogue dietary polyphenols-gut microbiota-host metabolism.

The studies presented in chapters I, II, III and IV support clear metabolic benefits of polyphenol-rich extracts to the detrimental consequences of diet-induced obesity (Table 1). The comprehensive analysis of the results presented throughout the four chapters of this thesis leads to the conclusion that the extent of these metabolic improvements was dependent on (*i*) the total amount of polyphenols present in the extracts, (*ii*) the polyphenolic signature of the extracts and (*iii*) the intensity of the diet-induced metabolic damage. When HFHS-fed mice were preventively treated with the cranberry (CE) or the camu camu (CC) extracts (*i.e.*, HFHS diet and treatment started concomitantly), visceral obesity was prevented in association with blunted metabolic endotoxemia and alleviated insulin resistance (chapters I and IV, Table 1, Figure 1). It is noteworthy that CE is extremely concentrated in polyphenols (37g of polyphenols/100g of extract), whereas CC, for being a raw extract, possess a more diverse repertoire of phytonutrients and complex polysaccharides in addition to a considerable abundance of polyphenols (6.5 g of polyphenols/100g of extract) (Table 2). Interestingly, while CE administration did not reverse diet-induced obesity, its

administration was associated with alleviated intestinal inflammation, metabolic endotoxemia, hepatic steatosis and insulin resistance, indicating that the positive metabolic effects of CE are obesity-independent in a reversal context (chapter II, Table 1, Figure 1). Similarly, the extracts of alpine bearberry, cloudberry and lingonberry improved insulin resistance, liver homeostasis and gut physiology without significantly affecting fat mass accretion when preventively administered to HFHS-fed mice (chapter III, Table 1, Figure 1).Overall it was observed that, when the effect of the polyphenol-rich extracts was toned down, either by an increase in the metabolic damage (chapter II) or by lower doses of polyphenols (chapter III), visceral fat mass accretion was unaffected while intestinal inflammation, hepatic homeostasis and insulin resistance remained improved (Figure 1, Table 1). Thus, taken together, the observations made in chapters I, II, III and IV suggest that polyphenols primarily act on the gut-liver axis to improve features of the metabolic syndrome in diet-induced obese mice. This is in agreement with the notion that diet-induced metabolic derangements are initiated by imbalanced intestinal homeostasis (146, 156, 157), which results from the primordial interaction between diet, gut microbes and enteric immune system (14, 146, 147). In the first months of my doctorate, I conducted studies that compared the effect of the daily administration of various polyphenolic-rich berry extracts on features of the metabolic syndrome in diet-induced obese mice. Prevention of hepatic triglyceride deposition was a major finding for almost all the berry extracts tested (Figure 2), which clearly corroborates the notion that polyphenols importantly target the gut-liver axis.

	CHAPTER I	CHAPTER II	CHAPTER III			CHAPTER IV
	Cranberry (preventive)	Cranberry (reversal)	Cloudberry	Alpine bearberry	Lingonberry	Camu camu
Weight/Fat mass gain	↓	–	–	–	–	↓
Instestinal inflammation/ Circulating LPS	↓		↓	↓	↓	↓
Hepatic steatosis	↓		↓	↓	↓	↓
Insulinemia	↓	↓	↓	↓	↓	↓
Glucose intolerance	–	↓	–	–	–	↓
Insulin resistance (Homa-IR)	↓	↓	↓	↓	↓	↓
F/B ratio	–	↓	–	–	–	↓
Main taxonomic features	↑*A. muciniphila*	↑*A. muciniphila,* ↑*Coprobacillus,* ↑ *Barnesiella*	↑*A. muciniphila,* ↑*Turicibacter,* ↑*Peptostreptococcaceae,* ↓*Lactobacillus* ↓*Bifidobacterium*	↑*A. muciniphila* ↑*Oscillibacter*	↑*A. muciniphila* ↑*Turicibacter*	↑*A. muciniphila* ↑*Bifidobacterium* ↑*Turicibacter* ↑ *Barnesiella* ↓*Lactobacillus*

Table 1: Summary of results.
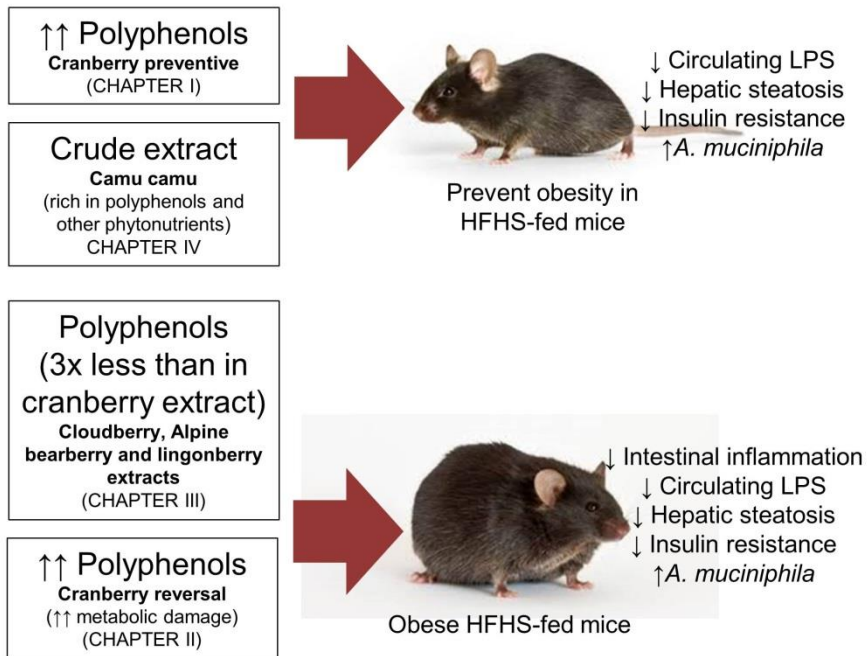
Figure 1: Summary of results
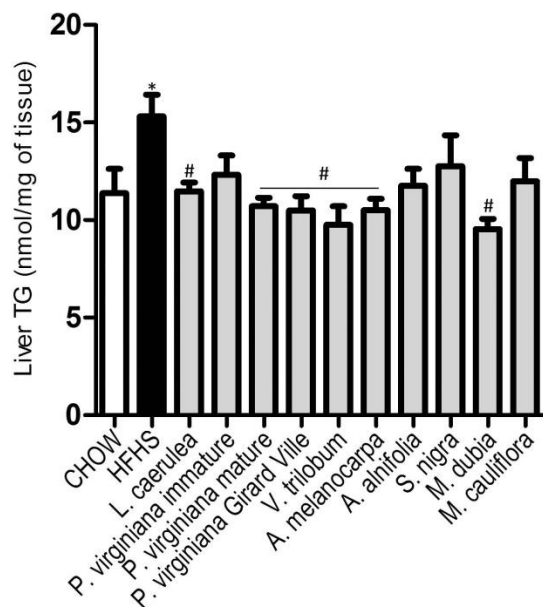
Figure 2: Liver triglyceride (TG) deposition in diet-induced obese mice treated with extracts of eight different berries.

Mice were fed either a HFHS or a normal CHOW diet and orally treated either with water (CHOW, HFHS) or one the berry extracts (200 mg of extract/kg of body weight) every day for 8 weeks. Liver TG (n=5) was extracted using a Folch solution and quantified by means of a specific colorimetric kit. * $P< 0.05$ vs. CHOW; # $P< 0.05$ vs. HFHS. Data are expressed as the mean ±SEM.

Another important observation is that the most efficient extracts against obesity and insulin resistance were rich in condensed or hydrolysable tannins (*i.e.*, proanthocyanidins and ellagitannins, respectively), which put forward these classes of polyphenols as promising molecules to fight obesity-related diseases through a targeted effect on the gut-liver axis (Table 3). Concordantly, the anti-inflammatory effect of cranberry proanthocyanidins have been demonstrated in human intestinal cell lines, with the high molecular weight fraction showing the more pronounced effects (416). This suggests that the pre-absorptive properties of this polyphenolic class have important impact *in vivo*. Indeed, in a recent report, Masumoto *et al*. showed that non-absorbable apple proanthocyanidins prevented diet-induced obesity in mice, which was associated with marked alleviation of intestinal inflammation and metabolic endotoxemia (417). The authors also confirmed the superiority of high molecular weight proanthocyanidins against features of the

metabolic syndrome, albeit oligomeric proanthocyanidins were also beneficial (417). Ellagitannins are another promising class of polyphenols pointed out in this thesis; however, the well-established health benefits of ellagitannins to humans (418) and animal models (419, 420) seems distinct from that of proanthocyanidins as ellagitannins' bioactivity is at least in part dependent on its gut microbial hydrolysis (yielding the monomer ellagic acid) and processing of ellagic acid into urolithins (421). In fact, as urolithin A is involved in mitophagy and prolonged lifespam in *C. elegans* (422), ellagic acid administration has been shown to improve metabolic health in HFHS-fed rats (423), suggesting that both molecules may be relevant to improve features of the metabolic syndrome. Altogether, these data support the observation made herein that proanthocyanidins and ellagitannins are promising polyphenolic subclasses against obesity-linked metabolic diseases. The findings presented in this thesis also pave the way for further research using polyphenolic fractions concentrated in these two polyphenolic subclasses in order to better understand their mode of action and unravel novel therapeutic targets to fight the metabolic syndrome. It is noteworthy that one third of the top twenty most prescribed drugs are plant-derived (424). For instance, Metformin (the most widely prescribed antidiabetic drug) and Aspirin (the prototypical nonsteroidal anti-inflammatory agent), are derived from French lilac (*Galega officinalis*) and the willow tree (*Silax spp*) bark, respectively.

	CHAPTERS I,II		CHAPTER III		CHAPTER IV
	Cranberry	Cloudberry	Alpine bearberry	Lingonberry	Camu camu
Total polyphenols (g/100g)	37.4	1.51	7.08	4.23	6.5
Anthocyanins (g/100g)	3.3	0.04	1.79	1.86	n.d.
Flavanols/ Flavonols (g/100g)	9.4	0.26	0.39	0.005	0.11
Ellagic acid (g/100g)	0.23	0.01	0.001	0.01	0.044
Ellagitannins (g/100g)	?	0.27	0.26	n.d.	0.45
Proantho cyanidins (g/100g)	10.0	0.084	1.497	2.121	n.d.

Table 2: Polyphenolic profile of the extracts of cranberry, cloudberry, alpine bearberry, lingonberry and camu camu.

The results presented in this thesis strongly support an association between changes in the gut microbiota and the beneficial effects of polyphenol-rich extracts on obesity and insulin resistance. In line with this evidence, a recent metagenome-wide association study has shown a strong relationship between the dietary intake of polyphenol-rich foods and higher gut microbial diversity (425). We have shown that expansion of *A. muciniphila* is a major gut microbial response to the introduction of dietary polyphenols to the gut lumen and, given the well-established positive role of this bacterium (164, 167), it possibly contributes to improve host metabolism. The findings described in chapter I were the first *in vivo* demonstration that a polyphenol-rich cranberry extract markedly alleviated several features of the metabolic syndrome in parallel to a drastic bloom of *A. muciniphila* in the gut microbiota. After the publication of this work, several authors showed similar findings using polyphenolic extracts of pomegranate (426), table grape (427),

concord grape (428), rhubarb (429), lingonberry (430) as well as non-absorbable apple proanthocyanidins (417) and caffeic acid (431). We have confirmed the expansion of *A. muciniphila* in lingonberry-treated mice (chapter III) and extended this finding to mice treated with extracts of alpine bearberry, cloudberry (chapter III) and camu camu (chapter IV). We also demonstrated that transplantation of a fecal microbiota rich in *A. muciniphila* from CC-treated mice to germ-free mice recapitulated the effects of CC administration on energy expenditure, suggesting that *A. muciniphila* is causally involved in regulating the host's energy expenditure. These results are supported by the recent demonstration that *A. muciniphila* controls host response to cold (13, 226).

Pomegranate, grapes and apples, as well as cranberries, camu camu, lingonberries, cloudberries and alpine bearberries are all abundant sources of proanthocyanidins and/or ellagitannins, which may suggest that these polyphenolic subclasses exert a stronger prebiotic effect on *A. muciniphila*. While more studies are warranted to confirm this hypothesis, it is likely that the effect of fruit phytonutrients on *A. muciniphila* is a result of additive or synergistic stimuli arising from various sources as, for example, phenolic acids (431), anthraquinones (429), quercetin (432) and resveratrol (433). Interestingly, resveratrol has also been shown to attenuate diet-induced obesity in association with reduced *A. muciniphila* population, which reveals the need for further investigation in this area. Culturing *A. muciniphila* in the presence of different polyphenols or polyphenolic classes is an interesting perspective to clarify this matter. For instance, Henning *et al.* have demonstrated that *A. muciniphila* can hydrolyze ellagitannins (yielding ellagic acid) and metabolize ellagic acid to an unknown metabolite (426). *In vivo*, it is also possible that polyphenols alter the niche occupied by *A. muciniphila* rather than directly acting on this bacterium. Our observations in this thesis led to the hypothesis that cranberry proanthocyanidins may increase mucus secretion thus creating a favorable environment for *A. muciniphila* to thrive. This is in line with the fact that cranberry proanthocyanidins ameliorated gut barrier integrity by increasing mucus secretion in a murine model of elemental enteral nutrition (434) and that dietary polyphenols were associated with increased mucin levels in the feces of

diet-induced obese rats (435). The putative mechanisms by which polyphenols alter *A. muciniphila* populations are illustrated in figure 3.
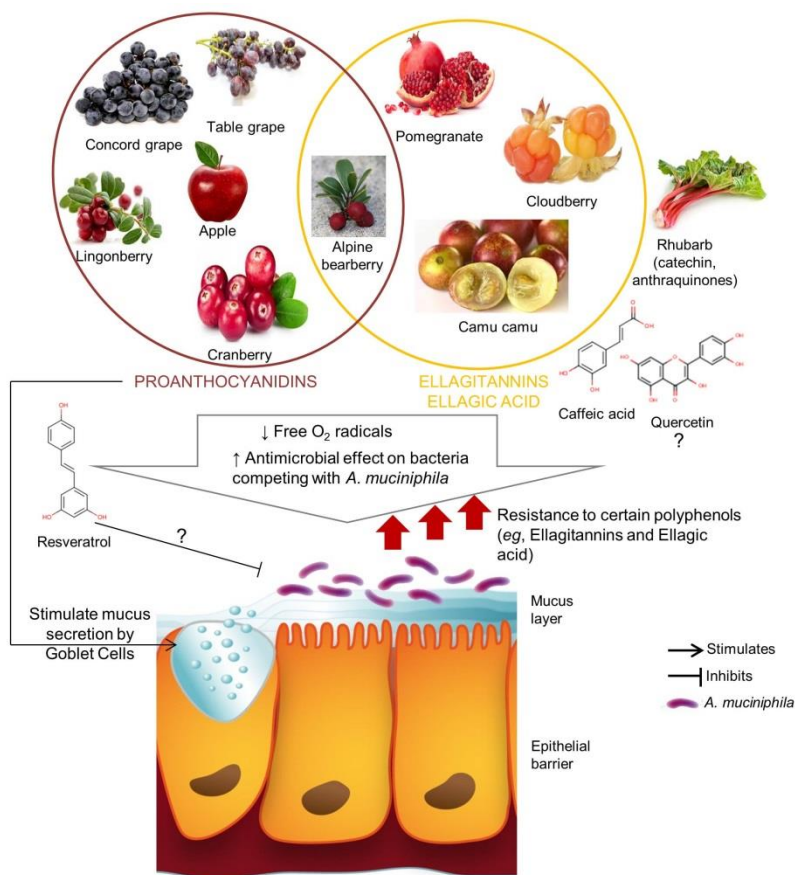
Figure 3: Polyphenol-rich extracts favour expansion of A. muciniphila in the gut microbiota.

Several proanthocyanidin-rich and ellagitannin-rich extracts, as well as caffeic acid and an extract of rhubarb, have been shown to favour expansion of *A. muciniphila* in the gut microbiota. The effect of quercetin and resveratrol on *A. muciniphila* needs further investigation: while administration of the former to rats only tended to increase *A. muciniphila* in fecal samples, the latter was associated with either reduction or expansion of *A. muciniphila*. Possible mechanisms by which polyphenols stimulate the growth of *A. muciniphila* in the gut microbiota involve (*i*) limitation of O_2 availability, which would favour the bloom of strict anaerobes and (*ii*) resistance of *A. muciniphila* to the antimicrobial effect of certain polyphenols. Moreover, proanthocyanidins may trigger mucus secretion by goblet cells, therefore creating a favourable environment for *A. muciniphila* to thrive.

A. muciniphila is deemed beneficial based on correlations between its abundance and specific phenotypes and on the oral administration of this bacterium to animal models. However, the targeted deletion of this bacterium in the

gut microbiota constitutes a promising alternative in order to clarify (*i*) the relevance of this bacterium to host physiology and (*ii*) to which extent this bacterium mediates the positive metabolic effects of polyphenols. Similarly to knocking out a gene in order to understand its function, targeting single species in the gut microbiota would bring the definitive proof of the impact of specific taxa on host physiology. These investigations are part of an ongoing project in collaboration with the group of Dr Sylvain Moineau. In our initial studies, we are currently working on the development of bacteriophages to target *A. muciniphila in vivo*. Because bacteria are highly predominat in the gut, the importance of other microorganims inhabiting our gastro-intestinal tract is considerably overlooked. However, bacteriophages exert major selective pressure on bacteria. Accordingly, the early life dynamics of the gut virome is marked by a transition from a higher to a lower ratio bacteriophages/bacteria (436), suggesting a predator-prey relationship with potential relevance to host metabolism. Indeed, obese mice have increased fecal viral content in comparison to lean mice (437), a trait that parallels to decreased bacterial richness. Investingating whether polyphenols affect the gut bacterial profile by means of altering gut bacteriophage population is a promising research perspective. Interestingly, some polyphenols are thought to exert anti-viral effects (438, 439).

How dietary polyphenols alter the host's response to the gut microbiota is another fertile and promising field of research. The recent demonstration that host intestinal miRNAs shape gut microbial communities (440) and the demonstration that polyphenols can target miRNAs (441, 442) leads to the question: can dietary polyphenols beneficially reshape the gut microbiota by altering host enteric miRNAs? Another interesting perspective involves PRR. Surprisingly, our understanding of how dietary phytonutrients modulate PRR biology is scarce. It has been shown that NLRP6 is necessary for mucus secretion in goblet cells (166), which leads to the hypothesis that the putative activation of the NLRP6-associated inflammasome response by certain phytonutrients may contribute to mucus secretion, therefore creating a favourable environment for *A. muciniphila* to thrive.

In the studies presented herein, the relevance of BAs to the anti-obesity effects of a crude extract of camu camu was proposed (chapter IV). BAs can reach concentrations at the high µM range in the gut lumen, and cycle about six times per day through the enterohepatic circulation (357). In addition to the great potential of BAs to modify the gut microbiota, BAs are important modulators of glucose and energy homeostasis (443), which highlight their relevance as major mediators in the dialogue gut microbiota-host. The findings presented in chapter IV suggest that camu camu phytonutrients increase the circulating levels of unconjugated secondary BAs, which seems relevant to enhance BAT activity. An interesting perspective of research is based on the putative link between higher secondary BAs and GLP1/2 production. Intestinal GLP 1/2-producing cells express the BA receptor TGR5, whose main ligands are secondary BA and whose activation enhances GLP1/2 secretion (444). GLP1/2 are therefore well-positioned as a promising mechanistic link between polyphenols, gut microbiota and BAs. This is particularly interesting because GLP1/2 regulate several aspects of metabolic health, such as intestinal permeability, satiety and glucose homeostasis (180, 445, 446). How BAs contribute to alter microbial populations in polyphenol-treated animals also warrants further investigation. For instance, it is currently unknown how *A. muciniphila* responds to the presence of BAs.

It is important, however, to acknowledge the limitations of the studies presented in this thesis. The relationship between the metabolic benefits of dietary polyphenols and changes in the gut microbiota was demonstrated, however further analysis with the extracts studied in chapters I, II and II are necessary to address causation. Moreover, although the use of PICRUSt enabled the prediction of functional alterations in the gut microbiome from the analysis of 16S rRNA-gene sequences, whole metagenomic shotgun sequencing would provide a better idea of microbial pathways altered after the intake of polyphenols. Finally, it is important to emphasize that the fecal microbiota does not represent the totality of the microbial populations living in the intestine. Different microbial communities colonize specific niches across the gut, and fecal samples are a better readout of bacterial taxa inhabiting the colonic lumen. In this thesis I focused on the fecal

microbiota because fecal pellets are easy to collect, very abundant, yield a great amount of DNA and can be sampled at distinct time points. However, it remains to be determined how specific gut microbial communities are modulated by dietary polyphenols and how these changes impact host physiology.

In sum, the research endeavour described throughout this thesis has considerably contributed to our understanding of how polyphenol-rich foods are beneficial to metabolic health. These studies underscore the role of the gut microbiota in the effects of dietary flavonoids while pointing to the gut-liver axis as a primary target of polyphenol-rich extracts. Here, we brought evidence to support the use of *A. muciniphila* as a "next-generation" probiotic and we showed that polyphenols are a promising dietary means to trigger the expansion of this bacterium. While the relevance of both condensed and hydrolysable tannins as therapeutic targets against obesity and its related comorbidities is suggested in the studies presented herein, this thesis brings unequivocal evidence to support the regular consumption of dietary sources of polyphenols in order to prevent the metabolic syndrome.

Bibliography

1.   Locke AE, Kahali B, Berndt SI, Justice AE, Pers TH, Day FR, et al. Genetic studies of body mass index yield new insights for obesity biology. Nature. 2015;518(7538):197-206. Epub 2015/02/13.

2.   Organization WH. Fact sheet on obesity and overweight. 2016 [cited 2017 26 April]; Available from: http://www.who.int/mediacentre/factsheets/fs311/en/.

3.   Organization WH. Global Health Observatory data. 2016 [cited 2017 26 April]; Available from: http://www.who.int/gho/ncd/risk_factors/overweight/en/.

4.   Finucane MM, Stevens GA, Cowan MJ, Danaei G, Lin JK, Paciorek CJ, et al. National, regional, and global trends in body-mass index since 1980: systematic analysis of health examination surveys and epidemiological studies with 960 country-years and 9.1 million participants. Lancet. 2011;377(9765):557-67. Epub 2011/02/08.

5.   Kelly T, Yang W, Chen CS, Reynolds K, He J. Global burden of obesity in 2005 and projections to 2030. Int J Obes (Lond). 2008;32(9):1431-7. Epub 2008/07/09.

6.   Locke AE, Kahali B, Berndt SI, Justice AE, Pers TH, Day FR, et al. Genetic studies of body mass index yield new insights for obesity biology. Nature. 2015;518(7538):197-206. Epub 2015/02/13.

7.   Speliotes EK, Willer CJ, Berndt SI, Monda KL, Thorleifsson G, Jackson AU, et al. Association analyses of 249,796 individuals reveal 18 new loci associated with body mass index. Nature genetics. 2010;42(11):937-48. Epub 2010/10/12.

8.   Maskarinec G, Lim U, Jacobs S, Monroe KR, Ernst T, Buchthal SD, et al. Diet Quality in Midadulthood Predicts Visceral Adiposity and Liver Fatness in Older Ages: The Multiethnic Cohort Study. Obesity (Silver Spring). 2017;25(8):1442-50. Epub 2017/07/27.

9.   Ebbeling CB, Swain JF, Feldman HA, Wong WW, Hachey DL, Garcia-Lago E, et al. Effects of dietary composition on energy expenditure during weight-loss maintenance. JAMA : the journal of the American Medical Association. 2012;307(24):2627-34. Epub 2012/06/28.

10.   Abubucker S, Segata N, Goll J, Schubert AM, Izard J, Cantarel BL, et al. Metabolic reconstruction for metagenomic data and its application to the human microbiome. PLoS computational biology. 2012;8(6):e1002358. Epub 2012/06/22.

11.   David LA, Maurice CF, Carmody RN, Gootenberg DB, Button JE, Wolfe BE, et al. Diet rapidly and reproducibly alters the human gut microbiome. Nature. 2014;505(7484):559-63. Epub 2013/12/18.

12.   Ridaura VK, Faith JJ, Rey FE, Cheng J, Duncan AE, Kau AL, et al. Gut microbiota from twins discordant for obesity modulate metabolism in mice. Science. 2013;341(6150):1241214. Epub 2013/09/07.

13.   Zietak M, Kovatcheva-Datchary P, Markiewicz LH, Stahlman M, Kozak LP, Backhed F. Altered Microbiota Contributes to Reduced Diet-Induced Obesity upon Cold Exposure. Cell metabolism. 2016;23(6):1216-23. Epub 2016/06/16.

14.   Le Chatelier E, Nielsen T, Qin J, Prifti E, Hildebrand F, Falony G, et al. Richness of human gut microbiome correlates with metabolic markers. Nature. 2013;500(7464):541-6. Epub 2013/08/30.

15.   Bammann K, Peplies J, De Henauw S, Hunsberger M, Molnar D, Moreno LA, et al. Early life course risk factors for childhood obesity: the IDEFICS case-control study. PloS one. 2014;9(2):e86914. Epub 2014/02/20.

16.   Gaillard R, Steegers EA, Duijts L, Felix JF, Hofman A, Franco OH, et al. Childhood cardiometabolic outcomes of maternal obesity during pregnancy: the Generation R Study. Hypertension. 2014;63(4):683-91. Epub 2014/01/01.

17.   Janesick AS, Shioda T, Blumberg B. Transgenerational inheritance of prenatal obesogen exposure. Molecular and cellular endocrinology. 2014;398(1-2):31-5. Epub 2014/09/15.

18.   Dabelea D, Harrod CS. Role of developmental overnutrition in pediatric obesity and type 2 diabetes. Nutrition reviews. 2013;71 Suppl 1:S62-7. Epub 2013/10/30.

19.   Bouchard C, Tremblay A, Despres JP, Nadeau A, Lupien PJ, Theriault G, et al. The response to long-term overfeeding in identical twins. The New England journal of medicine. 1990;322(21):1477-82. Epub 1990/05/24.

20.   Ravussin E. Metabolic differences and the development of obesity. Metabolism: clinical and experimental. 1995;44(9 Suppl 3):12-4. Epub 1995/09/01.

21.   Nedergaard J, Bengtsson T, Cannon B. Unexpected evidence for active brown adipose tissue in adult humans. Am J Physiol Endocrinol Metab. 2007;293(2):E444-52. Epub 2007/05/03.

22.   Saito M, Okamatsu-Ogura Y, Matsushita M, Watanabe K, Yoneshiro T, Nio-Kobayashi J, et al. High incidence of metabolically active brown adipose tissue in healthy adult humans: effects of cold exposure and adiposity. Diabetes. 2009;58(7):1526-31. Epub 2009/04/30.

23.   Ouellet V, Routhier-Labadie A, Bellemare W, Lakhal-Chaieb L, Turcotte E, Carpentier AC, et al. Outdoor temperature, age, sex, body mass index, and diabetic status determine the prevalence, mass, and glucose-uptake activity of 18F-FDG-detected BAT in humans. The Journal of clinical endocrinology and metabolism. 2011;96(1):192-9. Epub 2010/10/15.

24.   Virtanen KA, Lidell ME, Orava J, Heglind M, Westergren R, Niemi T, et al. Functional brown adipose tissue in healthy adults. The New England journal of medicine. 2009;360(15):1518-25. Epub 2009/04/10.

25.   Richard D, Monge-Roffarello B, Chechi K, Labbe SM, Turcotte EE. Control and physiological determinants of sympathetically mediated brown adipose tissue thermogenesis. Frontiers in endocrinology. 2012;3:36. Epub 2012/06/02.

26.   Spiegelman BM, Flier JS. Obesity and the regulation of energy balance. Cell. 2001;104(4):531-43. Epub 2001/03/10.

27.   Feldmann HM, Golozoubova V, Cannon B, Nedergaard J. UCP1 ablation induces obesity and abolishes diet-induced thermogenesis in mice exempt from thermal stress by living at thermoneutrality. Cell metabolism. 2009;9(2):203-9. Epub 2009/02/04.

28.   Nicholls DG, Locke RM. Thermogenic mechanisms in brown fat. Physiol Rev. 1984;64(1):1-64. Epub 1984/01/01.

29.   Bianco AC, Kim BW. Deiodinases: implications of the local control of thyroid hormone action. J Clin Invest. 2006;116(10):2571-9. Epub 2006/10/04.

30.   Fang S, Suh JM, Reilly SM, Yu E, Osborn O, Lackey D, et al. Intestinal FXR agonism promotes adipose tissue browning and reduces obesity and insulin resistance. Nature medicine. 2015;21(2):159-65. Epub 2015/01/07.

31.   Kwon MM, O'Dwyer SM, Baker RK, Covey SD, Kieffer TJ. FGF21-Mediated Improvements in Glucose Clearance Require Uncoupling Protein 1. Cell reports. 2015;13(8):1521-7. Epub 2015/11/21.

32.   Whittle AJ, Carobbio S, Martins L, Slawik M, Hondares E, Vazquez MJ, et al. BMP8B increases brown adipose tissue thermogenesis through both central and peripheral actions. Cell. 2012;149(4):871-85. Epub 2012/05/15.

33.   Watanabe M, Houten SM, Mataki C, Christoffolete MA, Kim BW, Sato H, et al. Bile acids induce energy expenditure by promoting intracellular thyroid hormone activation. Nature. 2006;439(7075):484-9. Epub 2006/01/10.

34.   Zietak M, Kozak LP. Bile acids induce uncoupling protein 1-dependent thermogenesis and stimulate energy expenditure at thermoneutrality in mice. Am J Physiol Endocrinol Metab. 2016;310(5):E346-54. Epub 2015/12/31.

35.   Gao Z, Yin J, Zhang J, Ward RE, Martin RJ, Lefevre M, et al. Butyrate improves insulin sensitivity and increases energy expenditure in mice. Diabetes. 2009;58(7):1509-17. Epub 2009/04/16.

36.   Kimura I, Inoue D, Maeda T, Hara T, Ichimura A, Miyauchi S, et al. Short-chain fatty acids and ketones directly regulate sympathetic nervous system via G protein-coupled receptor 41 (GPR41). Proceedings of the National Academy of Sciences of the United States of America. 2011;108(19):8030-5. Epub 2011/04/27.

37.   Kimura I, Ozawa K, Inoue D, Imamura T, Kimura K, Maeda T, et al. The gut microbiota suppresses insulin-mediated fat accumulation via the short-chain fatty acid receptor GPR43. Nature communications. 2013;4:1829. Epub 2013/05/09.

38.   Fedorenko A, Lishko PV, Kirichok Y. Mechanism of fatty-acid-dependent UCP1 uncoupling in brown fat mitochondria. Cell. 2012;151(2):400-13. Epub 2012/10/16.

39.   Dulloo AG, Seydoux J, Girardier L. Peripheral mechanisms of thermogenesis induced by ephedrine and caffeine in brown adipose tissue. International journal of obesity. 1991;15(5):317-26. Epub 1991/05/01.

40.   Dulloo AG, Seydoux J, Girardier L, Chantre P, Vandermander J. Green tea and thermogenesis: interactions between catechin-polyphenols, caffeine and sympathetic activity. Int J Obes Relat Metab Disord. 2000;24(2):252-8. Epub 2000/03/07.

41.   Thaiss CA, Itav S, Rothschild D, Meijer M, Levy M, Moresi C, et al. Persistent microbiome alterations modulate the rate of post-dieting weight regain. Nature. 2016. Epub 2016/12/03.

42.   Bartelt A, Heeren J. Adipose tissue browning and metabolic health. Nature reviews Endocrinology. 2014;10(1):24-36. Epub 2013/10/23.

43.   Cannon B, Nedergaard J. Brown adipose tissue: function and physiological significance. Physiol Rev. 2004;84(1):277-359. Epub 2004/01/13.

44.   Nguyen KD, Qiu Y, Cui X, Goh YP, Mwangi J, David T, et al. Alternatively activated macrophages produce catecholamines to sustain adaptive thermogenesis. Nature. 2011;480(7375):104-8. Epub 2011/11/22.

45.   Vegiopoulos A, Muller-Decker K, Strzoda D, Schmitt I, Chichelnitskiy E, Ostertag A, et al. Cyclooxygenase-2 controls energy homeostasis in mice by de novo recruitment of brown adipocytes. Science. 2010;328(5982):1158-61. Epub 2010/05/08.

46.   Martinez-Sanchez N, Moreno-Navarrete JM, Contreras C, Rial-Pensado E, Ferno J, Nogueiras R, et al. Thyroid hormones induce browning of white fat. The Journal of endocrinology. 2017;232(2):351-62. Epub 2016/12/04.

47.   Fisher FM, Kleiner S, Douris N, Fox EC, Mepani RJ, Verdeguer F, et al. FGF21 regulates PGC-1alpha and browning of white adipose tissues in adaptive thermogenesis. Genes & development. 2012;26(3):271-81. Epub 2012/02/04.

48.   Qian SW, Tang Y, Li X, Liu Y, Zhang YY, Huang HY, et al. BMP4-mediated brown fat-like changes in white adipose tissue alter glucose and energy homeostasis. Proceedings of the National Academy of Sciences of the United States of America. 2013;110(9):E798-807. Epub 2013/02/08.

49.   Lu Y, Fan C, Li P, Chang X, Qi K. Short Chain Fatty Acids Prevent High-fat-diet-induced Obesity in Mice by Regulating G Protein-coupled Receptors and Gut Microbiota. Scientific reports. 2016;6:37589. Epub 2016/11/29.

50.   Sahuri-Arisoylu M, Brody LP, Parkinson JR, Parkes H, Navaratnam N, Miller AD, et al. Reprogramming of hepatic fat accumulation and 'browning' of adipose tissue by the short-chain fatty acid acetate. Int J Obes (Lond). 2016;40(6):955-63. Epub 2016/03/16.

51.   Arias N, Pico C, Teresa Macarulla M, Oliver P, Miranda J, Palou A, et al. A combination of resveratrol and quercetin induces browning in white adipose tissue of rats fed an obesogenic diet. Obesity (Silver Spring). 2017;25(1):111-21. Epub 2016/11/23.

52.   Wang S, Liang X, Yang Q, Fu X, Rogers CJ, Zhu M, et al. Resveratrol induces brown-like adipocyte formation in white fat through activation of AMP-activated protein kinase (AMPK) alpha1. Int J Obes (Lond). 2015;39(6):967-76. Epub 2015/03/13.

53.   Azhar Y, Parmar A, Miller CN, Samuels JS, Rayalam S. Phytochemicals as novel agents for the induction of browning in white adipose tissue. Nutrition & metabolism. 2016;13(1):89.

54.   Mehran AE, Templeman NM, Brigidi GS, Lim GE, Chu KY, Hu X, et al. Hyperinsulinemia drives diet-induced obesity independently of brain insulin production. Cell metabolism. 2012;16(6):723-37. Epub 2012/12/12.

55.   Eckel RH, Grundy SM, Zimmet PZ. The metabolic syndrome. Lancet. 2005;365(9468):1415-28. Epub 2005/04/20.

56.   Organization WH. Fact sheet on Diabetes mellitus. 2017 [cited 2017 2 May]; Available from: http://www.who.int/mediacentre/factsheets/fs138/en/.

57.   organization Wh. Fact sheet on Diabetes. 2016 [cited 2017 2 May]; Available from: http://www.who.int/mediacentre/factsheets/fs312/en/.

58.   Morris RD, Rimm DL, Hartz AJ, Kalkhoff RK, Rimm AA. Obesity and heredity in the etiology of non-insulin-dependent diabetes mellitus in 32,662 adult white women. American journal of epidemiology. 1989;130(1):112-21. Epub 1989/07/01.

59.   Edelstein SL, Knowler WC, Bain RP, Andres R, Barrett-Connor EL, Dowse GK, et al. Predictors of progression from impaired glucose tolerance to NIDDM: an analysis of six prospective studies. Diabetes. 1997;46(4):701-10. Epub 1997/04/01.

60.   Burchfiel CM, Sharp DS, Curb JD, Rodriguez BL, Hwang LJ, Marcus EB, et al. Physical activity and incidence of diabetes: the Honolulu Heart Program. American journal of epidemiology. 1995;141(4):360-8. Epub 1995/02/15.

61.   Hu FB, van Dam RM, Liu S. Diet and risk of Type II diabetes: the role of types of fat and carbohydrate. Diabetologia. 2001;44(7):805-17. Epub 2001/08/18.

62.   Bray GA, Jablonski KA, Fujimoto WY, Barrett-Connor E, Haffner S, Hanson RL, et al. Relation of central adiposity and body mass index to the development of diabetes in the Diabetes Prevention Program. The American journal of clinical nutrition. 2008;87(5):1212-8. Epub 2008/05/13.

63.   Szczepaniak LS, Nurenberg P, Leonard D, Browning JD, Reingold JS, Grundy S, et al. Magnetic resonance spectroscopy to measure hepatic triglyceride content: prevalence of hepatic steatosis in the general population. Am J Physiol Endocrinol Metab. 2005;288(2):E462-8. Epub 2004/09/02.

64.   Cohen JC, Horton JD, Hobbs HH. Human fatty liver disease: old questions and new insights. Science. 2011;332(6037):1519-23. Epub 2011/06/28.

65.   Vernon G, Baranova A, Younossi ZM. Systematic review: the epidemiology and natural history of non-alcoholic fatty liver disease and non-alcoholic steatohepatitis in adults. Alimentary pharmacology & therapeutics. 2011;34(3):274-85. Epub 2011/06/01.

66.   Starley BQ, Calcagno CJ, Harrison SA. Nonalcoholic fatty liver disease and hepatocellular carcinoma: a weighty connection. Hepatology. 2010;51(5):1820-32. Epub 2010/05/01.

67.   Sherif ZA, Saeed A, Ghavimi S, Nouraie SM, Laiyemo AO, Brim H, et al. Global Epidemiology of Nonalcoholic Fatty Liver Disease and Perspectives on US Minority Populations. Digestive diseases and sciences. 2016;61(5):1214-25. Epub 2016/04/03.

68.   Newsholme P, Krause M. Nutritional regulation of insulin secretion: implications for diabetes. The Clinical biochemist Reviews. 2012;33(2):35-47. Epub 2012/08/17.

69.   Cong LN, Chen H, Li Y, Zhou L, McGibbon MA, Taylor SI, et al. Physiological role of Akt in insulin-stimulated translocation of GLUT4 in transfected rat adipose cells. Mol Endocrinol. 1997;11(13):1881-90. Epub 1998/02/12.

70.	Cross DA, Alessi DR, Cohen P, Andjelkovich M, Hemmings BA. Inhibition of glycogen synthase kinase-3 by insulin mediated by protein kinase B. Nature. 1995;378(6559):785-9. Epub 1995/12/21.

71.	Brunet A, Bonni A, Zigmond MJ, Lin MZ, Juo P, Hu LS, et al. Akt promotes cell survival by phosphorylating and inhibiting a Forkhead transcription factor. Cell. 1999;96(6):857-68. Epub 1999/04/02.

72.	Delplanque J, Devos D, Huin V, Genet A, Sand O, Moreau C, et al. TMEM240 mutations cause spinocerebellar ataxia 21 with mental retardation and severe cognitive impairment. Brain : a journal of neurology. 2014;137(Pt 10):2657-63. Epub 2014/07/30.

73.	Kern PA, Marshall S, Eckel RH. Regulation of lipoprotein lipase in primary cultures of isolated human adipocytes. J Clin Invest. 1985;75(1):199-208. Epub 1985/01/01.

74.	Weber C, Meiler S, Doring Y, Koch M, Drechsler M, Megens RT, et al. CCL17-expressing dendritic cells drive atherosclerosis by restraining regulatory T cell homeostasis in mice. J Clin Invest. 2011;121(7):2898-910. Epub 2011/06/03.

75.	Miyoshi H, Souza SC, Zhang HH, Strissel KJ, Christoffolete MA, Kovsan J, et al. Perilipin promotes hormone-sensitive lipase-mediated adipocyte lipolysis via phosphorylation-dependent and -independent mechanisms. The Journal of biological chemistry. 2006;281(23):15837-44. Epub 2006/04/06.

76.	Schmoll D, Walker KS, Alessi DR, Grempler R, Burchell A, Guo S, et al. Regulation of glucose-6-phosphatase gene expression by protein kinase Balpha and the forkhead transcription factor FKHR. Evidence for insulin response unit-dependent and -independent effects of insulin on promoter activity. The Journal of biological chemistry. 2000;275(46):36324-33. Epub 2000/08/29.

77.	Koo SH, Satoh H, Herzig S, Lee CH, Hedrick S, Kulkarni R, et al. PGC-1 promotes insulin resistance in liver through PPAR-alpha-dependent induction of TRB-3. Nature medicine. 2004;10(5):530-4. Epub 2004/04/27.

78.	Chen G, Liang G, Ou J, Goldstein JL, Brown MS. Central role for liver X receptor in insulin-mediated activation of Srebp-1c transcription and stimulation of fatty acid synthesis in liver. Proceedings of the National Academy of Sciences of the United States of America. 2004;101(31):11245-50. Epub 2004/07/22.

79.	Xu X, So JS, Park JG, Lee AH. Transcriptional control of hepatic lipid metabolism by SREBP and ChREBP. Seminars in liver disease. 2013;33(4):301-11. Epub 2013/11/14.

80.	Saltiel AR, Kahn CR. Insulin signalling and the regulation of glucose and lipid metabolism. Nature. 2001;414(6865):799-806. Epub 2001/12/14.

81.	Biddinger SB, Kahn CR. From mice to men: insights into the insulin resistance syndromes. Annu Rev Physiol. 2006;68:123-58. Epub 2006/02/08.

82.	Duckworth WC, Bennett RG, Hamel FG. The significance of intracellular insulin to insulin action. Journal of investigative medicine : the official publication of the American Federation for Clinical Research. 1997;45(2):20-7. Epub 1997/02/01.

83.	Flier J, Minaker K, Landsberg L, Young J, Pallotta J, Rowe J. Impaired in vivo insulin clearance in patients with severe target-cell resistance to insulin. Diabetes. 1982;31(2):132-5.

84.	Hojlund K, Wojtaszewski JF, Birk J, Hansen BF, Vestergaard H, Beck-Nielsen H. Partial rescue of in vivo insulin signalling in skeletal muscle by impaired insulin clearance in heterozygous carriers of a mutation in the insulin receptor gene. Diabetologia. 2006;49(8):1827-37. Epub 2006/06/09.

85.	Bonora E, Zavaroni I, Coscelli C, Butturini U. Decreased hepatic insulin extraction in subjects with mild glucose intolerance. Metabolism: clinical and experimental. 1983;32(5):438-46. Epub 1983/05/01.

86.   Peiris AN, Mueller RA, Smith GA, Struve MF, Kissebah AH. Splanchnic insulin metabolism in obesity. Influence of body fat distribution. J Clin Invest. 1986;78(6):1648-57. Epub 1986/12/01.

87.   Lee CC, Haffner SM, Wagenknecht LE, Lorenzo C, Norris JM, Bergman RN, et al. Insulin clearance and the incidence of type 2 diabetes in Hispanics and African Americans: the IRAS Family Study. Diabetes care. 2013;36(4):901-7. Epub 2012/12/12.

88.   Iwasaki Y, Ohkubo A, Kajinuma H, Akanuma Y, Kosaka K. Degradation and secretion of insulin in hepatic cirrhosis. The Journal of clinical endocrinology and metabolism. 1978;47(4):774-9. Epub 1978/10/01.

89.   Goto T, Onuma T, Takebe K, Kral JG. The influence of fatty liver on insulin clearance and insulin resistance in non-diabetic Japanese subjects. Int J Obes Relat Metab Disord. 1995;19(12):841-5. Epub 1995/12/01.

90.   Duckworth WC, Bennett RG, Hamel FG. Insulin degradation: progress and potential. Endocrine reviews. 1998;19(5):608-24. Epub 1998/10/30.

91.   Poy MN, Yang Y, Rezaei K, Fernstrom MA, Lee AD, Kido Y, et al. CEACAM1 regulates insulin clearance in liver. Nature genetics. 2002;30(3):270-6. Epub 2002/02/19.

92.   Formisano P, Najjar SM, Gross CN, Philippe N, Oriente F, Kern-Buell CL, et al. Receptor-mediated internalization of insulin. Potential role of pp120/HA4, a substrate of the insulin receptor kinase. The Journal of biological chemistry. 1995;270(41):24073-7. Epub 1995/10/13.

93.   Choice CV, Howard MJ, Poy MN, Hankin MH, Najjar SM. Insulin stimulates pp120 endocytosis in cells co-expressing insulin receptors. The Journal of biological chemistry. 1998;273(35):22194-200. Epub 1998/08/26.

94.   Najjar SM, Yang Y, Fernstrom MA, Lee SJ, Deangelis AM, Rjaily GA, et al. Insulin acutely decreases hepatic fatty acid synthase activity. Cell metabolism. 2005;2(1):43-53. Epub 2005/08/02.

95.   Xu E, Dubois MJ, Leung N, Charbonneau A, Turbide C, Avramoglu RK, et al. Targeted disruption of carcinoembryonic antigen-related cell adhesion molecule 1 promotes diet-induced hepatic steatosis and insulin resistance. Endocrinology. 2009;150(8):3503-12. Epub 2009/05/02.

96.   Park SY, Cho YR, Kim HJ, Hong EG, Higashimori T, Lee SJ, et al. Mechanism of glucose intolerance in mice with dominant negative mutation of CEACAM1. Am J Physiol Endocrinol Metab. 2006;291(3):E517-24. Epub 2006/04/28.

97.   DeAngelis AM, Heinrich G, Dai T, Bowman TA, Patel PR, Lee SJ, et al. Carcinoembryonic antigen-related cell adhesion molecule 1: a link between insulin and lipid metabolism. Diabetes. 2008;57(9):2296-303. Epub 2008/06/12.

98.   Farris W, Mansourian S, Chang Y, Lindsley L, Eckman EA, Frosch MP, et al. Insulin-degrading enzyme regulates the levels of insulin, amyloid beta-protein, and the beta-amyloid precursor protein intracellular domain in vivo. Proceedings of the National Academy of Sciences of the United States of America. 2003;100(7):4162-7. Epub 2003/03/14.

99.   Wei X, Ke B, Zhao Z, Ye X, Gao Z, Ye J. Regulation of insulin degrading enzyme activity by obesity-associated factors and pioglitazone in liver of diet-induced obese mice. PloS one. 2014;9(4):e95399. Epub 2014/04/18.

100.   Marangou AG, Weber KM, Boston RC, Aitken PM, Heggie JC, Kirsner RL, et al. Metabolic consequences of prolonged hyperinsulinemia in humans. Evidence for induction of insulin insensitivity. Diabetes. 1986;35(12):1383-9. Epub 1986/12/01.

101.   Martin BC, Warram JH, Krolewski AS, Bergman RN, Soeldner JS, Kahn CR. Role of glucose and insulin resistance in development of type 2 diabetes mellitus: results of a 25-year follow-up study. Lancet. 1992;340(8825):925-9. Epub 1992/10/17.

102.   Templeman NM, Clee SM, Johnson JD. Suppression of hyperinsulinaemia in growing female mice provides long-term protection against obesity. Diabetologia. 2015;58(10):2392-402. Epub 2015/07/15.

103.   Hotamisligil GS, Shargill NS, Spiegelman BM. Adipose expression of tumor necrosis factor-alpha: direct role in obesity-linked insulin resistance. Science. 1993;259(5091):87-91. Epub 1993/01/01.

104.   Hotamisligil GS, Arner P, Caro JF, Atkinson RL, Spiegelman BM. Increased adipose tissue expression of tumor necrosis factor-alpha in human obesity and insulin resistance. J Clin Invest. 1995;95(5):2409-15. Epub 1995/05/01.

105.   Wellen KE, Hotamisligil GS. Inflammation, stress, and diabetes. J Clin Invest. 2005;115(5):1111-9. Epub 2005/05/03.

106.   Brun A, Gutierrez-Adan A, Castilla J, Pintado B, Diaz-San Segundo F, Cano MJ, et al. Reduced susceptibility to bovine spongiform encephalopathy prions in transgenic mice expressing a bovine PrP with five octapeptide repeats. The Journal of general virology. 2007;88(Pt 6):1842-9. Epub 2007/05/09.

107.   Perreault M, Marette A. Targeted disruption of inducible nitric oxide synthase protects against obesity-linked insulin resistance in muscle. Nature medicine. 2001;7(10):1138-43. Epub 2001/10/09.

108.   Kaneto H, Nakatani Y, Miyatsuka T, Kawamori D, Matsuoka TA, Matsuhisa M, et al. Possible novel therapy for diabetes with cell-permeable JNK-inhibitory peptide. Nature medicine. 2004;10(10):1128-32. Epub 2004/09/28.

109.   Roytblat L, Rachinsky M, Fisher A, Greemberg L, Shapira Y, Douvdevani A, et al. Raised interleukin-6 levels in obese patients. Obesity research. 2000;8(9):673-5. Epub 2001/02/28.

110.   Aygun AD, Gungor S, Ustundag B, Gurgoze MK, Sen Y. Proinflammatory cytokines and leptin are increased in serum of prepubertal obese children. Mediators of inflammation. 2005;2005(3):180-3. Epub 2005/08/18.

111.   Herder C, Peltonen M, Koenig W, Kraft I, Muller-Scholze S, Martin S, et al. Systemic immune mediators and lifestyle changes in the prevention of type 2 diabetes: results from the Finnish Diabetes Prevention Study. Diabetes. 2006;55(8):2340-6. Epub 2006/07/29.

112.   Takahashi K, Mizuarai S, Araki H, Mashiko S, Ishihara A, Kanatani A, et al. Adiposity elevates plasma MCP-1 levels leading to the increased CD11b-positive monocytes in mice. The Journal of biological chemistry. 2003;278(47):46654-60. Epub 2003/09/18.

113.   Varma V, Yao-Borengasser A, Rasouli N, Nolen GT, Phanavanh B, Starks T, et al. Muscle inflammatory response and insulin resistance: synergistic interaction between macrophages and fatty acids leads to impaired insulin action. Am J Physiol Endocrinol Metab. 2009;296(6):E1300-10. Epub 2009/04/02.

114.   Weisberg SP, McCann D, Desai M, Rosenbaum M, Leibel RL, Ferrante AW, Jr. Obesity is associated with macrophage accumulation in adipose tissue. J Clin Invest. 2003;112(12):1796-808. Epub 2003/12/18.

115.   Stanton MC, Chen SC, Jackson JV, Rojas-Triana A, Kinsley D, Cui L, et al. Inflammatory Signals shift from adipose to liver during high fat feeding and influence the development of steatohepatitis in mice. J Inflamm (Lond). 2011;8:8. Epub 2011/03/18.

116.   Deng ZB, Liu Y, Liu C, Xiang X, Wang J, Cheng Z, et al. Immature myeloid cells induced by a high-fat diet contribute to liver inflammation. Hepatology. 2009;50(5):1412-20. Epub 2009/08/27.

117.   Rensen SS, Slaats Y, Nijhuis J, Jans A, Bieghs V, Driessen A, et al. Increased hepatic myeloperoxidase activity in obese subjects with nonalcoholic steatohepatitis. The American journal of pathology. 2009;175(4):1473-82. Epub 2009/09/05.

118.   Xu H, Barnes GT, Yang Q, Tan G, Yang D, Chou CJ, et al. Chronic inflammation in fat plays a crucial role in the development of obesity-related insulin resistance. J Clin Invest. 2003;112(12):1821-30. Epub 2003/12/18.

119.   Strissel KJ, Stancheva Z, Miyoshi H, Perfield JW, 2nd, DeFuria J, Jick Z, et al. Adipocyte death, adipose tissue remodeling, and obesity complications. Diabetes. 2007;56(12):2910-8. Epub 2007/09/13.

120.   Kanda H, Tateya S, Tamori Y, Kotani K, Hiasa K, Kitazawa R, et al. MCP-1 contributes to macrophage infiltration into adipose tissue, insulin resistance, and hepatic steatosis in obesity. J Clin Invest. 2006;116(6):1494-505. Epub 2006/05/13.

121.   Cinti S, Mitchell G, Barbatelli G, Murano I, Ceresi E, Faloia E, et al. Adipocyte death defines macrophage localization and function in adipose tissue of obese mice and humans. J Lipid Res. 2005;46(11):2347-55. Epub 2005/09/10.

122.   Lumeng CN, Bodzin JL, Saltiel AR. Obesity induces a phenotypic switch in adipose tissue macrophage polarization. J Clin Invest. 2007;117(1):175-84. Epub 2007/01/04.

123.   Nishimura S, Manabe I, Nagasaki M, Eto K, Yamashita H, Ohsugi M, et al. CD8+ effector T cells contribute to macrophage recruitment and adipose tissue inflammation in obesity. Nature medicine. 2009;15(8):914-20. Epub 2009/07/28.

124.   Ohmura K, Ishimori N, Ohmura Y, Tokuhara S, Nozawa A, Horii S, et al. Natural killer T cells are involved in adipose tissues inflammation and glucose intolerance in diet-induced obese mice. Arterioscler Thromb Vasc Biol. 2010;30(2):193-9. Epub 2009/11/17.

125.   Winer S, Chan Y, Paltser G, Truong D, Tsui H, Bahrami J, et al. Normalization of obesity-associated insulin resistance through immunotherapy. Nature medicine. 2009;15(8):921-9. Epub 2009/07/28.

126.   Elgazar-Carmon V, Rudich A, Hadad N, Levy R. Neutrophils transiently infiltrate intra-abdominal fat early in the course of high-fat feeding. J Lipid Res. 2008;49(9):1894-903. Epub 2008/05/27.

127.   Wu D, Molofsky AB, Liang HE, Ricardo-Gonzalez RR, Jouihan HA, Bando JK, et al. Eosinophils sustain adipose alternatively activated macrophages associated with glucose homeostasis. Science. 2011;332(6026):243-7. Epub 2011/03/26.

128.   Liu J, Divoux A, Sun J, Zhang J, Clement K, Glickman JN, et al. Genetic deficiency and pharmacological stabilization of mast cells reduce diet-induced obesity and diabetes in mice. Nature medicine. 2009;15(8):940-5. Epub 2009/07/28.

129.   Winer DA, Winer S, Shen L, Wadia PP, Yantha J, Paltser G, et al. B cells promote insulin resistance through modulation of T cells and production of pathogenic IgG antibodies. Nature medicine. 2011;17(5):610-7. Epub 2011/04/19.

130.   Despres JP, Lemieux I. Abdominal obesity and metabolic syndrome. Nature. 2006;444(7121):881-7. Epub 2006/12/15.

131.   Trayhurn P, Wang B, Wood IS. Hypoxia in adipose tissue: a basis for the dysregulation of tissue function in obesity? The British journal of nutrition. 2008;100(2):227-35. Epub 2008/04/10.

132.   Hummasti S, Hotamisligil GS. Endoplasmic reticulum stress and inflammation in obesity and diabetes. Circulation research. 2010;107(5):579-91. Epub 2010/09/04.

133.   Marette A. Mediators of cytokine-induced insulin resistance in obesity and other inflammatory settings. Current opinion in clinical nutrition and metabolic care. 2002;5(4):377-83. Epub 2002/07/11.

134.   Carvalho-Filho MA, Ueno M, Hirabara SM, Seabra AB, Carvalheira JB, de Oliveira MG, et al. S-nitrosation of the insulin receptor, insulin receptor substrate 1, and protein kinase B/Akt: a novel mechanism of insulin resistance. Diabetes. 2005;54(4):959-67. Epub 2005/03/29.

135.   White PJ, Charbonneau A, Cooney GJ, Marette A. Nitrosative modifications of protein and lipid signaling molecules by reactive nitrogen species. Am J Physiol Endocrinol Metab. 2010;299(6):E868-78. Epub 2010/09/30.

136.   Ischiropoulos H, al-Mehdi AB. Peroxynitrite-mediated oxidative protein modifications. FEBS Lett. 1995;364(3):279-82. Epub 1995/05/15.

137.   Higdon JV, Frei B. Obesity and oxidative stress: a direct link to CVD? Arterioscler Thromb Vasc Biol. 2003;23(3):365-7. Epub 2003/03/18.

138.   Cai H, Harrison DG. Endothelial dysfunction in cardiovascular diseases: the role of oxidant stress. Circulation research. 2000;87(10):840-4. Epub 2000/11/14.

139.   Maritim AC, Sanders RA, Watkins JB, 3rd. Diabetes, oxidative stress, and antioxidants: a review. Journal of biochemical and molecular toxicology. 2003;17(1):24-38. Epub 2003/03/05.

140.   Bailey CJ, Mynett KJ. Insulin requirement for the antihyperglycaemic effect of metformin. British journal of pharmacology. 1994;111(3):793-6. Epub 1994/03/01.

141.   Barrett EJ, Ferrannini E, Gusberg R, Bevilacqua S, DeFronzo RA. Hepatic and extrahepatic splanchnic glucose metabolism in the postabsorptive and glucose fed dog. Metabolism: clinical and experimental. 1985;34(5):410-20. Epub 1985/05/01.

142.   Maynard CL, Elson CO, Hatton RD, Weaver CT. Reciprocal interactions of the intestinal microbiota and immune system. Nature. 2012;489(7415):231-41. Epub 2012/09/14.

143.   Winer DA, Luck H, Tsai S, Winer S. The Intestinal Immune System in Obesity and Insulin Resistance. Cell metabolism. 2016;23(3):413-26. Epub 2016/02/09.

144.   Monteiro-Sepulveda M, Touch S, Mendes-Sa C, Andre S, Poitou C, Allatif O, et al. Jejunal T Cell Inflammation in Human Obesity Correlates with Decreased Enterocyte Insulin Signaling. Cell metabolism. 2015;22(1):113-24. Epub 2015/06/23.

145.   Veilleux A, Mayeur S, Berube JC, Beaulieu JF, Tremblay E, Hould FS, et al. Altered intestinal functions and increased local inflammation in insulin-resistant obese subjects: a gene-expression profile analysis. BMC gastroenterology. 2015;15:119. Epub 2015/09/18.

146.   Ding S, Chi MM, Scull BP, Rigby R, Schwerbrock NM, Magness S, et al. High-fat diet: bacteria interactions promote intestinal inflammation which precedes and correlates with obesity and insulin resistance in mouse. PloS one. 2010;5(8):e12191. Epub 2010/09/03.

147.   de La Serre CB, Ellis CL, Lee J, Hartman AL, Rutledge JC, Raybould HE. Propensity to high-fat diet-induced obesity in rats is associated with changes in the gut microbiota and gut inflammation. American journal of physiology Gastrointestinal and liver physiology. 2010;299(2):G440-8. Epub 2010/05/29.

148.   de Wit NJ, Bosch-Vermeulen H, de Groot PJ, Hooiveld GJ, Bromhaar MM, Jansen J, et al. The role of the small intestine in the development of dietary fat-induced obesity and insulin resistance in C57BL/6J mice. BMC medical genomics. 2008;1:14. Epub 2008/05/07.

149.   Hamilton MK, Boudry G, Lemay DG, Raybould HE. Changes in intestinal barrier function and gut microbiota in high-fat diet-fed rats are dynamic and region dependent. American journal of physiology Gastrointestinal and liver physiology. 2015;308(10):G840-51. Epub 2015/03/10.

150.   Garidou L, Pomie C, Klopp P, Waget A, Charpentier J, Aloulou M, et al. The Gut Microbiota Regulates Intestinal CD4 T Cells Expressing RORgammat and Controls Metabolic Disease. Cell metabolism. 2015;22(1):100-12. Epub 2015/07/15.

151.   Lam YY, Ha CW, Campbell CR, Mitchell AJ, Dinudom A, Oscarsson J, et al. Increased gut permeability and microbiota change associate with mesenteric fat inflammation and metabolic dysfunction in diet-induced obese mice. PloS one. 2012;7(3):e34233. Epub 2012/03/30.

152.   Li H, Lelliott C, Hakansson P, Ploj K, Tuneld A, Verolin-Johansson M, et al. Intestinal, adipose, and liver inflammation in diet-induced obese mice. Metabolism: clinical and experimental. 2008;57(12):1704-10. Epub 2008/11/18.

153.   Liu Z, Brooks RS, Ciappio ED, Kim SJ, Crott JW, Bennett G, et al. Diet-induced obesity elevates colonic TNF-alpha in mice and is accompanied by an activation of Wnt signaling: a

mechanism for obesity-associated colorectal cancer. The Journal of nutritional biochemistry. 2012;23(10):1207-13. Epub 2012/01/03.

154.   Johnson AM, Costanzo A, Gareau MG, Armando AM, Quehenberger O, Jameson JM, et al. High fat diet causes depletion of intestinal eosinophils associated with intestinal permeability. PloS one. 2015;10(4):e0122195. Epub 2015/04/04.

155.   Pendyala S, Neff LM, Suarez-Farinas M, Holt PR. Diet-induced weight loss reduces colorectal inflammation: implications for colorectal carcinogenesis. The American journal of clinical nutrition. 2011;93(2):234-42. Epub 2010/12/15.

156.   Luck H, Tsai S, Chung J, Clemente-Casares X, Ghazarian M, Revelo XS, et al. Regulation of obesity-related insulin resistance with gut anti-inflammatory agents. Cell metabolism. 2015;21(4):527-42. Epub 2015/04/12.

157.   Everard A, Geurts L, Caesar R, Van Hul M, Matamoros S, Duparc T, et al. Intestinal epithelial MyD88 is a sensor switching host metabolism towards obesity according to nutritional status. Nature communications. 2014;5:5648. Epub 2014/12/06.

158.   Cox LM, Yamanishi S, Sohn J, Alekseyenko AV, Leung JM, Cho I, et al. Altering the intestinal microbiota during a critical developmental window has lasting metabolic consequences. Cell. 2014;158(4):705-21. Epub 2014/08/16.

159.   Cani PD, Amar J, Iglesias MA, Poggi M, Knauf C, Bastelica D, et al. Metabolic endotoxemia initiates obesity and insulin resistance. Diabetes. 2007;56(7):1761-72. Epub 2007/04/26.

160.   Amar J, Chabo C, Waget A, Klopp P, Vachoux C, Bermudez-Humaran LG, et al. Intestinal mucosal adherence and translocation of commensal bacteria at the early onset of type 2 diabetes: molecular mechanisms and probiotic treatment. EMBO molecular medicine. 2011;3(9):559-72. Epub 2011/07/08.

161.   Denou E, Lolmede K, Garidou L, Pomie C, Chabo C, Lau TC, et al. Defective NOD2 peptidoglycan sensing promotes diet-induced inflammation, dysbiosis, and insulin resistance. EMBO molecular medicine. 2015;7(3):259-74. Epub 2015/02/11.

162.   Groschwitz KR, Hogan SP. Intestinal barrier function: molecular regulation and disease pathogenesis. The Journal of allergy and clinical immunology. 2009;124(1):3-20; quiz 1-2. Epub 2009/06/30.

163.   Vijay-Kumar M, Aitken JD, Carvalho FA, Cullender TC, Mwangi S, Srinivasan S, et al. Metabolic syndrome and altered gut microbiota in mice lacking Toll-like receptor 5. Science. 2010;328(5975):228-31. Epub 2010/03/06.

164.   Plovier H, Everard A, Druart C, Depommier C, Van Hul M, Geurts L, et al. A purified membrane protein from Akkermansia muciniphila or the pasteurized bacterium improves metabolism in obese and diabetic mice. Nature medicine. 2017;23(1):107-13. Epub 2016/11/29.

165.   Birchenough GM, Nystrom EE, Johansson ME, Hansson GC. A sentinel goblet cell guards the colonic crypt by triggering Nlrp6-dependent Muc2 secretion. Science. 2016;352(6293):1535-42. Epub 2016/06/25.

166.   Wlodarska M, Thaiss CA, Nowarski R, Henao-Mejia J, Zhang JP, Brown EM, et al. NLRP6 inflammasome orchestrates the colonic host-microbial interface by regulating goblet cell mucus secretion. Cell. 2014;156(5):1045-59. Epub 2014/03/04.

167.   Everard A, Belzer C, Geurts L, Ouwerkerk JP, Druart C, Bindels LB, et al. Cross-talk between Akkermansia muciniphila and intestinal epithelium controls diet-induced obesity. Proceedings of the National Academy of Sciences of the United States of America. 2013;110(22):9066-71. Epub 2013/05/15.

168.   Chassaing B, Koren O, Goodrich JK, Poole AC, Srinivasan S, Ley RE, et al. Dietary emulsifiers impact the mouse gut microbiota promoting colitis and metabolic syndrome. Nature. 2015;519(7541):92-6. Epub 2015/03/04.

169.   Cani PD, Delzenne NM, Amar J, Burcelin R. Role of gut microflora in the development of obesity and insulin resistance following high-fat diet feeding. Pathologie-biologie. 2008;56(5):305-9. Epub 2008/01/08.

170.   Brun P, Castagliuolo I, Di Leo V, Buda A, Pinzani M, Palu G, et al. Increased intestinal permeability in obese mice: new evidence in the pathogenesis of nonalcoholic steatohepatitis. American journal of physiology Gastrointestinal and liver physiology. 2007;292(2):G518-25. Epub 2006/10/07.

171.   Cario E, Rosenberg IM, Brandwein SL, Beck PL, Reinecker HC, Podolsky DK. Lipopolysaccharide activates distinct signaling pathways in intestinal epithelial cell lines expressing Toll-like receptors. J Immunol. 2000;164(2):966-72. Epub 2000/01/07.

172.   Schertzer JD, Tamrakar AK, Magalhaes JG, Pereira S, Bilan PJ, Fullerton MD, et al. NOD1 activators link innate immunity to insulin resistance. Diabetes. 2011;60(9):2206-15. Epub 2011/07/01.

173.   Youm YH, Adijiang A, Vandanmagsar B, Burk D, Ravussin A, Dixit VD. Elimination of the NLRP3-ASC inflammasome protects against chronic obesity-induced pancreatic damage. Endocrinology. 2011;152(11):4039-45. Epub 2011/08/25.

174.   Vandanmagsar B, Youm YH, Ravussin A, Galgani JE, Stadler K, Mynatt RL, et al. The NLRP3 inflammasome instigates obesity-induced inflammation and insulin resistance. Nature medicine. 2011;17(2):179-88. Epub 2011/01/11.

175.   Wolf AJ, Reyes CN, Liang W, Becker C, Shimada K, Wheeler ML, et al. Hexokinase Is an Innate Immune Receptor for the Detection of Bacterial Peptidoglycan. Cell. 2016;166(3):624-36. Epub 2016/07/05.

176.   Al-Sadi RM, Ma TY. IL-1beta causes an increase in intestinal epithelial tight junction permeability. J Immunol. 2007;178(7):4641-9. Epub 2007/03/21.

177.   Wang X, Ota N, Manzanillo P, Kates L, Zavala-Solorio J, Eidenschenk C, et al. Interleukin-22 alleviates metabolic disorders and restores mucosal immunity in diabetes. Nature. 2014;514(7521):237-41. Epub 2014/08/15.

178.   Cong Y, Feng T, Fujihashi K, Schoeb TR, Elson CO. A dominant, coordinated T regulatory cell-IgA response to the intestinal microbiota. Proceedings of the National Academy of Sciences of the United States of America. 2009;106(46):19256-61. Epub 2009/11/06.

179.   Shan CY, Yang JH, Kong Y, Wang XY, Zheng MY, Xu YG, et al. Alteration of the intestinal barrier and GLP2 secretion in Berberine-treated type 2 diabetic rats. The Journal of endocrinology. 2013;218(3):255-62. Epub 2013/06/13.

180.   Cani PD, Possemiers S, Van de Wiele T, Guiot Y, Everard A, Rottier O, et al. Changes in gut microbiota control inflammation in obese mice through a mechanism involving GLP-2-driven improvement of gut permeability. Gut. 2009;58(8):1091-103. Epub 2009/02/26.

181.   Drucker DJ. Glucagon-like peptides. Diabetes. 1998;47(2):159-69. Epub 1998/03/31.

182.   Syed SK, Bui HH, Beavers LS, Farb TB, Ficorilli J, Chesterfield AK, et al. Regulation of GPR119 receptor activity with endocannabinoid-like lipids. Am J Physiol Endocrinol Metab. 2012;303(12):E1469-78. Epub 2012/10/18.

183.   Cani PD, Plovier H, Van Hul M, Geurts L, Delzenne NM, Druart C, et al. Endocannabinoids--at the crossroads between the gut microbiota and host metabolism. Nature reviews Endocrinology. 2016;12(3):133-43. Epub 2015/12/19.

184.   Cani PD, Geurts L, Matamoros S, Plovier H, Duparc T. Glucose metabolism: focus on gut microbiota, the endocannabinoid system and beyond. Diabetes & metabolism. 2014;40(4):246-57. Epub 2014/03/19.

185.   Silvestri C, Di Marzo V. The endocannabinoid system in energy homeostasis and the etiopathology of metabolic disorders. Cell metabolism. 2013;17(4):475-90. Epub 2013/04/09.

186. Maccarrone M, Bab I, Biro T, Cabral GA, Dey SK, Di Marzo V, et al. Endocannabinoid signaling at the periphery: 50 years after THC. Trends in pharmacological sciences. 2015;36(5):277-96. Epub 2015/03/23.

187. Muccioli GG, Naslain D, Backhed F, Reigstad CS, Lambert DM, Delzenne NM, et al. The endocannabinoid system links gut microbiota to adipogenesis. Molecular systems biology. 2010;6:392. Epub 2010/07/29.

188. Geurts L, Muccioli GG, Delzenne NM, Cani PD. Chronic endocannabinoid system stimulation induces muscle macrophage and lipid accumulation in type 2 diabetic mice independently of metabolic endotoxaemia. PloS one. 2013;8(2):e55963. Epub 2013/02/09.

189. Alhouayek M, Lambert DM, Delzenne NM, Cani PD, Muccioli GG. Increasing endogenous 2-arachidonoylglycerol levels counteracts colitis and related systemic inflammation. FASEB J. 2011;25(8):2711-21. Epub 2011/05/10.

190. Alhamoruni A, Lee AC, Wright KL, Larvin M, O'Sullivan SE. Pharmacological effects of cannabinoids on the Caco-2 cell culture model of intestinal permeability. J Pharmacol Exp Ther. 2010;335(1):92-102. Epub 2010/07/02.

191. Alhamoruni A, Wright KL, Larvin M, O'Sullivan SE. Cannabinoids mediate opposing effects on inflammation-induced intestinal permeability. British journal of pharmacology. 2012;165(8):2598-610. Epub 2011/07/13.

192. Dehghan P, Gargari BP, Jafar-Abadi MA, Aliasgharzadeh A. Inulin controls inflammation and metabolic endotoxemia in women with type 2 diabetes mellitus: a randomized-controlled clinical trial. International journal of food sciences and nutrition. 2014;65(1):117-23. Epub 2013/09/26.

193. Lyte JM, Gabler NK, Hollis JH. Postprandial serum endotoxin in healthy humans is modulated by dietary fat in a randomized, controlled, cross-over study. Lipids in health and disease. 2016;15(1):186. Epub 2016/11/07.

194. Li J, Lin S, Vanhoutte PM, Woo CW, Xu A. Akkermansia Muciniphila Protects Against Atherosclerosis by Preventing Metabolic Endotoxemia-Induced Inflammation in Apoe-/- Mice. Circulation. 2016;133(24):2434-46. Epub 2016/05/05.

195. Ghoshal S, Witta J, Zhong J, de Villiers W, Eckhardt E. Chylomicrons promote intestinal absorption of lipopolysaccharides. J Lipid Res. 2009;50(1):90-7. Epub 2008/09/26.

196. Lin Y, Lee H, Berg AH, Lisanti MP, Shapiro L, Scherer PE. The lipopolysaccharide-activated toll-like receptor (TLR)-4 induces synthesis of the closely related receptor TLR-2 in adipocytes. The Journal of biological chemistry. 2000;275(32):24255-63. Epub 2000/05/24.

197. Jia L, Vianna CR, Fukuda M, Berglund ED, Liu C, Tao C, et al. Hepatocyte Toll-like receptor 4 regulates obesity-induced inflammation and insulin resistance. Nature communications. 2014;5:3878. Epub 2014/05/13.

198. Li J, Chen L, Zhang Y, Zhang WJ, Xu W, Qin Y, et al. TLR4 is required for the obesity-induced pancreatic beta cell dysfunction. Acta biochimica et biophysica Sinica. 2013;45(12):1030-8. Epub 2013/08/30.

199. Kopp A, Buechler C, Bala M, Neumeier M, Scholmerich J, Schaffler A. Toll-like receptor ligands cause proinflammatory and prodiabetic activation of adipocytes via phosphorylation of extracellular signal-regulated kinase and c-Jun N-terminal kinase but not interferon regulatory factor-3. Endocrinology. 2010;151(3):1097-108. Epub 2010/02/05.

200. Jang HJ, Kim HS, Hwang DH, Quon MJ, Kim JA. Toll-like receptor 2 mediates high-fat diet-induced impairment of vasodilator actions of insulin. Am J Physiol Endocrinol Metab. 2013;304(10):E1077-88. Epub 2013/03/28.

201.   Devaraj S, Tobias P, Kasinath BS, Ramsamooj R, Afify A, Jialal I. Knockout of toll-like receptor-2 attenuates both the proinflammatory state of diabetes and incipient diabetic nephropathy. Arterioscler Thromb Vasc Biol. 2011;31(8):1796-804. Epub 2011/05/28.

202.   Pierre N, Deldicque L, Barbe C, Naslain D, Cani PD, Francaux M. Toll-like receptor 4 knockout mice are protected against endoplasmic reticulum stress induced by a high-fat diet. PloS one. 2013;8(5):e65061. Epub 2013/06/07.

203.   Vijay-Kumar M, Sanders CJ, Taylor RT, Kumar A, Aitken JD, Sitaraman SV, et al. Deletion of TLR5 results in spontaneous colitis in mice. J Clin Invest. 2007;117(12):3909-21. Epub 2007/11/17.

204.   Schaffler A, Scholmerich J. Innate immunity and adipose tissue biology. Trends in immunology. 2010;31(6):228-35. Epub 2010/05/04.

205.   Broering R, Lu M, Schlaak JF. Role of Toll-like receptors in liver health and disease. Clin Sci (Lond). 2011;121(10):415-26. Epub 2011/07/30.

206.   Pillon NJ, Krook A. Innate immune receptors in skeletal muscle metabolism. Experimental cell research. 2017. Epub 2017/02/25.

207.   Lelouvier B, Servant F, Paisse S, Brunet AC, Benyahya S, Serino M, et al. Changes in blood microbiota profiles associated with liver fibrosis in obese patients: A pilot analysis. Hepatology. 2016;64(6):2015-27. Epub 2016/09/18.

208.   Chi W, Dao D, Lau TC, Henriksbo BD, Cavallari JF, Foley KP, et al. Bacterial peptidoglycan stimulates adipocyte lipolysis via NOD1. PloS one. 2014;9(5):e97675. Epub 2014/05/16.

209.   Chan KL, Tam TH, Boroumand P, Prescott D, Costford SR, Escalante NK, et al. Circulating NOD1 Activators and Hematopoietic NOD1 Contribute to Metabolic Inflammation and Insulin Resistance. Cell reports. 2017;18(10):2415-26. Epub 2017/03/09.

210.   Cavallari JF, Fullerton MD, Duggan BM, Foley KP, Denou E, Smith BK, et al. Muramyl Dipeptide-Based Postbiotics Mitigate Obesity-Induced Insulin Resistance via IRF4. Cell metabolism. 2017;25(5):1063-74 e3. Epub 2017/04/25.

211.   Veilleux A, Grenier E, Marceau P, Carpentier AC, Richard D, Levy E. Intestinal lipid handling: evidence and implication of insulin signaling abnormalities in human obese subjects. Arterioscler Thromb Vasc Biol. 2014;34(3):644-53. Epub 2014/01/11.

212.   Honka H, Makinen J, Hannukainen JC, Tarkia M, Oikonen V, Teras M, et al. Validation of [18F]fluorodeoxyglucose and positron emission tomography (PET) for the measurement of intestinal metabolism in pigs, and evidence of intestinal insulin resistance in patients with morbid obesity. Diabetologia. 2013;56(4):893-900. Epub 2013/01/22.

213.   Couture P, Tremblay AJ, Kelly I, Lemelin V, Droit A, Lamarche B. Key intestinal genes involved in lipoprotein metabolism are downregulated in dyslipidemic men with insulin resistance. J Lipid Res. 2014;55(1):128-37. Epub 2013/10/22.

214.   Phillips C, Mullan K, Owens D, Tomkin GH. Intestinal microsomal triglyceride transfer protein in type 2 diabetic and non-diabetic subjects: the relationship to triglyceride-rich postprandial lipoprotein composition. Atherosclerosis. 2006;187(1):57-64. Epub 2005/09/27.

215.   Krebs HA. Some aspects of the regulation of fuel supply in omnivorous animals. Advances in enzyme regulation. 1972;10:397-420. Epub 1972/01/01.

216.   Mithieux G, Rajas F, Zitoun C. Glucose utilization is suppressed in the gut of insulin-resistant high fat-fed rats and is restored by metformin. Biochemical pharmacology. 2006;72(2):198-203. Epub 2006/06/02.

217.   Tobin V, Le Gall M, Fioramonti X, Stolarczyk E, Blazquez AG, Klein C, et al. Insulin internalizes GLUT2 in the enterocytes of healthy but not insulin-resistant mice. Diabetes. 2008;57(3):555-62. Epub 2007/12/07.

218.   Ait-Omar A, Monteiro-Sepulveda M, Poitou C, Le Gall M, Cotillard A, Gilet J, et al. GLUT2 accumulation in enterocyte apical and intracellular membranes: a study in morbidly obese human subjects and ob/ob and high fat-fed mice. Diabetes. 2011;60(10):2598-607. Epub 2011/08/20.
219.   Mithieux G, Gautier-Stein A. Intestinal glucose metabolism revisited. Diabetes research and clinical practice. 2014;105(3):295-301. Epub 2014/06/28.
220.   Croset M, Rajas F, Zitoun C, Hurot JM, Montano S, Mithieux G. Rat small intestine is an insulin-sensitive gluconeogenic organ. Diabetes. 2001;50(4):740-6. Epub 2001/04/06.
221.   Mithieux G, Misery P, Magnan C, Pillot B, Gautier-Stein A, Bernard C, et al. Portal sensing of intestinal gluconeogenesis is a mechanistic link in the diminution of food intake induced by diet protein. Cell metabolism. 2005;2(5):321-9. Epub 2005/11/08.
222.   De Vadder F, Kovatcheva-Datchary P, Goncalves D, Vinera J, Zitoun C, Duchampt A, et al. Microbiota-generated metabolites promote metabolic benefits via gut-brain neural circuits. Cell. 2014;156(1-2):84-96. Epub 2014/01/15.
223.   Cani PD, Bibiloni R, Knauf C, Waget A, Neyrinck AM, Delzenne NM, et al. Changes in gut microbiota control metabolic endotoxemia-induced inflammation in high-fat diet-induced obesity and diabetes in mice. Diabetes. 2008;57(6):1470-81. Epub 2008/02/29.
224.   Backhed F, Ding H, Wang T, Hooper LV, Koh GY, Nagy A, et al. The gut microbiota as an environmental factor that regulates fat storage. Proceedings of the National Academy of Sciences of the United States of America. 2004;101(44):15718-23. Epub 2004/10/27.
225.   Turnbaugh PJ, Ley RE, Mahowald MA, Magrini V, Mardis ER, Gordon JI. An obesity-associated gut microbiome with increased capacity for energy harvest. Nature. 2006;444(7122):1027-31. Epub 2006/12/22.
226.   Chevalier C, Stojanovic O, Colin DJ, Suarez-Zamorano N, Tarallo V, Veyrat-Durebex C, et al. Gut Microbiota Orchestrates Energy Homeostasis during Cold. Cell. 2015;163(6):1360-74. Epub 2015/12/08.
227.   Whitman WB, Coleman DC, Wiebe WJ. Prokaryotes: the unseen majority. Proceedings of the National Academy of Sciences of the United States of America. 1998;95(12):6578-83. Epub 1998/06/17.
228.   Qin J, Li R, Raes J, Arumugam M, Burgdorf KS, Manichanh C, et al. A human gut microbial gene catalogue established by metagenomic sequencing. Nature. 2010;464(7285):59-65. Epub 2010/03/06.
229.   Scheithauer TP, Dallinga-Thie GM, de Vos WM, Nieuwdorp M, van Raalte DH. Causality of small and large intestinal microbiota in weight regulation and insulin resistance. Molecular metabolism. 2016;5(9):759-70. Epub 2016/09/13.
230.   Sender R, Fuchs S, Milo R. Revised Estimates for the Number of Human and Bacteria Cells in the Body. PLoS biology. 2016;14(8):e1002533. Epub 2016/08/20.
231.   Luckey TD. Introduction to intestinal microecology. The American journal of clinical nutrition. 1972;25(12):1292-4. Epub 1972/12/01.
232.   Backhed F, Ley RE, Sonnenburg JL, Peterson DA, Gordon JI. Host-bacterial mutualism in the human intestine. Science. 2005;307(5717):1915-20. Epub 2005/03/26.
233.   Ley RE, Peterson DA, Gordon JI. Ecological and evolutionary forces shaping microbial diversity in the human intestine. Cell. 2006;124(4):837-48. Epub 2006/02/25.
234.   Rodriguez JM, Murphy K, Stanton C, Ross RP, Kober OI, Juge N, et al. The composition of the gut microbiota throughout life, with an emphasis on early life. Microbial ecology in health and disease. 2015;26:26050. Epub 2015/02/06.
235.   Lozupone CA, Stombaugh JI, Gordon JI, Jansson JK, Knight R. Diversity, stability and resilience of the human gut microbiota. Nature. 2012;489(7415):220-30. Epub 2012/09/14.

236.   Yatsunenko T, Rey FE, Manary MJ, Trehan I, Dominguez-Bello MG, Contreras M, et al. Human gut microbiome viewed across age and geography. Nature. 2012;486(7402):222-7. Epub 2012/06/16.

237.   Backhed F, Roswall J, Peng Y, Feng Q, Jia H, Kovatcheva-Datchary P, et al. Dynamics and Stabilization of the Human Gut Microbiome during the First Year of Life. Cell host & microbe. 2015;17(6):852. Epub 2015/08/27.

238.   Olszak T, An D, Zeissig S, Vera MP, Richter J, Franke A, et al. Microbial exposure during early life has persistent effects on natural killer T cell function. Science. 2012;336(6080):489-93. Epub 2012/03/24.

239.   Goodrich JK, Waters JL, Poole AC, Sutter JL, Koren O, Blekhman R, et al. Human genetics shape the gut microbiome. Cell. 2014;159(4):789-99. Epub 2014/11/25.

240.   Hopkins MJ, Sharp R, Macfarlane GT. Age and disease related changes in intestinal bacterial populations assessed by cell culture, 16S rRNA abundance, and community cellular fatty acid profiles. Gut. 2001;48(2):198-205. Epub 2001/01/13.

241.   Martinez I, Stegen JC, Maldonado-Gomez MX, Eren AM, Siba PM, Greenhill AR, et al. The gut microbiota of rural papua new guineans: composition, diversity patterns, and ecological processes. Cell reports. 2015;11(4):527-38. Epub 2015/04/22.

242.   Wu GD, Chen J, Hoffmann C, Bittinger K, Chen YY, Keilbaugh SA, et al. Linking long-term dietary patterns with gut microbial enterotypes. Science. 2011;334(6052):105-8. Epub 2011/09/03.

243.   Rajilic-Stojanovic M, de Vos WM. The first 1000 cultured species of the human gastrointestinal microbiota. FEMS microbiology reviews. 2014;38(5):996-1047. Epub 2014/05/28.

244.   Derrien M, Collado MC, Ben-Amor K, Salminen S, de Vos WM. The Mucin degrader Akkermansia muciniphila is an abundant resident of the human intestinal tract. Applied and environmental microbiology. 2008;74(5):1646-8. Epub 2007/12/18.

245.   Tap J, Mondot S, Levenez F, Pelletier E, Caron C, Furet JP, et al. Towards the human intestinal microbiota phylogenetic core. Environmental microbiology. 2009;11(10):2574-84. Epub 2009/07/16.

246.   Arumugam M, Raes J, Pelletier E, Le Paslier D, Yamada T, Mende DR, et al. Enterotypes of the human gut microbiome. Nature. 2011;473(7346):174-80. Epub 2011/04/22.

247.   Hildebrand F, Nguyen TL, Brinkman B, Yunta RG, Cauwe B, Vandenabeele P, et al. Inflammation-associated enterotypes, host genotype, cage and inter-individual effects drive gut microbiota variation in common laboratory mice. Genome biology. 2013;14(1):R4. Epub 2013/01/26.

248.   Gorvitovskaia A, Holmes SP, Huse SM. Interpreting Prevotella and Bacteroides as biomarkers of diet and lifestyle. Microbiome. 2016;4:15. Epub 2016/04/14.

249.   De Filippo C, Cavalieri D, Di Paola M, Ramazzotti M, Poullet JB, Massart S, et al. Impact of diet in shaping gut microbiota revealed by a comparative study in children from Europe and rural Africa. Proceedings of the National Academy of Sciences of the United States of America. 2010;107(33):14691-6. Epub 2010/08/04.

250.   Huse SM, Ye Y, Zhou Y, Fodor AA. A core human microbiome as viewed through 16S rRNA sequence clusters. PloS one. 2012;7(6):e34242. Epub 2012/06/22.

251.   Koren O, Knights D, Gonzalez A, Waldron L, Segata N, Knight R, et al. A guide to enterotypes across the human body: meta-analysis of microbial community structures in human microbiome datasets. PLoS computational biology. 2013;9(1):e1002863. Epub 2013/01/18.

252.   Roager HM, Licht TR, Poulsen SK, Larsen TM, Bahl MI. Microbial enterotypes, inferred by the prevotella-to-bacteroides ratio, remained stable during a 6-month randomized controlled diet

intervention with the new nordic diet. Applied and environmental microbiology. 2014;80(3):1142-9. Epub 2013/12/04.

253.   Ramirez-Farias C, Slezak K, Fuller Z, Duncan A, Holtrop G, Louis P. Effect of inulin on the human gut microbiota: stimulation of Bifidobacterium adolescentis and Faecalibacterium prausnitzii. The British journal of nutrition. 2009;101(4):541-50. Epub 2008/07/02.

254.   Turnbaugh PJ, Backhed F, Fulton L, Gordon JI. Diet-induced obesity is linked to marked but reversible alterations in the mouse distal gut microbiome. Cell host & microbe. 2008;3(4):213-23. Epub 2008/04/15.

255.   Hjorth MF, Roager HM, Larsen TM, Poulsen SK, Licht TR, Bahl MI, et al. Pre-treatment microbial Prevotella-to-Bacteroides ratio, determines body fat loss success during a 6-month randomized controlled diet intervention. Int J Obes (Lond). 2017. Epub 2017/09/09.

256.   Samuel BS, Gordon JI. A humanized gnotobiotic mouse model of host-archaeal-bacterial mutualism. Proceedings of the National Academy of Sciences of the United States of America. 2006;103(26):10011-6. Epub 2006/06/20.

257.   Pedersen HK, Gudmundsdottir V, Nielsen HB, Hyotylainen T, Nielsen T, Jensen BA, et al. Human gut microbes impact host serum metabolome and insulin sensitivity. Nature. 2016;535(7612):376-81. Epub 2016/07/15.

258.   Troy EB, Kasper DL. Beneficial effects of Bacteroides fragilis polysaccharides on the immune system. Front Biosci (Landmark Ed). 2010;15:25-34. Epub 2009/12/29.

259.   Newgard CB, An J, Bain JR, Muehlbauer MJ, Stevens RD, Lien LF, et al. A branched-chain amino acid-related metabolic signature that differentiates obese and lean humans and contributes to insulin resistance. Cell metabolism. 2009;9(4):311-26. Epub 2009/04/10.

260.   Elinav E, Strowig T, Kau AL, Henao-Mejia J, Thaiss CA, Booth CJ, et al. NLRP6 inflammasome regulates colonic microbial ecology and risk for colitis. Cell. 2011;145(5):745-57. Epub 2011/05/14.

261.   Knights D, Ward TL, McKinlay CE, Miller H, Gonzalez A, McDonald D, et al. Rethinking "enterotypes". Cell host & microbe. 2014;16(4):433-7. Epub 2014/10/10.

262.   Zhou Y, Mihindukulasuriya KA, Gao H, La Rosa PS, Wylie KM, Martin JC, et al. Exploration of bacterial community classes in major human habitats. Genome biology. 2014;15(5):R66. Epub 2014/06/03.

263.   Jeffery IB, Claesson MJ, O'Toole PW, Shanahan F. Categorization of the gut microbiota: enterotypes or gradients? Nature reviews Microbiology. 2012;10(9):591-2. Epub 2012/10/16.

264.   Cotillard A, Kennedy SP, Kong LC, Prifti E, Pons N, Le Chatelier E, et al. Dietary intervention impact on gut microbial gene richness. Nature. 2013;500(7464):585-8. Epub 2013/08/30.

265.   Turnbaugh PJ, Hamady M, Yatsunenko T, Cantarel BL, Duncan A, Ley RE, et al. A core gut microbiome in obese and lean twins. Nature. 2009;457(7228):480-4. Epub 2008/12/02.

266.   Manichanh C, Rigottier-Gois L, Bonnaud E, Gloux K, Pelletier E, Frangeul L, et al. Reduced diversity of faecal microbiota in Crohn's disease revealed by a metagenomic approach. Gut. 2006;55(2):205-11. Epub 2005/09/29.

267.   Claesson MJ, Jeffery IB, Conde S, Power SE, O'Connor EM, Cusack S, et al. Gut microbiota composition correlates with diet and health in the elderly. Nature. 2012;488(7410):178-84. Epub 2012/07/17.

268.   Macfarlane S, Macfarlane GT. Regulation of short-chain fatty acid production. The Proceedings of the Nutrition Society. 2003;62(1):67-72. Epub 2003/05/13.

269.   Cummings JH, Macfarlane GT. The control and consequences of bacterial fermentation in the human colon. The Journal of applied bacteriology. 1991;70(6):443-59. Epub 1991/06/01.

270.   Cummings JH, Pomare EW, Branch WJ, Naylor CP, Macfarlane GT. Short chain fatty acids in human large intestine, portal, hepatic and venous blood. Gut. 1987;28(10):1221-7. Epub 1987/10/01.

271. Cox LM, Blaser MJ. Pathways in microbe-induced obesity. Cell metabolism. 2013;17(6):883-94. Epub 2013/06/12.

272. Lin HV, Frassetto A, Kowalik EJ, Jr., Nawrocki AR, Lu MM, Kosinski JR, et al. Butyrate and propionate protect against diet-induced obesity and regulate gut hormones via free fatty acid receptor 3-independent mechanisms. PloS one. 2012;7(4):e35240. Epub 2012/04/17.

273. Tolhurst G, Heffron H, Lam YS, Parker HE, Habib AM, Diakogiannaki E, et al. Short-chain fatty acids stimulate glucagon-like peptide-1 secretion via the G-protein-coupled receptor FFAR2. Diabetes. 2012;61(2):364-71. Epub 2011/12/23.

274. den Besten G, Bleeker A, Gerding A, van Eunen K, Havinga R, van Dijk TH, et al. Short-Chain Fatty Acids protect against High-Fat Diet-Induced Obesity via a PPARgamma-dependent switch from lipogenesis to fat oxidation. Diabetes. 2015. Epub 2015/02/20.

275. Demigne C, Morand C, Levrat MA, Besson C, Moundras C, Remesy C. Effect of propionate on fatty acid and cholesterol synthesis and on acetate metabolism in isolated rat hepatocytes. The British journal of nutrition. 1995;74(2):209-19. Epub 1995/08/01.

276. Sakakibara S, Yamauchi T, Oshima Y, Tsukamoto Y, Kadowaki T. Acetic acid activates hepatic AMPK and reduces hyperglycemia in diabetic KK-A(y) mice. Biochem Biophys Res Commun. 2006;344(2):597-604. Epub 2006/04/25.

277. Canfora EE, Jocken JW, Blaak EE. Short-chain fatty acids in control of body weight and insulin sensitivity. Nature reviews Endocrinology. 2015;11(10):577-91. Epub 2015/08/12.

278. Smith PM, Howitt MR, Panikov N, Michaud M, Gallini CA, Bohlooly YM, et al. The microbial metabolites, short-chain fatty acids, regulate colonic Treg cell homeostasis. Science. 2013;341(6145):569-73. Epub 2013/07/06.

279. Arpaia N, Campbell C, Fan X, Dikiy S, van der Veeken J, deRoos P, et al. Metabolites produced by commensal bacteria promote peripheral regulatory T-cell generation. Nature. 2013;504(7480):451-5. Epub 2013/11/15.

280. Furusawa Y, Obata Y, Fukuda S, Endo TA, Nakato G, Takahashi D, et al. Commensal microbe-derived butyrate induces the differentiation of colonic regulatory T cells. Nature. 2013;504(7480):446-50. Epub 2013/11/15.

281. Atarashi K, Tanoue T, Shima T, Imaoka A, Kuwahara T, Momose Y, et al. Induction of colonic regulatory T cells by indigenous Clostridium species. Science. 2011;331(6015):337-41. Epub 2011/01/06.

282. Bosi E, Molteni L, Radaelli MG, Folini L, Fermo I, Bazzigaluppi E, et al. Increased intestinal permeability precedes clinical onset of type 1 diabetes. Diabetologia. 2006;49(12):2824-7. Epub 2006/10/10.

283. Secondulfo M, Iafusco D, Carratu R, deMagistris L, Sapone A, Generoso M, et al. Ultrastructural mucosal alterations and increased intestinal permeability in non-celiac, type I diabetic patients. Digestive and liver disease : official journal of the Italian Society of Gastroenterology and the Italian Association for the Study of the Liver. 2004;36(1):35-45. Epub 2004/02/20.

284. Chang PV, Hao L, Offermanns S, Medzhitov R. The microbial metabolite butyrate regulates intestinal macrophage function via histone deacetylase inhibition. Proceedings of the National Academy of Sciences of the United States of America. 2014;111(6):2247-52. Epub 2014/01/07.

285. Hester CM, Jala VR, Langille MG, Umar S, Greiner KA, Haribabu B. Fecal microbes, short chain fatty acids, and colorectal cancer across racial/ethnic groups. World journal of gastroenterology : WJG. 2015;21(9):2759-69. Epub 2015/03/12.

286. Liou AP, Paziuk M, Luevano JM, Jr., Machineni S, Turnbaugh PJ, Kaplan LM. Conserved shifts in the gut microbiota due to gastric bypass reduce host weight and adiposity. Science translational medicine. 2013;5(178):178ra41. Epub 2013/03/29.

287.   Schnorr SL, Candela M, Rampelli S, Centanni M, Consolandi C, Basaglia G, et al. Gut microbiome of the Hadza hunter-gatherers. Nature communications. 2014;5:3654. Epub 2014/04/17.

288.   Fernandes J, Su W, Rahat-Rozenbloom S, Wolever TM, Comelli EM. Adiposity, gut microbiota and faecal short chain fatty acids are linked in adult humans. Nutrition & diabetes. 2014;4:e121. Epub 2014/07/01.

289.   Singh V, Chassaing B, Zhang L, San Yeoh B, Xiao X, Kumar M, et al. Microbiota-Dependent Hepatic Lipogenesis Mediated by Stearoyl CoA Desaturase 1 (SCD1) Promotes Metabolic Syndrome in TLR5-Deficient Mice. Cell metabolism. 2015;22(6):983-96. Epub 2015/11/04.

290.   Marette A, Jobin C. SCFAs Take a Toll En Route to Metabolic Syndrome. Cell metabolism. 2015;22(6):954-6. Epub 2015/12/05.

291.   Backhed F, Manchester JK, Semenkovich CF, Gordon JI. Mechanisms underlying the resistance to diet-induced obesity in germ-free mice. Proceedings of the National Academy of Sciences of the United States of America. 2007;104(3):979-84. Epub 2007/01/11.

292.   Ley RE, Backhed F, Turnbaugh P, Lozupone CA, Knight RD, Gordon JI. Obesity alters gut microbial ecology. Proceedings of the National Academy of Sciences of the United States of America. 2005;102(31):11070-5. Epub 2005/07/22.

293.   Ley RE, Turnbaugh PJ, Klein S, Gordon JI. Microbial ecology: human gut microbes associated with obesity. Nature. 2006;444(7122):1022-3. Epub 2006/12/22.

294.   Santacruz A, Collado MC, Garcia-Valdes L, Segura MT, Martin-Lagos JA, Anjos T, et al. Gut microbiota composition is associated with body weight, weight gain and biochemical parameters in pregnant women. The British journal of nutrition. 2010;104(1):83-92. Epub 2010/03/09.

295.   Armougom F, Henry M, Vialettes B, Raccah D, Raoult D. Monitoring bacterial community of human gut microbiota reveals an increase in Lactobacillus in obese patients and Methanogens in anorexic patients. PloS one. 2009;4(9):e7125. Epub 2009/09/24.

296.   Schwiertz A, Taras D, Schafer K, Beijer S, Bos NA, Donus C, et al. Microbiota and SCFA in lean and overweight healthy subjects. Obesity (Silver Spring). 2010;18(1):190-5. Epub 2009/06/06.

297.   Duncan SH, Lobley GE, Holtrop G, Ince J, Johnstone AM, Louis P, et al. Human colonic microbiota associated with diet, obesity and weight loss. Int J Obes (Lond). 2008;32(11):1720-4. Epub 2008/09/10.

298.   Ussar S, Griffin NW, Bezy O, Fujisaka S, Vienberg S, Softic S, et al. Interactions between Gut Microbiota, Host Genetics and Diet Modulate the Predisposition to Obesity and Metabolic Syndrome. Cell metabolism. 2015;22(3):516-30. Epub 2015/08/25.

299.   Ericsson AC, Davis JW, Spollen W, Bivens N, Givan S, Hagan CE, et al. Effects of vendor and genetic background on the composition of the fecal microbiota of inbred mice. PloS one. 2015;10(2):e0116704. Epub 2015/02/13.

300.   Rausch P, Basic M, Batra A, Bischoff SC, Blaut M, Clavel T, et al. Analysis of factors contributing to variation in the C57BL/6J fecal microbiota across German animal facilities. International journal of medical microbiology : IJMM. 2016;306(5):343-55. Epub 2016/04/08.

301.   Lozupone CA, Stombaugh J, Gonzalez A, Ackermann G, Wendel D, Vazquez-Baeza Y, et al. Meta-analyses of studies of the human microbiota. Genome research. 2013;23(10):1704-14. Epub 2013/07/19.

302.   Duncan SH, Belenguer A, Holtrop G, Johnstone AM, Flint HJ, Lobley GE. Reduced dietary intake of carbohydrates by obese subjects results in decreased concentrations of butyrate and butyrate-producing bacteria in feces. Applied and environmental microbiology. 2007;73(4):1073-8. Epub 2006/12/26.

303.   Li R, Wang H, Shi Q, Wang N, Zhang Z, Xiong C, et al. Effects of oral florfenicol and azithromycin on gut microbiota and adipogenesis in mice. PloS one. 2017;12(7):e0181690. Epub 2017/07/26.

304.   Payne AN, Chassard C, Zimmermann M, Muller P, Stinca S, Lacroix C. The metabolic activity of gut microbiota in obese children is increased compared with normal-weight children and exhibits more exhaustive substrate utilization. Nutrition & diabetes. 2011;1:e12. Epub 2011/01/01.

305.   Zhang H, DiBaise JK, Zuccolo A, Kudrna D, Braidotti M, Yu Y, et al. Human gut microbiota in obesity and after gastric bypass. Proceedings of the National Academy of Sciences of the United States of America. 2009;106(7):2365-70. Epub 2009/01/24.

306.   Lee MW, Odegaard JI, Mukundan L, Qiu Y, Molofsky AB, Nussbaum JC, et al. Activated type 2 innate lymphoid cells regulate beige fat biogenesis. Cell. 2015;160(1-2):74-87. Epub 2014/12/30.

307.   Hu J, Kyrou I, Tan BK, Dimitriadis GK, Ramanjaneya M, Tripathi G, et al. Short-Chain Fatty Acid Acetate Stimulates Adipogenesis and Mitochondrial Biogenesis via GPR43 in Brown Adipocytes. Endocrinology. 2016;157(5):1881-94. Epub 2016/03/19.

308.   Ley RE, Hamady M, Lozupone C, Turnbaugh PJ, Ramey RR, Bircher JS, et al. Evolution of mammals and their gut microbes. Science. 2008;320(5883):1647-51. Epub 2008/05/24.

309.   Belzer C, de Vos WM. Microbes inside--from diversity to function: the case of Akkermansia. The ISME journal. 2012;6(8):1449-58. Epub 2012/03/23.

310.   Derrien M, Vaughan EE, Plugge CM, de Vos WM. Akkermansia muciniphila gen. nov., sp. nov., a human intestinal mucin-degrading bacterium. International journal of systematic and evolutionary microbiology. 2004;54(Pt 5):1469-76. Epub 2004/09/25.

311.   Wang L, Christophersen CT, Sorich MJ, Gerber JP, Angley MT, Conlon MA. Low relative abundances of the mucolytic bacterium Akkermansia muciniphila and Bifidobacterium spp. in feces of children with autism. Applied and environmental microbiology. 2011;77(18):6718-21. Epub 2011/07/26.

312.   Png CW, Linden SK, Gilshenan KS, Zoetendal EG, McSweeney CS, Sly LI, et al. Mucolytic bacteria with increased prevalence in IBD mucosa augment in vitro utilization of mucin by other bacteria. The American journal of gastroenterology. 2010;105(11):2420-8. Epub 2010/07/22.

313.   Swidsinski A, Dorffel Y, Loening-Baucke V, Theissig F, Ruckert JC, Ismail M, et al. Acute appendicitis is characterised by local invasion with Fusobacterium nucleatum/necrophorum. Gut. 2011;60(1):34-40. Epub 2009/11/21.

314.   Zhang X, Shen D, Fang Z, Jie Z, Qiu X, Zhang C, et al. Human gut microbiota changes reveal the progression of glucose intolerance. PloS one. 2013;8(8):e71108. Epub 2013/09/10.

315.   Karlsson FH, Tremaroli V, Nookaew I, Bergstrom G, Behre CJ, Fagerberg B, et al. Gut metagenome in European women with normal, impaired and diabetic glucose control. Nature. 2013;498(7452):99-103. Epub 2013/05/31.

316.   Dao MC, Everard A, Aron-Wisnewsky J, Sokolovska N, Prifti E, Verger EO, et al. Akkermansia muciniphila and improved metabolic health during a dietary intervention in obesity: relationship with gut microbiome richness and ecology. Gut. 2016;65(3):426-36. Epub 2015/06/24.

317.   Derrien M, Van Baarlen P, Hooiveld G, Norin E, Muller M, de Vos WM. Modulation of Mucosal Immune Response, Tolerance, and Proliferation in Mice Colonized by the Mucin-Degrader Akkermansia muciniphila. Frontiers in microbiology. 2011;2:166. Epub 2011/09/10.

318.   Lukovac S, Belzer C, Pellis L, Keijser BJ, de Vos WM, Montijn RC, et al. Differential modulation by Akkermansia muciniphila and Faecalibacterium prausnitzii of host peripheral lipid metabolism and histone acetylation in mouse gut organoids. mBio. 2014;5(4). Epub 2014/08/15.

319.   Seth EC, Taga ME. Nutrient cross-feeding in the microbial world. Frontiers in microbiology. 2014;5:350. Epub 2014/07/30.

320.   Fusunyan RD, Quinn JJ, Fujimoto M, MacDermott RP, Sanderson IR. Butyrate switches the pattern of chemokine secretion by intestinal epithelial cells through histone acetylation. Mol Med. 1999;5(9):631-40. Epub 1999/11/07.

321.   Alenghat T, Osborne LC, Saenz SA, Kobuley D, Ziegler CG, Mullican SE, et al. Histone deacetylase 3 coordinates commensal-bacteria-dependent intestinal homeostasis. Nature. 2013;504(7478):153-7. Epub 2013/11/05.

322.   Anhe FF, Marette A. A microbial protein that alleviates metabolic syndrome. Nature medicine. 2017;23(1):11-2. Epub 2017/01/07.

323.   Shin NR, Lee JC, Lee HY, Kim MS, Whon TW, Lee MS, et al. An increase in the Akkermansia spp. population induced by metformin treatment improves glucose homeostasis in diet-induced obese mice. Gut. 2014;63(5):727-35. Epub 2013/06/28.

324.   Greer RL, Dong X, Moraes AC, Zielke RA, Fernandes GR, Peremyslova E, et al. Akkermansia muciniphila mediates negative effects of IFNgamma on glucose metabolism. Nature communications. 2016;7:13329. Epub 2016/11/15.

325.   Nath N, Khan M, Paintlia MK, Singh I, Hoda MN, Giri S. Metformin attenuated the autoimmune disease of the central nervous system in animal models of multiple sclerosis. J Immunol. 2009;182(12):8005-14. Epub 2009/06/06.

326.   de la Cuesta-Zuluaga J, Mueller NT, Corrales-Agudelo V, Velasquez-Mejia EP, Carmona JA, Abad JM, et al. Metformin Is Associated With Higher Relative Abundance of Mucin-Degrading Akkermansia muciniphila and Several Short-Chain Fatty Acid-Producing Microbiota in the Gut. Diabetes care. 2017;40(1):54-62. Epub 2016/12/22.

327.   Wu H, Esteve E, Tremaroli V, Khan MT, Caesar R, Manneras-Holm L, et al. Metformin alters the gut microbiome of individuals with treatment-naive type 2 diabetes, contributing to the therapeutic effects of the drug. Nature medicine. 2017. Epub 2017/05/23.

328.   Thomas C, Pellicciari R, Pruzanski M, Auwerx J, Schoonjans K. Targeting bile-acid signalling for metabolic diseases. Nature reviews Drug discovery. 2008;7(8):678-93. Epub 2008/08/02.

329.   Lefebvre P, Cariou B, Lien F, Kuipers F, Staels B. Role of bile acids and bile acid receptors in metabolic regulation. Physiol Rev. 2009;89(1):147-91. Epub 2009/01/08.

330.   Goodwin B, Jones SA, Price RR, Watson MA, McKee DD, Moore LB, et al. A regulatory cascade of the nuclear receptors FXR, SHP-1, and LRH-1 represses bile acid biosynthesis. Mol Cell. 2000;6(3):517-26. Epub 2000/10/13.

331.   Sinal CJ, Tohkin M, Miyata M, Ward JM, Lambert G, Gonzalez FJ. Targeted disruption of the nuclear receptor FXR/BAR impairs bile acid and lipid homeostasis. Cell. 2000;102(6):731-44. Epub 2000/10/13.

332.   Inagaki T, Choi M, Moschetta A, Peng L, Cummins CL, McDonald JG, et al. Fibroblast growth factor 15 functions as an enterohepatic signal to regulate bile acid homeostasis. Cell metabolism. 2005;2(4):217-25. Epub 2005/10/11.

333.   Potthoff MJ, Kliewer SA, Mangelsdorf DJ. Endocrine fibroblast growth factors 15/19 and 21: from feast to famine. Genes & development. 2012;26(4):312-24. Epub 2012/02/04.

334.   Kong B, Wang L, Chiang JY, Zhang Y, Klaassen CD, Guo GL. Mechanism of tissue-specific farnesoid X receptor in suppressing the expression of genes in bile-acid synthesis in mice. Hepatology. 2012;56(3):1034-43. Epub 2012/04/03.

335.   Zhu Y, Li F, Guo GL. Tissue-specific function of farnesoid X receptor in liver and intestine. Pharmacological research. 2011;63(4):259-65. Epub 2011/01/08.

336.   Wang H, Chen J, Hollister K, Sowers LC, Forman BM. Endogenous bile acids are ligands for the nuclear receptor FXR/BAR. Mol Cell. 1999;3(5):543-53. Epub 1999/06/09.

337. Mueller M, Thorell A, Claudel T, Jha P, Koefeler H, Lackner C, et al. Ursodeoxycholic acid exerts farnesoid X receptor-antagonistic effects on bile acid and lipid metabolism in morbid obesity. Journal of hepatology. 2015;62(6):1398-404. Epub 2015/01/27.

338. Gonzalez FJ, Jiang C, Bisson WH, Patterson AD. Inhibition of farnesoid X receptor signaling shows beneficial effects in human obesity. Journal of hepatology. 2015;62(6):1234-6. Epub 2015/03/10.

339. Ma K, Saha PK, Chan L, Moore DD. Farnesoid X receptor is essential for normal glucose homeostasis. J Clin Invest. 2006;116(4):1102-9. Epub 2006/03/25.

340. Lambert G, Amar MJ, Guo G, Brewer HB, Jr., Gonzalez FJ, Sinal CJ. The farnesoid X-receptor is an essential regulator of cholesterol homeostasis. The Journal of biological chemistry. 2003;278(4):2563-70. Epub 2002/11/08.

341. Zhang Y, Wang X, Vales C, Lee FY, Lee H, Lusis AJ, et al. FXR deficiency causes reduced atherosclerosis in Ldlr-/- mice. Arterioscler Thromb Vasc Biol. 2006;26(10):2316-21. Epub 2006/07/11.

342. Zhang Y, Ge X, Heemstra LA, Chen WD, Xu J, Smith JL, et al. Loss of FXR protects against diet-induced obesity and accelerates liver carcinogenesis in ob/ob mice. Mol Endocrinol. 2012;26(2):272-80. Epub 2012/01/21.

343. Parseus A, Sommer N, Sommer F, Caesar R, Molinaro A, Stahlman M, et al. Microbiota-induced obesity requires farnesoid X receptor. Gut. 2017;66(3):429-37. Epub 2016/01/08.

344. Prawitt J, Abdelkarim M, Stroeve JH, Popescu I, Duez H, Velagapudi VR, et al. Farnesoid X receptor deficiency improves glucose homeostasis in mouse models of obesity. Diabetes. 2011;60(7):1861-71. Epub 2011/05/20.

345. Hanniman EA, Lambert G, McCarthy TC, Sinal CJ. Loss of functional farnesoid X receptor increases atherosclerotic lesions in apolipoprotein E-deficient mice. J Lipid Res. 2005;46(12):2595-604. Epub 2005/09/28.

346. Schmitt J, Kong B, Stieger B, Tschopp O, Schultze SM, Rau M, et al. Protective effects of farnesoid X receptor (FXR) on hepatic lipid accumulation are mediated by hepatic FXR and independent of intestinal FGF15 signal. Liver international : official journal of the International Association for the Study of the Liver. 2015;35(4):1133-44. Epub 2014/08/27.

347. Mudaliar S, Henry RR, Sanyal AJ, Morrow L, Marschall HU, Kipnes M, et al. Efficacy and safety of the farnesoid X receptor agonist obeticholic acid in patients with type 2 diabetes and nonalcoholic fatty liver disease. Gastroenterology. 2013;145(3):574-82 e1. Epub 2013/06/04.

348. Neuschwander-Tetri BA, Loomba R, Sanyal AJ, Lavine JE, Van Natta ML, Abdelmalek MF, et al. Farnesoid X nuclear receptor ligand obeticholic acid for non-cirrhotic, non-alcoholic steatohepatitis (FLINT): a multicentre, randomised, placebo-controlled trial. Lancet. 2015;385(9972):956-65. Epub 2014/12/04.

349. Jiang C, Xie C, Lv Y, Li J, Krausz KW, Shi J, et al. Intestine-selective farnesoid X receptor inhibition improves obesity-related metabolic dysfunction. Nature communications. 2015;6:10166. Epub 2015/12/17.

350. Li F, Jiang C, Krausz KW, Li Y, Albert I, Hao H, et al. Microbiome remodelling leads to inhibition of intestinal farnesoid X receptor signalling and decreased obesity. Nature communications. 2013;4:2384. Epub 2013/09/26.

351. Devkota S, Wang Y, Musch MW, Leone V, Fehlner-Peach H, Nadimpalli A, et al. Dietary-fat-induced taurocholic acid promotes pathobiont expansion and colitis in Il10-/- mice. Nature. 2012;487(7405):104-8. Epub 2012/06/23.

352. Kawamata Y, Fujii R, Hosoya M, Harada M, Yoshida H, Miwa M, et al. A G protein-coupled receptor responsive to bile acids. The Journal of biological chemistry. 2003;278(11):9435-40. Epub 2003/01/14.

353. Maruyama T, Miyamoto Y, Nakamura T, Tamai Y, Okada H, Sugiyama E, et al. Identification of membrane-type receptor for bile acids (M-BAR). Biochem Biophys Res Commun. 2002;298(5):714-9. Epub 2002/11/07.

354. Vassileva G, Golovko A, Markowitz L, Abbondanzo SJ, Zeng M, Yang S, et al. Targeted deletion of Gpbar1 protects mice from cholesterol gallstone formation. The Biochemical journal. 2006;398(3):423-30. Epub 2006/05/27.

355. Chen X, Lou G, Meng Z, Huang W. TGR5: a novel target for weight maintenance and glucose metabolism. Experimental diabetes research. 2011;2011:853501. Epub 2011/07/15.

356. Thomas C, Gioiello A, Noriega L, Strehle A, Oury J, Rizzo G, et al. TGR5-mediated bile acid sensing controls glucose homeostasis. Cell metabolism. 2009;10(3):167-77. Epub 2009/09/03.

357. Wahlstrom A, Sayin SI, Marschall HU, Backhed F. Intestinal Crosstalk between Bile Acids and Microbiota and Its Impact on Host Metabolism. Cell metabolism. 2016;24(1):41-50. Epub 2016/06/21.

358. Inagaki T, Moschetta A, Lee YK, Peng L, Zhao G, Downes M, et al. Regulation of antibacterial defense in the small intestine by the nuclear bile acid receptor. Proceedings of the National Academy of Sciences of the United States of America. 2006;103(10):3920-5. Epub 2006/02/14.

359. Grzybowski A, Pietrzak K. Albert Szent-Gyorgyi (1893-1986): the scientist who discovered vitamin C. Clinics in dermatology. 2013;31(3):327-31. Epub 2013/06/07.

360. Rusznyak S, Szent-Gyorgyi A. Vitamin P: flavonols as vitamins. Nature. 1936;138.

361. Hertog MG, Kromhout D, Aravanis C, Blackburn H, Buzina R, Fidanza F, et al. Flavonoid intake and long-term risk of coronary heart disease and cancer in the seven countries study. Archives of internal medicine. 1995;155(4):381-6. Epub 1995/02/27.

362. Arts IC, Hollman PC. Polyphenols and disease risk in epidemiologic studies. The American journal of clinical nutrition. 2005;81(1 Suppl):317S-25S. Epub 2005/01/11.

363. Hirvonen T, Virtamo J, Korhonen P, Albanes D, Pietinen P. Flavonol and flavone intake and the risk of cancer in male smokers (Finland). Cancer causes & control : CCC. 2001;12(9):789-96. Epub 2001/11/21.

364. Lambert JD, Hong J, Yang GY, Liao J, Yang CS. Inhibition of carcinogenesis by polyphenols: evidence from laboratory investigations. The American journal of clinical nutrition. 2005;81(1 Suppl):284S-91S. Epub 2005/01/11.

365. Williamson G, Manach C. Bioavailability and bioefficacy of polyphenols in humans. II. Review of 93 intervention studies. The American journal of clinical nutrition. 2005;81(1 Suppl):243S-55S. Epub 2005/01/11.

366. Cesoniene L, Jasutiene I, Sarkinas A. Phenolics and anthocyanins in berries of European cranberry and their antimicrobial activity. Medicina (Kaunas, Lithuania). 2009;45(12):992-9.

367. Cushnie T, Lamb A. Recent advances in understanding the antibacterial properties of flavonoids. International journal of antimicrobial agents. 2011;38(2):99-107.

368. Heim K, Tagliaferro A, Bobilya D. Flavonoid antioxidants: chemistry, metabolism and structure-activity relationships. The Journal of nutritional biochemistry. 2002;13(10):572-84.

369. Manach C, Williamson G, Morand C, Scalbert A, Rémésy C. Bioavailability and bioefficacy of polyphenols in humans. I. Review of 97 bioavailability studies. The American journal of clinical nutrition. 2005;81(1 Suppl).

370. Harborne J, Williams C. Advances in flavonoid research since 1992. Phytochemistry. 2000;55(6):481-504.

371. Crozier A, Clifford, M. N. and Ashihara, H. Frontmatter. Plant Secondary Metabolites: Blackwell Publishing Ltd; 2007. p. i-xii.

372.   Day A, Cañada F, Díaz J, Kroon P, McLauchlan R, Faulds C, et al. Dietary flavonoid and isoflavone glycosides are hydrolysed by the lactase site of lactase phlorizin hydrolase. FEBS letters. 2000;468(2-3):166-70.

373.   Day A, DuPont M, Ridley S, Rhodes M, Morgan M, Williamson G. Deglycosylation of flavonoid and isoflavonoid glycosides by human small intestine and liver beta-glucosidase activity. FEBS letters. 1998;436(1):71-5.

374.   Gee J, DuPont M, Day A, Plumb G, Williamson G, Johnson I. Intestinal transport of quercetin glycosides in rats involves both deglycosylation and interaction with the hexose transport pathway. The Journal of nutrition. 2000;130(11):2765-71.

375.   Moco S, Martin F-PJ, Rezzi S. Metabolomics View on Gut Microbiome Modulation by Polyphenol-rich Foods. Journal of proteome research. 2012;11(10):4781-90.

376.   Anhê FF, Desjardins Y, Pilon G, Dudonné S, Genovese MI, Lajolo FM, et al. Polyphenols and type 2 diabetes: A prospective review. PharmaNutrition. 2013;1(4):105-14.

377.   Fraga CG, Galleano M, Verstraeten SV, Oteiza PI. Basic biochemical mechanisms behind the health benefits of polyphenols. Molecular aspects of medicine. 2010;31(6):435-45. Epub 2010/09/22.

378.   Moskaug JO, Carlsen H, Myhrstad MC, Blomhoff R. Polyphenols and glutathione synthesis regulation. The American journal of clinical nutrition. 2005;81(1 Suppl):277S-83S. Epub 2005/01/11.

379.   Hayeshi R, Mutingwende I, Mavengere W, Masiyanise V, Mukanganyama S. The inhibition of human glutathione S-transferases activity by plant polyphenolic compounds ellagic acid and curcumin. Food and Chemical Toxicology. 2007;45(2):286-95.

380.   Khan SM. Protective effect of black tea extract on the levels of lipid peroxidation and antioxidant enzymes in liver of mice with pesticide-induced liver injury. Cell biochemistry and function. 2006;24(4):327-32. Epub 2005/07/02.

381.   Hanhineva K, Törrönen R, Bondia-Pons I, Pekkinen J, Kolehmainen M, Mykkänen H, et al. Impact of dietary polyphenols on carbohydrate metabolism. International journal of molecular sciences. 2010;11(4):1365-402.

382.   Montopoli M, Ragazzi E, Froldi G, Caparrotta L. Cell-cycle inhibition and apoptosis induced by curcumin and cisplatin or oxaliplatin in human ovarian carcinoma cells. Cell Proliferation. 2009;42(2):195-206.

383.   Ohara K, Uchida A, Nagasaka R, Ushio H, Ohshima T. The effects of hydroxycinnamic acid derivatives on adiponectin secretion. Phytomedicine : international journal of phytotherapy and phytopharmacology. 2009;16(2-3):130-7. Epub 2008/11/18.

384.   Kim SO, Kundu JK, Shin YK, Park JH, Cho MH, Kim TY, et al. [6]-Gingerol inhibits COX-2 expression by blocking the activation of p38 MAP kinase and NF-kappaB in phorbol ester-stimulated mouse skin. Oncogene. 2005;24(15):2558-67. Epub 2005/03/01.

385.   Kim C-S, Kawada T, Kim B-S, Han I-S, Choe S-Y, Kurata T, et al. Capsaicin exhibits anti-inflammatory property by inhibiting IkB-a degradation in LPS-stimulated peritoneal macrophages. Cellular Signalling. 2003;15(3):299-306.

386.   Park J-Y, Kawada T, Han I-S, Kim B-S, Goto T, Takahashi N, et al. Capsaicin inhibits the production of tumor necrosis factor α by LPS-stimulated murine macrophages, RAW 264.7: a PPARγ ligand-like action as a novel mechanism. FEBS letters. 2004;572(1–3):266-70.

387.   Kang J-H, Kim C-S, Han I-S, Kawada T, Yu R. Capsaicin, a spicy component of hot peppers, modulates adipokine gene expression and protein release from obese-mouse adipose tissues and isolated adipocytes, and suppresses the inflammatory responses of adipose tissue macrophages. FEBS letters. 2007;581(23):4389-96.

388. Chun KS, Sohn Y, Kim HS, Kim OH, Park KK, Lee JM, et al. Anti-tumor promoting potential of naturally occurring diarylheptanoids structurally related to curcumin. Mutat Res. 1999;428(1-2):49-57. Epub 1999/10/13.

389. Chacon MR, Ceperuelo-Mallafre V, Maymo-Masip E, Mateo-Sanz JM, Arola L, Guitierrez C, et al. Grape-seed procyanidins modulate inflammation on human differentiated adipocytes in vitro. Cytokine. 2009;47(2):137-42. Epub 2009/06/30.

390. Chung JY, Park JO, Phyu H, Dong Z, Yang CS. Mechanisms of inhibition of the Ras-MAP kinase signaling pathway in 30.7b Ras 12 cells by tea polyphenols (-)-epigallocatechin-3-gallate and theaflavin-3,3'-digallate1. The FASEB Journal. 2001.

391. Muraoka K, Shimizu K, Sun X, Tani T, Izumi R, Miwa K, et al. Flavonoids exert diverse inhibitory effects on the activation of nf-κb. Transplantation proceedings. 2002;34(4):1335-40.

392. Ahn J, Lee H, Kim S, Ha T. Resveratrol inhibits TNF-α-induced changes of adipokines in 3T3-L1 adipocytes. Biochemical and biophysical research communications. 2007;364(4):972-7.

393. Zhu J, Yong W, Wu X, Yu Y, lv J, Liu C, et al. Anti-inflammatory effect of resveratrol on TNF-α-induced MCP-1 expression in adipocytes. Biochemical and biophysical research communications. 2008;369(2):471-7.

394. Olholm J, Paulsen SK, Cullberg KB, Richelsen B, Pedersen SB. Anti-inflammatory effect of resveratrol on adipokine expression and secretion in human adipose tissue explants. Int J Obes (Lond). 2010;34(10):1546-53. Epub 2010/06/10.

395. Wang A, Liu M, Liu X, Dong LQ, Glickman RD, Slaga TJ, et al. Up-regulation of Adiponectin by Resveratrol. Journal of Biological Chemistry. 2011;286(1):60-6.

396. Chuang C-C, Martinez K, Xie G, Kennedy A, Bumrungpert A, Overman A, et al. Quercetin is equally or more effective than resveratrol in attenuating tumor necrosis factor-α–mediated inflammation and insulin resistance in primary human adipocytes. The American journal of clinical nutrition. 2010;92(6):1511-21.

397. Qureshi AA, Tan X, Reis JC, Badr MZ, Papasian CJ, Morrison DC, et al. Suppression of nitric oxide induction and pro-inflammatory cytokines by novel proteasome inhibitors in various experimental models. Lipids in health and disease. 2011;10:177. Epub 2011/10/14.

398. Dulloo AG, Duret C, Rohrer D, Girardier L, Mensi N, Fathi M, et al. Efficacy of a green tea extract rich in catechin polyphenols and caffeine in increasing 24-h energy expenditure and fat oxidation in humans. Am J Clin Nutr. 1999;70(6):1040-5. Epub 1999/12/03.

399. Borchardt RT, Huber JA. Catechol O-methyltransferase. 5. Structure-activity relationships for inhibition by flavonoids. Journal of medicinal chemistry. 1975;18(1):120-2. Epub 1975/01/01.

400. Gugler R, Dengler HJ. Inhibition of human liver catechol-O-methyltransferase by flavonoids. Naunyn-Schmiedeberg's archives of pharmacology. 1973;276(2):223-33. Epub 1973/02/23.

401. Chen D, Wang CY, Lambert JD, Ai N, Welsh WJ, Yang CS. Inhibition of human liver catechol-O-methyltransferase by tea catechins and their metabolites: structure-activity relationship and molecular-modeling studies. Biochemical pharmacology. 2005;69(10):1523-31. Epub 2005/04/29.

402. Ku CR, Cho YH, Hong ZY, Lee H, Lee SJ, Hong SS, et al. The Effects of High Fat Diet and Resveratrol on Mitochondrial Activity of Brown Adipocytes. Endocrinol Metab (Seoul). 2016;31(2):328-35. Epub 2016/04/15.

403. Diepvens K, Westerterp KR, Westerterp-Plantenga MS. Obesity and thermogenesis related to the consumption of caffeine, ephedrine, capsaicin, and green tea. American journal of physiology Regulatory, integrative and comparative physiology. 2007;292(1):R77-85. Epub 2006/07/15.

404.   Lee YM, Choi JS, Kim MH, Jung MH, Lee YS, Song J. Effects of dietary genistein on hepatic lipid metabolism and mitochondrial function in mice fed high-fat diets. Nutrition. 2006;22(9):956-64. Epub 2006/07/04.

405.   Lee MS, Kim CT, Kim IH, Kim Y. Effects of capsaicin on lipid catabolism in 3T3-L1 adipocytes. Phytotherapy research : PTR. 2011;25(6):935-9. Epub 2011/06/01.

406.   Chung S, Yao H, Caito S, Hwang JW, Arunachalam G, Rahman I. Regulation of SIRT1 in cellular functions: role of polyphenols. Arch Biochem Biophys. 2010;501(1):79-90. Epub 2010/05/11.

407.   Howitz KT, Bitterman KJ, Cohen HY, Lamming DW, Lavu S, Wood JG, et al. Small molecule activators of sirtuins extend Saccharomyces cerevisiae lifespan. Nature. 2003;425(6954):191-6. Epub 2003/08/27.

408.   Lagouge M, Argmann C, Gerhart-Hines Z, Meziane H, Lerin C, Daussin F, et al. Resveratrol improves mitochondrial function and protects against metabolic disease by activating SIRT1 and PGC-1alpha. Cell. 2006;127(6):1109-22. Epub 2006/11/23.

409.   Pearson KJ, Baur JA, Lewis KN, Peshkin L, Price NL, Labinskyy N, et al. Resveratrol delays age-related deterioration and mimics transcriptional aspects of dietary restriction without extending life span. Cell Metab. 2008;8(2):157-68. Epub 2008/07/05.

410.   Qiang L, Wang L, Kon N, Zhao W, Lee S, Zhang Y, et al. Brown remodeling of white adipose tissue by SirT1-dependent deacetylation of Ppargamma. Cell. 2012;150(3):620-32. Epub 2012/08/07.

411.   Ganesan S, Faris AN, Comstock AT, Chattoraj SS, Chattoraj A, Burgess JR, et al. Quercetin prevents progression of disease in elastase/LPS-exposed mice by negatively regulating MMP expression. Respiratory research. 2010;11:131. Epub 2010/10/06.

412.   Davis JM, Murphy EA, Carmichael MD, Davis B. Quercetin increases brain and muscle mitochondrial biogenesis and exercise tolerance. American journal of physiology Regulatory, integrative and comparative physiology. 2009;296(4):R1071-7. Epub 2009/02/13.

413.   de Boer VC, de Goffau MC, Arts IC, Hollman PC, Keijer J. SIRT1 stimulation by polyphenols is affected by their stability and metabolism. Mech Ageing Dev. 2006;127(7):618-27. Epub 2006/04/11.

414.   de Moreno de LeBlanc A, del Carmen S, Chatel J-M, Miyoshi A, Azevedo V, Langella P, et al. Current Review of Genetically Modified Lactic Acid Bacteria for the Prevention and Treatment of Colitis Using Murine Models. Gastroenterology Research and Practice. 2015;2015:8.

415.   Mooney RA, Senn J, Cameron S, Inamdar N, Boivin LM, Shang Y, et al. Suppressors of cytokine signaling-1 and -6 associate with and inhibit the insulin receptor. A potential mechanism for cytokine-mediated insulin resistance. The Journal of biological chemistry. 2001;276(28):25889-93. Epub 2001/05/09.

416.   Denis MC, Desjardins Y, Furtos A, Marcil V, Dudonne S, Montoudis A, et al. Prevention of oxidative stress, inflammation and mitochondrial dysfunction in the intestine by different cranberry phenolic fractions. Clin Sci (Lond). 2015;128(3):197-212. Epub 2014/07/30.

417.   Masumoto S, Terao A, Yamamoto Y, Mukai T, Miura T, Shoji T. Non-absorbable apple procyanidins prevent obesity associated with gut microbial and metabolomic changes. Scientific reports. 2016;6:31208. Epub 2016/08/11.

418.   Hosseini B, Saedisomeolia A, Wood LG, Yaseri M, Tavasoli S. Effects of pomegranate extract supplementation on inflammation in overweight and obese individuals: A randomized controlled clinical trial. Complementary therapies in clinical practice. 2016;22:44-50. Epub 2016/02/07.

419.   Yang J, Henning SM, Lee R, Hsu M, Grojean EM, Ly A, et al. Effects of Pomegranate Extract on High Fat/High Sucrose Diet induced Obesity are Dependent on the Intestinal Formation of Urolithin A. The FASEB Journal. 2016;30(1 Supplement):691.28.

420.   Neyrinck AM, Van Hee VF, Bindels LB, De Backer F, Cani PD, Delzenne NM. Polyphenol-rich extract of pomegranate peel alleviates tissue inflammation and hypercholesterolaemia in high-fat diet-induced obese mice: potential implication of the gut microbiota. The British journal of nutrition. 2013;109(5):802-9. Epub 2012/06/09.

421.   Espin JC, Larrosa M, Garcia-Conesa MT, Tomas-Barberan F. Biological significance of urolithins, the gut microbial ellagic Acid-derived metabolites: the evidence so far. Evidence-based complementary and alternative medicine : eCAM. 2013;2013:270418. Epub 2013/06/20.

422.   Ryu D, Mouchiroud L, Andreux PA, Katsyuba E, Moullan N, Nicolet-Dit-Felix AA, et al. Urolithin A induces mitophagy and prolongs lifespan in C. elegans and increases muscle function in rodents. Nature medicine. 2016;22(8):879-88. Epub 2016/07/12.

423.   Panchal SK, Ward L, Brown L. Ellagic acid attenuates high-carbohydrate, high-fat diet-induced metabolic syndrome in rats. European journal of nutrition. 2013;52(2):559-68. Epub 2012/04/28.

424.   Howitz KT, Sinclair DA. Xenohormesis: sensing the chemical cues of other species. Cell. 2008;133(3):387-91. Epub 2008/05/06.

425.   Zhernakova A, Kurilshikov A, Bonder MJ, Tigchelaar EF, Schirmer M, Vatanen T, et al. Population-based metagenomics analysis reveals markers for gut microbiome composition and diversity. Science. 2016;352(6285):565-9. Epub 2016/04/30.

426.   Henning SM, Summanen PH, Lee RP, Yang J, Finegold SM, Heber D, et al. Pomegranate ellagitannins stimulate the growth of Akkermansia muciniphila in vivo. Anaerobe. 2017;43:56-60. Epub 2016/12/13.

427.   Baldwin J, Collins B, Wolf PG, Martinez K, Shen W, Chuang CC, et al. Table grape consumption reduces adiposity and markers of hepatic lipogenesis and alters gut microbiota in butter fat-fed mice. The Journal of nutritional biochemistry. 2016;27:123-35. Epub 2015/10/02.

428.   Roopchand DE, Carmody RN, Kuhn P, Moskal K, Rojas-Silva P, Turnbaugh PJ, et al. Dietary Polyphenols Promote Growth of the Gut Bacterium Akkermansia muciniphila and Attenuate High-Fat Diet-Induced Metabolic Syndrome. Diabetes. 2015;64(8):2847-58. Epub 2015/04/08.

429.   Neyrinck AM, Etxeberria U, Taminiau B, Daube G, Van Hul M, Everard A, et al. Rhubarb extract prevents hepatic inflammation induced by acute alcohol intake, an effect related to the modulation of the gut microbiota. Mol Nutr Food Res. 2017;61(1). Epub 2016/03/19.

430.   Heyman-Linden L, Kotowska D, Sand E, Bjursell M, Plaza M, Turner C, et al. Lingonberries alter the gut microbiota and prevent low-grade inflammation in high-fat diet fed mice. Food & nutrition research. 2016;60:29993. Epub 2016/04/30.

431.   Zhang Z, Wu X, Cao S, Wang L, Wang D, Yang H, et al. Caffeic acid ameliorates colitis in association with increased Akkermansia population in the gut microbiota of mice. Oncotarget. 2016;7(22):31790-9. Epub 2016/05/14.

432.   Etxeberria U, Arias N, Boque N, Macarulla MT, Portillo MP, Martinez JA, et al. Reshaping faecal gut microbiota composition by the intake of trans-resveratrol and quercetin in high-fat sucrose diet-fed rats. The Journal of nutritional biochemistry. 2015;26(6):651-60. Epub 2015/03/13.

433.   Chen ML, Yi L, Zhang Y, Zhou X, Ran L, Yang J, et al. Resveratrol Attenuates Trimethylamine-N-Oxide (TMAO)-Induced Atherosclerosis by Regulating TMAO Synthesis and Bile Acid Metabolism via Remodeling of the Gut Microbiota. mBio. 2016;7(2):e02210-15. Epub 2016/04/07.

434. Pierre JF, Heneghan AF, Feliciano RP, Shanmuganayagam D, Roenneburg DA, Krueger CG, et al. Cranberry proanthocyanidins improve the gut mucous layer morphology and function in mice receiving elemental enteral nutrition. JPEN Journal of parenteral and enteral nutrition. 2013;37(3):401-9. Epub 2012/10/16.

435. Taira T, Yamaguchi S, Takahashi A, Okazaki Y, Yamaguchi A, Sakaguchi H, et al. Dietary polyphenols increase fecal mucin and immunoglobulin A and ameliorate the disturbance in gut microbiota caused by a high fat diet. Journal of clinical biochemistry and nutrition. 2015;57(3):212.

436. Lim ES, Zhou Y, Zhao G, Bauer IK, Droit L, Ndao IM, et al. Early life dynamics of the human gut virome and bacterial microbiome in infants. Nature medicine. 2015;21(10):1228-34. Epub 2015/09/15.

437. Yadav H, Jain S, Nagpal R, Marotta F. Increased fecal viral content associated with obesity in mice. World journal of diabetes. 2016;7(15):316-20. Epub 2016/08/25.

438. Friedman M. Overview of antibacterial, antitoxin, antiviral, and antifungal activities of tea flavonoids and teas. Mol Nutr Food Res. 2007;51(1):116-34. Epub 2006/12/30.

439. Sekizawa H, Ikuta K, Mizuta K, Takechi S, Suzutani T. Relationship between polyphenol content and anti-influenza viral effects of berries. J Sci Food Agric. 2013;93(9):2239-41. Epub 2013/01/29.

440. Liu S, da Cunha AP, Rezende RM, Cialic R, Wei Z, Bry L, et al. The Host Shapes the Gut Microbiota via Fecal MicroRNA. Cell host & microbe. 2016;19(1):32-43. Epub 2016/01/15.

441. Baselga-Escudero L, Blade C, Ribas-Latre A, Casanova E, Suarez M, Torres JL, et al. Resveratrol and EGCG bind directly and distinctively to miR-33a and miR-122 and modulate divergently their levels in hepatic cells. Nucleic acids research. 2014;42(2):882-92. Epub 2013/10/30.

442. Milenkovic D, Deval C, Gouranton E, Landrier JF, Scalbert A, Morand C, et al. Modulation of miRNA expression by dietary polyphenols in apoE deficient mice: a new mechanism of the action of polyphenols. PloS one. 2012;7(1):e29837. Epub 2012/01/19.

443. Li T, Chiang JY. Bile acids as metabolic regulators. Current opinion in gastroenterology. 2015;31(2):159-65. Epub 2015/01/15.

444. Brighton CA, Rievaj J, Kuhre RE, Glass LL, Schoonjans K, Holst JJ, et al. Bile Acids Trigger GLP-1 Release Predominantly by Accessing Basolaterally Located G Protein-Coupled Bile Acid Receptors. Endocrinology. 2015;156(11):3961-70. Epub 2015/08/19.

445. Drucker DJ, Nauck MA. The incretin system: glucagon-like peptide-1 receptor agonists and dipeptidyl peptidase-4 inhibitors in type 2 diabetes. Lancet. 2006;368(9548):1696-705. Epub 2006/11/14.

446. Dailey MJ, Moran TH. Glucagon-like peptide 1 and appetite. Trends in endocrinology and metabolism: TEM. 2013;24(2):85-91. Epub 2013/01/22.